Report

Investigation of the fish die-off in the Oder River in August 2022

30.05.2023
BfG-2143_EN

BfG Federal Institute of Hydrology

Report

Investigation of the fish die-off in the Oder River in August 2022

Short title	Investigation of the fish die-off in the Oder River in August 2022

Authors	Wiederhold, Jan; Buchinger, Sebastian; Duester, Lars; Fischer, Helmut; Hahn, Jens; Helms, Martin; Hermes, Nina; Jewell, Kevin; Kleinteich, Julia; Krenek, Sascha; Loeffler, Dirk; Mora, Demetrio; Rademacher, Silke; Schluesener, Michael; Schuetze, Katharina; Wahrendorf, Dierk-Steffen; Wick, Arne; Ternes, Thomas **Federal Institute of Hydrology (BfG)**

Project number	M39600001000
BfG number	BfG-2143_EN
DOI	10.5675/BfG-2143_EN

Publication details

Publisher

Federal Institute of Hydrology (BfG)
Am Mainzer Tor 1
56068 Koblenz
Germany

Phone: +49 261 1306-0
Fax: +49 261 1306-5302

Email: posteingang@bafg.de
Website: www.bafg.de/EN

Translation

Linguatext Ltd., Edinburgh, UK
Ruth Trautmann, BfG

The original German version of this report BfG-2143 ("Untersuchungen zum Fischsterben in der Oder im August 2022") was published in June 2023.

Suggested citation

WIEDERHOLD, J.; BUCHINGER, S.; DUESTER, L.; FISCHER, H.; HAHN, J.; HELMS, M.; HERMES, N.; JEWELL, K.; KLEINTEICH, J.; KRENEK, S.; LOEFFLER, D.; MORA, D.; RADEMACHER, S.; SCHLUESENER, M.; SCHUETZE, K.; WAHRENDORF, D.-S.; WICK, A.; TERNES, T. (2023) Investigation of the fish die-off in the Oder River in August 2022. [Online]. Koblenz, Federal Institute of Hydrology, Report BfG-2143_EN. DOI: 10.5675/BfG-2143_EN.

Cover photo

The Oder River near Eisenhüttenstadt, August 2018
(photo: Markus Kiefer, BfG)

Contents

Brief summary

- In August 2022, massive numbers of fish died in the Polish and German parts of the Oder River. The cause of this fish die-off was initially unknown.
- BfG was heavily involved in the investigations to elucidate the fish die-off, using its interdisciplinary expertise from the fields of hydrology, analytical chemistry, ecotoxicology and ecology.
- The availability of daily composite samples that were collected automatically at the Oder monitoring station in Hohenwutzen, which is jointly operated by the federal state of Brandenburg and BfG, proved to be extremely valuable. They enabled the investigation of the river water before, during and after the event.
- The prolonged low-flow conditions of the Oder in summer 2022 were one of the influential factors in the development of the fish die-off event. Comparable low-flow conditions in the Oder can be expected in the future, when considering the examinations of the recent years.
- The substantially elevated salt concentrations in the Oder during the fish die-off were primarily caused by sodium chloride (table salt). However, for many years elevated salt concentrations have regularly been recorded in the Oder.
- The combination of elevated salt content, high temperatures, strong sunlight and prolonged low-flow conditions facilitated the widespread mass proliferation of the brackish water microalga *Prymnesium parvum* in the Oder in summer 2022.
- The microscopic and molecular biological identification of *Prymnesium parvum* and the detection of prymnesin-B1 by LC-MS/MS attest to the high likelihood that the prymnesins, which are toxic to fish, led to the mass die-off of fish and other organisms in the Oder.
- Numerous analyses by BfG showed that a large number of anthropogenic substances were discharged into the river, but it is unlikely that these substances were one of the direct factors responsible for the fish die-off.

1 Introduction and overview

The fish die-off in the Oder in August 2022 is one of the biggest ecological disasters to strike Central European watercourses in recent years. Shortly after dead fish were first seen – initially in the Polish part of the Oder, but then in the German section, too – developments took place thick and fast within just a few days. The unexpected large number of dead fish and the simultaneously observed deaths of other organisms in the river caused great concern, not only amongst all the authorities affected, but also among the public, which was rapidly informed about the disaster by the media. Besides a focus on the organisation of measures by the local authorities to deal directly with the consequences of the fish die-off (e.g. disposing of the dead fish), interest soon centred around the question of what had caused the event. Since it was initially impossible to identify any direct cause of the fish die-off, there was a great deal of speculation and many hypotheses that needed to be tested.

The Federal Institute of Hydrology (BfG) joined the search for potential causes of the fish kill at an early stage and conducted many analyses of samples from the Oder. Following requests for administrative assistance from the State Laboratory Berlin-Brandenburg (Landeslabor Berlin-Brandenburg – LBB) and the Brandenburg State Office for the Environment (Landesamt für Umwelt (LfU) Brandenburg) and in coordination with the Federal Ministry for the Environment, Nature Conservation, Nuclear Safety and Consumer Protection (BMUV), BfG provided scientific support in a variety of areas. The availability of daily composite samples of water from the Oder from the Hohenwutzen monitoring station, which is operated jointly by the federal state of Brandenburg and BfG, from 1 July 2022 onwards, proved particularly helpful in this regard. This is because these samples made it possible to retrospectively examine the temporal evolution of the composition of the water of the Oder before, during and after the fish die-off. All three BfG divisions were involved in the investigations into the fish die-off in the Oder in summer 2022. They were able to draw on BfG's broad expertise in the fields of hydrology, analytical chemistry, ecotoxicology, molecular biology and algology.

This report provides a comprehensive overview of the work carried out at BfG from August 2022 in relation to the fish die-off in the Oder. Certain results presented in detail here previously appeared in a more concise form in the status report published on 30 September 2022 by the German expert group on the fish die-off in the Oder River. This expert group also included BfG staff members (BMUV 2022). Following a general introduction and a description of the event, this BfG report sets out the results of the various investigations conducted by BfG in detail. It also discusses these results and presents conclusions and recommendations for dealing with and/or preventing similar extreme ecological events in the future.

2 General introduction regarding the water quality of the Oder

2.1 Description of the catchment area and general characteristics

The Oder rises in the Czech Republic in the Oder Mountains – a south-eastern range of the Sudeten Mountains – at an altitude of 632 metres above sea level. According to the International Commission for the Protection of the Odra River against Pollution (IKSO 2022b), the Oder's main course to the mouth of the river at the Baltic Sea is 855 km long. Its catchment area (see Figure 2.1.1) measures approximately 124,050 km^2, with more than 86% of this area on Polish territory, 6% on Czech territory and 8% on German territory.

The Oder's biggest tributary is the Warta, which flows into the Oder approximately 30 km downstream of Frankfurt (at Oder km 617.5) and drains just under half of the entire Oder catchment area. The Oder's other principal tributaries include the Bober (mouth at Oder km 514) and the Lusatian Neisse (mouth at Oder km 542.5, approximately 12 km upstream of Eisenhüttenstadt). The section that is downstream of the mouth of the Lusatian Neisse runs along the border between Germany and Poland for around 160 kilometres.

The prevalent climate in the Oder catchment area is a temperate continental one, with the continental influence increasing from west to east. The mean annual precipitation depths at the ridges of the upper mountain regions are between 1,000 and 1,400 mm. However, the majority of the catchment area has mean annual precipitation depths of between 500 and 600 mm (IKSO 2020).

According to BFG (2021), the conditions of this natural environment result in a nivo-pluvial flow regime that is characterised by a highly volatile flow level extending far beyond the upper reach. It is only after the inflow of the Warta that the lower reach of the Oder, which starts there, takes on the typical, even flow character of a low-gradient lowland river. Overall, the river is characterised by high flows in spring as a result of snow-melt and low flows from June to November, with minimum levels in September and October. However, it is not uncommon for the low-flow phases to be punctuated by short, steep flood waves after heavy precipitation.

There are many dams in the Oder catchment area, but their total water storage capacity is considerably lower than that of the dams in the neighbouring Elbe catchment area, for example. According to IKSO (2022b), the dams with an individual water storage capacity of more than 5 million m^3 have a combined storage capacity of around 1.2 billion m^3, and of these, dams with a total storage capacity of around 860 million m^3 help, at least to some extent, to increase water levels in low-flow conditions. In addition, large sections of the Oder are impounded in Poland. However, the section of the Oder that runs along the border between Poland and Germany is free-flowing. Finally, anthropogenic interventions that affect the water balance of the Oder catchment area also include the abstraction of water for lignite opencast mining in Lusatia. The sustainability deficiencies this has caused will continue to have an impact for decades to come (BFG 2021).

Figure 2.1.1 *The Oder catchment area with major bodies of water and gauging stations. Source: BFG 2021.*

The hydrological primary values presented in Table 2.1.1 portray the fundamental flow conditions at the main German gauging stations on the Oder – Eisenhüttenstadt (Oder km 554.1) and Hohensaaten-Finow (Oder km 664.9).

Table 2.1.1 *Hydrological primary values (MAD – mean annual discharge (in German: MQ), MAPD – mean annual peak discharge (in German: MHQ), MAMD – mean annual minimum discharge (in German: MNQ)) at the Eisenhüttenstadt and Hohensaaten-Finow Oder gauging stations, according to BFG (2021). The values relate to the hydrological years (MAD, MAPD) and water-balance years (MAMD) 1961 to 2018.*

Gauging station	MAD (m^3/s)	MAPD (m^3/s)	MAMD (m^3/s)
Eisenhüttenstadt	297	884	131
Hohensaaten-Finow	522	1,200	246

2.2 Long-term trends in water quality

The water quality of the Oder varies spatially along its length and seasonally under the influence of temperature and flow conditions. It also varies over the long term, both as a function of anthropogenic inputs and their associated long-term effects and as a result of regional climate developments. Unless otherwise stated, the trend analyses of the various water quality parameters described in this section relate to the period from 2000 to 2022 and are based on data supplied by the Brandenburg State Office for the Environment (LfU) and the International Commission for the Protection of the Odra River against Pollution (ICPO). The aim of this section of the report is to illustrate the long-term trends in water quality from the recent past to the present, based on this reference period. There is a particular focus on the physicochemical parameters that showed anomalies during the fish die-off (see section 5.2).

In addition to the long-term trends, a summary of anomalous water-quality parameters is also provided to give an insight into the aquatic ecological and chemical characteristics of the Oder prior to the start of the fish die-off in 2022. Water quality is assessed in line with the specifications of the EU Water Framework Directive (EU 2000). The assessment involves determining the ecological status and the chemical status of a surface water body on the basis of its catchment area and categorising it in a rating system comprising five classes (high, good, moderate, poor and bad). Under European law, the EU Member States are therefore required by the WFD to set threshold values for the assessment of the ecological status and chemical status of watercourses. In terms of the assessment of the ecological status and ecological potential, these values include physicochemical parameters, nutrient elements and their compounds, and specific pollutants. The chemical status, on the other hand, is assessed on the basis of threshold values for priority substances. In terms of content, this section of the report focuses on the “anomalous” parameters in respect of which relevant threshold values were exceeded in the recent past and which are recorded close to real-time or online. It should be noted that the threshold values may differ from one riparian state of the Oder to another. This is due to the fact that the Member States implement the WFD requirements through national legislation.

Development trends in physicochemical water quality properties and total chlorophyll

To infer the long-term trends in physicochemical water quality properties, sensor data (electrical conductivity, water temperature, oxygen content and pH) supplied by LfU Brandenburg was assessed. The trend diagrams for some of the sensor data from the Hohenwutzen monitoring station (Oder km 661) for the years 2000 to 2022 are presented in Figures 2.2.2 to 2.2.7. In these diagrams, original data (daily mean values) is shown in grey, and the time series derived from this data (median of four-week intervals) is shown in blue. The trend line determined from the time-series values is shown in red. LOWESS refers to locally weighted scatterplot smoothing, which makes changes within the time series visible that cannot be identified via the trend line (BAGGELAAR & VAN DER MEULEN 2012). The reference gauge for this monitoring station is Hohensaaten-Finow (Oder km 665). Further information about monitoring stations on the Oder can be accessed at https://undine.bafg.de/index_en.html and https://lfu.brandenburg.de. The data shown here originates from LfU Brandenburg and the Pegelonline hydrological information system operated by Germany's Federal Waterways and Shipping Administration (WSV). Table 2.2.1 presents a summary overview of the trend analyses

conducted and the statistical method that best fits the respective time series (for details, see Annex 1 and BAGGELAAR & VAN DER MEULEN 2012).

Table 2.2.1 *Trend assessment of sensor data from the Hohenwutzen monitoring station (MK = Mann-Kendall test, a = autocorrelation correction, LR = extended linear regression, s = seasonal).*

Parameter	Test	Significant trend (95%)?	Assessed period
Electrical conductivity	LRsa LRsa	Yes Yes	2000-2022 2013-2022
Water temperature	LRs	Yes	2000-2022
Oxygen	MKsa	Yes	2000-2022
pH	LRs	No	2000-2022

Over the last 22 years, discharge at the Hohensaaten-Finow gauging station showed a mean level that largely remained constant up to around 2013. However, in the years that followed, discharge was low (Figure 2.2.1). As a consequence, the mean annual discharge (MAD) values at this gauging station for the years 2015 to 2020 exhibit mean discharge volumes that are consistently below average compared to the 1951 to 2015 reference period (ABBAS et al. 2022). During these low-discharge years from 2014 onwards, extreme low-flow phases occurred in 2015, 2018, 2019 and, most recently, 2022. No trend was detected that was significant in the long term (from 1961) in terms of low-flow parameters (see section 5.1).

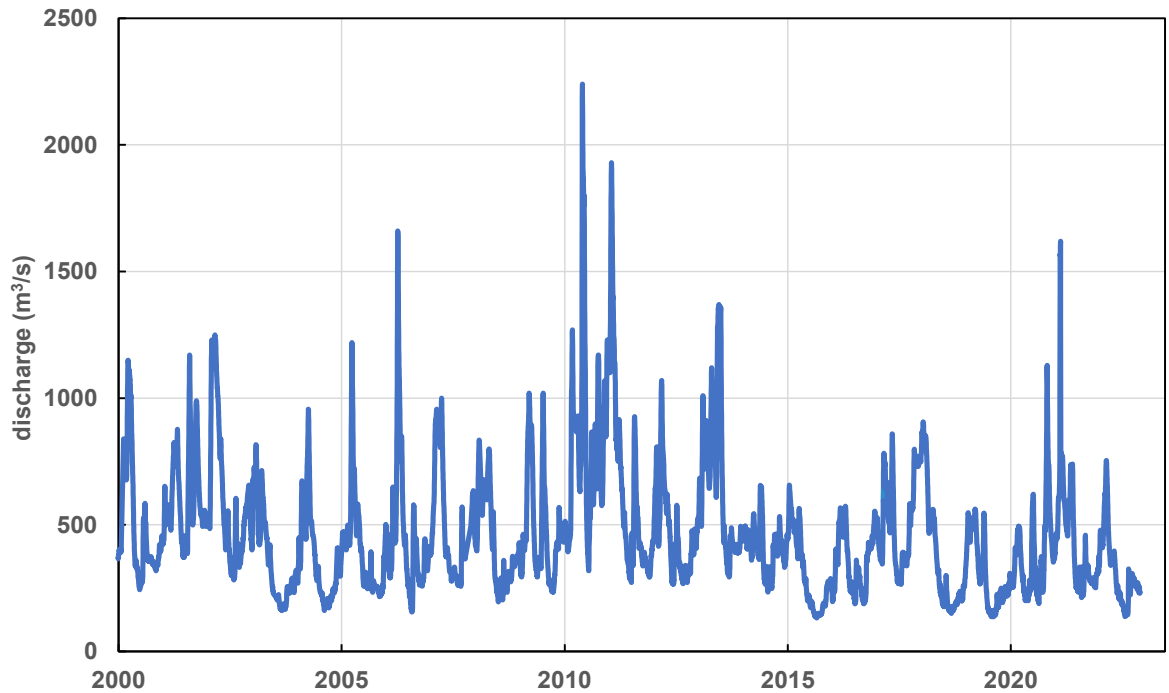

Figure 2.2.1 *Discharge (m^3/s) at the Hohensaaten-Finow gauging station for the years 2000 to 2022.*

With regard to electrical conductivity (Figure 2.2.2) and water temperature (Figure 2.2.3), rising trends are significant. Over the last 10 years, the increasing trend in terms of electrical conductivity was even more strongly pronounced than across the time period as a whole.

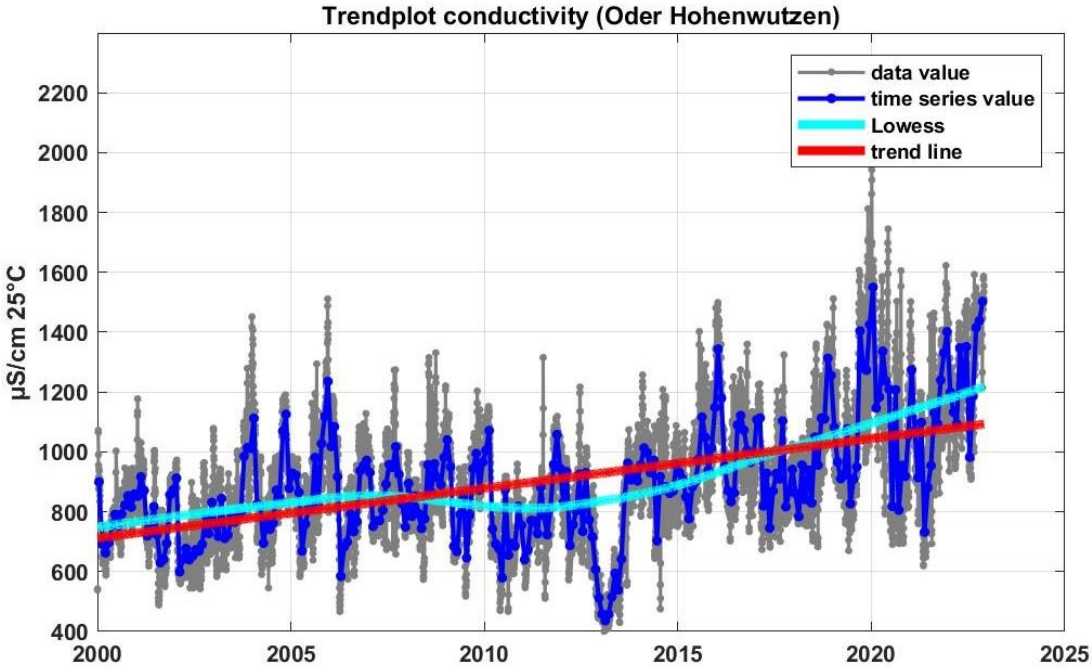

Figure 2.2.2 *Electrical conductivity (µS/cm) for the years 2000 to 2022. The relative trend across the time period as a whole was +16.6 µS/cm (25 °C) (equivalent to +1.9%) per year. Over the last 10 years (2013 to 2022), the annual trend was as high as +44.3 µS/cm (25 °C) (equivalent to +5.1%). The "data values" shown are daily mean values. Time series values correspond to the median of four-week intervals.*

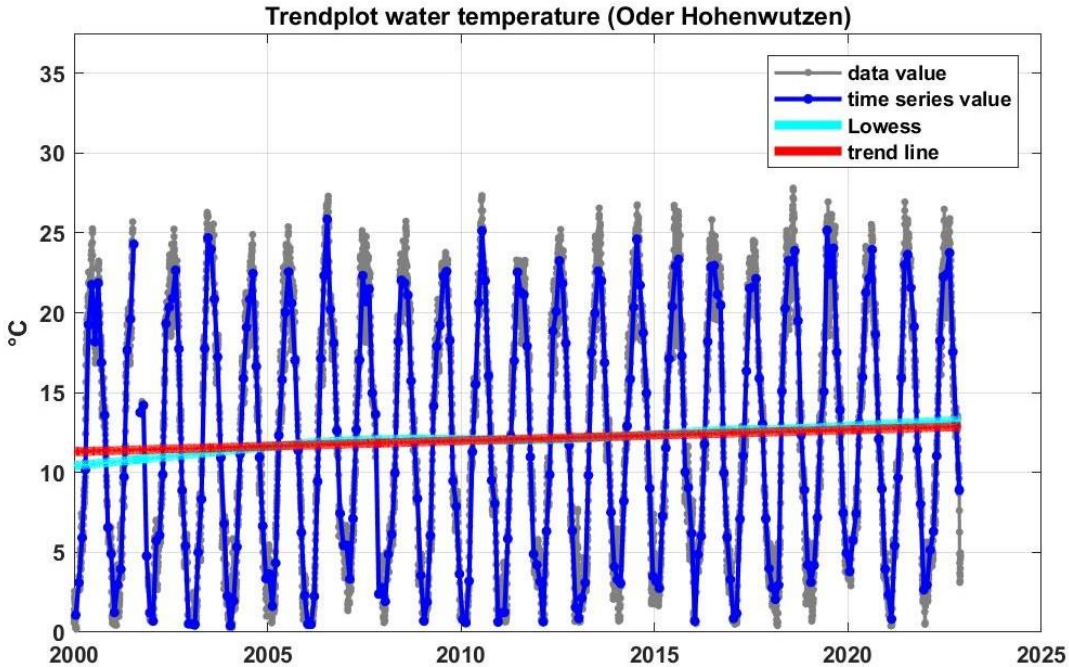

Figure 2.2.3 *Water temperature (°C) for the years 2000 to 2022. The "data values" shown are daily mean values. Time series values correspond to the median of four-week intervals.*

The statistical analysis revealed slightly decreasing trends in terms of the concentrations of total chlorophyll (Figure 2.2.4) and dissolved oxygen (Figure 2.2.5). However, the very large variations in these parameters and gaps in the data mean there is great uncertainty about these trends, so they should not be used to infer future developments. In addition, comparison measurements during the *Prymnesium* bloom revealed an undervaluation of the chlorophyll concentrations measured with the probe in Hohenwutzen.

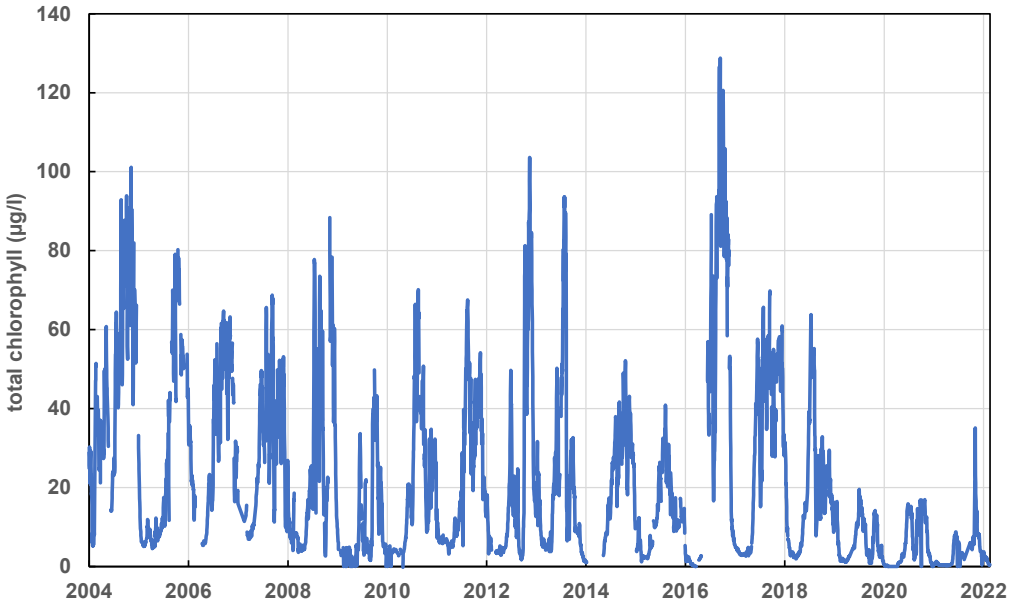

Figure 2.2.4 *Concentration of total chlorophyll (µg/l) in Hohenwutzen from October 2004 to November 2022 (there was no available data for 2000 to 2004). Daily mean values are shown. There are concerns over the plausibility of the data from the years 2020 to 2022, since comparison measurements suggest an undervaluation in respect of these figures during this period.*

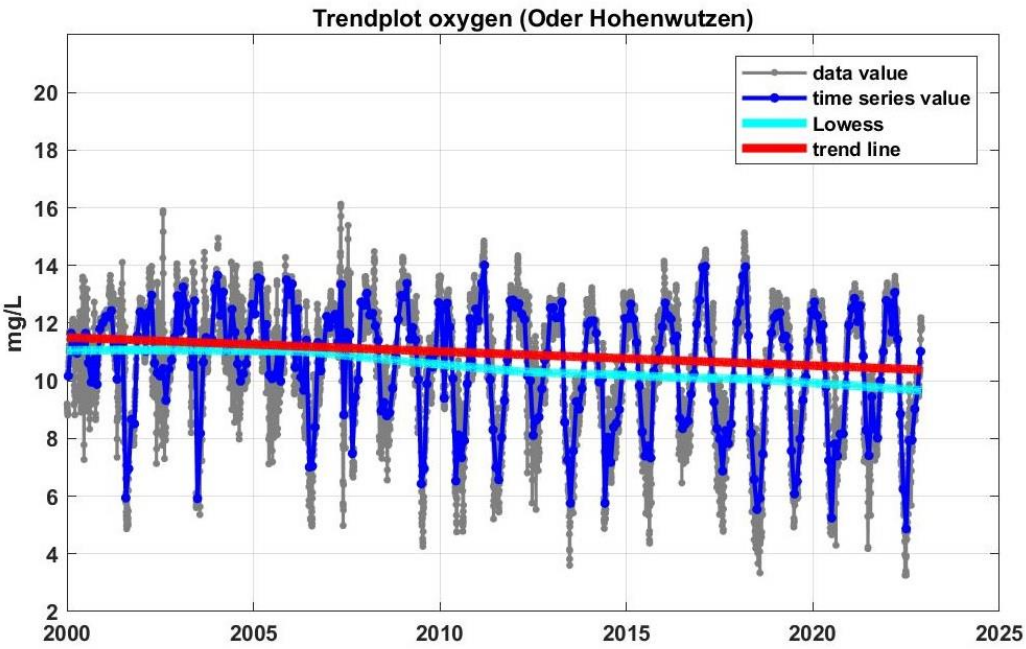

Figure 2.2.5 *Dissolved oxygen (mg/l) for the years 2000 to 2022. The "data values" shown are daily mean values. Time series values correspond to the median of four-week intervals. Differences relating to the time of day (day/night) may show even bigger fluctuation intervals and are not shown here.*

In terms of pH, no long-term trend was detected. However, as can be seen in Figure 2.2.6, the variations within an identifiable reference year demonstrate that, similar to the parameters already outlined, pH is subject to a pronounced seasonal effect.

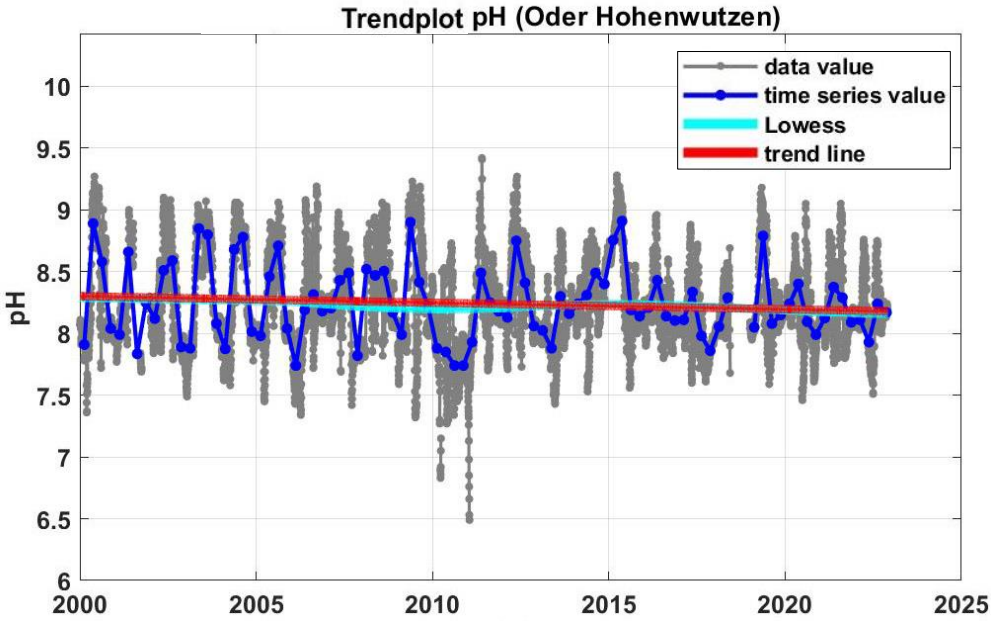

Figure 2.2.6 *Variations in pH for the years 2000 to 2022. The "data values" shown are daily mean values. Time series values correspond to the median of four-week intervals.*

As in the case of oxygen content and total chlorophyll, this effect in the spring and summer is largely biologically controlled. The extent of seasonal differences in pH is shown in Figure 2.2.7, where the data is sorted and presented in quarters so that possible seasonal differences in pH can be seen.

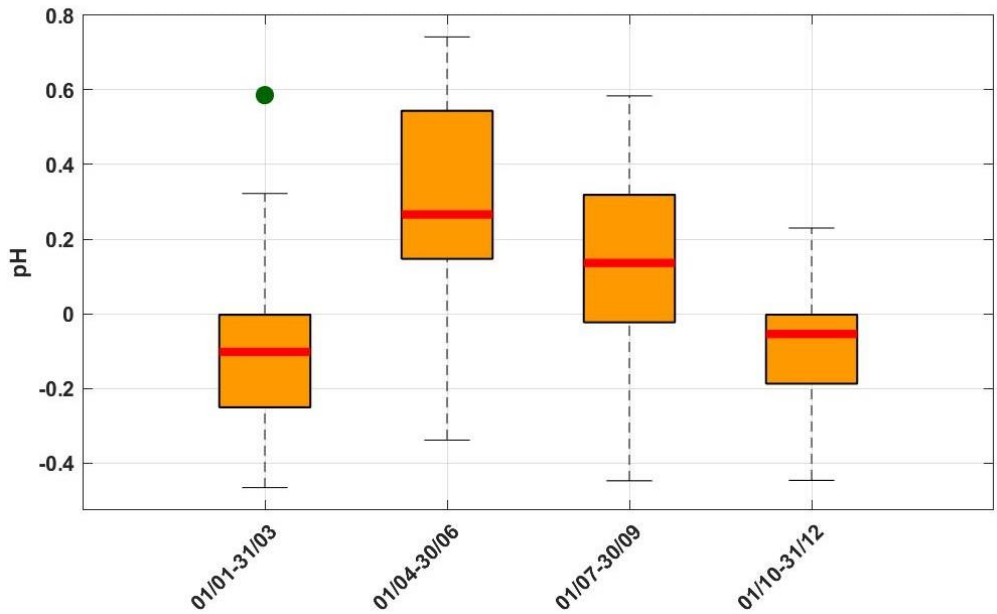

Figure 2.2.7 *Trend-corrected box and whisker plots of pH based on quarters Jan.-Mar., Apr.-Jun., Jul.-Sep. and Oct.-Dec. of years 2000 to 2022.*

When the selected data from the monitoring stations at Hohenwutzen and Hohensaaten−Finow (discharge) is summarised, the recent low-flow years and the significantly increasing trends in terms of electrical conductivity and temperature indicate a deterioration in water quality in recent years. Even without considering other factors, the high electrical conductivity, which is above average compared to other watercourses, particularly presents a picture of an aquatic system with very high levels of anthropogenic pressure. Adverse effects of the consequences of climate change, in the form of a multiple-year low-flow phase and rising water temperatures, along with increasing anthropogenic usage manifested in rising electrical conductivity, appear to accumulate more intensely towards the present day. The sometimes critically low oxygen concentrations (< 4 mg/l) in the early summer indicate increased oxygen consumption processes, e.g. due to decaying phytoplankton. It can be assumed that this negative development in the parameters presented by way of example is also coupled with a decreasing resilience to pollution that is present (e.g. organic contaminants or algal toxins) and to future pollution if this development continues (e.g. if water temperatures continue to rise as flow levels drop further and the input of substances remains the same).

Nutrient concentrations

During the last decade, the surface waters of the Oder catchment area in Czech, Polish and German territory have predominantly not achieved good ecological status. In terms of the biological components, this was particularly caused by the macrozoobenthos. In addition, the frequently elevated nutrient concentrations, especially in the form of phosphorus (total phosphorus, orthophosphate), did also not meet the requirements for good ecological status or good ecological potential (IKSO 2022b).

An overview of the longitudinal course of the Oder and its main tributaries is made possible by data from the following monitoring stations: Bohumín (Oder, CZ), Wroclaw (Oder, PL), Połęcko (Oder, PL), Hrádek nad Nisou (Lusatian Neisse, CZ), Hrádek nad Nisou (Lusatian Neisse, PL), Guben (Lusatian Neisse, DE), Kostrzyn nad Odrą (Warta, PL), Hohenwutzen (Oder, DE) and Krajnik Dolny (Oder, PL). Between 2011 and 2018, the concentrations of total nitrogen (TN) at these monitoring stations varied between 0.76 mg/l and 11 mg/l, and the mean values ranged from 2.4 mg/l to 4.3 mg/l (IKSO 2022a). Over the course of the year, the maximum TN concentrations particularly occurred in the upper Oder during low-flow phases.

During the same period, total phosphorus (TP) varied between 0.03 mg/l and 1 mg/l, with the annual mean values ranging from 0.08 to 0.22 mg/l. For the most part, only slight differences in TP concentration occurred along the longitudinal profile of the Oder. The annual mean values from almost all the permanent monitoring stations listed do not therefore meet the requirements for good ecological status as set out by OGewV (2016), which stipulates a TP concentration of ≤ 0.10 mg/l as a mean value for three consecutive years.

It can be inferred from the measurement values that there is a clear need to reduce nutrient loads – especially phosphorus compounds – in parts of the Oder to meet the WFD objective (IKSO 2022a). Aside from legal provisions, it should be noted that the TP concentration during the period from 2011 to 2018 showed repeated increases while flows were decreasing (IKSO 2022a). A future escalation of the summertime low-flow situation could consequently also mean an increase in total phosphorus concentrations in

the summer. This would run counter to achieving good ecological status and could facilitate summer algal blooms.

Priority substances

The classification of the chemical status of the Oder and its associated water bodies in line with the applicable environmental quality standard (EQS) directive (Directive 2013/39/EU) is implemented through national law. As with the ecological status classification, the requirements for achieving “good chemical status” may vary between the different riparian states of the Oder. For the reference period 2013 to 2019, the chemical quality of the water bodies of the Oder catchment area was published by the three riparian states in IKSO (2022b) and classified on the basis of priority substance concentrations as follows:

- In the Czech Republic, the chemical quality of the water in a total of 118 bodies of water was successfully analysed. Of these, 115 were classified as “not good”, and this was primarily due to the concentrations of polycyclic aromatic hydrocarbons (PAHs) that were present.
- In Poland, the chemical quality of the water was declared “not good” for 53.5% of the water bodies analysed. This was primarily due to PAH, Cd and Hg pollution.
- In Germany, all the water bodies belonging to the Oder catchment had to be classified as “not good” due to EQS thresholds of certain contaminants being exceeded. This applied frequently to ubiquitous contaminants such as mercury and polybrominated diphenyl ethers and to PAHs in many cases, too. Levels that exceeded EQS thresholds for nickel, di(2-ethylhexyl)phthalate (DEHP), cypermethrin, dichlorvos, trichloromethane and isoproturon were detected in individual cases; however, they represented only < 5% of the total number of cases in which EQS thresholds were exceeded in bodies of surface water in Germany.

Based on this state of affairs, it can be noted, in summary, that there is a need for improvements to achieve the “good chemical status” of surface water. However, since EQSs are, for the most part, breached by the concentrations of ubiquitous substances within the catchment area, no specific pollution of the Oder by contaminants should be assumed. It is true that above-average accumulations of contaminants, especially in the form of metals and PAHs, were detected in many locations along the length of the Oder in the past (MEYER 2002). Moreover, elevated concentrations of contaminants in water and sediment samples from the Oder have been described in numerous scientific publications (e.g. MÜLLER et al. 2003; CISZEWSKI & TURNER 2009; STEPIEN & PUTTMANN 2014; FAMERA et al. 2021; JASKULA & SOJKA 2022). However, an assessment of upper sediment layers along the part of the Oder that runs along the border between Poland and Germany (km 542.5-704) in 2021 (INSTITUT DR. NOWAK 2021) revealed the extensive presence of sands and gravels with little or no contamination. It is therefore likely that, in the case of the ubiquitous substances at least, the EQS breaches described above are attributable to historical contamination, presumably with distribution in a few specific locations.

2.3 Information about anthropogenic influences

The Oder catchment area has been greatly affected by anthropogenic influences for a long time. There is a long tradition of coal mining around the upper reaches of the Oder in Upper Silesia, for example – a tradition that dates from the Middle Ages, with mining on an industrial scale taking place from the 19th century (DULIAS 2016). Coal mining in Poland reached its peak in 1979, when the annual quantity mined was 201 million metric tons of coal (SZPOR & ZIÓŁKOWSKA 2018). Even though Polish coal production has declined since then, there are still around 30 active coal mines in the Upper Silesian Coal Basin (see Figure 2.3.1A) producing approximately 80 million metric tons per year (CHALUPNIK et al. 2017). Drainage of underground mines results in large quantities of effluents with a high salt content. A large proportion of these effluents are released, directly or indirectly, into Poland's two major rivers – the Oder (Odra) and the Vistula (Wisla). The total quantity of salt (with its main constituent being sodium chloride) entering rivers in Poland in effluents from coal mining operations is stated to be approximately 4 million metric tons per year (MITKO et al. 2021). The salination of Polish rivers as a result of mining has been recognised as a serious environmental problem for several decades now (e.g. KCEPIŃSKI 1980; ANDERSSON 1999; WOLKERSDORFER et al. 2005; GZYL et al. 2017). Even if various technical methods for treating and desalinating effluents from mining operations have been proposed (e.g. ERICSSON & HALLMANS 1996; TUREK et al. 2005), these have so far only been put into use at individual pilot plants (MITKO et al. 2021; TSALIDIS et al. 2022). It takes high levels of energy to desalinate effluents from mining operations, so high costs are also involved. The EU has co-financed the "Zero Brine" project (https://zerobrine.eu), for example, and this included studying ways of treating effluents from Polish coal mines.

In the Oder catchment area, the majority of the input of salt from coal mining operations takes place around the upper reaches of the river in the Upper Silesian Coal Basin region. The Klodnica (respectively the Gliwice Canal), a right tributary of the Oder, plays a particular role in this respect, since particularly high quantities of effluents from mining operations and other industrial effluents are released into it (MATYSIK 2019; ZGORSKA et al. 2020; WIESNER-SĘKALA & KOŃCZAK 2023). One measure that was initiated to protect smaller watercourses was the construction of an artificial canal (the Olza Collector, see Figure 2.3.1B and Annex 2 Figure A2.2.3.1 (in German only)). From there, discharges from mining operations are released directly into the Oder in a controlled and metered way (HARAT et al. 2015; SWOLKIEŃ & FILEK 2012). In Poland, the total of chloride and sulphate is used to regulate the input of saline effluents into rivers. Once the effluents have been fully mixed into the river, this sum should not exceed 1 g/l (GZYL et al. 2017; ZIELIŃSKI et al. 2021). However, many breaches of this threshold have been documented (GZYL et al. 2017).

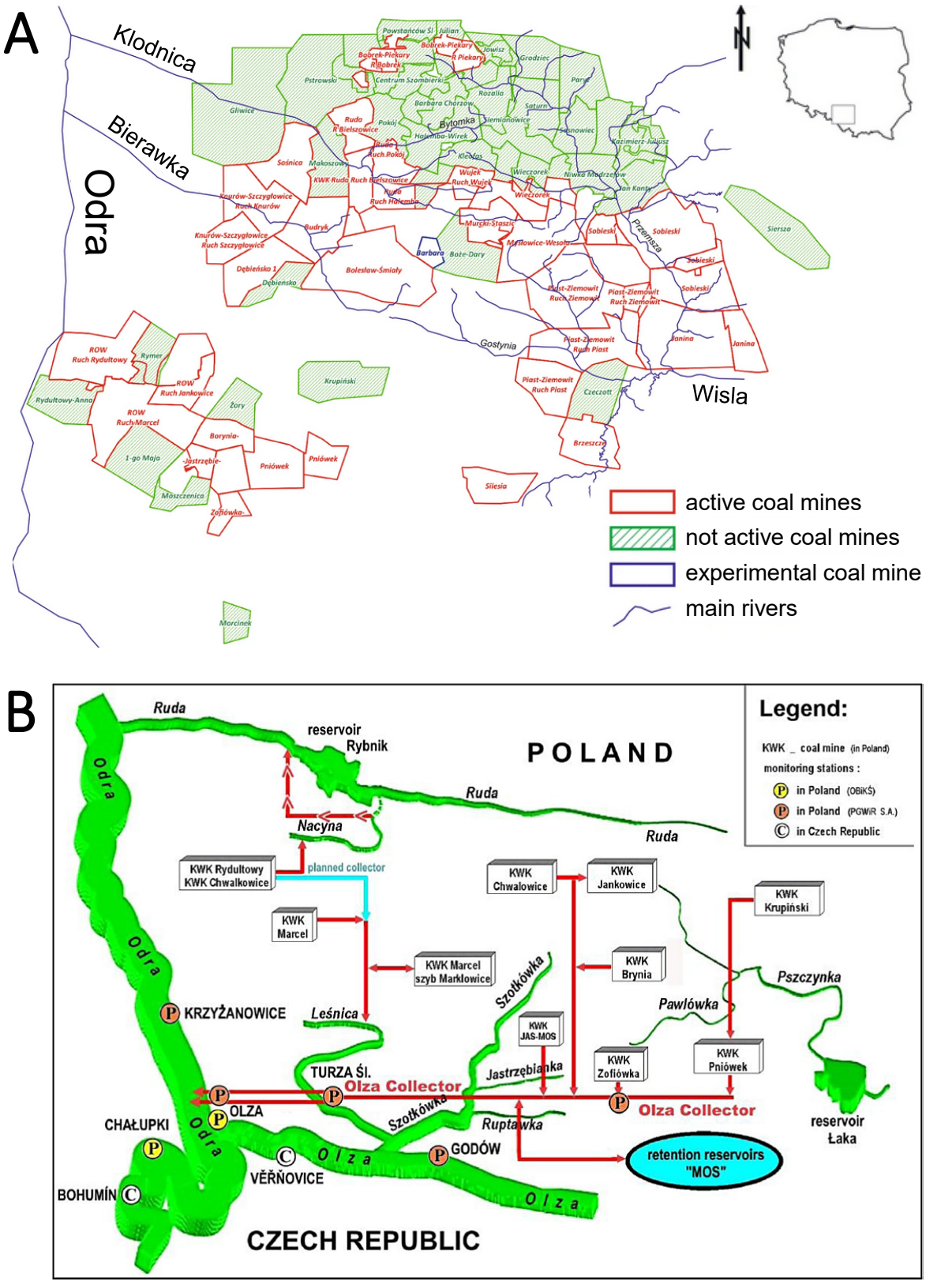

Figure 2.3.1 *(A) Overview of active and not-active coal mines in the Upper Silesian Coal Basin with the main surface waters (slightly modified, based on* WYSOCKA *et al. 2019).(B) Schematic diagram of the Olza Collector drainage system into the Oder (*HARAT *et al. 2015; also see Annex 2, Figure A2.2.3.1 (in German only)).*

In addition to coal mines, other mining operations and industries also play a role in the salination of the Oder. One example is the large KGHM copper mine in Lower Silesia. Effluents from this mine are released into the Oder close to Glogów (Figure 2.3.2A). Collected effluents and residues from several mines and ore processing plants are discharged into the "Zelazny Most" artificial pond. Surrounded by a dam measuring between 41 and 65 m in height and 14.3 km in length (Figure 2.3.2B), this is Europe's biggest mine tailings pond (KARCZEWSKA et al. 2017). It contains approximately 652 million m^3 of tailings and 8 million m^3 of water (LYDZBA et al. 2022), and capacity is currently being expanded to 950 million m^3 (DUCZMAL-CZERNIKIEWICZ et al. 2021). Ores containing copper have been mined and smelted on an industrial scale in various mines in the surrounding area since the 1950s (KARCZEWSKA et al. 2017). Until the mid-1980s, water was taken from the Oder for these operations and for processing residues (WITECKI & GROTOWSKI 2019). However, changes to the mine drainage systems and water management reversed the water balance. Since then, excess residual water has been discharged into the Oder at the former abstraction site near Glogów. In 2021, the discharge station was modernised. As a result, saline effluent can now be pumped into the Oder at a rate of up to 2 m^3/s via a pipe section that is 50 m in length and contains a number of outlets (ZIELIŃSKI et al. 2021). Here again, the target is that the water of the Oder should contain less than 1 g/l chloride and sulphate once the effluent has been fully mixed in. The excess residual water that is transported from the "Zelazny Most" pond via a pipeline that is more than 15 km in length contains around 40 g/l NaCl. Every year, around 25 million m^3 are discharged into the Oder (i.e. approximately 0.8 m^3/s on average) (ZIELIŃSKI et al. 2021).

In addition to the inputs from coal and copper mining operations described above, which are probably the main sources of the salt load, many other industrial enterprises are located in the Oder catchment whose effluents are directly or indirectly released into the Oder. Annex 4 of the "Havarieplan für die Oder", the emergency plan for the Oder published by the International Commission for the Protection of the Odra River against Pollution (IKSO 2018), contains a map of potential sources of pollution. This map is reproduced in Figure A2.2.3.2 in Annex 2 of this report (in German only).

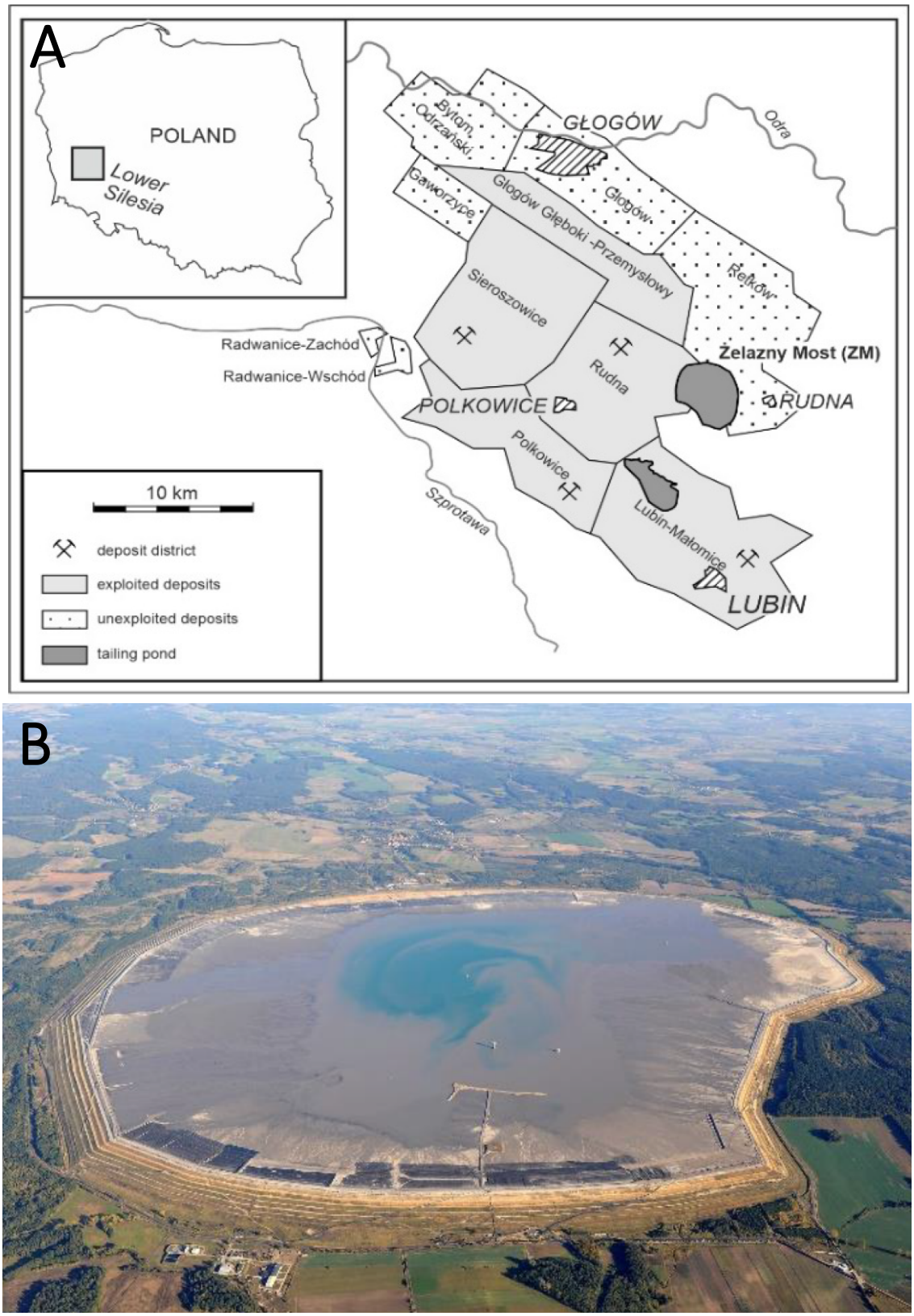

Figure 2.3.2 *(A) Overview of the Lubin-Glogów copper mining region (DUCZMAL-CZERNIKIEWICZ et al. 2021) and (B) aerial view of the Zelazny Most mine tailings pond (LYDZBA et al. 2022), from which saline effluents are pumped into the Oder near Glogów (ZIELIŃSKI et al. 2021).*

3 Description of the fish die-off event in August 2022

As described in greater detail in the sections that follow, the period from July to mid-August 2022 in the Oder catchment area was characterised by high temperatures, strong solar irradiation, low levels of precipitation and, consequently, decreasing water levels. In Poland, a sizeable volume of dead fish (920 kg) was observed in the Gliwice Canal (section II), a tributary of the Oder in Upper Silesia, in as early as mid-July 2022 (IOŚ-PIB 2022). However, it is unclear whether this event was connected with the large fish die-off that occurred later, i.e. starting in late July and in August 2022. In late July 2022, the first large fish die-offs were observed in the Polish part of the Oder (e.g. 3,350 kg of dead fish on 30 July 2022 near Oława in Lower Silesia, IOŚ-PIB 2022). From late July until 12 September 2022, a total of 249 metric tons of dead fish were recorded in the Polish part of the Oder. The spatial and temporal distribution of these dead fish is described in detail in the Polish study report (IOŚ-PIB 2022). This was not, therefore, one single, continuous event; instead, dead fish were observed at different times in various reaches of the Oder (IOŚ-PIB 2022).

The fish die-off was first discovered on the German side by a ship operator on 9 August 2022, and the discovery was reported to the State Laboratory Berlin-Brandenburg (LBB). On 11 August 2022, the July 2022 daily composite samples from the BfG monitoring station in Hohenwutzen (see section 4.1) arrived at the BfG premises in Koblenz for the routine analysis associated with the monitoring of environmental radioactivity in Germany's federal waterways. In view of the first media reports about the fish die-off in the Oder, aliquots of these water samples were immediately put into containers and prepared for various analyses so that the composition of the Oder river water before the period of the fish die-off could be determined. On Friday, 12 August 2022, the State Laboratory Berlin-Brandenburg (LBB) and the Brandenburg State Office for the Environment (LfU) officially requested administrative assistance from the German Environment Agency (UBA) and the Federal Institute of Hydrology (BfG) via the Federal Ministry for the Environment, Nature Conservation, Nuclear Safety and Consumer Protection (BMUV). On Monday, 15 August 2022, BfG held its first internal meeting about the fish die-off in the Oder and drew up its first investigation concept.

Shortly afterwards, individual water samples from the federal state monitoring stations at Frankfurt (Oder) and Hohenwutzen were sent to BfG. These samples arrived in Koblenz on 17 August 2022. On 16 August 2022, a group of experts from the German authorities in Brandenburg, Mecklenburg-Vorpommern and the German Federal Government (including from BfG) was formed to investigate the possible causes of the fish die-off on the basis of information and monitoring data. On 16 August 2022, a BfG staff member picked up the daily composite samples from the BfG monitoring station in Hohenwutzen for 1 to 15 August 2022, along with grab samples of Oder river water taken on 16 August 2022 and a composite sample of suspended particulate matter from the period 1 to 15 August 2022. These samples arrived in Koblenz on 17 August 2022 and were immediately prepared for a range of analyses. On 24 August 2022, a BfG staff member picked up the daily composite samples from the BfG monitoring station in Hohenwutzen for 16 to 23 August 2022, along with grab samples of Oder river water taken on 24 August 2022 and a composite sample of suspended particulate matter from the period

16 to 24 August 2022. LBB also supplied a grab sample from the Frankfurt (Oder) federal state monitoring station. Finally, on 6 September 2022, a BfG staff member picked up the daily composite samples from the BfG monitoring station in Hohenwutzen for 24 August to 6 September 2022. He also picked up a composite sample of suspended particulate matter from the period 24 to 31 August 2022 and took grab samples of Oder river water in Hohenwutzen on 6 September 2022. On 6 September 2022, two water samples were also taken from the Oder-Spree Canal, close to Eisenhüttenstadt. More details about the monitoring stations and the samples analysed can be found in sections 4.1 and 4.2 of this report.

BfG's analysis results, which are described in detail in the sections that follow, were evaluated directly and made available to other parties, including the German expert group on the fish die-off in the Oder River. In September 2022, BfG carried out intensive support for the compilation of the status report on the fish die-off in the Oder River that was published by the German expert group on 30 September 2022 (BMUV 2022). The Polish expert group had published its provisional report on the situation in the Oder one day earlier, i.e. on 29 September 2022 (IOŚ-PIB 2022). An English version of the German status report was made available on the BMUV website in October 2022.

Observations and scientific reports on the fish die-off in the Oder were also published. Based on anglers' observations of a number of live fish in the Oder, the Institute of Inland Fisheries in Potsdam-Sacrow (Institut für Binnenfischerei e.V. Potsdam-Sacrow – IfB) carried out some test fishing in the Oder, close to Brieskow-Finkenheerd, on 19 and 30 August 2022 and found 19 fish species typical of the Oder (IFB 2023). On 12 September 2022, the Leibniz Institute of Freshwater Ecology and Inland Fisheries (IGB) published a policy brief entitled "The future of the River Oder – research-based recommendations for action in the wake of the man-made environmental disaster" (IGB 2022b). On 29 September 2022, Greenpeace published a fact sheet about the fish die-off, complete with its own analysis results (GREENPEACE 2022). In the months that followed, IGB reported on 27 October 2022 (IGB 2022c) and 20 December 2022 (IGB 2022a) on results of test fishing campaigns in the Oder. On 14 February 2023, the BMUV announced funding for the special investigative project for the Oder River ("Sonderuntersuchungsvorhaben Oder") being conducted by IGB. This funding, which covers the period from 1 February 2023 to 30 April 2026, is worth more than 4.8 million euros (BMUV 2023). On 17 February 2023, a report by the EU Joint Research Center (JRC) on the fish die-off in the Oder in summer 2022 was published (FREE et al. 2023). This report included references to the contents of the Polish and German expert reports. On 2 March 2023, Greenpeace published a report about its own analyses of salt discharges from Polish mines into the Oder and Vistula (PAZDERSKI et al. 2023). On 8 March 2023, an article appeared in a scientific journal, publishing chlorophyll data that had been collected along the Oder with a multi-parameter probe during the period 15 to 24 July 2022. This was combined with analysis of satellite images and discussed with reference to the situation before and during the fish die-off (ABSALON et al. 2023). On 31 March 2023, the Polish Institute of Environmental Protection – National Research Institute (IEP-NRI) published a final report about the fish die-off in the Oder (IOŚ-PIB 2023).

4 BfG's investigations

4.1 Description of sites / monitoring stations

As part of its water quality monitoring network (LFU 2009), the Brandenburg State Office for the Environment (LfU Brandenburg) maintains two automatic monitoring stations on the Oder in Frankfurt (Oder) (river km 584) and Hohenwutzen (river km 661) (Figure 4.1.1). At these stations, the following physicochemical parameters are monitored on a continuous basis in the water of the Oder (samples are taken from a depth of approximately 1.5 m below the surface of the water): water temperature, oxygen content, pH, electrical conductivity, turbidity, UV absorption (254 nm), total chlorophyll and nitrate. At the Hohenwutzen monitoring station, ammonium is also measured, and a Daphnia toximeter is in operation, too. Due to a power failure, no measurement data was collected at the Hohenwutzen monitoring station during the period from 6 to 8 August 2022.

As part of its statutory mandate to monitor environmental radioactivity (section 161 of the German Radiation Protection Act, StrlSchG), BfG operates 40 monitoring stations in Germany's federal waterways. One of these stations is located in Hohenwutzen on the Oder (river km 661), on the same site as the federal state's monitoring station. Here, in addition to online measurements of total gamma activity concentration, continuous daily composite samples of river water and a monthly composite sample of suspended particulate matter are taken automatically. The suspended particulate matter is collected in a sedimentation tank (integral collector) developed in-house at BfG. Since the online measurement of total gamma activity concentration revealed no anomalous values for the period being investigated (see Annex 2 – in German only), the input of radioactive substances into the Oder as a possible cause of the fish die-off could be ruled out at an early stage.

Figure 4.1.1 *Overview of the Oder catchment area, with the locations of the monitoring stations in Frankfurt (Oder) and Hohenwutzen marked on it (source: Wikipedia Commons).*

4.2 Overview of the samples tested

As part of the BfG investigations, the following samples were tested:

- 70 daily composite samples of water from the Oder from Hohenwutzen (BfG monitoring station: 1 July to 6 September 2022; Brandenburg federal state monitoring station (LfU): 10 to 12 August 2022)
- 7 daily composite samples or grab samples of water from the Oder from Frankfurt (Oder) (Brandenburg federal state monitoring station (LfU): 5 to 8, 10, 12 and 24 August 2022)
- 8 suspended particulate matter samples from the Oder in Hohenwutzen (BfG monitoring station: monthly composite samples for March, April, May, June and July 2022, and composite samples for 1 to 15 August 2022, 16 to 23 August 2022 and 24 to 31 August 2022)
- 2 samples of water taken from the Oder-Spree Canal close to Eisenhüttenstadt on 6 September 2022 (grab samples, unfiltered and filtered on site): km 125.68 (Oder-Spree Canal, in German: Spree-Oder-Kanal: SOK) and km 127.14 (Zwillingsschachtschleuse lock: ZSS)

The water sample IDs used in this report are made up of the location code (HW = Hohenwutzen, FFO = Frankfurt (Oder), EHS = Eisenhüttenstadt), the sample type code (TM = daily composite sample, S = grab sample) and the date (day/month: e.g. 12/08 = 12 August) in 2022, with each of these three elements separated by an underscore. Where necessary, the name of the monitoring station (e.g. BfG or LfU in Hohenwutzen) or of the sampling site (EHS: SOK or ZSS) is also specified. For example, “HW_TM_15/08” is the ID for the daily composite sample taken in Hohenwutzen on 15 August 2022, while “EHS_ZSS_S_06/09” describes a grab sample taken in Eisenhüttenstadt (at the Zwillingsschachtschleuse sampling site) on 6 September 2022. In Annex 3 (in German only), there is a table (A3.4.2.1) for matching these sample IDs with other IDs used (e.g. BfG in-house sample numbers).

When interpreting some of the measurement data, it is important to know whether the water samples were stored and transported under cooled conditions, since degradation processes in uncooled samples can cause changes in various parameters. Conversely, algal cells in uncooled samples may survive better than in cooled samples in some circumstances. As a general rule, the continuous water sampling at the BfG monitoring station in Hohenwutzen is carried out by an automatic sampler with a cooling function. However, the cooling function was deactivated in July 2022. This was due to technical problems, which would have led to the formation of ice and thus caused the sampler to fail. Consequently, the water samples from up to and including 15 August 2022 that were analysed were not cooled either while being stored at the local site or during transport. It was only when the samples arrived at the BfG premises on 11 August 2022 (July 2022 samples) and on 17 August 2022 (samples for 1 to 15 August 2022 and grab sample taken on 16 August) that these samples were put into cold storage at 4 °C. On 16 August 2022, the sampler cooling function in the monitoring station in Hohenwutzen was reactivated. The water samples that were picked up in Hohenwutzen on 24 August 2022 (samples for 16 to 23 August 2022 and grab sample taken on 24 August) were therefore stored at the local site under cooled conditions at 4 °C. These samples were also transported under cooled conditions to Koblenz, in electric cool boxes at 4 °C. Directly on arrival at the BfG premises on 25 August 2022, they were put into the cold-

storage rooms there. As regards the water samples that the State Laboratory Berlin-Brandenburg (LBB) sent to BfG, the samples from the Frankfurt (Oder) federal state monitoring station for the period 5 to 8 August 2022 were uncooled, whereas the samples from Frankfurt (Oder) taken on 10, 12 and 24 August 2022 and those from the Hohenwutzen federal state monitoring station for 10 to 12 August 2022 were cooled. When these samples arrived at the BfG premises in Koblenz on 17 August 2022, they were also put into cold storage at 4 °C.

5 Results

5.1 Hydrology (discharge situation during the low-flow conditions in 2022)

The daily discharge hydrographs from the Eisenhüttenstadt and Hohensaaten-Finow gauging stations show the discharge conditions in 2022 on the section of the Oder that runs along the border between Germany and Poland (Figure 5.1.1). As a result of the dry weather conditions in winter and spring 2022 – when no flood occurred in the Oder and the mean annual discharge (MAD) was only exceeded for four to five weeks and relatively early in the year (February/March) – the flow levels fell below the mean annual minimum discharge (MAMD) on as early as 23/24 May. Due to the low baseflow level (low level of groundwater recharge in the spring), the discharge continued to drop rapidly towards the summer and reached the extreme low-flow range (Eisenhüttenstadt < 71 m^3/s, Hohensaaten-Finow < 140 m^3/s). Following a precipitation event in the southern part of the catchment area on 5 August, discharge levels increased slightly until 6/9 August (to 103 m^3/s at the Eisenhüttenstadt gauging station and 168 m^3/s at the Hohensaaten-Finow gauging station). However, they then dropped back into the extreme low-flow range, at around 72 and 144 m^3/s respectively. It was only after abundant precipitation over a large area from 20 August that the discharge rose above MAMD again, and it then remained in the moderate low-flow range at both gauging stations until around the end of the year.

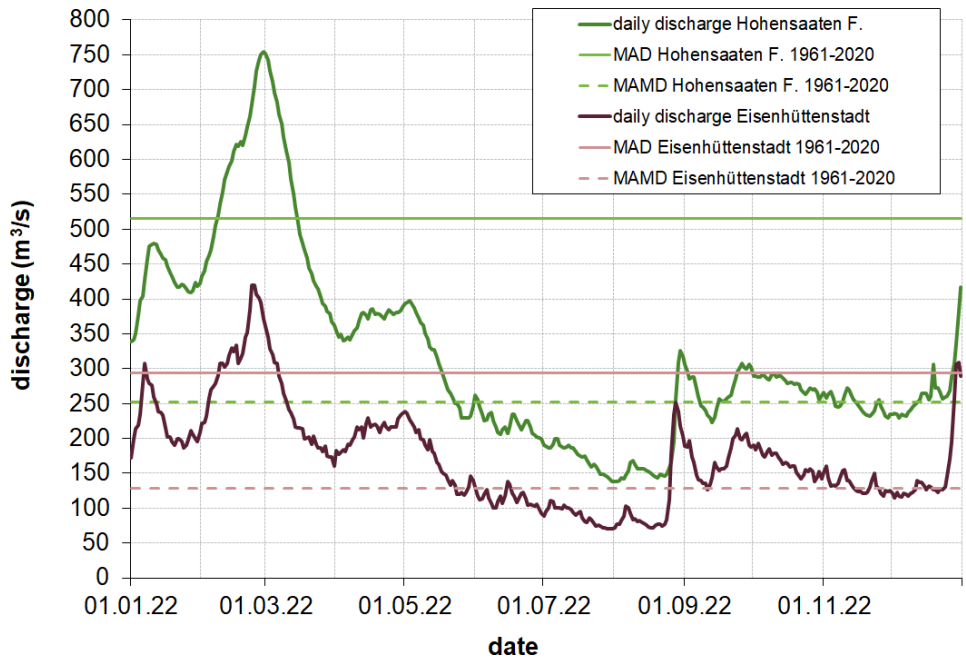

Figure 5.1.1 *Daily discharge hydrographs from the Eisenhüttenstadt and Hohensaaten-Finow gauging stations on the Oder in 2022, with the hydrological primary values MAD (mean annual discharge, in German: MQ) and MAMD (mean annual minimum discharge, in German: MNQ) as a reference.*

To analyse this low-flow event in terms of its critical impact on fish fauna, various aspects need to be taken into account. These relate to the life cycle of fish species found in the river and other boundary conditions in respect of their habitats (including water

temperature, the oxygen content of the water, the occurrence of algae or pathogens and, where applicable, the drying up of the water in parts). SOLLINGER et al. (2023) specify characteristic features of low-flow events. In addition to amplitude (including the lowest discharge or water level), the timing (during the course of the year), the frequency of the events and, above all, the duration of the low-flow events can have consequences for the fish fauna of watercourses.

In this section of the report, the 2022 low-flow event is classified statistically on the basis of these aspects and compared to the long-term discharge process of the Oder. This classification is carried out on the basis of the daily discharge data series from the gauging stations specified above. These are of high informative value for the entire section of the Oder that runs along the border between Poland and Germany. With the exception of discharge year 1945 (November 1944 to October 1945), the discharge data series from these gauging stations are available without interruption starting from November 1921. As in the case of BFG (2021), the analysis and classification is carried out with particular regard to the reference period from 1961 onwards (the two last climatic reference periods: 1961 to 2020). However, (extreme) events and parameters from the years preceding 1961 are also included in the assessment as a reference.

Figure 5.1.2 shows a comparison of the discharge hydrograph of water-balance year 2022 (1 April 2022 to 31 March 2023) with the long-term reference of the date-based minimum values, maximum values and quantiles (deciles) for the years 1961 to 2020. Even in the spring, the 2022 discharge hydrographs were at a relatively low level. In contrast to other low-flow years in the recent past (2015, 2019 and, in the case of the Hohensaaten-Finow gauging station, 2018, too), they hardly exceeded the date-based 10% quantile up to the start of July and they never exceeded – or even came close to exceeding – the MAD. Compared to low-flow years 2015, 2018 and 2019 and the date-based quantiles in the low-flow range, there were atypically rapid decreases in discharge from the start of July 2022 until the start of August. At the Hohensaaten-Finow gauging station, discharge dropped from the date-based 10% quantile to almost the date-based minimum values from years 1961-2020, while at the Eisenhüttenstadt gauging station, discharge actually fell below this. These rapid decreases in discharge in July 2022 can be considered extreme. Despite slight interim increases, discharge at both gauging stations remained below the date-based 10% quantiles until 24/25 August, before subsequently increasing into the date-based mid-range.

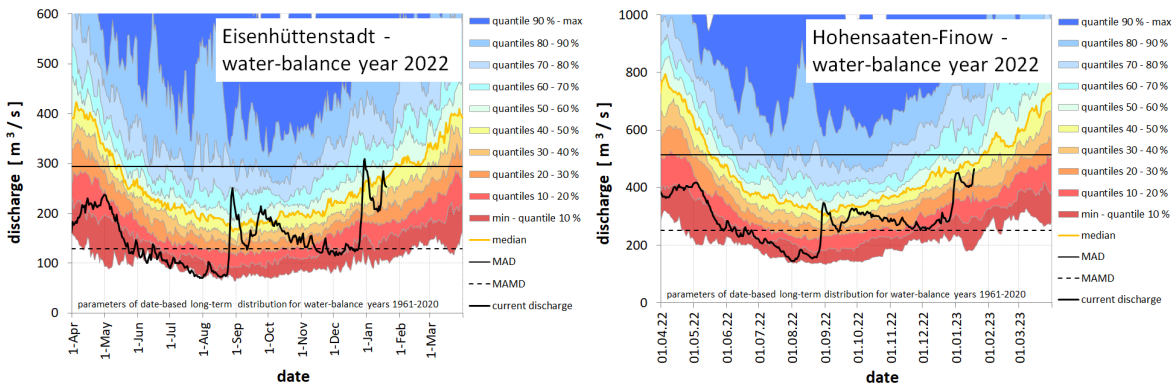

Figure 5.1.2 *Daily discharge hydrographs from the Eisenhüttenstadt (left) and Hohensaaten-Finow (right) gauging stations in comparison with date-based parameters of discharge distribution during the period 1961 to 2020 (minimum value, maximum value, deciles). MAD is the mean annual discharge (in German: MQ), MAMD is the mean annual minimum discharge (in German: MNQ).*

In addition to the development described, the 2022 discharge hydrographs reveal minimum values at the start of August that are comparable to – or even lower than – the minimum values of the previous extreme years. Although the overall duration of the period in which the discharge is lower than MAMD is shorter than in the previous extreme years, discharge fell below MAMD in late May, i.e. relatively early in the year. To further evaluate these event characteristics in a long-term context, annual series of the AM7D (annual minimum of 7-day mean discharge in the water-balance year) and sumD (sum duration of the period in which the discharge was below MAMD in the water-balance year) parameters were created.

Figure 5.1.3 shows the AM7D 1921 to 2022 series from the Eisenhüttenstadt and Hohensaaten-Finow gauging stations with 30-year moving averages (TUSZYNSKI 2014) that highlight the mean long-term development. At 72 and 140 m^3/s respectively, the AM7D 2022 values are some of the lowest AM7D values since 1921, although there have been several years with AM7D values that are comparable or – especially in the case of the Hohensaaten-Finow gauging station – even lower. Many of these years have been in the recent past (water-balance years 2015, with an AM7D of 69 and 135 m^3/s respectively; 2018, with 76 and 154 m^3/s respectively; and 2019, with 74 and 139 m^3/s respectively). As the moving averages also show, it is therefore recent years in particular that have been characterised by extreme AM7D values. However, an analysis of the period 1961 to 2022, taking account of autocorrelation, did not reveal any significant deterioration trends so far (p value > 0.05). The trends were calculated using a Theil-Sen estimator and evaluated for significance via a Mann-Kendall test in an iterative process in connection with prewhitening (FREI 2013; cf. BFG 2021). Similarly, for AM30D (annual minimum of 30-day mean discharge in the water-balance year) and for series of graduated length (1951-2022, 1961-2022, 1971-2022, ..., 2001-2022) for AM7D and AM30D, no significant trends (p>0.05) were found for either of the gauging stations specified above. Moreover, they are also characterised by a high level of variability in (and thus uncertainty over) their slope coefficients. Low moving averages for the AM7D series can also be observed in the first half of the 20th century, although there was a weaker dam effect at that time (cf. section 2.1). Other years with extreme AM7D values are 2003, 1992, 1922 and 1921. In 1921 especially, the AM7D value at the Hohensaaten-Finow gauging station – 112 m^3/s – was substantially lower than in 2022. It is against this background that, in this study, an assumption is made that past years have been strongly characterised by low-flow conditions within the context of decadal climate variability, but not (so far) by long-term non-stationary patterns in the low-flow conditions in the section of the Oder that runs along the border between Poland and Germany. In this context, recent years (from 2015) have overall been characterised by relatively low mean discharges in the Oder, too (ABBAS et al. 2022). Further development of low-flow conditions on the (entire) Oder should be carefully observed, analysed and, if necessary, reassessed.

In order to classify the likelihood of occurrence, extreme value statistics were drawn up for the AM7D series on the basis of BFG (2021). Accordingly, a statistical recurrence interval of a little more than 20 years is to be assigned to the AM7D 2022 in Hohensaaten-Finow, making this a rare but not an exceptional extreme event in this regard. In terms of the timing of the AM7D 2022 in the midsummer (end of July / start of August), there is also equivalence in the given reference years of 1922 (mid-July) and 2019 (also the start of August), whereas the AM7D for the other years mentioned did not occur until the end of August (1992) or the month of September (1921, 2015 and 2018).

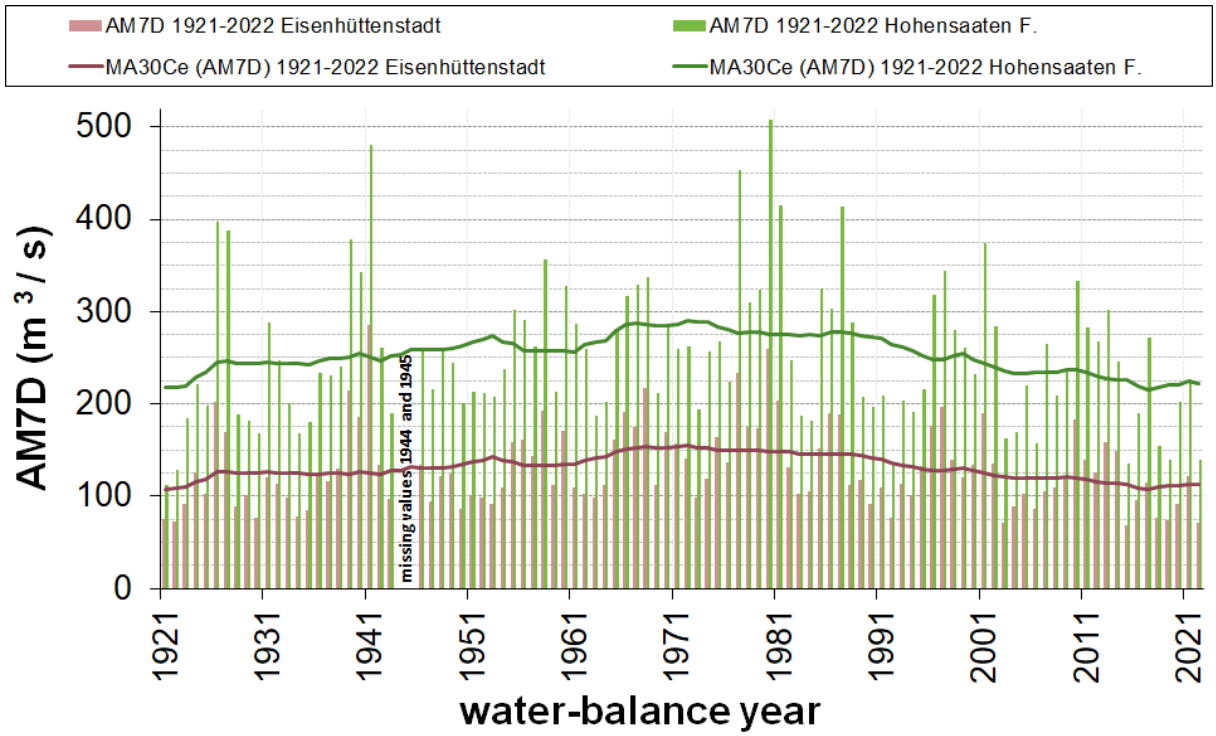

Figure 5.1.3 *AM7D series 1921-2022 for the Eisenhüttenstadt and Hohensaaten-Finow gauging stations, with 30-year moving averages MA30Ce (based on the middle of the 30-a time window in each case). AM7D is the annual minimum of the 7-day mean discharge (in German: NM7Q).*

Using the sumD(<MAMD) parameter, the durations of the periods with discharge below MAMD are initially assessed for the *entire* water-balance year; however, the durations up to the fish die-off phase that is of particular interest here, which occurred in the Oder in August, are not explicitly analysed. A supplementary evaluation on the basis of *maximum uninterrupted* durations of periods with discharge below MAMD for each water-balance year was not undertaken, however, due to high levels of uncertainty as regards the efficacy and the methodical handling of short-term interruptions to the phases with discharge below MAMD (pooling problem). Instead, series of the more robust total durations of periods with discharge below MAMD were formed for the water-balance year up to the selected dates (31 July and 25/27 August, where the latter dates are directly before the end of the period with discharge below MAMD in August 2022). Figure 5.1.4 shows all three series – sumD(<MAMD), $sumD_{31.7.}$(<MAMD) and $sumD_{25.8.\text{ or }27.8.}$(<MAMD) – for the Eisenhüttenstadt and Hohensaaten-Finow gauging stations in a stacked bar chart. In the case of the sumD(<MAMD) parameter, water-balance year 2022, with 118 (Eisenhüttenstadt) and 132 (Hohensaaten-Finow) days with discharge below MAMD, was only ranked in 13th and 11th place respectively out of the 100 years in total since 1921. Compared to the extreme value statistics drawn up for this parameter and the Hohensaaten-Finow gauging station (reference period 1961 to 2018) in BFG (2021), a statistical recurrence interval of a little over 10 years is to be assigned to the specified value.

In a long-term comparison, the $sumD_{31.7.}$(<MAMD) parameter, at 63 and 68 days respectively, and the $sumD_{25./27.8.}$(<MAMD) parameter, at 88 and 95 days respectively, were considerably more extreme. Extreme value statistics have so far not been available for these specific parameters. However, their extreme nature in 2022 is evident solely on

the basis of their rankings. From 1921 onwards, the numbers of days with discharge below MAMD in 2022 were exceeded only in water-balance year 1934, also following a dry spring. The figures are 75 and 84 days respectively and 100 and 111 days respectively, but the minimum discharge values in 1934 remained substantially above those of 2022 ($AM7D_{1934}$ = 78 m^3/s and 168 m^3/s respectively) and occurred relatively early (end of June). At the Hohensaaten-Finow gauging station, the figures for the years that come next in the rankings are considerably lower – up to 55 and 81 days. At the Eisenhüttenstadt gauging station, however, the year 2018, with 62 and 87 days, was also comparable to 2022. At both gauging stations, it is striking that there is a cluster of these years in the recent past (2015, 2018, 2019 and 2020). Moreover, these years, with the exception of 2020, also saw low minimum discharge values in high summer.

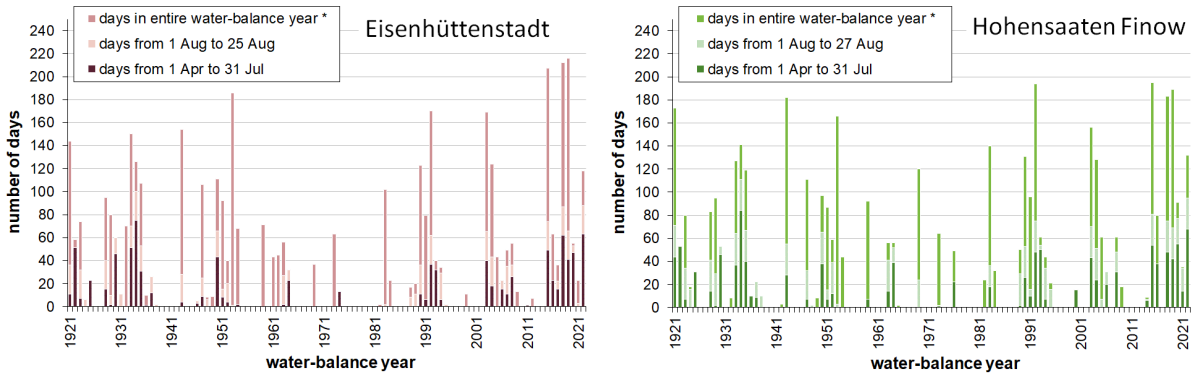

Figure 5.1.4 *Series of the numbers of days with discharge below MAMD per water-balance year from 1921 to 2022 at the Eisenhüttenstadt (left) and Hohensaaten-Finow (right) gauging stations. The numbers of these days already recorded by 31 July and by 25 or 27 August are also shown. * In water-balance year 2022 according to status as at 31 January 2023.*

In summary, water-balance year 2022 showed several extreme characteristics in the Oder discharge data series in long-term comparison. These characteristics were the result of dry conditions that were already pronounced in spring and continued especially in high summer. In addition to AM7D, with a statistical recurrence interval of a little more than 20 years (Hohensaaten-Finow gauging station), it is important to highlight the unusually rapid decrease in discharge down into this extreme range in July and the unusually long duration of the low-flow conditions already seen in the early summer. The latter – albeit less extreme – also occurred in four of the seven previous years since 2015.

5.2 Presentation and analysis of the online data from the federal state monitoring stations

Figures 5.2.1 and 5.2.2 show the electrical conductivity, oxygen, pH, temperature, total chlorophyll, turbidity and discharge parameters for the Frankfurt (Oder) and Hohenwutzen monitoring stations for the period from 1 January 2022 to 30 November 2022. The period between the two red dotted lines (28 July to 19 August 2022) immediately stands out – and it was during this period that the peaks occurred of both the algal bloom and the fish die-off. This is shown again for Frankfurt (Oder) in higher resolution in Figure 5.2.3. Data supplied by LfU Brandenburg shows that, in the case of the Frankfurt (Oder) site, the conductivity values had already previously been around and in excess of 2,000 µS/cm. As already stated in section 2.2, high electrical conductivity values in excess of 1000 µS/cm are not unusual in the Oder. In addition to conductivity, the profiles for total chlorophyll content and pH are also anomalous, with the latter jumping by one pH unit. Alongside these parameters, it should also be taken into account that very low discharge volumes were observed at this point in time, as were very high temperatures during the course of the year. For both these parameters, similar circumstances were observed at the Hohenwutzen monitoring station, too. However, all other parameters can be assessed as being considerably less anomalous than they were in Frankfurt (Oder).

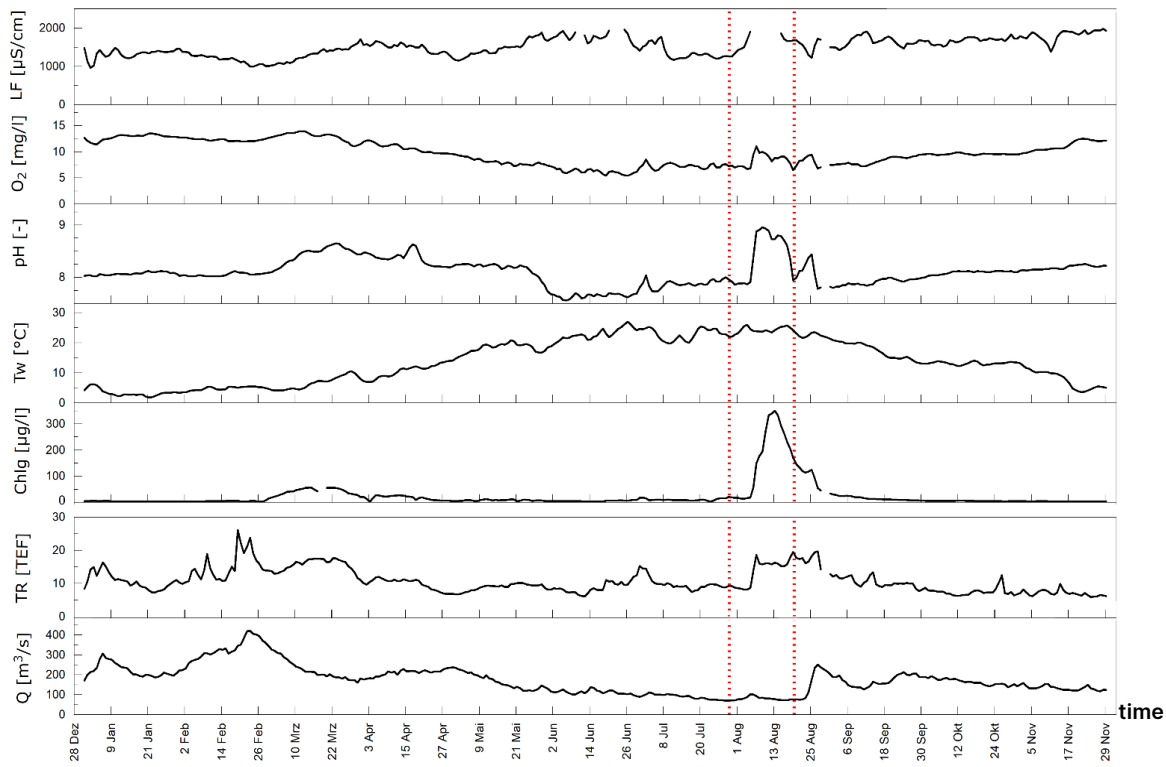

Figure 5.2.1 *Online measurement data from the federal state monitoring station in Frankfurt (Oder) (km 584) for the period between 1 January 2022 and 30 November 2022 (from top to bottom: electrical conductivity (LF), oxygen content, pH, water temperature (Tw), total chlorophyll concentration (Chlg), turbidity (TR) and discharge (Q) at the Eisenhüttenstadt reference gauging station, Oder km 554). The red dotted lines delineate the period from 28 July to 19 August 2022, which is shown again in higher resolution in Figure 5.2.3. It was during this period that the peak of both the algal bloom and the fish die-off occurred. (Data: LfU Brandenburg)*

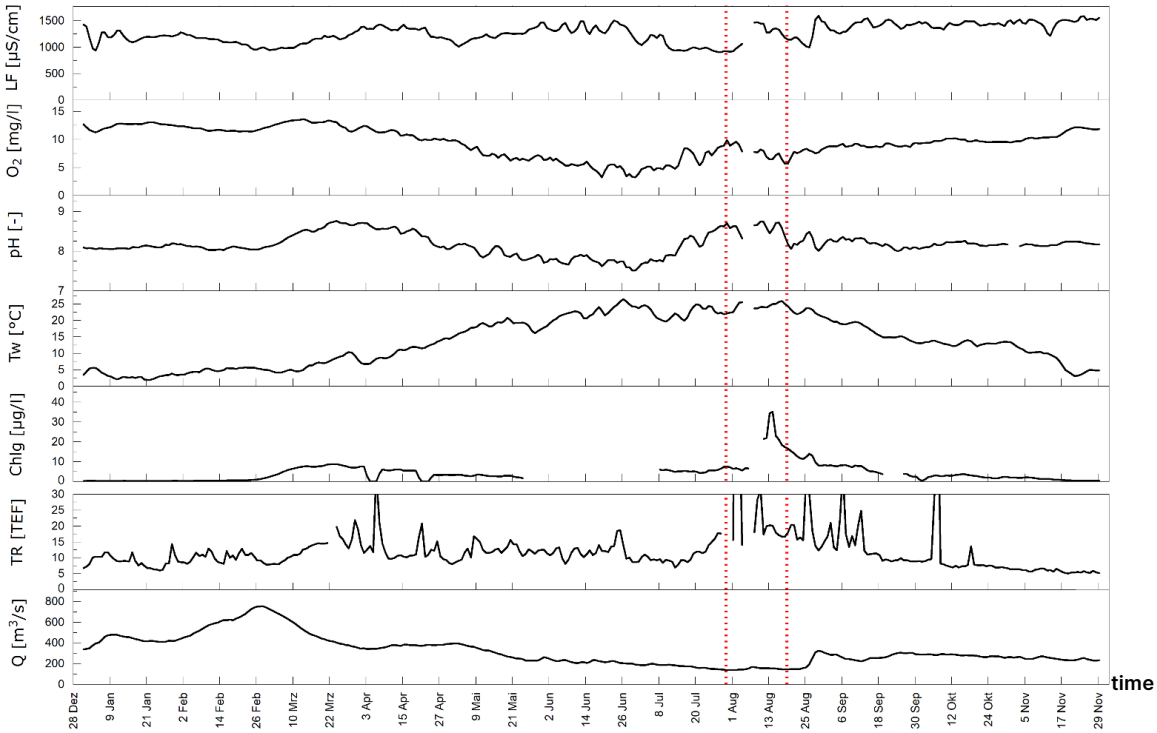

Figure 5.2.2 *Online measurement data from the federal state monitoring station in Hohenwutzen (Oder km 661) for the period from 1 January 2022 to 30 November 2022 (from top to bottom: electrical conductivity (LF), oxygen content, pH, water temperature (Tw), total chlorophyll concentration (Chlg) (comparative measurements indicate an undervaluation of the measurement data), turbidity (TR) and discharge (Q) at Hohensaaten-Finow gauging station (Oder km 665), which is the closest gauging station to the Hohenwutzen monitoring station). The red dotted lines delineate the period from 28 July to 19 August 2022, during which the peak of both the algal bloom and the fish die-off occurred. (Data: LfU Brandenburg)*

In summary, it can be noted that the parameters shown here are certainly striking when compared to other rivers in Central Europe. However, the individual values are in themselves not particularly exceptional for the Oder, especially when compared with the data in section 2.2. It is only by combining the various parameters and the prevalent environmental conditions in August 2022 that the extreme ecological event can be retrospectively reconstructed on the basis of the online measurement data. This makes it more difficult to set alarm thresholds, because elevated individual values alone do not need to be anomalous; it is much more the combination of different parameters that needs to be taken into account (also see section 6.4).

In Table 5.2.1, the mean electrical conductivity values for various German rivers for the years 2019 to 2021 are shown for comparison purposes. This table shows that the major rivers Rhine, Danube and Elbe have lower mean electrical conductivity values than the Oder. However, a number of tributaries also show elevated salinity, and these therefore increase electrical conductivity after their confluence (e.g. after the Moselle confluences with the Rhine). The Saale and, in particular, the Werra show substantially elevated mean electrical conductivity values, which are even higher than the mean values for the Oder and cause increased conductivity values in the Elbe and Weser, respectively, after their confluence points. The substantially elevated salinity of the Werra can be attributed to inputs associated with the mining and processing of potash salts for the production of fertilisers (FGG WESER 2020).

Table 5.2.1 *Mean electrical conductivity (EC) values at various monitoring stations on German rivers for the period 2019 to 2021.*

River	Monitoring station	River km	EC (µS/cm)	Data source
Oder	Frankfurt (Oder)	584	**1,258**	1
Oder	Hohenwutzen	661	**1,101**	1
Rhine	Koblenz	590.3	**447**	2
Moselle	Koblenz	2.0	**946**	2
Rhine	Bimmen	865	**642**	2
Danube	Ulm-Wiblingen	2,589	**616**	3
Isar	Plattling	9.1	**474**	4
Inn	Ingling	3.1	**299**	4
Danube	Jochenstein	2,204	**367**	4
Elbe	Schmilka	3.9	**427**	5
Mulde	Dessau	7.6	**591**	5
Saale	Rosenburg	4.5	**2,828**	5
Havel	Potsdam	Humboldt Bridge	**941**	5
Elbe	Schnackenburg	474.5	**1,039**	5
Elbe	Bunthaus	609.8	**962**	5
Werra	Witzenhausen	13.0	**4,245**	6
Fulda	Wahnhausen	15.5	**445**	6
Weser	Porta	199.3	**1,636**	6
Weser	Hemelingen	361.1	**1,309**	6

[1] LfU Brandenburg, [2] ICPR tables of figures, [3] data and map service provided by the Baden-Württemberg State Institute for the Environment (LUBW), [4] Gewässerkundlicher Dienst Bayern (hydrology service for Bavaria), [5] River Basin Community Elbe (FGG-Elbe) data portal, [6] River Basin Community Weser (FGG-Weser) data portal

However, the mean electrical conductivity values presented in Table 5.2.1 for a three-year period (2019 to 2021) do not provide any information about temporal variability or possible extreme values. As can be seen in Figure 2.2.2, the salt load of the Oder exhibits strong, short-term fluctuations over time. It is precisely these rapidly changing conditions that can be a considerable stress factor for fish and other organisms in the river. Even though electrical conductivity values in excess of 2,000 µS/cm occurred earlier in the year, the sharp rise during the period from 3 to 7 August 2022 also occurred very rapidly.

The high temporal resolution of the online data from the federal state monitoring stations in Frankfurt (Oder) and Hohenwutzen was very significant when investigating the fish die-off of August 2022. The two graphs shown above were produced on the basis of daily mean values, but the striking day and night fluctuations in the data with higher resolution (measurement interval: 10 minutes) for various parameters were a strong indication of a dynamic shaped by an algal bloom with regard to the physicochemical parameters in the water of the Oder during the period of the fish die-off (Figure 5.2.3). These include, for example, oxygen and pH (Figure 5.2.3 B).

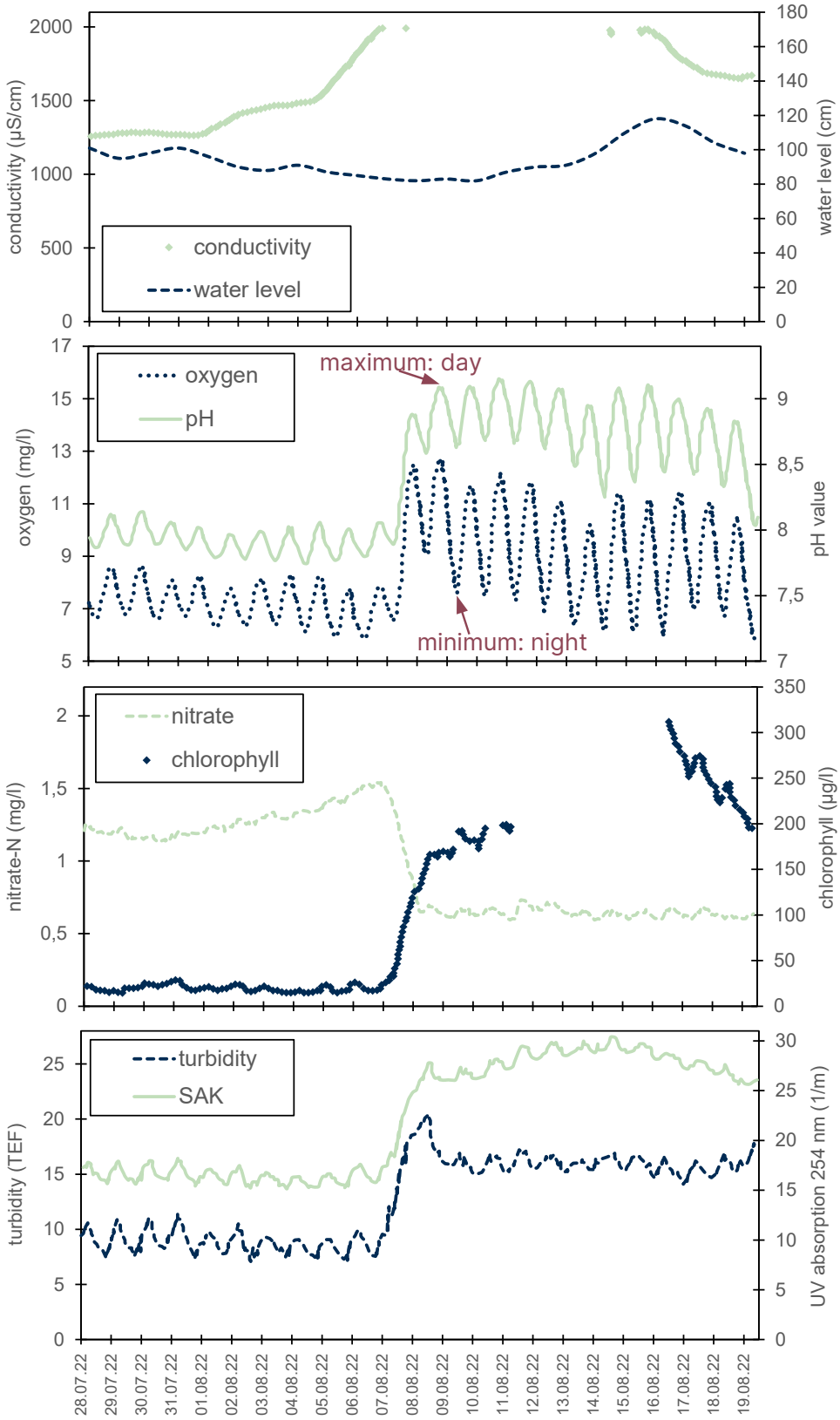

Figure 5.2.3 *Measurement values for selected online parameters from the federal state monitoring station in Frankfurt (Oder) during the period 28 July to 19 August 2022 (LfU Brandenburg). In terms of conductivity, there are no values >2,000 µS/cm (exceedance of measurement range). There is a gap in the chlorophyll measurement data between 11 and 16 August 2022. SAK is the spectral absorption coefficient.*

5.3 Element composition

To analyse the elements present, BfG used triple quadrupole inductively coupled plasma mass spectrometry (ICP-QQQ-MS) to conduct measurements on daily composite samples of Oder river water from Hohenwutzen (BfG monitoring station, 1 July to 6 September 2022) and Frankfurt (Oder) (federal state monitoring station: 5 to 8, 10 and 12 August 2022) and on digested suspended particulate matter samples from Hohenwutzen (BfG monitoring station, monthly composite samples from March to July 2022 and composite samples for 1 to 15 August 2022, 16 to 23 August 2022 and 24 to 31 August 2022). The water samples were analysed both filtered (<0.45 µm) and unfiltered as whole water samples following aqua regia digestion (see Annex 1 for details about the method).

The element measurements were used to verify and further investigate the temporal profile of the elevated salt load in the Oder river water during the period of the fish die-off. This temporal profile was already known from the electrical conductivity online measurement values recorded at the Frankfurt (Oder) and Hohenwutzen LfU monitoring stations. The predominant main elements in the water of the Oder are chlorine (Cl) and sodium (Na), followed by calcium (Ca) and sulphur (S). While the concentrations of Cl and Na approximately doubled in the first half of August, in parallel with the electrical conductivity profile, the concentration of Ca dropped by around 25% during this period, and the concentration of S changed only slightly (Figure 5.3.1).

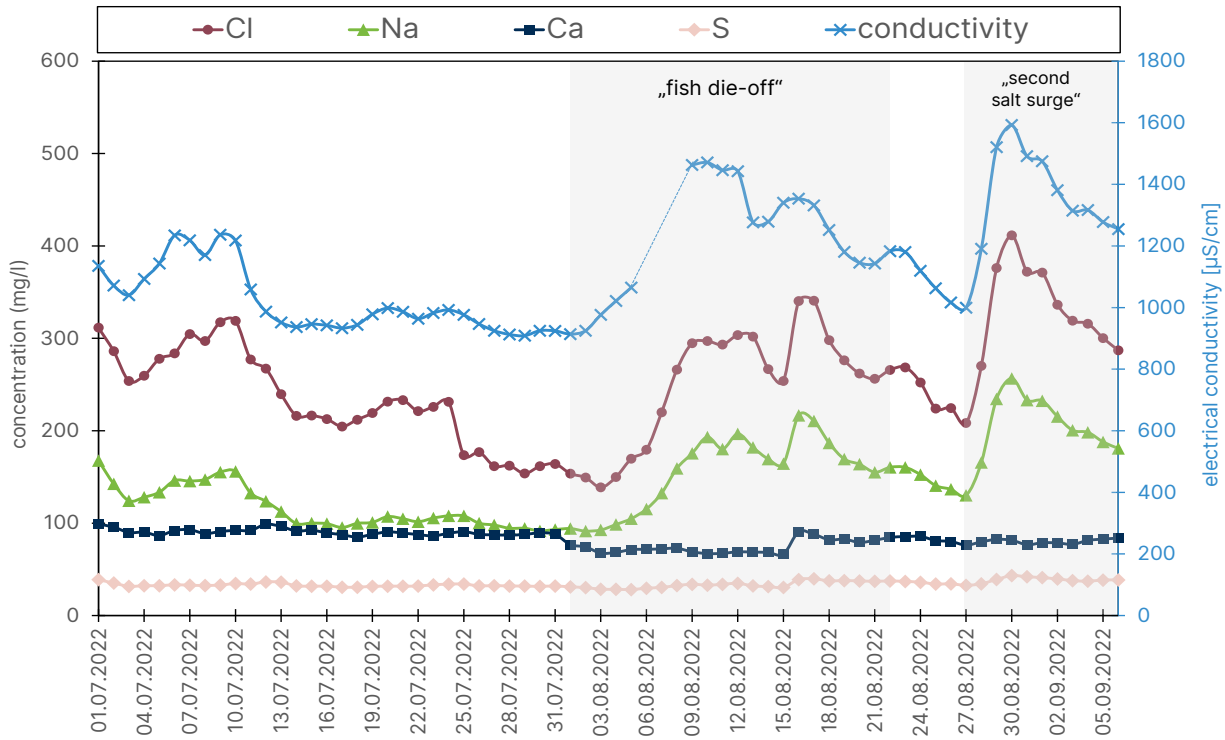

Figure 5.3.1 *Changes in the concentrations of chlorine (Cl), sodium (Na), calcium (Ca) and sulphur (S) (left y-axis) and in electrical conductivity (right y-axis) in the water of the Oder (<0.45 µm) in Hohenwutzen during the period from 1 July to 6 September 2022. The dotted line during the period from 6 to 8 August 2022 shows an assumed linear interpolation of the online measurements that are missing due to a power failure. The areas shaded in grey represent the approximate periods of the fish die-off (1 to 22 August 2022) and the second salt surge (27 August to 6 September 2022).*

Since the chlorine values measured by means of ICP-QQQ-MS closely match the chloride measurements that were conducted in parallel using ion chromatography (see section 5.4.3), it can be assumed – as expected – that the element chlorine is present in the form of the chloride anion. The maximum dissolved concentrations in the tested samples were found in Frankfurt (Oder) on 12 August 2022 (304 mg/l Na and 558 mg/l Cl). Downstream in Hohenwutzen, the maximum concentrations were somewhat lower (Figure 5.3.1), due to the dilution of the salt load by the inflow of the Warta tributary between Frankfurt (Oder) and Hohenwutzen. The Na/Cl ratio in the water samples tested was close to the stoichiometric molar ratio of the atomic mass of Na (23 g/mol) to the atomic mass of Cl (35.5 g/mol). By way of illustration, dissolving 1 g NaCl in one litre of water produces concentrations of 393 mg/l Na and 607 mg/l Cl, and a solution of this kind has an electrical conductivity (25 °C) of around 2,100 µS/cm. The electrical conductivity of an NaCl solution with 1 g/l chloride (= 1.65 g/l NaCl) is approximately 3,250 µS/cm. The target applicable in Poland with regard to the input of saline effluents into rivers – i.e. that the sum total of chloride and sulphate must not exceed 1 g/l once the effluent has been fully mixed into the river (see section 2.3) – lies approximately in this range. The rise in salt load from 5/6 August 2022 is clearly discernible from the daily composite samples from Hohenwutzen, with the sharpest increase occurring during the period from 7 to 9 August 2022. During the last week of July 2022, i.e. immediately prior to the fish die-off, the concentrations of Na and Cl in Hohenwutzen were approximately 100 and 150 mg/l respectively. These values then doubled to around 200 and 300 mg/l respectively by 12 August 2022. Following an occasional drop in electrical conductivity and concentrations of Na and Cl up to 27 August 2022, there was then another sharp parallel rise in these parameters, which reached their peak on 30 August 2022. This second increase is hereinafter referred to as the “second salt surge”, while the rise during the fish die-off period at the start of August 2022 is referred to as the “first salt surge”.

5.3.1 Salt load volume estimates

From the element analyses, it is clear that sodium chloride (NaCl, table salt) can be held responsible for the increase in salt load in the Oder during the period investigated. Compared to NaCl, other elements associated with the input of saline effluents into rivers, such as sulphur (S, in the form of sulphate) and potassium (K), did not play any appreciable role in the Oder during this period. To estimate the additional volumes of NaCl that were input into the Oder during the period of the fish die-off, the mean value for the period of the last week in July 2022 was used as the reference period for the “normal” salt load in the Oder. Given the major fluctuations in the electrical conductivity of the water of the Oder and the long-term rise in this parameter over recent decades (see section 2.2, Figure 2.2.2), it is not possible to explicitly define a “normal” background value for the salt load in the Oder. However, for the purposes of a simplified illustration of the volumes of salt that were being transported in the Oder during the period around the fish die-off, this assumption should nevertheless suffice. To estimate the absolute volume of salt that was transported, it is not only the concentrations of the elements Na and Cl that need to be taken into account – the watercourse discharge needs to be considered, too. Normally, when discharge increases (e.g. due to heavy rain), a drop in the electrical conductivity of the river water would be expected due to the effects of dilution. Such a correlation between discharge and electrical conductivity was observed in spring 2022 in Hohenwutzen, for example (see Annex 2, Figure A2.5.3.3 – in German only). A sharp rise in the discharge of the Oder in February 2022 led to a corresponding decrease in

electrical conductivity due to the dilution of the dissolved ions in the much bigger volume of water. In March 2022, the discharge dropped, and the electrical conductivity increased again accordingly. However, this inverse trend between discharge and electrical conductivity was not observed in August 2022. In fact, in this case, the increase in discharge coincided far more with an increase in conductivity and dissolved ions, as can be seen from the parallel profiles of discharge and dissolved Na and Cl concentrations in Figure 5.3.2A. During this period, the Oder was therefore not only transporting more water – the higher volume of water actually also exhibited a higher salt concentration. This can be deemed a clear indication of the anthropogenic input of substantial volumes of highly saline effluents into the Oder. Even if the increase in discharge in the Oder during the period being investigated can be explained by natural rain events in the Oder catchment area (see section 5.1), the parallel increase in concentrations of dissolved Na and Cl clearly points to the input of highly saline effluents from anthropogenic sources (see, for example, section 2.3).

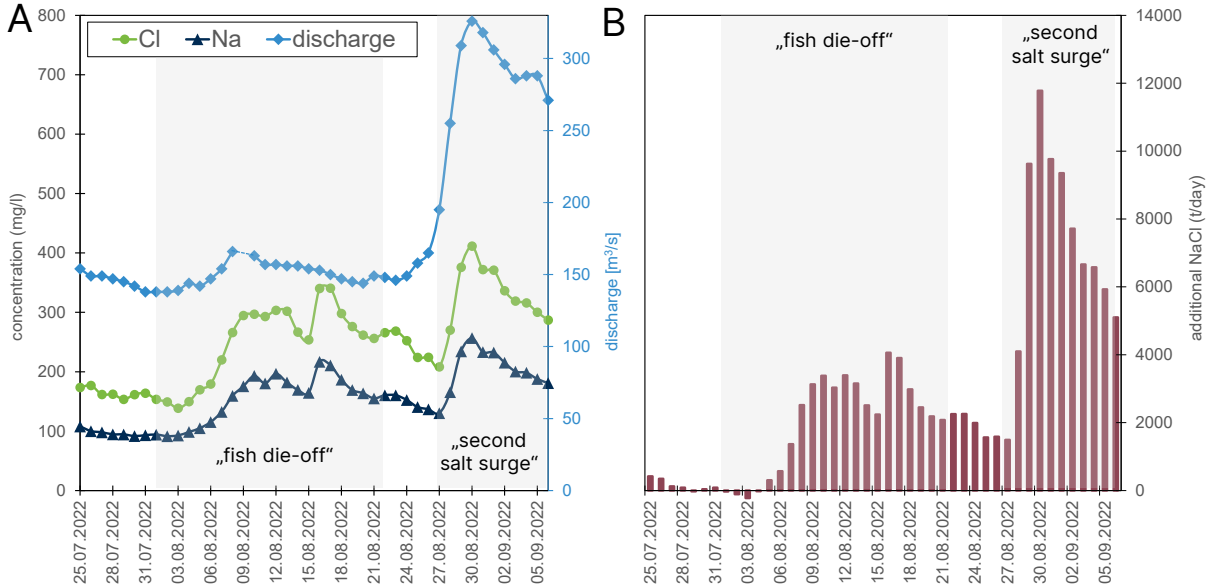

Figure 5.3.2 *(A) Temporal profile of Na and Cl concentrations in Hohenwutzen (left y-axis) and discharge at the Hohensaaten-Finow gauging station (right y-axis) and (B) estimate of the additional volume of NaCl transported each day during the period of the two salt surges in Hohenwutzen in summer 2022 (25 July to 6 September 2022, assumption: “normal” salt load during the last week of July 2022).*

Based on the combined concentration and discharge data and the assumption of a “normal” salt concentration during the last week of July, it can be estimated that an additional volume of 25,600 metric tons of NaCl was transported at Hohenwutzen during the period from 5 to 15 August 2022 (“first salt surge”). For the period from 28 August to 6 September (“second salt surge”), the extrapolated volume of additional NaCl is as much as 76,600 metric tons, due to the higher discharge. For the entire period from 5 August to 6 September 2022, the estimate suggests that the additional NaCl volume was 131,000 metric tons, which is around 4,000 metric tons per day (Figure 5.3.2B). As a guide, 4,000 metric tons of NaCl in the form of solid table salt would fill around 200 railway freight wagons. However, it is likely that the salt input into the Oder was in the form of saline solutions. Assuming an NaCl concentration of 40 g/l, which can serve as an estimated typical value for saline effluents from mining operations (see section 2.3), 4,000 metric tons of NaCl are equivalent to a solution volume of 100,000 m^3.

This volume equates to a square tank measuring 100 m x 100 m, and filled to a depth of 10 m, being emptied into the Oder each day. An average rate of 1.16 m^3/s would be needed to pump this volume of saline solution into the Oder continuously over 24 hours. These rough estimates are not precise calculations of the salt load; instead, they are merely intended to illustrate the huge scale of the salt inputs into the Oder. However, given the information that is known about the input volumes of saline mining effluents into the Oder (including from coal and copper mines, see section 2.3), these salt volume extrapolations for August 2022 are nevertheless within a plausible range in respect of the anthropogenic salt pollution of the Oder ascertained to date. As can be seen from the conductivity measurement values up to the end of November 2022, which are shown in Figures 5.2.1 and 5.2.2 (current measurement values: https://undine.bafg.de/oder/guetemessstellen/oder_mst_auswahl.html), the inputs of salt continued after the fish die-off.

5.3.2 Temporal trends of main elements and trace elements

Of the 69 chemical elements (including Re) measured using the multi-element method according to BELKOUTEB et al. (2023) by means of triple quadrupole inductively coupled plasma mass spectrometry (ICP-QQQ-MS), a total of 65 of them were detected in measurable concentrations in the samples of water and suspended particulate matter investigated. Only Nb, Ru, Te and Ta were below the limit of quantification in all samples. In the filtered water samples, the median values for the determined concentrations of elements extended over more than eight orders of magnitude, and only six elements (Cl, Na, Ca, S, Mg and K) had results in the >1 mg/l range. The concentrations of Si and C are probably also in this range; however, these were not included in the quantitative evaluation for the majority of the samples due to an elevated background signal and/or possible losses during sample preparation. The elements H, O and N are also not detected by this method. These main elements were followed by Br, Sr, P, B, Ba, Li and Rb in the 10-1,000 µg/l range and Zn, Mo, Cu, As, Fe, Ni, Re and Al in the 1-10 µg/l range. These were then followed by the median values of 12 elements in the 100-1,000 ng/l range (Cs, V, U, W, Tl, Sb, Se, Mn, Pd, Co, Sc and Cr), 9 elements in the 1-100 ng/l range (Gd, Cd, Ge, Y, Ga, Ag, Yb, Eu and Er) and 6 further elements in the < 1 ng/l range (La, Dy, Sm, Lu, Ho and Tm). In comparison with analyses of water samples from other river basins in Germany, the concentrations of rhenium (Re) – an element which is otherwise only very rarely detectable – were unusually high in the water from the Oder, with values of around 1-3 µg/l. It is possible that there may be a connection with the input of effluents into the Oder from the KGHM copper mines near Glogów, since rhenium is one of the elements extracted from ores and processed there (https://kghm.com/en/our-business/products/rhenium).

For the purposes of a comparative illustration of the temporal profile of concentrations of elements in water from the Oder during the fish die-off period and the second salt surge, the mean value of the concentrations measured in the last week in July (25 to 31 July 2022) is set to 100% in the diagrams below, and the subsequent relative changes in concentration are shown. It can be seen from Figure 5.3.3 that, in contrast to the sharp increase in Na (to approximately 200%, along with Cl) and the decrease in Ca to around 75%, there were no major changes in the concentrations of S, Mg or K during the period of the fish die-off.

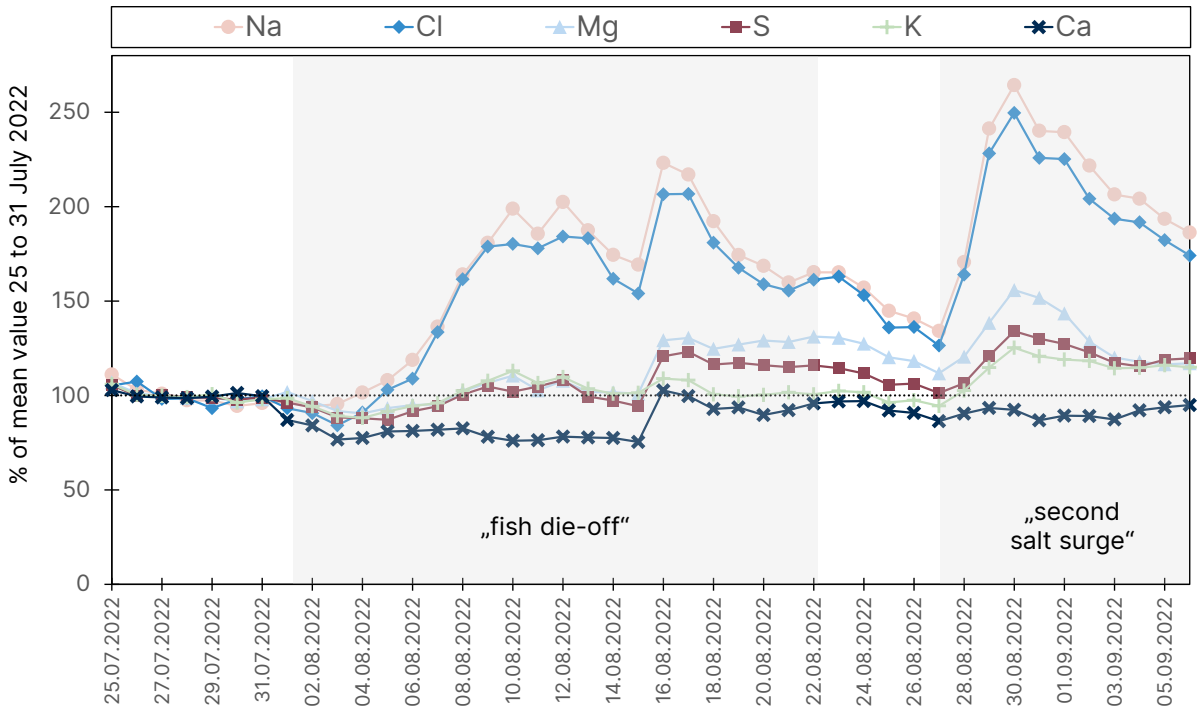

Figure 5.3.3 *Relative changes in the concentrations of the main elements Na, Cl, Mg, S, K and Ca in filtered samples of water from the Oder from Hohenwutzen for 25 July to 6 September 2022. The values are shown in relation to the mean value for the last week in July (25 to 31 July 2022), which has been set as 100%.*

However, during the second salt surge, there were also increases in Mg (up to around 150%) and in S and K (up to around 120-130%), although these increases were substantially smaller than the rise in Na (to >250%). The concentration of Ca did not change during the second salt surge. The reduction in the dissolved Ca concentration by around 25% in the first half of August was probably caused by the process of biogenic decalcification linked to the simultaneous occurrence of the algal bloom (see section 5.6). Biogenic decalcification represents the formation of calcium carbonate minerals under the influence of photosynthetically active aquatic organisms (e.g. algae). The binding of carbon dioxide (CO_2) from hydrogencarbonate (HCO_3^-) that is dissolved in the water leads to the release of OH^- ions and thus to a pH increase. This, in turn, alters the solubility equilibria, causing precipitation of calcium carbonate minerals and thus a reduction in the dissolved calcium concentration in the river water.

Along with Na and Cl, there were also increases in the concentrations of bromine (Br), lithium (Li) and caesium (Cs) during both salt surges (Figure 5.3.4). This can be explained by the relatively similar geochemical behaviour of Li and Cs compared to Na, and of Br compared to Cl. It seems reasonable to conjecture that these elements also occur in the areas of origin (mining) in association with NaCl and that they are transported in the water of the Oder along with the salt load. In contrast, some elements displayed differing concentration trends in the two salt surges investigated. These were elements connected with ore mining (e.g. sulphide ores). Just like the elements mentioned above, there was an increase in thallium (Tl) during both salt surges (Figure 5.3.4), whereas the concentration of nickel (Ni) only increased during the second salt surge, and the concentrations of molybdenum (Mo) and rhenium (Re) fell considerably during the second salt surge (see Annex A2, Figure A2.5.3.4 – in German only). Since, just like rhenium, molybdenum is one of the resources produced by the

copper mines near Glogów (KGHM, see link above), it could possibly be concluded from the relative changes in the concentrations of the various elements that, in contrast to the first salt surge, when there were increased values of Mo and Re, the input of effluents from the copper mines near Glogów may have played only a subordinate role in the salt load of the second surge.

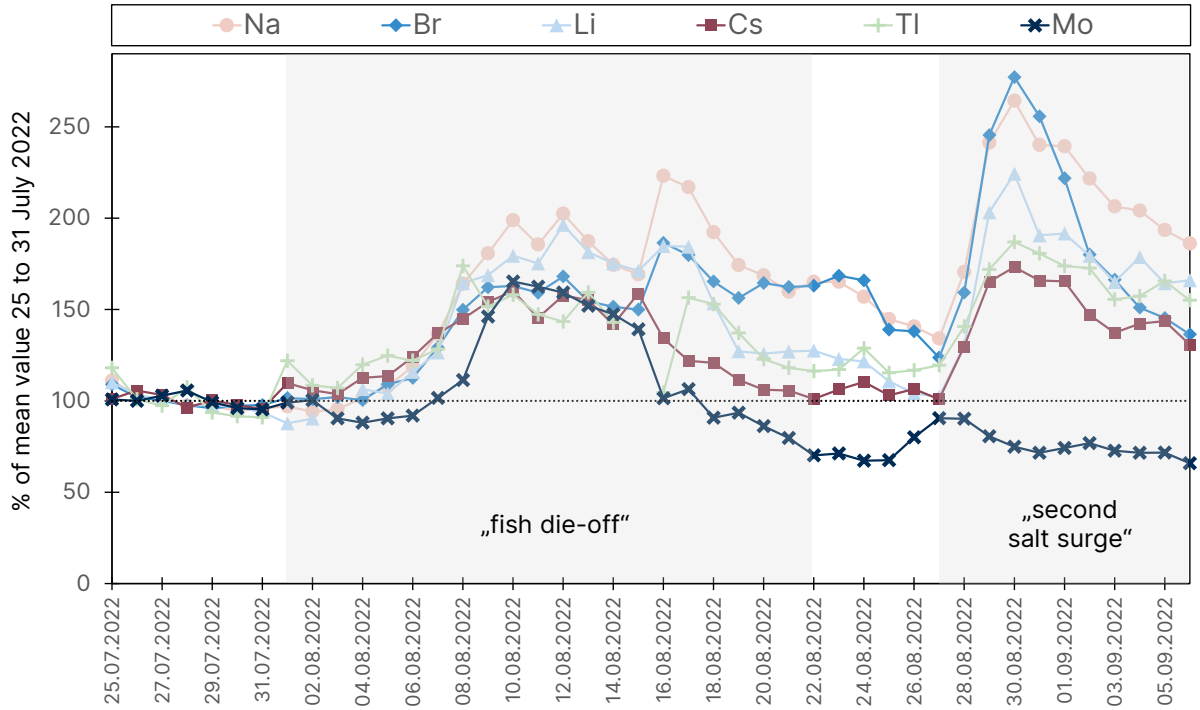

Figure 5.3.4 *Relative changes in the concentrations of the elements that increased during both salt surges – Na, Br, Li, Cs, Tl and Mo – in filtered samples of water from the Oder from Hohenwutzen for 25 July to 6 September 2022. The values are shown in relation to the mean value for the last week in July (25 to 31 July 2022), which has been set as 100%.*

In the unfiltered whole water samples (after aqua regia digestion), the measured concentrations of most elements were in the same order of magnitude as the measured values of the filtered samples, or only slightly above them. Notable exceptions were the elements Fe, Al and Mn, which were more abundant in the unfiltered samples by several orders of magnitude (median values in the 100-1,000 µg/l range), and Br and Zn, each of which was more abundant by one order of magnitude. The preferential occurrence of Fe, Al and Mn in the particulate fraction relative to the dissolved fraction is generally typical for surface waters. However, proportions in the dissolved fraction that were elevated – at least in the case of manganese (Mn), exceptionally so – were measured during the period around 15 August 2022 in Hohenwutzen (Figure 5.3.5), at the time when the chlorophyll concentrations were at their peak (see section 5.6). No unusual concentrations of elements were measured in the analysed samples of suspended particulate matter from the period from March to August 2022. The concentrations of potentially toxic trace elements were actually lower in August than in March in most cases – probably as a result of dilution with more organic matter – while the concentrations of calcium in the suspended particulate matter in August were substantially elevated (see Annex 2, Figure A2.5.3.2.3 – in German only), consistent with the process of biogenic decalcification (see above).

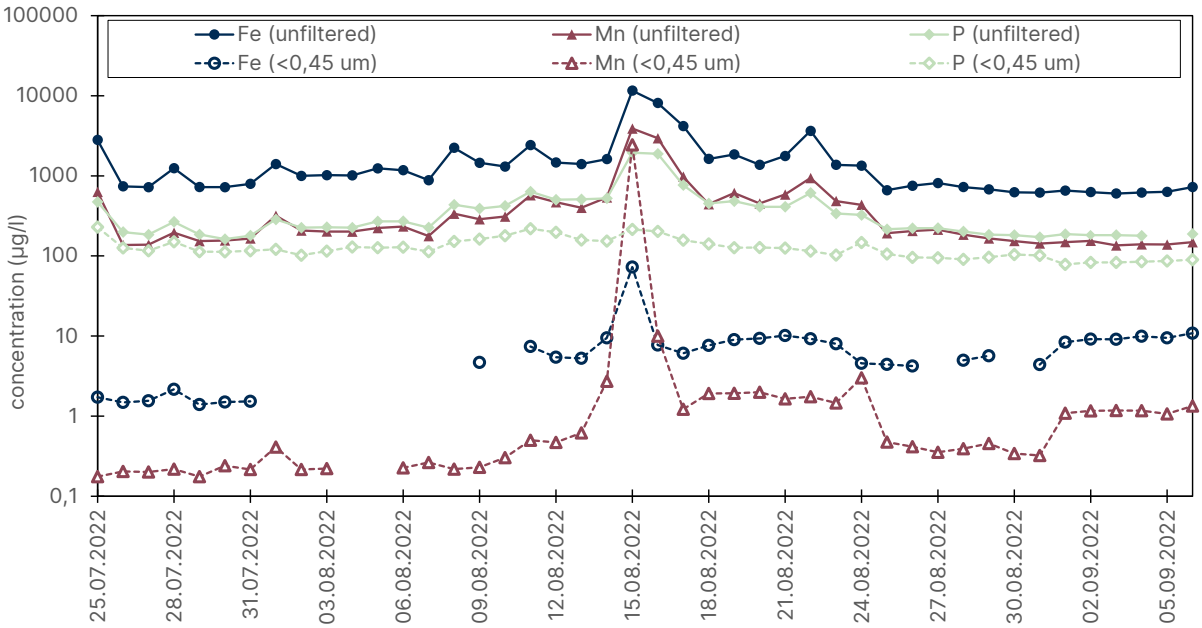

Figure 5.3.5 *Changes in the concentrations of Fe, Mn and P in unfiltered (whole water digestion) and filtered (<0.45 µm) water samples from Hohenwutzen for 25 July to 6 September 2022, in a logarithmic display. The substantially increased concentrations of manganese on 15 August 2022 were 3.9 mg/l (unfiltered) and 2.4 mg/l (<0.45 µm).*

5.4 Organic compounds

At BfG, organic compounds in the Oder were analysed using a range of techniques:

- Non-target screening using LC-QqToF-MS
- Target screening using GC-MS/MS
- Target analysis using IC-MS

Water samples (LC, IC) and suspended particulate matter samples (LC, GC) from Hohenwutzen and Frankfurt (Oder) were analysed. Details can be found in the relevant sub-sections.

5.4.1 Non-target screening using LC-QqToF-MS

Various methods were used to analyse organic compounds in the Oder, including non-target screening (NTS) by means of LC-QqToF-MS. NTS is a generic measurement method, which – in contrast to target methods – does not involve any pre-selection of the substances to be analysed. Instead, NTS detects all organic compounds in a sample that can be found with the measurement method in question on the basis of the method parameters (choice of column, solvent, gradient, MS parameters). The aim of NTS is to look for trace organic compounds which are not covered by the specialised target analysis methods used or which have not previously been recognised as river contaminants. A comprehensive spectral library is an essential tool for identifying the compounds detected by means of NTS. The BfG's spectral library, which was developed in cooperation with the Bavarian Environment Agency and the German Environment Agency (UBA), contains mass spectrometra for more than 1,200 substances from a variety of substance classes (including pharmaceuticals, industrial chemicals and pesticides). In addition to the precursor compounds, this database also includes human metabolites and transformation products of these compounds that are formed through human metabolism or in the environment. When measured non-target data is compared with the spectral library, many trace organic compounds can be identified directly and automatically. However, the high number of unknown detections means the data needs to be carefully evaluated using various algorithms. These algorithms, which are adapted to the current study, are used to rank the detections according to different criteria, and detections of interest are selected for identification by structural elucidation on a case-by-case basis. In this case, NTS was performed on various matrices using LC-QqToF-MS: water (section 5.4.1.1), suspended particulate matter (section 5.4.1.2) and algal biomass (section 5.6).

5.4.1.1 Water

NTS was performed on daily composite samples from the Hohenwutzen monitoring station (BfG monitoring station: 1 July to 23 August 2022) and the Frankfurt (Oder) monitoring station (federal state monitoring station: 5 to 8, 10 and 12 August 2022). The evaluation was performed in three separate steps:

1) A screening for organic compounds that could potentially be connected to the fish die-off was carried out first. The time series from Hohenwutzen was divided into two time periods for this purpose – 1) 1 to 31 July 2022 and 2) 6 to 14 August 2022. For each detected compound, the mean intensity values in each period were calculated and compared. If there was a significantly higher mean

intensity in August compared to July, and if the compound could also be detected in the samples from Frankfurt (Oder), it was categorised as relevant.

2) The organic compounds that showed peaks of intensity in the time series, meaning they could be attributed with greater probability to discontinuous (anthropogenic) input, were selected.

3) The organic compounds specific to the Oder, compared to the Rhine and Moselle (daily composite samples from the period 1 January 2020 to 31 December 2020), were determined. Compounds were considered to be specific to the Oder if they were detected in the Oder only or if their intensity in the Oder was higher by a factor of 10 compared to the highest intensity in the Rhine and Moselle.

The steps described were each performed separately, and the results subsequently summarised.

The substances that were identified using the in-house spectral library and categorised as relevant across all three screening steps were 2,4-dichlorophenoxyacetic acid (2,4-D), 2,6-D and 2,4,6-trichlorophenoxyacetic acid (2,4,6-T). All three substances show correlating time profiles in the data from both Hohenwutzen and Frankfurt (Oder), with a clearly delineated peak in intensity at the time of the fish die-off (Figure 5.4.1).

Both 2,6-D and 2,4,6-T are technical by-products from the production of 2,4-D. The joint occurrence of these by-products is therefore an indication of input resulting from the industrial production of pesticides. Correlation analyses between the temporal profile of 2,4-D and all other detected compounds were performed in order to obtain organic compounds that are connected to this type of production but are so far unknown. Through manual interpretation of the mass spectrometry data, it was possible to tentatively identify dichlorophenol sulfonic acid and trichlorophenol sulfonic acid. A subsequent quantification of 2,4-D, 2,6-D and 2,4,6-T revealed concentrations well over 1 µg/l, with maximum concentrations in Frankfurt (Oder) of 17 µg/l for 2,6-D, 8 µg/l for 2,4-D and 6 µg/l for 2,4,6-T. These concentrations verified the results that were obtained in parallel by the State Laboratory Berlin-Brandenburg.

Another herbicide – bentazon – was prioritised due to a discontinuous intensity profile at the Hohenwutzen monitoring station. The time series shows two peaks of intensity – one in July and one during the fish die-off period in August (Figure 5.4.1). Bentazon was also detected in the samples from the Frankfurt (Oder) monitoring station. However, in this case, the peak in intensity must have occurred shortly before the first sampling and must thus have taken place shortly before the fish die-off. One organic compound, which was initially unknown and which was categorised as relevant for identification due to its peak intensity at the time of the fish die-off and, therefore, its discontinuous profile (Figure 5.4.1), and because it was specific to the Oder, was tentatively identified as O,O-diethyl thiophosphate by carrying out research in online spectral libraries. This compound is a synthesis by-product or degradation product of certain insecticides. The detection of bentazon and O,O-diethyl thiophosphate could also be linked to input resulting from the industrial production of pesticides, as is suspected for 2,4-D.

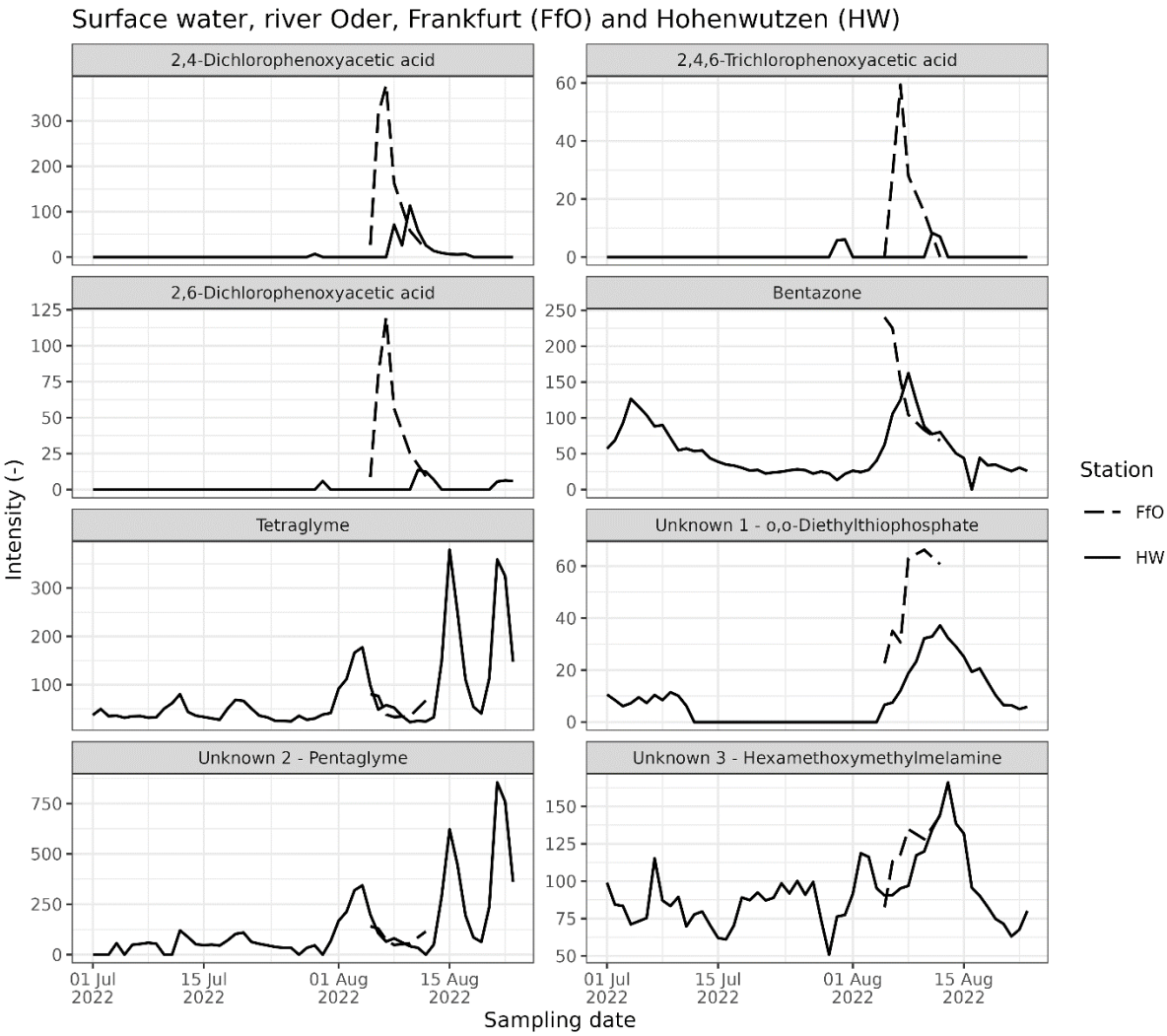

Figure 5.4.1 *Time series of identified substances at the Hohenwutzen (HW) and Frankfurt (Oder) (FfO) monitoring stations.*

Although the industrial chemical tetraglyme (Figure 5.4.1) was not directly linked to the fish die-off, it was prioritised due to a discontinuous intensity profile in Hohenwutzen. The time series in Hohenwutzen reveals several peaks of intensity, which increase in height over time and reach their maximum values at the time of the fish die-off. A retrospective quantification revealed a peak value of approximately 2 µg/l in Hohenwutzen. Tetraglyme was also detected in Frankfurt (Oder), but with substantially lower intensities and a maximum concentration of around 0.5 µg/l. The profile in Frankfurt (Oder) suggests that, as in the case of bentazon, the maximum intensity occurred shortly before the start of the first sampling. Correlation analyses between the tetraglyme profile and all other time series delivered an initially unknown compound with a correlating intensity profile (Figure 5.4.1). Given its similarity in the fragmentation spectrum, this was tentatively identified as pentaglyme. In a comparison with the Rhine and Moselle, pentaglyme was also flagged as specific to the Oder. An input of industrial effluent, such as from battery production, is also suspected as being responsible for the presence of tetraglyme and pentaglyme.

The substance provisionally identified as hexa(methoxymethyl)melamine, which shows a maximum intensity in Hohenwutzen and Frankfurt (Oder) at the time of the fish die-off

(Figure 5.4.1), is indicative of another possible industrial source, and the likely focus here is on the production of coatings.

By applying NTS and the subsequent analysis steps, a large number of organic compounds were prioritised that showed peaks of intensity at the time of the fish die-off and/or in the temporal profile generally and were also specific to the Oder in some cases. To date, it has only been possible to identify a small proportion of these by means of comparison with the in-house spectral library, research in online spectral libraries or manual interpretation of the data. However, the substances that have been identified already point to inputs relating to various industrial production processes. Although it is not yet possible to postulate a direct link between any of the identified substances and the fish die-off, there is evidence of high levels of chemical pollution in the Oder due to inputs of industrial substances. These inputs are in addition to the continuous inputs into the water from municipal wastewater treatment plants, which have also been detected. Overall, for both locations together, it was possible to directly identify 71 substances using the in-house spectral library. These included 28 pharmaceuticals or products of daily use with concentrations in the 0.05 to 1.5 µg/l range and continuous intensity profiles in the Hohenwutzen time series. These are substances such as candesartan, carbamazepine, oxipurinol and telmisartan that are typically released by municipal wastewater treatment plants.

5.4.1.2 Suspended particulate matter

In addition to the water samples from Hohenwutzen and Frankfurt (Oder), samples of suspended particulate matter from Hohenwutzen were also tested. Two composite samples from the periods 1 to 31 July and 1 to 15 August were available initially. These samples were prepared (BOULARD et al. 2020) and then measured by applying the non-target method. A total of 60 substances were identified through the screening process using the in-house spectral library. Of these substances, five were detected in August only (Table 5.4.1). In addition, a suspect screening was performed using the algal toxins list from the NORMAN Susdat database (https://www.norman-network.com/nds/susdat). Microcystin-LR and microcystin-YR were identified as a result of this screening (Table 5.4.1). Algal toxins were not detected in the water samples. A more precise analysis and quantification of algal toxins was carried out with adapted sample preparation (see section 5.6.4).

Table 5.4.1 *Annotated substances in the suspended particulate matter samples that showed higher intensities in August than in July.*

Substance	Use	Substance categorisation by
Didecyldimethylammonium	Biocide	m/z, t_R, MS^2
2-Oxaspiro[4.5]decan-3-one	Unknown	m/z, t_R, MS^2
Methyltriphenylphosphonium	Industrial chemical	m/z, t_R, MS^2
Tryptamine	Natural metabolite, basic material of chem. syntheses	m/z, t_R, MS^2
Benzyl butyl phthalate	Plasticiser	m/z, t_R, MS^2
Microcystin-LR	Cyanobacteria toxins	m/z, t_R, MS^2
Microcystin-YR	Cyanobacteria toxins	m/z, t_R

5.4.2 Target screening using GC-MS/MS

GC-MS/MS was used to determine polycyclic aromatic hydrocarbons (PAHs), various chlorinated organic compounds (especially chlorobenzenes, hexachlorocyclohexanes, polychlorinated biphenyls (PCBs), and the pesticide DDT and its transformation products), polybrominated diphenyl ethers (PBDEs) and organotin compounds in the suspended particulate matter composite samples. Furthermore, GC-FID was used to determine mineral oil hydrocarbons in the samples.

Monthly composite samples were used for the period from March to July 2022, whereas the suspended particulate matter composite samples that were analysed for the organic compounds in August 2022 came from three collection periods – 1 to 15 August, 16 to 23 August and 24 to 31 August 2022.

Across the substance groups analysed, the highest concentrations over the period investigated occurred most often in the months of March and April (Annex 3, Tables A3.5.4.2.1 and A3.5.4.2.2 – in German only). Over the period as a whole, a decreasing trend in the concentrations of PAHs and many chloro-organic compounds can be observed. The lowest concentrations were found in August. However, during the last week of August, in parallel with an increase in discharge volumes, there was a slight increase in the concentrations of some contaminants. The concentrations of PAHs and chlorinated organic compounds that were reached during the last week of August were mostly substantially below the mean concentrations for the investigated period of March to August 2022.

In terms of organic compounds, no elevated concentrations were detected in the suspended particulate matter samples in the months of July and August.

5.4.3 Target analysis using ion chromatography MS

IC-MS can be used to analyse organic compounds that are carrying a charge. These include anions such as chloride and bromide, as well as carboxylic acids, haloacetic acids, sulfonic acids and others. Haloacetic acids (HAAs) are chlorination disinfection by-products and are of high toxicological relevance. Sulfonic acids are used in a wide variety of ways, including in cleaning products and organic synthesis. As part of the

investigations into the fish die-off in the Oder, a target approach was used to analyse and quantify a total of 15 sulfonic acids and HAAs in the samples from Hohenwutzen (1 to 15 August 2022) and Frankfurt (Oder) (5 to 8, 10 and 12 August 2022). Values that were above the limit of quantification were found only for sulfamic acid. A rapid degradation of the substance was observed at both locations – from 9 August 2022 in Frankfurt (Oder) and from 10 August 2022 in Hohenwutzen (Figure 5.4.2). Sulfamic acid is recalcitrant in the environment and is released in high concentrations and on an ongoing basis by wastewater treatment plants. Since it is a small molecule that contains nitrogen, it is assumed that its rapid degradation is due to sulfamic acid being used by algae as a source of nitrogen.

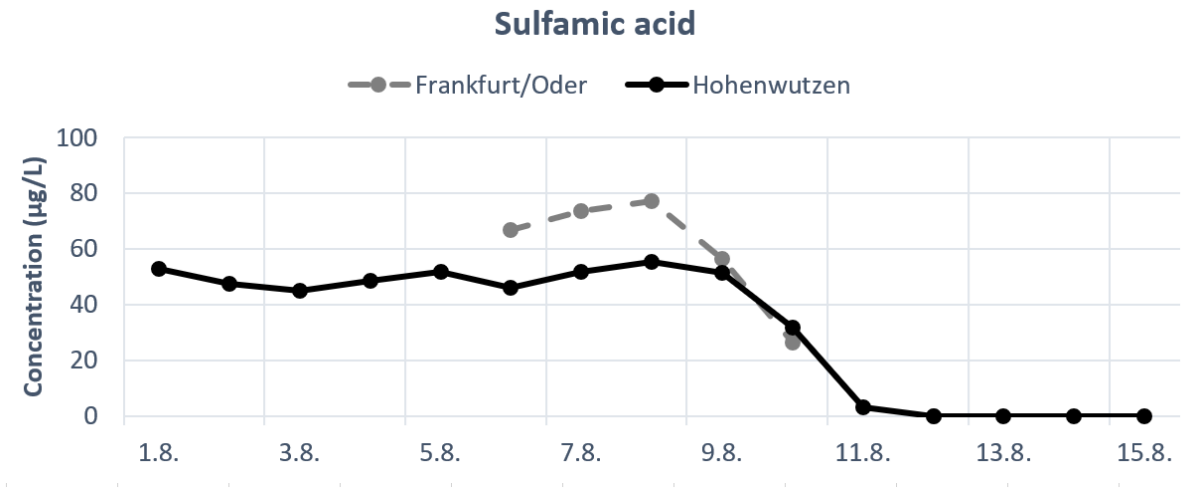

Figure 5.4.2 *Sulfamic acid detected at the Hohenwutzen and Frankfurt (Oder) monitoring stations during the period from 1 to 15 August 2022.*

5.5 Ecotoxicology

In addition to its chemical analyses, BfG also used several bioassay methods to conduct ecotoxicological tests to detect pollution and toxic effects present in the water samples from the Oder.

In these bioassays, the various test species were used as a model to represent the different trophic levels of the aquatic ecosystem. Bioassays indicate the cumulative effect of all bioavailable contaminants on the test organisms. For these tests, neither the contaminants nor their concentrations need to be known. Analytical chemistry to detect known and problematic substances and ecotoxicological tests to record the harmful effects that are present therefore complement one another perfectly. By combining both approaches, samples can be comprehensively analysed.

Ecotoxicological tests were performed on water samples provided by the State Laboratory and on daily composite samples from the BfG monitoring station in Hohenwutzen. Between 5 and 24 August 2022, 10 water samples were collected by scoop from the LfU monitoring station in Frankfurt (Oder) and tested. Three grab water samples from the LfU monitoring station in Hohenwutzen between 10 and 12 August 2022 were tested. A total of 15 daily composite samples from the BfG monitoring station in Hohenwutzen that had been taken between 1 and 15 August 2022 were tested. Tests were also carried out on two surface water samples from the Spree-Oder Waterway close to Eisenhüttenstadt that BfG had taken on 6 September 2022. This sampling site was chosen by taking account of the current *Prymnesium* concentrations at the federal state monitoring stations.

Depending on the date on which the samples were taken and the point at which BfG became involved, it was not always possible to test the samples directly. The samples that were tested first were not transported under cooled conditions. Due to the small sample volumes of the LfU samples taken from 5 to 8 August 2022, it was only possible to test these samples by means of the luminescent bacteria test in the screening procedure.

Figure 4.1.1 shows an overview of the sampling site locations. Table A3.5.5 in Annex 3 (in German only) provides detailed information about the sampling sites, sampling dates and the water parameters measured on site.

5.5.1 Bioassays used and ecotoxicological assessment

The water samples from the Oder were tested using three different bioassay organisms. The luminescent bacteria test, freshwater algal growth inhibition test and Daphnia acute immobilisation test were used. The test methods are briefly described in Annex 1.

Assessment of the ecotoxicological test results

Dilution series were used to test the water samples. This procedure allows for better differentiation of the toxic effects measured, and any impairment caused by confounding factors can also be reduced.

The results from the bioassays were categorised by means of the LID values and the pT values (*potentia Toxicologiae*) derived from these. The lowest sample dilution that no longer causes a significant effect in the bioassay is denominated as LID value. The higher the LID value, the more toxic a sample is. The pT value is derived from the LID value and specifies how often a sample needs to be diluted in a ratio of 1 to 2 so that it

no longer has a toxic effect (KREBS 1988; KREBS 2000). All results of a sample obtained using the bioassays are summarised by the pT_{max} value. This value is determined by the most sensitive bioassay and results from the highest pT value of the applied bioassays.

5.5.2 Ecotoxicological results

A total of 30 water samples were tested using the bioassays. A summary of the results is presented in Table 5.5.1. The main accompanying water parameters and the measurement results of the dilution series are listed in Annex 3 (Tables A3.5.5 – in German only).

None of the water samples tested showed any significant inhibition at the highest studied test substance concentration of 45% in response to the luminescent bacteria test on a microplate (MPL), adapted in line with DIN EN ISO 11348-2. Similarly, the tests performed in line with the standard method after the first screening tests did not show any significant inhibition in the G1 dilution of 80% for any of the samples tested.

Since the samples sometimes contained considerable quantities of other algae, they were tested both in filtered and unfiltered form in the freshwater algal growth inhibition test (DIN 38412-33). Neither the unfiltered nor the filtered samples revealed any significant effects on the algal growth.

In the Daphnia acute immobilisation test according to DIN 38412-30, no inhibition was detected for the majority of the samples either. However, potent toxic effects were recorded in the two samples taken from the LfU monitoring station in Frankfurt (Oder) on 10 and 12 August 2022 (FFO_TM_10/08 and FFO_TM_12/08) and in the unfiltered and filtered BfG sample from the Spree-Oder Waterway (EHS_SOK_S06/09).

The accompanying water parameters that were recorded (pH, oxygen content, conductivity/salinity, concentration of ammonium) could be excluded as the cause of the toxicities observed. However, conductivity in both LfU samples was higher than in all other samples, at >2,000 µS/cm. Nevertheless, the elevated salt content is to be ruled out as a direct cause of the inhibition observed.

The LID values for the samples from Frankfurt (Oder) were 16 and 32, while the pT values were pT 4 and pT 5. These samples were tested again after they had been stored in a refrigerator for a prolonged period of time. After this period – 16 weeks at 4 °C – the potent toxic effects on the Daphnia that had previously been observed were no longer detected.

Table 5.5.1 Ecotoxicological results for the samples from the LfU Brandenburg monitoring stations, the BfG monitoring station in Hohenwutzen and from the Spree-Oder Waterway.

Sample ID	Sampling site	Sampling date	**Lum. bacteria test** DIN EN ISO 11348-2		**Freshwater algal growth inhibition test** DIN 38412-33		**Daphnia acute immobili-sation test** DIN 38412-30		max. LID value	**pT_{max} value**
			MPL pT value	Stan-dard pT value	Unfil-tered pT value	Fil-tered pT value	24 h pT value	48 h pT value		
FFO_TM_05/08 to 08/08	Frankfurt (Oder), LfU monitoring station	05-08/08/2022	1.1	-	-	-	-	-	2.2	0
FFO_TM_10/08		10/08/2022	1.1	0	0	0	4	4	16	**4**
FFO_TM_10/08 (follow-up test)		10/08/2022	1.1	-	-	-	0	0	1	**0**
FFO_TM_12/08		12/08/2022	1.1	0	0	0	4	5	32	**5**
FFO_TM_12/08 (follow-up test)		12/08/2022	1.1	-	-	-	0	0	1	**0**
FFO_BP_12/08		12/08/2022	1.1	-	-	-	-	-	2.2	**0**
FFO_BP_15/08		15/08/2022	1.1	0	0	0	0	0	1	**0**
FFO_S_24/08 (unfiltered)		24/08/2022	1.1	0	0	-	0	0	1	**0**
FFO_S_24/08 (filtered)		24/08/2022	1.1	0	0	-	0	0	1	**0**
HW_LfU_TM_10/08 to 12/08	HW, LfU monitoring station	10-12/08/2022	1.1	0	0	-	0	0	1	**0**
HW_TM_01/08 to 15/08	HW, BfG monitoring station	01-15/08/2022	1.1	0	0	0	0	0	1	**0**
EHS_SOK_S_06/09 (unfiltered)	Eisenhüttenstadt, Bridge Str. d. Republik	06/09/2022	1.1	0	0	-	2	3	8	**3**
EHS_SOK_S_06/09 (filtered)		06/09/2022	1.1	0	0	-	2	2	4	**2**

The results for the EHS sample were LID values of 4 and 8 and pT values of pT 2 and pT 3. To determine whether the toxic effect is particle-bound or whether it is present in the aqueous phase, both filtered and unfiltered specimen of the EHS sample were tested in parallel. The inhibition, LID values and pT values were slightly lower in the filtered sample than in the unfiltered sample (see Figure 5.1.1). After 48 hours, the LID value was just 4 and the pT value was 2, whereas previously the LID value was 8 and the pT value was 3.

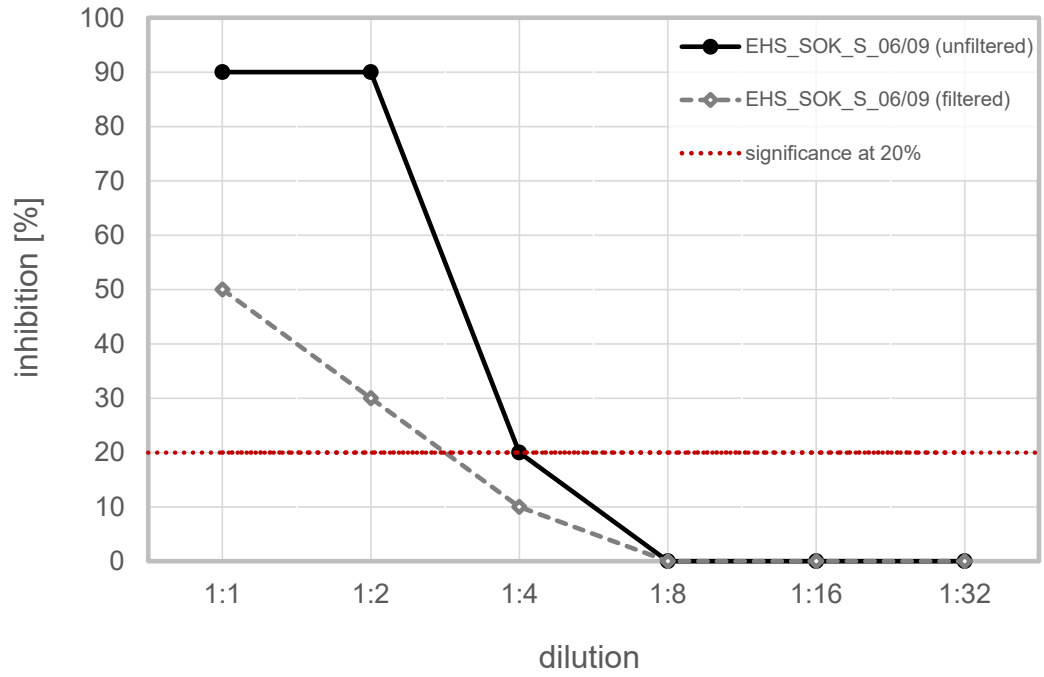

Figure 5.5.1 *Results for the unfiltered and filtered water sample from the Spree-Oder Waterway, inhibition in the Daphnia acute immobilisation test after 48 hours.*

5.5.3 Interpretation of the ecotoxicological results

Increased conductivity was detected in the Oder during the period of the fish die-off. However, direct damage to freshwater organisms cannot be explained by the elevated salt concentrations alone. As the brackish water alga *Prymnesium parvum* was deemed the most likely cause of the fish die-off, filtered and unfiltered samples with established Daphnia toxicity were tested to determine whether the toxic effect is particle-bound. Although the toxic effect was reduced by filtering the sample through a glass fibre filter, toxic effects on Daphnia were also detected in the filtrate. This indicates that the compounds responsible for the toxicity were present to some extent in particle-bound form. It is possible that the algae-associated prymnesins were released by dead, decomposing algae. The release of such exotoxins is consistent with the study performed by FISTAROL et al. (2003); it describes the haemolytic activity in the cell-free filtrate of *P. parvum* cultures.

When the test systems are compared with one another and the different samples considered, the measured toxic effects are consistent. The results of the sometimes strong inhibition in the Daphnia acute immobilisation test match the Daphnia toximeter measurements[1]; these measurements exceeded the alarm threshold almost continuously, especially around mid-August. During this period, more Daphnia had to be added to this test system on multiple occasions due to the death of the exposed test organisms in the water from the Oder (BMUV 2022).

In a few samples, the BfG tests were unable to verify the toxicity that the LfU had detected in the water of the Oder near Hohenwutzen. However, this discrepancy could be explained by the degradation of the prymnesins, since the samples were not always transported under cooled conditions. Moreover, stability experiments conducted at BfG demonstrated that the toxic effect was no longer detectable when the samples had been stored for a prolonged period at 4 °C. This finding is consistent with the short half-life of the prymnesins. SCHWIERZKE-WADE et al. (2011) and JAMES et al. (2011) have reported that, when algal toxins produced by *P. parvum* are exposed to full sunlight, they have a half-life of less than one hour due to photodegradation. BLOSSOM et al. (2014) also report that the prymnesins are very unstable and lose their lytic effect after three days when they are stored at -20 °C, and after just 24 hours when they are stored at 4 °C. This observation and the in-house measurements highlight the necessity of both storing collected samples appropriately and testing samples with this type of pollution very promptly.

[1] The Daphnia toximeter is a continuous biomonitor that is operated by the LfU at the Hohenwutzen monitoring station. With this system, various swimming parameters of the water flea used are monitored with a camera and computationally evaluated. The behavioural data captured in this way is used to calculate an alarm index.

5.6 Phytoplankton

5.6.1 Light microscopy analysis of environmental samples and temporal trends of chlorophyll and algal abundances

Online data from the LfU Brandenburg monitoring station in Frankfurt (Oder) showed that there was a massive increase in the concentration of chlorophyll *a* (Chla) in the Oder, rising from around 20 to 160 µg Chla/l on 7 and 8 August 2022 (Figure 5.2.3C). Chlorophyll *a* is used as an indicator of algal biomass. Since such a sudden and strong increase in algal biomass can trigger doubts about the correct functioning of the measuring probe, consideration is simultaneously given to measurement parameters that are also influenced by algal growth. The increase in oxygen concentration to maximum values in excess of 12 mg/l O_2, in pH to maximum values in excess of pH 9 and in UV absorption, along with the daily periodic fluctuations in these variables, are also clear indicators of a strong algal bloom (Figure 5.2.3). In the days that followed, the Chla concentration increased further to over 300 µg/l, before decreasing again from 16 August. The values were below 50 µg Chla/l again from around 29 August 2022 (source: LfU Brandenburg online measurement data from the Frankfurt (Oder) monitoring station).

Given the indications of an algal bloom, live samples were taken in Hohenwutzen (BfG monitoring station) on 16 August and examined by microscope at BfG on 17 August 2022. Additional grab samples were preserved with Lugol's iodine and thus prepared for the subsequent algal community count. Mobile, single-celled microalgae that were green-gold in colour dominated the microscopic image of the live sample. The predominance of this taxon was also visible in the preserved sample. It was assumed (based on knowledge from the LfU and IGB investigations) that this was *Prymnesium parvum*. The preserved samples were assessed by AquaEcology GmbH (Oldenburg) and counts were conducted on the basis of MISCHKE & BEHRENDT (2015). The predominant taxon was categorised – provisionally in the first instance and subject to further assessment – as being of the *Prymnesium parvum* species (Figure 5.6.1, Table A.5.6.1).

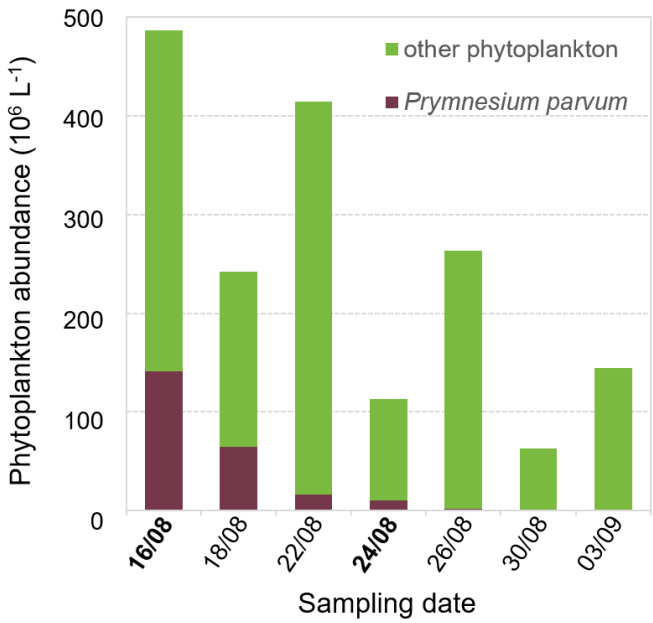

Figure 5.6.1 *Abundance of Prymnesium parvum and proportion of the total phytoplankton abundance at the Hohenwutzen monitoring station (in bold) and Lunow. The results from LfU and BfG samples are included. Assessed and counted by: AquaEcology GmbH, Oldenburg.*

The results show mass developments of *Prymnesium parvum* across the entire stretch of the Oder from which samples were taken (between Frankfurt (Oder) and the Lower Oder Valley). The maximum cell count detected – 141 million cells per litre – was in Hohenwutzen on 16 August 2022. Concentrations of 28 million cells per litre were found in the Western Oder in the Lower Oder Valley until 26 August 2022. It is likely that the sample taken in Hohenwutzen on 16 August 2022 was at the peak of the algal bloom, while the samples taken in Lebus (near Frankfurt (Oder)) on 19 August 2022 reflect the algal densities that were already declining. Results from Poland revealed cell counts of up to 160 million per litre as early as on 12 August 2022 (Oder near Słubice, IOŚ-PIB 2022). Since it is highly likely that *Prymnesium parvum* dominated the algal bloom from the outset, it can be assumed, based on the available chlorophyll data, that there was a period of around two weeks during which there were high, potentially fish-toxic *Prymnesium* counts (in excess of 20 million cells per litre) in the entire course of the Oder between Frankfurt (Oder) and the Lower Oder Valley.

Prymnesium cells also made their way into tributaries of the Oder via locks and outlets and, to some extent, remained there due to lack of current. Over a protracted time period of at least 27 August to 4 September 2022, there were cell counts of over 50 million cells per litre in the Oder-Spree Canal in Eisenhüttenstadt. The *Prymnesium* bloom presumably reached the Wriezener Alte Oder in the Oder Marshes via the Reitwein channel, the Förstersee lake and the Quappendorfer canal, where fish die-off was also reported.

5.6.2 Identification of *Prymnesium parvum*

5.6.2.1 Establishing unialgal clonal cultures

Enrichment cultures with different salt concentrations were prepared from the grab sample taken in Hohenwutzen (BfG monitoring station) on 16 August. This involved making 50 ml culture preparations with a general algal culture medium (Alga-Gro; Carolina Biology Supply Comp.) and sea salt (Sea salts; Sigma Aldrich, final concentration 5, 10 and 20 g/l) and inoculating them with 2 ml of the original sample. Observations by light microscopy (Figure 5.6.2.1) revealed that the cultures with 10 g/l and 20 g/l sea salt contained large quantities of *Prymnesium*-typical cells after 11 days; these co-occurred with centric diatoms. Approximately 40 single cells were isolated from the enrichment culture with 1% salt concentration, and these were used both to extract DNA (see section 5.6.2.2) and to establish clonal cultures. Aliquots of the clonal cultures were then used both for the DNA extraction to identify the species and phylotype by molecular techniques (see section 5.6.2.2) and for studies on the production of algal toxins (see section 5.6.4). The four successfully established clonal cultures were stored in the Central Collection of Algal Cultures (CCAC) at the University of Duisburg-Essen with the strain IDs CCAC 9414 - 9417.

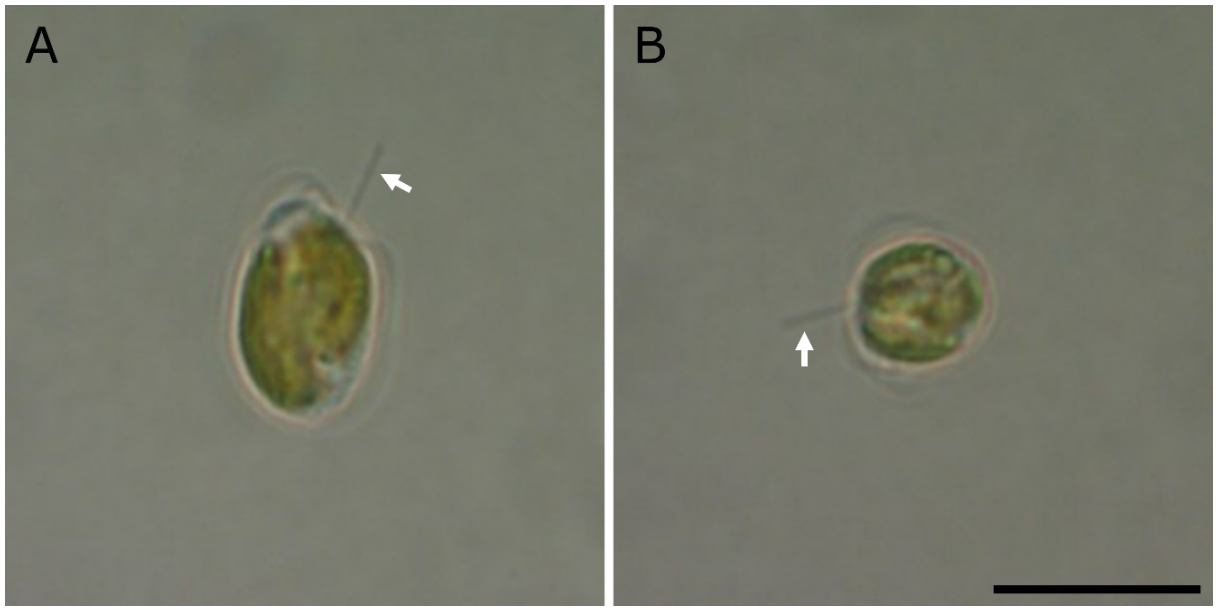

Figure 5.6.2.1 *Light microscopy images of two cells of Prymnesium parvum from the enrichment cultures. Both cells show the flagella (lying around the cell body) and the haptonema (indicated by the arrows). A = oval shape, B = round shape. Scale bar = 10 µm. Photo: D. Mora, BfG.*

5.6.2.2 Molecular phylogenetic species and phylotype identification

The species identification of the predominant algal species in the samples taken on 16 August (BfG monitoring station, Hohenwutzen II) first needed to be verified by means of molecular phylogenetics. The Chelex 100 method (WALSH et al. 1991) was used to extract DNA from single cells, which had been isolated from an enrichment culture with 1% salt concentration (see section 5.5.2.1). The DNA was then used for the amplification of the hypervariable V4 region of the 18S rRNA gene and subsequent Sanger sequencing. Details about the method can be found in Annex A1.5.6.2.2. The sequencing of a total of eight single cells yielded sequence results that could be successfully analysed for three single cells. They were classified as being of the *Prymnesium parvum* or *Prymnesium nemamethecum* species. Although both *Prymnesium* species reveal identical sequences in the DNA region analysed, *Prymnesium nemamethecum* is so far known only from marine environments, so it is possible to conclude that the species in question is *Prymnesium parvum*, which is also found in brackish water.

For the purposes of an unequivocal taxonomic classification of the identified *Prymnesium* species, DNA was therefore extracted from 7 ml of the culture fluid from the clonal cultures (see section 5.6.2.1). This DNA was then used for the amplification and sequencing of the almost complete 18S rRNA gene and the ITS (internal transcribed spacer) region. Details about the method can be found in Annex A1.5.6.2.2. All the sequences obtained were of high sequencing quality and could be unequivocally classified as being of the *Prymnesium parvum* species. As can be seen in the phylogenetic tree based on 18S rDNA sequence data (Figure 5.6.2.2.1), the sequence of the *Prymnesium* culture from the Oder (strain ID CCAC 9414) is grouped with a *P. parvum* sequence from Norway (strain ID K-0081) with 100% sequence similarity. Furthermore, a clear separation between *P. parvum* and its most closely related species *P. nemamethecum* can be seen. Their close phylogenetic relationship on the basis of the 18S rRNA gene is due to the extremely small genetic differences, which represent only a 2 bp difference in the alignment comprising 1,762 positions.

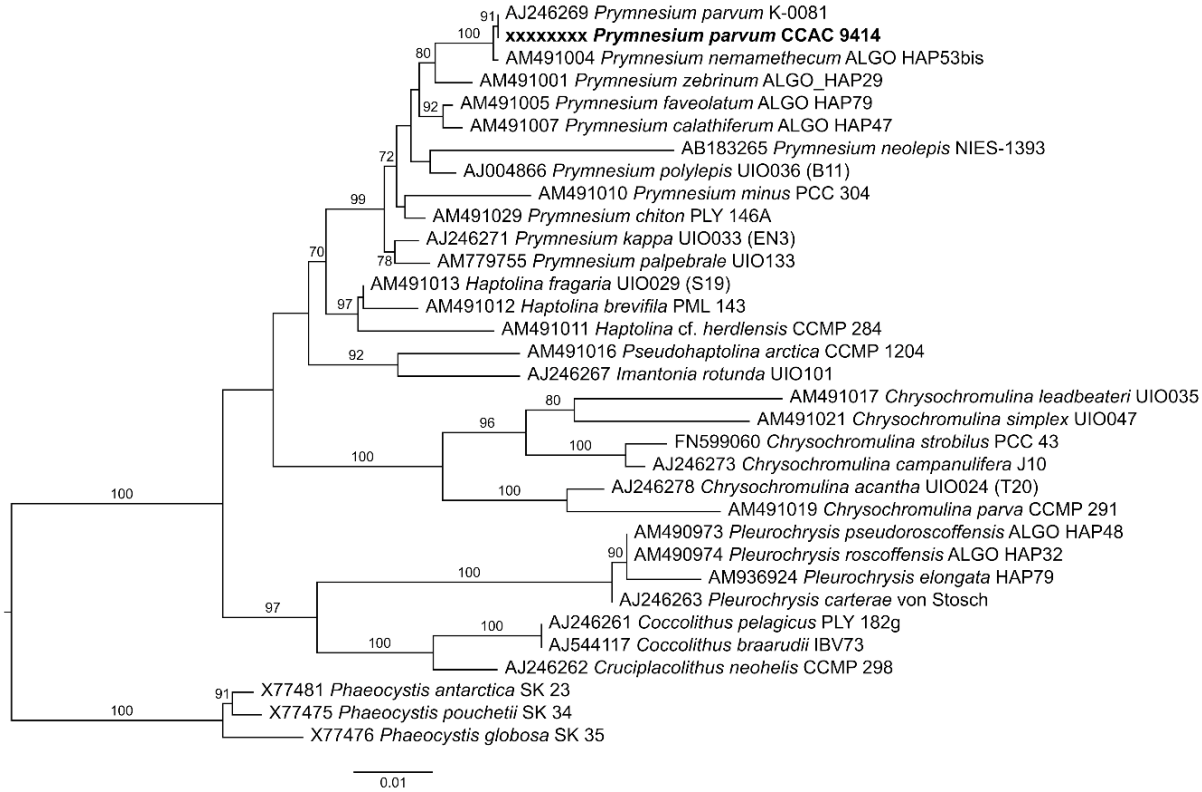

Figure 5.6.2.2.1 *Maximum likelihood phylogeny of selected strains within the Haptophyta, with the Phaeocystis genus as the outgroup, based on a 1,762-position alignment of 18S rRNA genes, including a representative sequence from a clonal Oder culture (in bold). Bootstrap values ≥70 are shown. Scale = number of substitutions per base.*

The phylogenetic analysis on the basis of the ITS region (ITS1-5.8S-ITS2) reveals three different clades (related groups) within the *Prymnesium parvum* species. According to BINZER et al. (2019), the representatives in the three clades are characterised by the production of a specific type of metabolites – prymnesins (A, B or C) – which are toxic to fish. As can be seen in Figure 5.6.2.2.2, the cultivated strains from the Oder are clustered in the B-type prymnesin producer clade (in the analysis, only Oder strain CCAC 9414 was used as an example). This group also includes strain SAG 18.97, for example, which is likewise of German origin and was isolated and cultivated after a fish die-off in a eutrophic pond (SAG CULTURE COLLECTION 2023).

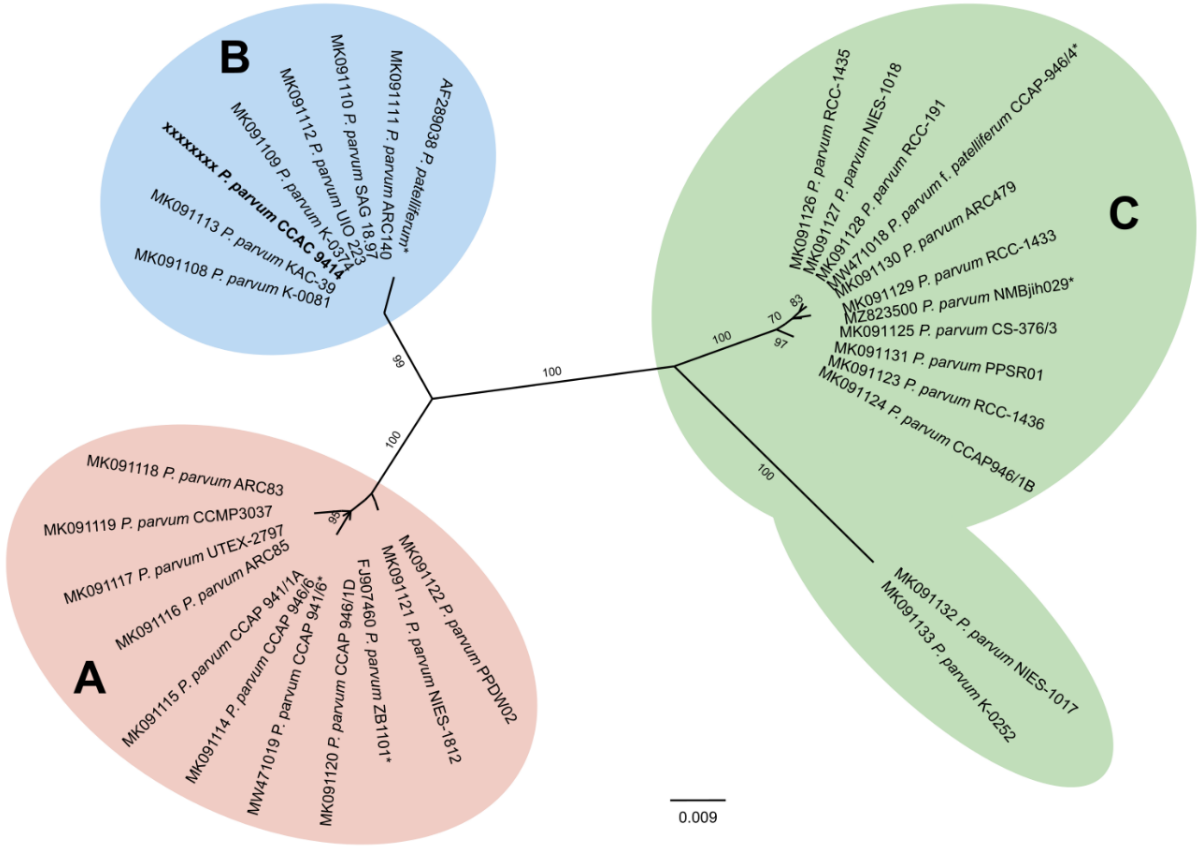

Figure 5.6.2.2.2 *Maximum likelihood phylogeny (unrooted) of selected strains of Prymnesium parvum, including a representative sequence from a clonal Oder culture (in bold), based on a 692-position alignment of the ITS1-5.8S-ITS2 region. * designates strains for which there is no reference to toxin production. The strain with the Acc. No. AF289038 (clade B) is classified as P. patelliferum and is currently considered synonymous with P. parvum. Bootstrap values ≥70 are shown. Scale = number of substitutions per base.*

5.6.3 Molecular biological detection of *Prymnesium parvum* in environmental samples

5.6.3.1 Rapid detection by PCR method

Two different molecular biological methods based on the polymerase chain reaction (PCR) technique were used to verify and quantify *Prymnesium parvum* in water samples from the Oder. In order to trace the temporal development of the occurrence of *P. parvum* in the Oder, the daily composite samples of water from the Oder from Hohenwutzen (BfG monitoring station, period from 4 to 14 August 2022) and grab samples of surface water from Hohenwutzen (BfG monitoring station, 16 and 24 August 2022) and the Frankfurt (Oder) water quality monitoring station (LfU Brandenburg, 24 August 2022) were used. The water samples were filtered for this purpose, and the DNA was extracted from the filter residue and the algae contained within it. The extracted DNA was then used for a PCR specific to *Prymnesium parvum*, with three different molecular markers, to detect the presence of *P. parvum* DNA in the water samples tested. Moreover, the DNA was used for droplet digital PCR (ddPCR) specific to *P. parvum*, so that the abundance of *P. parvum* in the water samples tested could also be determined. The DNA extraction methods, primers, reaction conditions and analysis processes used for this purpose are listed and explained in greater detail in Annex A1.5.6.3.1.

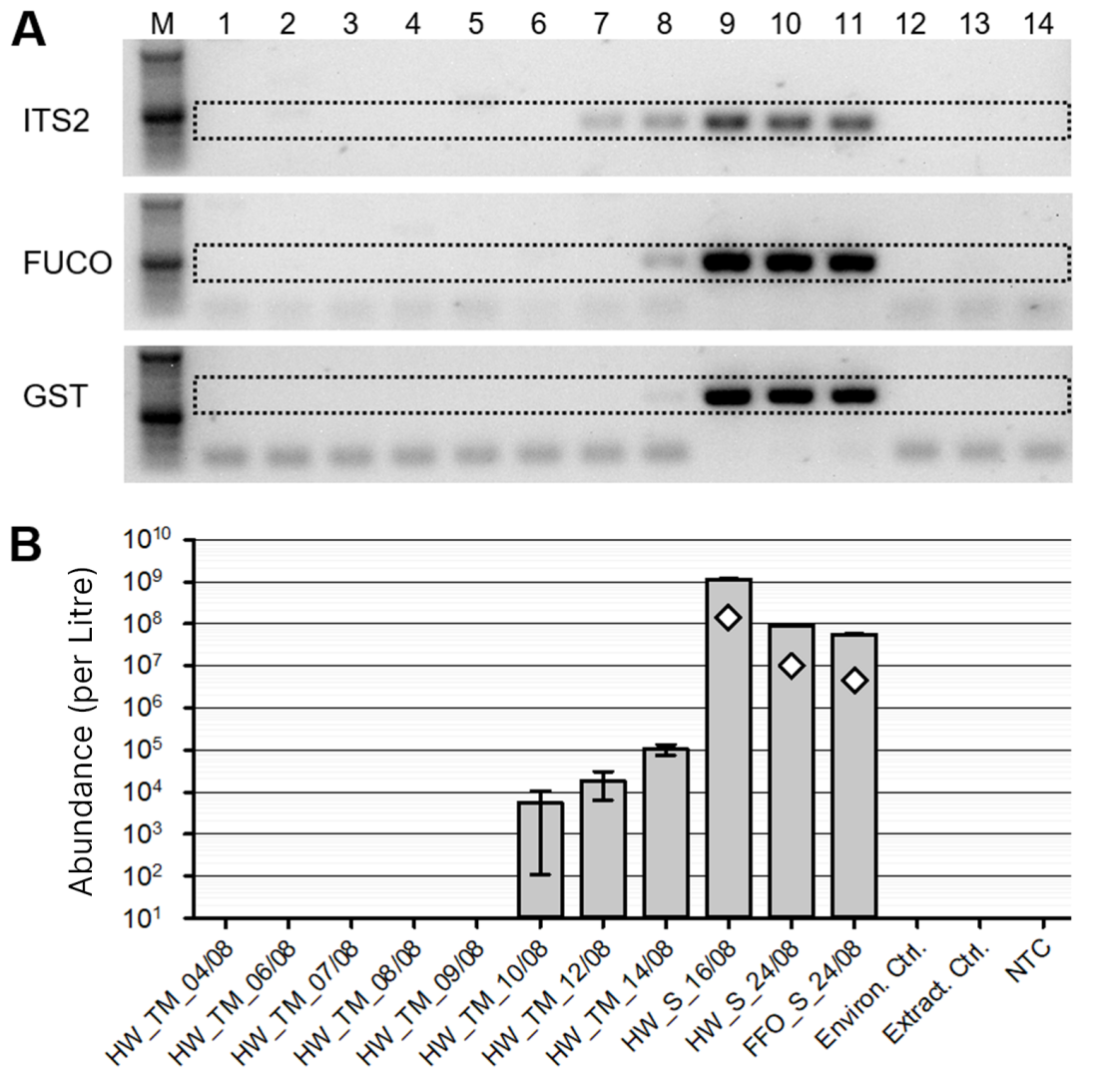

Figure 5.6.3.1 *(A) Gel image of 11 analysed DNA samples plus three negative controls, which were amplified by means of conventional PCR and P.-parvum-specific primers for three molecular markers (ITS2 – internal transcribed spacer 2, FUCO – fucoxanthin chlorophyll a/c-binding protein, GST – glutathione S-transferase). Lanes 1 – 14 correspond to the x-axis labels in Figure B. The molecular weight marker (50 bp; New England Biolabs GmbH) is visible in lane "M". (B) Concentration (copies/l) of the P. parvum ITS2 region in 11 analysed DNA samples plus three negative controls (mean value ± 95% confidence interval) and the cell counts (cells/l) determined by light microscopy for the three grab samples tested (white rhombi).*

As can be seen in Figure 5.6.3.1-A, *P. parvum* could first be detected by means of conventional PCR in the sample taken on 12 August (weak amplicon band for the ITS2 (internal transcribed spacer 2) molecular marker). None of the daily composite samples from Hohenwutzen from 4 to 10 August that were tested showed a positive signal. In the case of the samples taken on 16 and 24 August (Hohenwutzen and Frankfurt (Oder)), strong amplicon bands can be seen in the agarose gel for all three of the markers used, which indicates high concentrations of *P. parvum*. Quantitative ddPCR was also performed, which made it possible to determine the number of DNA copies for the ITS2 marker as proxy for the cell abundance of *P. parvum* in the samples. This revealed a

similar pattern to the one for conventional PCR (comparison of Figures 5.6.3.1 A and B). The daily composite samples from Hohenwutzen from 4 to 9 August were also negative for *P. parvum*, and the daily composite samples for 10, 12 and 14 August revealed comparatively low values (5.47 x 10^3 to 1.05 x 10^5 DNA copies/l). The positive result on 10 August (in contrast to the negative result from the conventional PCR) is attributable to just four detected DNA molecules in the ddPCR reaction. The highest number – approximately 1.14 x 10^9 DNA copies/l – was detected in the grab sample taken in Hohenwutzen on 16 August. The two grab samples taken in Hohenwutzen and Frankfurt (Oder) on 24 August, at approximately 9.04 x 10^7 and 5.61 x 10^7 DNA copies/l respectively, still showed comparatively high values, but they are nevertheless lower than the highest detected value by more than one order of magnitude.

The results of the conventional and droplet digital PCR therefore clearly demonstrate the presence of *P. parvum* in Hohenwutzen from 12 August 2022. However, since the daily composite samples were stored at ambient temperature and in the dark in the sampler in Hohenwutzen until they were removed from the sampler on 16 August, it is possible that disintegration of the algal biomass and degradation of the DNA occurred. The possibility that *P. parvum* was present from an earlier date cannot therefore be ruled out. For the same reason, the weak amplicon bands and relatively low numbers of DNA copies on 10, 12 and 14 August 2022 do not necessarily indicate low *Prymnesium* abundances. Overall, however, the ddPCR results correlate well with the *P. parvum* abundances determined (cf. Table 5.6.2.1). The highest number of DNA copies (1.14 x 10^9 copies/l) and the highest cell counts (1.41 x 10^8 cells/l) were found in the sample from Hohenwutzen taken on 16 August 2022 by both the ddPCR and light microscopy method. The higher number of DNA copies compared to the cell count can be explained by the presence of multiple copies of the target gene in each cell (YARIMIZU et al. 2021). Nevertheless, when the samples taken in Hohenwutzen and Frankfurt (Oder) on 16 and 24 August 2022 are compared, similar relative ratios between the numbers of DNA copies and the cell counts are observed. For example, the results of both abundance estimates for the sample from Hohenwutzen taken on 24 August 2022 (9.04 x 10^7 DNA copies/l and 1.0 x 10^7 cells/l) are lower by more than one order of magnitude than the results for the sample taken on 16 August (Figure 5.6.3.1.B).

In summary, it can be stated that both the strong signals from the conventional PCR and the high numbers of DNA copies detected in the grab samples taken on 16 and 24 August 2022 show that the methodology presented here provides reliable evidence of high *Prymnesium* densities. Even smaller abundances (≤ 1 x 10^5 DNA copies/l) can be detected by means of conventional PCR and ddPCR. Methodology is therefore available that can be used to quickly and reliably detect *Prymnesium parvum* in environmental samples, even without microscopic evidence, and, where applicable, to quantify it. However, further sensitivity tests with defined cell and DNA concentrations of *P. parvum* are required in order to determine the limit of detection (LOD) and the limit of quantification (LOQ).

5.6.3.2 DNA metabarcoding

The DNA metabarcoding method offers another DNA-based technique for identifying organisms in environmental samples. This technology makes it possible to simultaneously analyse almost the entire species community in one sample and thus trace, for example, changes in the mix of species in the plankton community during the algal bloom in the Oder. For the DNA metabarcoding of the water samples already tested

as set out in section 5.6.3.1, the extracted DNA was analysed by means of amplification and sequencing of the hypervariable V4 region of the 18S rRNA gene and subsequent bioinformatic evaluation. Since the analysis of the 18S rDNA is targeted at eukaryotic organisms, the proportion of cyanobacteria in the phytoplankton was not recorded here. Methodological details about the process can be found in Annex A1.5.6.3.2.

In total, more than one million sequence reads were generated for the 11 samples tested and used for the analysis. The percentage of reads that could be ascribed to the algae ranged from 51.2% to 88.6%, depending on the sample. Diatoms, which accounted for 84.5% of these “algal reads” and 57% of the total reads, were the predominant group in all samples overall.

Only two sequence variants (amplicon sequence variants — ASVs) were found in the data set that were classified as haptophytes. One of the two ASVs belongs taxonomically to the *Prymnesium* genus and was detected in all 11 samples (Figure 5.6.3.2 B). Using DNA metabarcoding, it was therefore possible to detect the *Prymnesium* genus in samples from the Oder near Hohenwutzen from as early as 4 August. However, the relative abundance of this ASV in the entirety of all reads for all samples was below 0.6%, with the exception of the sample taken in Hohenwutzen on 16 August, in which the corresponding ASV accounted in total for 7.8% of all reads. The low relative abundance of *Prymnesium* and the strong predominance of diatoms can probably be attributed to technical artefacts from the DNA extraction and PCR amplification (primer bias). It was not possible to classify the *Prymnesium* ASVs at species level, since the taxonomic resolution of the 18S-V4 marker used was too low (see also section 5.6.2.2). To be able to use DNA metabarcoding as a basis for making clear statements about occurrence and relative abundances in the case of future toxic algal blooms with a focus on *Prymnesium parvum*, other molecular markers or longer DNA sections may need to be analysed. Multi-marker approaches are also particularly recommended for this purpose so that the group-specific resolution of individual markers can be applied for an overall higher taxonomic resolution (GAONKAR & CAMPBELL 2023).

The predominant genera in the entire data set were centric diatoms (*Actinocyclus* and *Cyclotella*), which are also typical representatives of plankton communities (Figure 5.6.3.2 A). It was noticeable that one single sequence variant, which was classified as member of the *Actinocyclus* genus, made up the largest percentage of the total reads (29%). Given the insufficient coverage of this genus in the reference database used (PR2, GUILLOU et al. 2013), this ASV, with a sequence similarity of less than 97.8%, could not be classified down to species level. However, in the samples examined by light microscopy (see section 5.5.2.1), the *Actinocyclus normanii* species was found, which probably corresponds to the ASV detected. This species frequently occurs in eutrophic, brackish inland waters with an optimum salinity of 0.9 to 1.8‰ (VAN DAM et al. 1994; SPAULDING et al. 2021). It is also regarded as an invasive species in freshwater (see references in SPAULDING et al. 2010). *A. normanii* has also already been detected, for example, in other strongly altered waterways in Europe, such as in the Danube-Tisa-Danube canal (VIDAKOVIĆ et al. 2016), and upstream in the Volga, where it has come from the Caspian Sea (KORNEVA 2007).

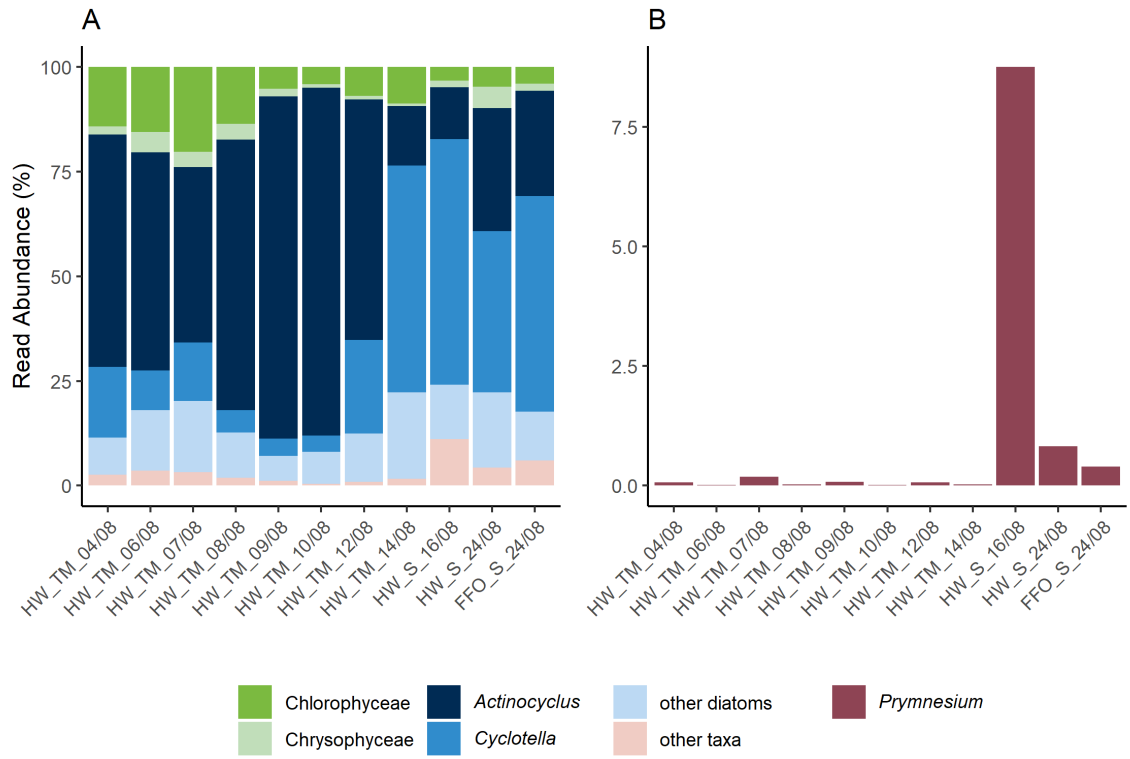

Figure 5.6.3.2 *Proportion of sequence reads per taxonomic unit in the 11 analysed samples, based on all classified "algal reads" in the entire data set. A) Relative abundance of selected algal taxa, including the two most abundant diatom genera (Ochrophyta phylum, Bacillariophyta class). B) Relative abundance of the ASV classified as Prymnesium (included in "other taxa" in Figure A).*

5.6.4 Algal toxins

The mixotrophic haptophyte *Prymnesium parvum* is one of the main causes of harmful algal blooms that can trigger massive fish die-off events. The fish-toxic effect is attributed to the formation of allelochemical toxins known as prymnesins, which can be divided into three groups – A, B and C (RASMUSSEN et al. 2016). Figure 5.6.4.1 shows an example of the molecular structure of prymnesin-B1, a polyether with a ladder frame structure.

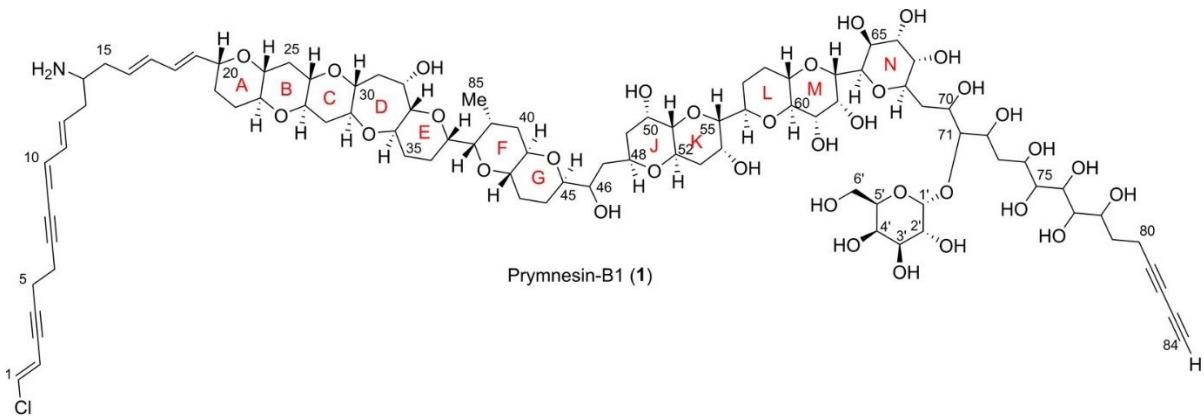

Figure 5.6.4.1 *Molecular structure of prymnesin-B1 (from RASMUSSEN et al. 2016; reprinted with permission of the American Chemical Society).*

In addition to the examination of water samples from the Oder for prymnesins, the analysis of algal toxins (according to SVENSSEN et al. 2019) also included microcystins, which are formed by cyanobacteria (blue-green algae). The extraction and processing method is described in Annex A1.5.6.4.

Algal toxins were detected exclusively in the intracellular fraction (filter residue) of the examined water samples from Hohenwutzen and Frankfurt (Oder). Prymnesin-B1 (prym-B1), some monosaccharides and disaccharides, which are characteristic of prymnesin conjugates, and microcystins were clearly detected in these samples. Since no reference standards are available for prymnesins, only the measured intensities could be determined for the detected prymnesins. These do not allow for any statements to be made about their absolute concentrations, but they can be used to draw conclusions about the relative differences in the prymnesin concentrations. A water sample from Hohenwutzen II (HW) taken on 16 August 2022 and a water sample from Frankfurt (Oder) taken on 24 August 2022 were tested first. As the prymnesins are considered very unstable outside the cells, the samples were taken directly from the closed circular pipeline of the monitoring stations and transported within 24 hours under cool, dark conditions to the BfG laboratory for analysis. The prym-B1 algal toxin and the monohexoses and dihexoses were identified in both samples. Prymnesins were identified by their exact mass (mass error < 2 ppm), their characteristic isotope patterns, their sodium adducts, the in-source fragmentation of the sugar units to aglycone and their MS^2 spectra (mass error < 10 ppm, see Annex 2 – in German only). The concentration or measured intensity of the sample taken in HW on 16 August was higher than the later sample from Frankfurt (Oder) by a factor of 50 to 400 (see Annex 2, Figure A2.5.6.4.1 – in German only). This is also consistent with a considerably higher density (by a factor of around 30) of *Prymnesium parvum* (cf. Table 5.6.2.1).

Residual samples (stored in dark conditions) from the BfG Hohenwutzen monitoring station from 1 August 2022 to 23 August 2022 were subsequently analysed for algal toxins. From 10 August 2022 Prym-B1 could be detected (Figure 5.6.4.2), which is consistent with the detection of *P. parvum* by PCR method (section 5.6.3.1). Although the stability of prymnesins under cell-free conditions is not temperature-dependent (JAMES et al. 2011), it cannot be completely ruled out that microbial degradation of the toxin took place during the unrefrigerated storage of the daily mixed samples (1 to 15 August). The peak maximum was between 17 and 20 August 2022. From 21 August 2022, the measured intensities of prym-B1 in Hohenwutzen decreased again. Microcystins were also detectable from 10 August 2022 (Figure 5.6.4.2). Maximum concentration was reached around 16 August 2022.

Microcystins were also detected and quantified in the water samples from 16 August and 24 August (Table 5.6.4.1). The detected microcystin concentrations are too low to have a toxic impact on fish (e.g. MALBROUCK & KESTEMONT 2006). WHO recommends a drinking water guideline value of 1 µg/l for microcystin-LR. Nevertheless, the temporal occurrence of microcystins in the water of the Oder (Hohenwutzen) provides an indication of the presence of cyanobacteria, associated with the *Prymnesium parvum* bloom (Figure 5.6.4.3).

Table 5.6.4.1 *Concentrations of microcystins in water samples (from algal biomass) from Hohenwutzen (HW) and Frankfurt (Oder) (FFO).*

	Microcystin RR	Microcystin YR	Microcystin LR
Whole water sample 16 August 2022 HW	30 ng/l	90 ng/l	300 ng/l
Whole water sample 24 August 22 FFO	0.3 ng/l	9 ng/l	5 ng/l

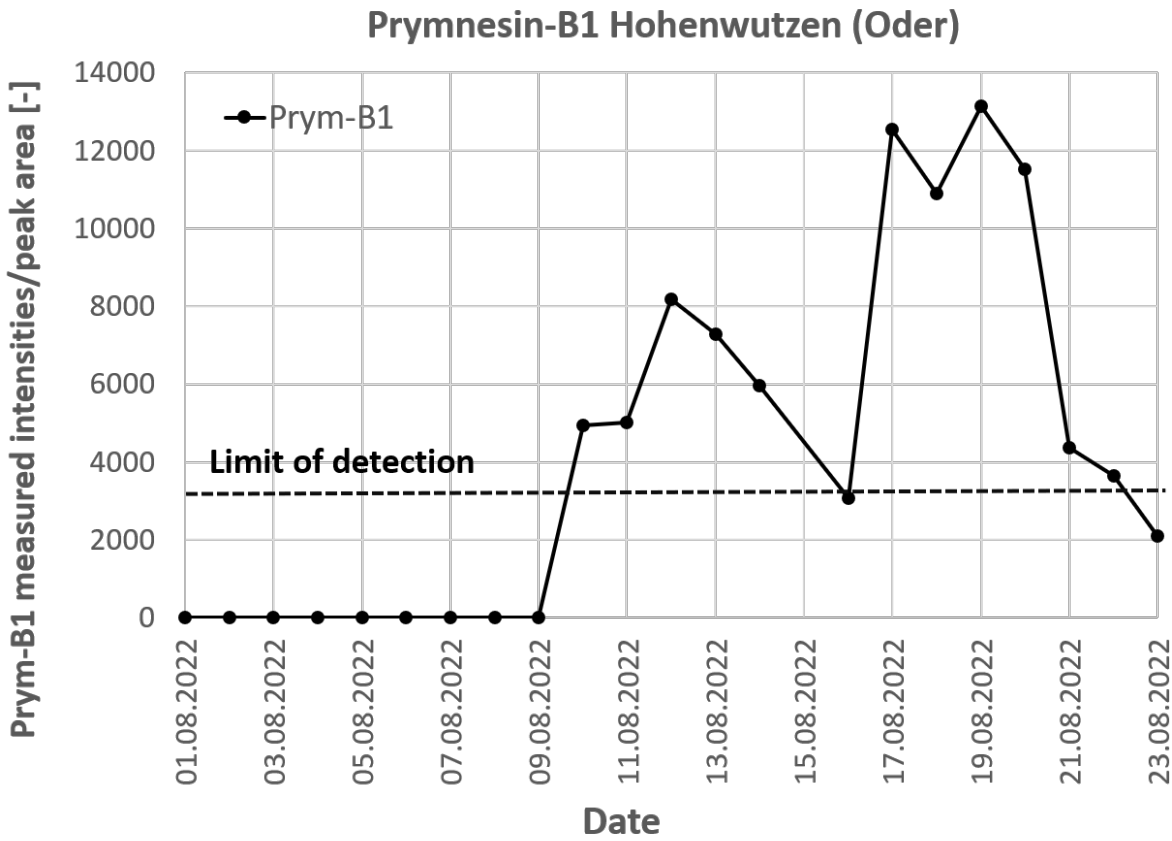

Figure 5.6.4.2 *Temporal profile of the measured intensity of the algal toxin prymnesin-B1 produced by Prymnesium parvum in daily composite samples from the BfG Hohenwutzen monitoring station.*

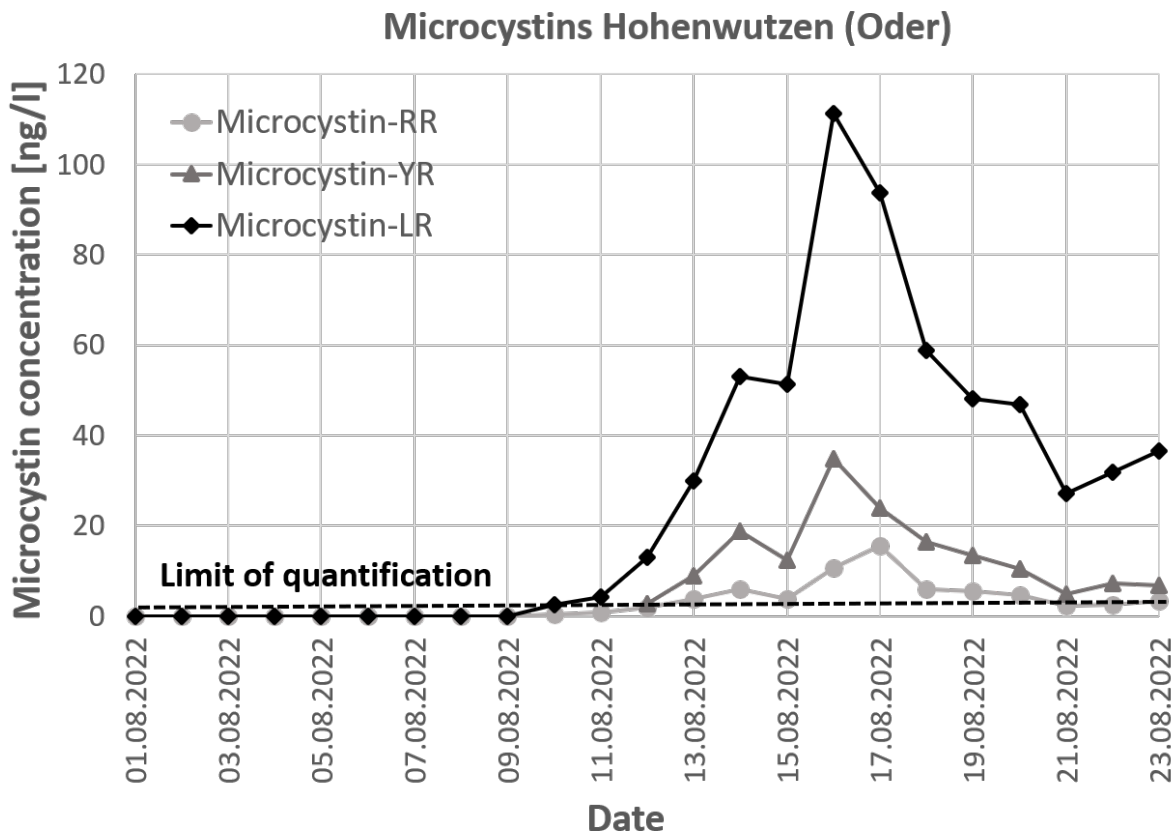

Figure 5.6.4.3 *Temporal profile of the concentrations in nanograms per litre (ng/l) of the microcystins produced by cyanobacteria at the BfG Hohenwutzen monitoring station.*

In clonal cultures of *Prymnesium parvum*, generated from samples of water from the Oder (see section 5.6.2.1), high measured intensities of prym-B1 were detected (see Annex 2, Figure A2.5.6.4.2 – in German only).

To clarify the question as regards the extent to which 2,4-dichlorophenoxyacetic acid (2,4-D) – the herbicide found in samples from the Oder (see section 5.4.1) – and its technical by-products (2,6-dichlorophenoxyacetic acid (2,6-D) and 2,4,6-trichlorophenoxyacetic acid (2,4,6-T)) have an influence on algal and toxin production, a mix of 2,4-D; 2,6-D and 2,4,6-T was added to additional clonal algal cultures (n=3). No inhibition and no increased growth of the algal population was detected, even at concentrations of up to 100 µg/l. Prym-B1 was detected at consistently high intensities in all of these samples (Figure 5.6.4.4).

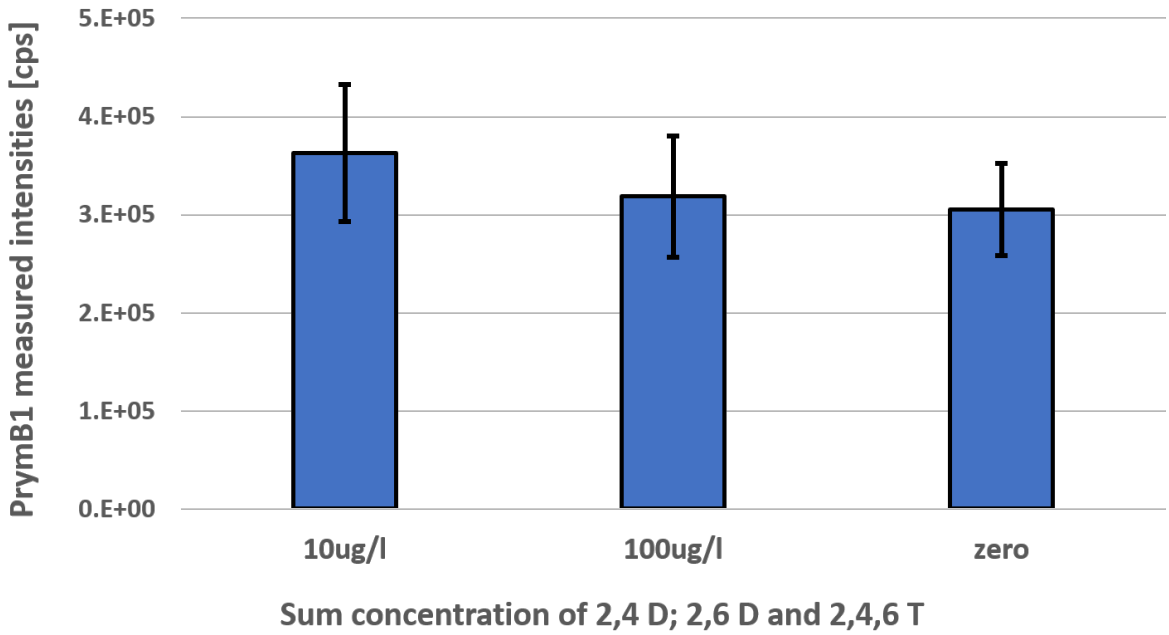

Figure 5.6.4.4 *Influence of 2,4-dichlorophenoxyacetic acid (2,4-D), 2,6 dichlorophenoxyacetic acid (2,6-D) and 2,4,6-trichlorophenoxyacetic acid (2,4,6-T) on the prymnesin-B1 concentration (uncalibrated signal intensity in counts per second (cps)) in algal incubation experiments (n=3).*

Conclusion:

- The detection of prym-B1 in clonal cultures of *Prymnesium parvum*, generated from samples from the Oder, identifies this as the producer of the algal toxin detected in samples of water from the Oder. This result also correlates with the phylogenetic classification of the *P. parvum* strain as a potential producer of B-type prymnesins (see section 5.6.2.2).
- The direct evidence of prymnesins (B-type) confirms the presence of *Prymnesium parvum* at the time of the fish die-off and the occurrence of compounds that are extremely toxic to fish, probably in very high concentrations.
- The detected microcystin concentrations were too low (ng/l) to have a toxic effect on fish. They were also below the microcystin drinking water guideline value of 1 µg/l.
- An algal incubation experiment with herbicides from the synthetic auxin group (phenoxyacetic acid derivatives) showed no influence on the toxin production.

6 Discussion and conclusions

6.1 Synoptic discussion of the investigation results

It is only the combined examination of the investigation results set out in the previous section that gives rise to a complete, overall picture of the events in the Oder in August 2022. The combination of the prevalent environmental conditions in August 2022 in interaction with the known anthropogenic interventions in the Oder ecosystem ultimately led to the ecological disaster. At the outset of the broad-based investigations, it was also initially important to test various hypotheses and rule out potential causes and contaminants.

The hydrological assessment of the low-flow event in the Oder in summer 2022 was carried out for the Eisenhüttenstadt and Hohensaaten-Finow gauging stations on the Oder in Germany with particular consideration of characteristics that could have a critical impact on the fish fauna (amplitude, timing, frequency and duration of the low-flow event and the discharge or water levels associated with it). Water-balance year 2022 showed several extreme characteristics in the Oder discharge data series in a long-term comparison. These characteristics were the result of dry conditions that were already pronounced in spring and continued especially in high summer. In addition to the AM7D low-flow parameter, with a statistical recurrence interval of a little more than 20 years (Hohensaaten-Finow gauging station), it is important to highlight the unusually rapid decrease in discharge down into this extreme range in July and the unusually long duration of the low-flow conditions already seen in the early summer. The latter occurred in four of the seven previous years since 2015, albeit to a less extreme extent.

The online measurement data from the LfU Brandenburg state monitoring stations in Frankfurt (Oder) and Hohenwutzen supplied valuable insights into the changes in physicochemical parameters and total chlorophyll content during the fish die-off in August 2022. Shortly after the rise in electrical conductivity (and thus a substantially elevated salt content in the water of the Oder), there was a sharp increase in chlorophyll. This, along with increased oxygen content and pH values, which fluctuated in a diurnal manner, indicated an algal bloom. This also resulted in increasing turbidity and decreasing nitrate values in the water of the Oder, caused by algal uptake of nitrate. The high water temperatures and low discharge were also important influential factors in relation to the extreme ecological event. However, the fish die-off was not foreseeable based on the interpretation of the online measurement data alone, and more detailed investigations were needed.

From the chemical element analyses of the Oder river water before, during and after the event, it was possible, in the first instance, to determine the composition of the salt load that was responsible for the elevated electrical conductivity. Both the first salt surge that passed through the Oder during the period of the fish die-off and the second surge, which took place in higher discharge conditions at the end of August and transported even more salt, largely consisted of table salt (NaCl), i.e. the elements sodium and chloride. The reduced calcium concentration during the first salt surge was an indication of the precipitation of calcium carbonate minerals by biogenic decalcification, and this was confirmed by increased calcium content in the samples of suspended particulate matter. The analysis of the trace element composition of the water of the Oder indicated that, alongside table salt, there was also an increase in the concentrations of various

elements, which had probably originated from mining operations. For example, the concentrations of the very rare element rhenium (Re) were substantially elevated. The analysis of the unfiltered whole water samples also revealed that the increased particle load at the peak of the algal bloom resulted in elevated concentrations of iron, manganese and phosphorus in the Oder river water. Overall, however, no concentrations of elements were found that even came anywhere close to the range that would be associated with direct toxicity to fish. Amongst other elements, this included the concentration of mercury, which was discussed in the press at the start of the fish die-off.

Analysis of organic compounds was carried out by means of non-target screening using LC-QqToF-MS and target screening using GC-MS/MS, GC-FID and IC-MS/MS. Water samples (LC, IC) and suspended particulate matter samples (LC, GC) from Hohenwutzen and Frankfurt (Oder) were measured. General chemical contamination of the Oder was apparent. The non-target screening, for example, detected a large number of organic compounds in the water samples. These showed cyclically recurring maximum intensity values, which can be attributed to various factors, including the input of industrial effluents. These are in addition to the substances that municipal wastewater treatment plants release into the river on a continuous basis. The suspended particulate matter samples that were analysed by means of GC-MS/MS and GC-FID also revealed general contamination. Various PAHs, organotin compounds, chloro-organic compounds and polybrominated diphenyl ethers were detected throughout the entire period from March to August 2022. None of the organic compounds identified so far by means of the various techniques and matrices could be directly linked to the fish die-off.

BfG conducted ecotoxicological tests to detect toxic effects present in the water samples from the Oder. The water samples showed no significant inhibition in the luminescent bacteria and freshwater algal growth inhibition tests. In the Daphnia acute immobilisation test, however, inhibition was measured – and was very strong in some cases – meaning that these organisms were considerably more sensitive to the pollution. Direct damage as a result of the elevated salt concentrations detected could be ruled out.

The samples that caused inhibition were tested in both filtered and unfiltered states to determine whether the toxic effect is particle-bound. Although the toxicity was reduced by filtering the sample through a glass fibre filter, toxic effects were still also observed in the filtrate. From this, it was possible to conclude that the toxic compounds were, to some extent, particle bound, i.e. in the algae. This finding is consistent with other tests.

The measured toxic effects are consistent both when the test systems are compared with one another and in comparison with other measurements. Moreover, tests performed to ascertain the stability of the toxic effects demonstrated that these effects were no longer detectable when the samples had been stored for a prolonged period at 4 °C. This finding is congruent with the results from other studies and is consistent with the known short half-life of the prymnesins. These results clearly highlight the necessity of both storing collected samples appropriately and testing samples with this type of pollution very promptly.

The aims of the phytoplankton tests were, in particular, the reliable molecular biological detection and quantification of *P. parvum* during and after the event. In addition, the *P. parvum* strain occurring in the Oder was cultivated so that it is now available to experts for further analyses. The molecular biological methods that were used were able to reliably verify and quantify the *P. parvum* algal species in the samples of water from the Oder that were investigated. DNA metabarcoding was also used to trace the temporal

profile of the *Prymnesium* bloom, and this demonstrated that *P. parvum* formed part of the algal bloom from the outset. However, it was never the exclusively dominant species (cf. Figures 5.6.1 and 5.6.3.2). This is consistent with the knowledge that *P. parvum* particularly produces its toxins in situations where it is competing with other phytoplankton taxa (e.g. ROELKE et al. 2016).

Relatively low abundances (≤ 1 x 10^5 DNA copies/l) of *P. parvum* can be detected both with conventional PCR and, in particular, with the droplet digital PCR method. Methodology is therefore available that can be used to quickly and reliably detect *Prymnesium parvum* in environmental samples, even without microscopic evidence, and, where applicable, to quantify it. This can be of key importance, especially when it comes to monitoring programmes for the early detection of *P. parvum* (see section 6.3.1). However, when there is appropriate species knowledge, a quick microscopic analysis can also detect a mass occurrence of *P. parvum*.

Based on earlier methods that were developed at BfG for the chemical detection of algal toxins (e.g. in connection with the cyanobacteria blooms in the Moselle), it was possible to identify the algal toxin of *P. parvum* in the samples of water from the Oder as being the substance prymnesin-B1. However, since there is no standard available for this substance, it was only possible to describe the relative intensity profile – it was not possible to quantify concentrations. Although it was possible to determine the concentrations of microcystins that were also detected in the water of the Oder, these were relatively low and thus played no part in the fish die-off.

The combined examination of the different analysis results produced a comprehensive overall picture of the chain of effects that played out in the Oder in August 2022. Based on the insights presented in this report, the clear anthropogenic influence on the sensitive ecosystem of the Oder, combined with the prevalent environmental factors in summer 2022, led to the fish die-off. There is a very high likelihood that, without the strongly increased salt content of the Oder resulting from anthropogenic influence, mass growth of the brackish water alga *Prymnesium parvum* – the excreted toxins (prymnesins) of which ultimately led to the die-off of fish and other organisms in the Oder – would not have been possible. The two sections of this report that follow present recommendations for improved monitoring and for possible measures for detecting and preventing future algal blooms of *Prymnesium parvum*.

6.2 Monitoring requirements

A river water monitoring concept that is both effective and has the highest possible resolution in time and space, along with prompt public provision of measurement data, is a key requirement for being able to detect comparable future events quickly in order to initiate measures to control or minimise potential damage. The measures proposed in the report by the Polish Institute of Environmental Protection – National Research Institute (IOŚ-PIB 2022) include extending monitoring and improving online provision as the first point listed in the recommendations. This appears to be urgently required given the spatial and temporal density of the data. Joint public provision of data by all riparian states, as quickly as possible, continues to be just as important, as is the creation of redundant systems that will ensure the supply of data if an event occurs, even if technical downtimes occur within an event. On the German side, intensifying cooperation between the Federal Government and the federal states could ensure additional safeguards for

this very personnel-intensive work. Recommendations for extending online monitoring and the public availability of measurement data and for improving cross-border communication and emergency planning are also contained in the EU report on the fish die-off in the Oder (FREE et al. 2023) and in the IGB policy brief (IGB 2022b).

6.3 Options for detecting and preventing *Prymnesium parvum*

6.3.1 Molecular biological methods as "rapid tests" for early detection

Molecular biological detection methods offer a valuable alternative or complementary technique to conventional light microscopy. Since these methods are targeted at the detection of species-specific DNA sequences, they can be used to detect organisms quickly and reliably in environmental samples. They are particularly useful when it comes to detecting only small concentrations of the target organism in large-volume samples or when it is hard to identify the target species on the basis of morphological characteristics.

In recent years, various molecular biological methods have been developed to detect *Prymnesium parvum* in environmental samples. Of these, the most commonly used techniques are conventional polymerase chain reaction (PCR) and quantitative PCR (qPCR) (e.g. GALLUZZI et al. 2008, MANNING & LA CLAIRE 2010, ECKFORD-SOPER & DAUGBJERG 2015, WAGSTAFF et al. 2021). The ITS (internal transcribed spacer) region is a molecular marker that is frequently used for detecting DNA specific to *P. parvum* (FEIST & LANCE 2021). Given the high number of copies per genome, this region is particularly suitable for ensuring the method has a high level of sensitivity. The quantitative PCR method is thus already used in *P. parvum* algal bloom monitoring programmes (WAGSTAFF et al. 2018). The ITS region was therefore also used for both conventional PCR and quantitative ddPCR in this report. Both techniques are thus available as potential monitoring methods and for ad hoc investigations by BfG.

In addition to the PCR-based techniques, isothermal amplification methods are increasingly being used to detect DNA specifically in environmental samples without any need for complex, special equipment such as a thermal cycler. The LAMP (loop-mediated isothermal amplification) and RPA (recombinase polymerase amplification) methods can be combined with other DNA detection methods such as gel electrophoresis, fluorescence-based assays and lateral flow tests to visualise the specifically amplified DNA fragments. Both isothermal amplification methods were already established in combination with the lateral flow dipstick (LFD) method as a cost-effective, rapid and specific means of detecting *P. parvum* in environmental samples (ZHU et al. 2019, LUO et al. 2022). Furthermore, the results showed that the RPA-LFD assay is much more sensitive when it comes to detecting *P. parvum* than conventional PCR-based approaches (LUO et al. 2022).

In terms of future monitoring initiatives on the Oder and other salt-influenced or brackish waters in which *P. parvum* could pose a risk, the various DNA-based detection methods offer a relatively simple and practical technique both for routine use and, where necessary, as an early-warning system for *P. parvum* blooms. Early detection could prove helpful for initiating appropriate management measures for controlling and containing algal blooms in a timely manner, thus minimising the detrimental effects.

6.3.2 Prevention of factors that promote algal blooms

Measures to prevent harmful algal blooms in general and *Prymnesium parvum* blooms in particular should be the top priority for preventing a repeat of the serious impact on water quality and the environment that was observed in the Oder disaster in 2022. As can be seen from the investigations in this report and the provisional Polish report (IOŚ-PIB 2022), elevated salt loads were detected in the Oder during the period around the massive fish die-off. It is likely that this, combined with high temperatures, strong solar irradiation and low water levels, provided favourable conditions for the growth of the brackish water alga *Prymnesium parvum* in the Oder.

So far, it is not known what concentrations or quantities of *P. parvum* entered the river from tributaries with high salinity or how strongly this species grew in the Oder itself. To date, there is no available data relating to the concentration of *P. parvum* in tributaries for the period preceding the algal bloom in the main course of the Oder. However, high concentrations of *P. parvum* in the Gliwice Canal in the weeks during and after the algal bloom in the main course of the Oder point to this highly saline body of water as a possible *P. parvum* input source. In September 2022, for example, up to 383 million cells of *P. parvum* per litre were found in the Gliwice Canal (IOŚ-PIB 2022). A reservoir of algal cells would therefore be available in this body of water, with the potential effect of inoculating the Oder on an ongoing basis as it flows into it. In the event that the Gliwice Canal is identified as a main input source for the Oder, control or prevention measures should be put in place here in particular.

Especially in view of the future climatic conditions that are to be expected, with increased periods of heat and drought, along with intense solar irradiation and evaporation, adapted management of substance releases is generally necessary as a means of limiting chemical substance contamination as a key stressor of aquatic ecosystems to a level they can tolerate.

Another, frequently successful aquatic management measure aimed at preventing harmful algal blooms involves reducing the input of nutrients such as nitrogen (N) and phosphorus (P), which promote the growth of plants and algae in general (FISTAROL et al. 2003, GOBLER et al. 2016, SCHINDLER et al. 2016). Despite substantial improvements in terms of reducing nutrients and contaminants, treated wastewater still exhibits much higher chemical substance contamination than natural river water. In low-flow situations, disposal of wastewater via rivers thus poses a particular hazard to river ecosystems due to increasing toxic effects of contaminants on the one hand and strong eutrophication in the wake of nutrient enrichment on the other. In view of climate change and the associated longer periods of drought, this nutrient enrichment needs to be reduced further and, if possible, stopped in the long term, by recycling the nutrients contained in wastewater in the sense of a circular economy. However, in respect of *P. parvum*, it should be noted that, in laboratory experiments involving N and/or P limitation, increased toxicity was detected, with strong P limitation leading to considerably higher toxicities than strong N limitation (JOHANSSON & GRANÉLI 1999, HAMBRIGHT et al. 2014). This is probably due to a biochemical need (e.g. auxotrophy) under nutrient limitation. It was also shown in field studies, for example, that *P. parvum* lost its competitive advantage to other phytoplankton species under non-limiting nutrient conditions and that toxicity was also greatly reduced or completely eliminated (ROELKE et al. 2007, ERRERA et al. 2008). Instead of individual measures, e.g. in relation to a reduced input of nutrients into the Oder, there seems to be a need for cross-border integrated water management that

takes account of the wide-ranging aspects and effects of management options for preventing future algal blooms of *P. parvum* as part of a holistic concept.

In addition to official regulations that limit or even prohibit the abstraction of river water in low-flow situations, flow management during such situations could also be of key importance. For instance, this could involve using water resources from impounded areas and reservoirs to maintain the flow that is necessary from an ecological perspective. However, especially in periods of drought, the flow conditions should also be viewed in connection with the regional water balance, since the flow draws heavily from the near-surface groundwater during such periods. Climate scenarios predict, for example, that there will be a shift in precipitation from the summer months to the winter (KAHLENBORN et al. 2021), which will increase the likelihood of prolonged periods without precipitation in the summer and flood hazards in the winter. Measures that improve the retention of water in the landscape and thus help protect and improve bodies of groundwater are therefore of key importance for preventing algal blooms, too. For example, these measures could involve de-sealing areas of land or removing drainage systems in agricultural areas to facilitate a slow percolation of water rather than a rapid run-off. In addition to these adaptation measures, consideration should also be given to direct action against climate change, e.g. reducing greenhouse gas emissions. Heightening public awareness of the link between climate change and the occurrence of toxic algal blooms can also help increase understanding of and support for measures to combat climate change.

6.3.3 Controlling and containing harmful algal blooms

Due to their production of cytotoxins – prymnesins – algal blooms of the *Prymnesium parvum* brackish water alga pose a concrete hazard to aquatic ecosystems. Given their toxic impact on fish, they also pose a threat to the economy (fishing, tourism) in affected areas. This is why, in addition to measures to prevent harmful algal blooms of *P. parvum* (see section 6.3.2), explicit measures to combat the algae and their toxins have been – and continue to be – developed and tested. These measures can be divided into chemical, biological and physical methods.

The efficacy of conventional chemical methods involving algicides and herbicides, such as ammonium sulphate and various copper compounds, has been successfully proven in field studies (SAGER et al. 2007, RODGERS et al. 2010). However, these algicides can have serious negative effects on other organisms and on ecosystems. Examples include the release of toxins, high oxygen consumption due to increased rates of degradation, as well as bioaccumulation and accumulation in sediments (GIBSON 1972, KENEFICK et al. 1993, LEAL et al. 2018). Although these methods have often been used to control and mitigate *P. parvum* blooms in view of their relatively cost-effective application and rapid effect, there is an increasing move away from this practice worldwide due to the undesirable effects (HAGSTRÖM et al. 2010). In recent years, there has therefore been an increasing focus on hydrogen peroxide in particular as an alternative method of combating these algal blooms. Studies have demonstrated that hydrogen peroxide, even in low concentrations that are deemed to have little or no toxic impact on fish, was able to reduce *P. parvum* effectively within one day (SOUTHARD 2005, WAGSTAFF et al. 2021). However, the effect in the field study was only of limited duration (WAGSTAFF et al. 2021), so regular application appears to be necessary. As a general rule, the use of chemicals must be carefully weighed up and the effects meticulously controlled to prevent or minimise any negative ecological impact resulting from the chemicals used. Given the

strong dilution effect in running waters, they can also only be used effectively in impounded or standing water.

To prevent or control harmful algal blooms by means of biological and less invasive methods, many studies have been conducted with barley straw and leaf litter, with some successful results (see HAGSTRÖM et al. (2010) and the references therein). The biological materials serve as an important substrate for invertebrates and zooplankton, for example, which increases the abundance of these organisms and thus the grazing on phytoplankton (NEWMAN 2004). However, it emerged that the effects vary greatly, depending on the prevalent taxa in the plankton communities, and that, overall, barley straw is regarded as being ineffective against *P. parvum* blooms (HAGSTRÖM et al. 2010). In addition to the top-down control through grazing by zooplankton, research has also been conducted into algicidal bacteria and viruses as biological agents to combat harmful algal blooms (HAGSTRÖM et al. (2010) and references therein). However, the possible effects of such biomanipulation measures on the ecosystems are unknown, which is why these measures are not currently considered a viable option. In recent years, there has been an increasing focus on allelochemicals with algicidal effects as further biological agents for combating harmful algal blooms (TANG & GOBLER 2011, BEN GHARBIA et al. 2017, XU et al. 2022). These allelochemicals are chemical compounds that are produced by organisms and affect other organisms by influencing their physiology or growth, for instance. In a study by MARY et al. (2021), for example, the alkaloid ellipticine, which was extracted from the neophyte *Arundo donax* (giant reed), was shown to be a highly potent, natural algicide against *P. parvum*. However, before this alkaloid can be used extensively as a natural, environmentally friendly method of controlling harmful algal blooms in natural ecosystems, further research and development is needed.

Clay is used as a natural flocculant and is an effective physical measure for controlling algal blooms. Clay slurry is sprayed onto the surface of the water to stop a bloom progressing. The clay particles adhere to the algal cells and sediment out with them (e.g. SHIROTA 1989, NA et al. 1996, SENGCO & ANDERSON 2005). However, the efficacy of the method very much depends on use of the right type of clay, combined with flocculants, and on the nutrient and salt content (HAGSTRÖM 2006, HAGSTRÖM et al. 2010). The direct impact on other, non-planktonic organisms, such as fish and benthic species, is estimated to be minor overall, although there is a negative effect on the respiration process in fish and the filtration rate of mussels, for example (SHUMWAY et al. 2003, RENSEL & ANDERSON 2004). It is also important to note that *Prymnesium parvum* can form dormant cysts (GREEN et al. 1982, LARSEN & EDVARDSEN 1998), and that the precipitation of the algae into the water sediment thus probably constitutes a temporary solution only. However, it was also shown that the toxins formed by *P. parvum* can be removed or neutralised by adding certain clay slurries (HAGSTRÖM & GRANÉLI 2005, SENGCO et al. 2005). Even though the use of clay slurry to treat water bodies is considered a very promising natural method of combating *P. parvum* blooms, further research is needed to gain an understanding of the precise mechanism of action and the specific application methods in the natural ecosystem, and thus to ensure effective control of the algal blooms.

In addition to these containment measures, creating refuge habitats for natural river fauna is also a suitable management technique. If these areas provide refuge habitats for organisms that are being negatively affected during system-wide algal blooms, thus protecting parts of the populations, this could speed up the recovery of the populations (ZAMOR et al. 2014). In waterways, connected oxbows that can be actively managed

could provide such refuge habitats. The active removal and short-term relocation of affected organisms such as fish is another possible option – albeit a time-consuming one – for rescuing parts of populations from watercourses for subsequent repopulation (UK GOV. ENVIRONMENT AGENCY 2015). However, an early warning system is needed for these measures so that the refuge habitats can be cut off from the affected aquatic system at the right time and the rescue operations can be initiated early on.

6.4 Knowledge gaps and needs for applied research

Based on the results of this investigation into the fish die-off in the Oder in August 2022, the following gaps in knowledge (amongst others) can be identified and the need for future applied research described:

- Closer overview of inputs of industrial and municipal effluents and the way these are controlled under different flow conditions is needed to improve understanding of the chemical substance contamination of the Oder. This particularly applies to inputs of saline effluents from mining (see section 2.3), but is also applicable to inputs of (in)organic contaminants, for example.
- Expanding and improving international networking in relation to online monitoring of key water quality parameters (including electrical conductivity, chlorophyll, pH and oxygen) along the Oder would lead to a better understanding of the influence that various environmental parameters have on the Oder ecosystem and make it possible to establish a better early warning system before extreme events.
- Since it is not possible to detect an extreme ecological event such as the fish die-off in August 2022 on the basis of alarm thresholds for individual measurement parameters being exceeded, there is an increased need to develop automated analysis systems for multiple parameters, which can help support the course of action when an event occurs.
- Given the background of a pronounced low-flow character in recent years, careful monitoring and, potentially, reassessment of the long-term development of the flow conditions in the Oder should be carried out. This should focus particularly on the question of whether this involves an emerging trend or a temporary fluctuation (decadal variability). A coherent procedure within the river basin is also needed for hydrological research in the context of international cooperation in the Oder region.
- There is insufficient knowledge about the effects of substantially elevated and greatly fluctuating salt concentrations on complex and dynamic aquatic ecosystems such as the Oder. This creates an increased need for interdisciplinary measurement programmes and field studies in relation to this topic.
- The lack of an available *Prymnesin* standard material poses a key limitation when it comes to quantifying algal toxins of *Prymnesium parvum* in the environment. Although the synthesis of the complex molecule (see Figure 5.6.4.1) involves high outlay, the production and provision of a standard material for specialist laboratories at both national and international level would represent an important step for determining the concentration of the algal toxin in environmental samples. The availability of a standard material would potentially also be of interest for studies into the ecotoxicology and behaviour of the substance under a variety of environmental conditions.

- In terms of the measures described in section 6.3.3 for controlling and containing *Prymnesium parvum* algal blooms, there is still insufficient experience of the practicality and efficacy of applying these measures to larger watercourses such as the Oder. Even though prevention should be paramount, possible control and containment concepts should also be devised and experimentally tested where appropriate.
- One important gap in knowledge is an understanding of the environmental conditions under which *Prymnesium parvum* can develop, through mass proliferation, into an algal bloom and, in particular, an understanding of which factors (e.g. nutrient situation, salt content, competition) trigger and control the formation and excretion of toxic prymnesins.
- To date, there is also insufficient information about the behaviour and stability of prymnesins in natural watercourse systems (e.g. partitioning between the water and suspended particulate matter phases, degradation pathways and degradation rates under different conditions), and research is therefore needed.

7 Summary and outlook

This report presents BfG's comprehensive investigation into the fish die-off in the Oder in August 2022. The cross-divisional collaboration, which was initiated just a few days after the first reports of dead fish in the German part of the Oder, made it possible to analyse the event quickly from a range of perspectives and subsequently work through it in detail.

The hydrological analysis revealed that the prevalent conditions in July and the first three weeks of August 2022 had involved a prolonged low-flow event with water levels that dropped relatively quickly at times, but that similar events – even if less extreme in manifestation – had already occurred in the Oder in four of the seven previous years since 2015. Abundant rainfall in the Oder catchment area from 20 August 2022 then led to a sharp increase in flow and ended the low-water phase. The low flow in the Oder was an important contributing factor to the combination of environmental conditions that made the mass proliferation of *Prymnesium parvum* possible, especially under the influence of high salt concentrations, and thus ultimately contributed to the onset of the fish die-off event. Given the pronounced low-flow character of recent years, the possibility that similar conditions will also arise in the Oder in the summers to come cannot be ruled out.

A comparison of the water quality online measurement data from the LfU Brandenburg monitoring stations in Frankfurt (Oder) and Hohenwutzen from July and August 2022 with the historical mean values and ranges of fluctuation for the respective parameters revealed that elevated values of electrical conductivity, which indicate high salt concentrations in the water of the Oder, have already occurred in the past. However, the increase in salt load at the start of the event occurred very quickly. Shortly after the increase in electrical conductivity, there was then a clear rise in oxygen content and pH in Frankfurt (Oder) from 7 August 2022. The typical fluctuations in oxygen content and pH in a diurnal pattern, together with the sharp increase in total chlorophyll content, indicated the arrival of the algal bloom. The availability of continuous measurement values from LfU Brandenburg's automatic monitoring stations proved extremely helpful for understanding the event. The expansion and further development of effective online monitoring systems is an important step along the way to improving the monitoring of rivers and ensuring the ability to react quickly if an extreme event occurs.

Analyses of the element composition revealed that the elevated salt load in the Oder during the fish die-off primarily consisted of sodium chloride (table salt). Compared to the values from the last week of July, an additional volume of around 25,600 metric tons of NaCl was transported in the Oder during the period from 5 to 15 August 2022. Following the increase in flow at the end of August as a result of rainfall, there was a second salt surge, during which an additional volume of around 76,600 metric tons of NaCl was transported in the period from 28 August to 6 September 2022. These estimated volumes of salt closely match the available information about the scale of anthropogenic inputs of saline effluents from Polish mining operations into the Oder. The trace element analysis of the Oder river water also provided indications that pointed to a source related to mining operations. The multi-element method used for this analysis, which was newly developed at BfG for quantifying 68 elements in river water samples, will prove useful for rapidly shedding light on possible sources of contaminants and identifying potentially toxic trace elements in future extreme events, too.

Various target and non-target methods were used to determine organic compounds. These results not only highlighted that the water of the Oder was contaminated with

various organic compounds (including from pesticide production), but also played a key role in ruling out potentially fish-toxic concentrations of many known organic compounds as the cause of the fish die-off. The conspicuous decline in the concentration of sulfamic acid during the fish die-off indicated that the algae were using this compound as a source of nitrogen. When analysing samples from the Oder, it was also possible to swiftly apply the algal toxin detection methods that had been developed in recent years at BfG in connection with the cyanobacteria blooms in the Moselle. Besides detecting small quantities of microcystins produced by cyanobacteria, these methods also made it possible to detect the algal toxin prymnesin-B1, which was a key element for clarifying the causes of the fish die-off. The identification of prymnesin-B1 – a substance which is produced by the brackish water alga *Prymnesium parvum* and is toxic to fish – in the samples of water from the Oder during the fish die-off confirmed the hypothesis that the algal bloom was responsible for triggering the event. The availability of a prymnesin standard would allow its concentration in environmental samples to be quantified in future investigations and facilitate further studies into the environmental behaviour and impact of the algal toxin.

In Daphnia acute immobilisation tests, the ecotoxicological studies showed considerable inhibition for some of the samples of water from the Oder. Although this inhibition was reduced when the samples were filtered, it did not disappear completely. In contrast, no inhibition occurred in the luminescent bacteria and freshwater algal growth inhibition tests. Since the toxic effect on the Daphnia no longer occurred following prolonged storage at 4 °C, it was possible to conclude that the toxin responsible has low levels of stability, and this is consistent with the available information about the prymnesins produced by *Prymnesium parvum*. For future studies, it is therefore important to note that, once samples have been taken, they need to be appropriately stored and tested very promptly. The suitability of bioassays for monitoring the quality of river water was also confirmed by the death of the organisms in the Daphnia toximeter at the LfU monitoring station in Hohenwutzen during the period of the fish die-off.

Studying the phytoplankton that occurred in the samples of water from the Oder ultimately provided another vital piece of the puzzle that makes up the overall picture of the fish die-off in the Oder. Light microscopy analysis detected the predominant presence of a single-cell microalga that was green-gold in colour. During the course of further investigations, it was subsequently identified as *Prymnesium parvum*. The highest density observed was 141 million cells per litre in Hohenwutzen on 16 August 2022. DNA was extracted from enrichment cultures of this sample, and clonal cultures were established. Molecular biological methods were then applied to perform a precise taxonomic classification, and a PCR method was used for the rapid detection and the quantification of *Prymnesium parvum* in environmental samples. Suitable methods are therefore available that can also be rapidly deployed if algal blooms reoccur in the Oder or other rivers to contribute to an early-stage risk assessment.

In addition to detecting the brackish water microalga *Prymnesium parvum* and identifying the algal toxin prymnesin in environmental samples, future studies should also focus more on possible strategies for preventing and controlling future algal blooms. To minimise future risk, one important objective would be reducing the salt concentrations in the Oder that have increased due to anthropogenic factors. As outlined in the previous section of this report, there are also various approaches for actively combating algal blooms of *Prymnesium parvum*. However, to date, there is insufficient knowledge about the practicability of these approaches in large watercourses such as the Oder, and this

should therefore be investigated in future studies. Based on the discussion of the results of the investigations and the conclusions drawn from them, a number of gaps in knowledge were identified, and the need for future applied research was described. An important finding from BfG's investigations presented in this report is also that a broad, interdisciplinary approach and close interaction between the various specialist fields involved are needed, so as to understand the complex interrelationships involved in extreme ecological events such as the fish die-off in the Oder in August 2022 and be able to derive effective measures for the future on the basis of such insights.

Acknowledgements

The study was conducted on behalf of the Federal Ministry for the Environment, Nature Conservation, Nuclear Safety and Consumer Protection (BMUV) and to provide administrative assistance to the State Laboratory Berlin-Brandenburg (LBB) and the Brandenburg State Office for the Environment (LfU). We are grateful for this trust in BfG's work.

We would like to thank the State Laboratory Berlin-Brandenburg and the Brandenburg State Office for the Environment for their good cooperation. Our particular thanks go to Mr Detlef Schmaler for providing the online measurement data and Mr Jörg Schönfelder for providing phytoplankton abundance data.

We thank Ms Tanja Burgmer and Mr Claus-Dieter Dürselen (AquaEcology GmbH) for the microscopic identification and quantification of phytoplankton.

We are grateful to all BfG staff who were involved in the investigations into the fish die-off in the Oder in summer 2022. In addition to the authors of this report, the following individuals made particular contributions:

- Transporting sample material from the Oder to the BfG premises in Koblenz: Stefan Kiefer, Ingo Habermann, Sascha Koch, Alexander Zavarsky
- Organising sample receipt and sample distribution: Corinna Brinkmann
- Supplying suspended particulate matter samples: Christine Sachsinger
- Data research and conductivity measurements: Anna-Lena Gerloff
- Assistance with sample preparation and conducting whole water digestion and chemical analyses: Michelle Feit, Iris Brühl
- Assistance with sample preparation and conducting element analyses: Nadine Belkouteb, Lorenz Gfeller, Rolf Hartmann, Mohamed Harhash
- Assistance with sample preparation and conducting organic compound analyses: Björn Ehlig, Lennart Lörke, Manoj Schulz
- Sample preparation and conducting ecotoxicological tests: Angela Koppers, Denise Spira, Michaela Theis, Anna Maria Bell
- Assistance with sample preparation and conducting phytoplankton analyses: Annette Becker, Phillip Jung, Johannes Lingen

8 Bibliography

ABBAS, B., C. HOFMANN, J. SCHÖNFELDER, L. NOACK, A. NAWROCKI, M. JUNGE, S. ROHDE, J. HAHN, A. BAKIEROWSKA, I. KAŁUZIŃSKA, M. MASŁOWSKA, M. RANISZEWSKA, E. SROKA, L. SŁOWIŃSKA, A. SIWKA & P. SUSEK Bericht über die Beschaffenheit der deutsch – polnischen Grenzgewässer. Deutsch-Polnische Grenzgewässerkommission, 72, **2022**. https://www.wasserblick.net/servlet/is/219446/

ABSALON, D., M. MATYSIK, A. WOŹNICA & N. JANCZEWSKA Detection of changes in the hydrobiological parameters of the Oder River during the ecological disaster in July 2022 based on multi-parameter probe tests and remote sensing methods. *Ecological Indicators*, **2023**, 148, 110103. doi: 10.1016/j.ecolind.2023.110103

ALTSCHUL, S. F., W. GISH, W. MILLER, E. W. MYERS & D. J. LIPMAN Basic local alignment search tool. *Journal of Molecular Biology*, **1990**, 215(3), 403-410. doi: 10.1016/S0022-2836(05)80360-2

ANDERSSON, M. Saline waste water from the hard coal sector. In M. ANDERSSON ed. *Change and Continuity in Poland's Environmental Policy.* Springer, **1999**, p. 153-174. doi: 10.1007/978-94-011-4517-6_7

BAGGELAAR, P. K. & E. C. J. VAN DER MEULEN Trendanalyse op maat voor een meetnet waterkwaliteit. *Stromingen*, **2012**, 18(2), 77-96. doi: https://www.nhv.nu/wp-content/uploads/2020/06/2012-2_trendanalyse_op_maat_voor_een_meetnet_waterkwaliteit.pdf

BELKOUTEB, N., H. SCHROEDER, J. ARNDT, J. G. WIEDERHOLD, T. A. TERNES & L. DUESTER Quantification of 68 elements in river water monitoring samples in single-run measurements. *Chemosphere*, **2023**, 320, 138053. doi: 10.1016/j.chemosphere.2023.138053

BEN GHARBIA, H., O. KÉFI-DALY YAHIA, P. CECCHI, E. MASSERET, Z. AMZIL, F. HERVE, G. ROVILLON, H. NOURI, C. M'RABET, D. COUET, H. ZMERLI TRIKI & M. LAABIR New insights on the species-specific allelopathic interactions between macrophytes and marine HAB dinoflagellates. *PLOS ONE*, **2017**, 12(11), e0187963. doi: 10.1371/journal.pone.0187963

BFG Die Niedrigwassersequenz der Jahre 2015 bis 2018 in Deutschland – Analyse, Einordnung und Auswirkungen. Koblenz: Bundesanstalt für Gewässerkunde, BfG-Mitteilungen 35, 412 Seiten, **2021**. doi: 10.5675/BfG_Mitteilungen_35.2021

BINZER, S. B., D. K. SVENSSEN, N. DAUGBJERG, C. ALVES-DE-SOUZA, E. PINTO, P. J. HANSEN, T. O. LARSEN & E. VARGA A-, B- and C-type prymnesins are clade specific compounds and chemotaxonomic markers in Prymnesium parvum. *Harmful Algae*, **2019**, 81, 10-17. doi: 10.1016/j.hal.2018.11.010

BLOSSOM, H. E., N. G. ANDERSEN, S. A. RASMUSSEN & P. J. HANSEN Stability of the intra- and extracellular toxins of *Prymnesium parvum* using a microalgal bioassay. *Harmful Algae*, **2014**, 32, 11-21. doi: 10.1016/j.hal.2013.11.006

BMUV Fischsterben in der Oder, August 2022 (Statusbericht, Stand 30.09.2022). 34 Seiten, **2022**. https://www.bmuv.de/fileadmin/Daten_BMU/Download_PDF/Binnengewaesser/Bericht_-_Fischsterben_in_der_Oder_20220929_bf.pdf

BMUV Bundesumweltministerium fördert Forschungsprojekt für bessere Frühwarnung an der Oder. 2023, https://www.bmuv.de/pressemitteilung/bundesumweltministerium-foerdert-forschungsprojekt-fuer-bessere-fruehwarnung-an-der-oder, abgerufen am 25.03.2023

BOLYEN, E., J. R. RIDEOUT, M. R. DILLON, N. A. BOKULICH, C. C. ABNET, G. A. AL-GHALITH, H. ALEXANDER, E. J. ALM, M. ARUMUGAM, F. ASNICAR, Y. BAI, J. E. BISANZ, K. BITTINGER, A. BREJNROD, C. J. BRISLAWN, C. T. BROWN, B. J. CALLAHAN, A. M. CARABALLO-RODRIGUEZ, J. CHASE, E. K. COPE, R. DA SILVA, C. DIENER, P. C. DORRESTEIN, G. M. DOUGLAS, D. M. DURALL, C. DUVALLET, C. F. EDWARDSON, M. ERNST, M. ESTAKI, J. FOUQUIER, J. M. GAUGLITZ, S. M. GIBBONS, D. L. GIBSON, A. GONZALEZ, K. GORLICK, J. GUO, B. HILLMANN, S. HOLMES, H. HOLSTE, C. HUTTENHOWER, G. A. HUTTLEY, S. JANSSEN, A. K. JARMUSCH, L. JIANG, B. D. KAEHLER, K. B. KANG, C. R. KEEFE, P. KEIM, S. T. KELLEY, D. KNIGHTS, I. KOESTER, T. KOSCIOLEK, J. KREPS, M. G. I. LANGILLE, J. LEE, R. LEY, Y. X. LIU, E. LOFTFIELD, C. LOZUPONE, M. MAHER, C. MAROTZ, B. D. MARTIN, D. MCDONALD, L. J. MCIVER, A. V. MELNIK, J. L. METCALF, S. C. MORGAN, J. T. MORTON, A. T. NAIMEY, J. A. NAVAS-MOLINA, L. F. NOTHIAS, S. B. ORCHANIAN, T. PEARSON, S. L. PEOPLES, D. PETRAS, M. L. PREUSS, E. PRUESSE, L. B. RASMUSSEN, A. RIVERS, M. S. ROBESON, 2ND, P. ROSENTHAL, N. SEGATA, M. SHAFFER, A. SHIFFER, R. SINHA, S. J. SONG, J. R. SPEAR, A. D. SWAFFORD, L. R. THOMPSON, P. J. TORRES, P. TRINH, A. TRIPATHI, P. J. TURNBAUGH, S. UL-HASAN, J. J. J. VAN DER HOOFT, F. VARGAS, Y. VAZQUEZ-BAEZA, E. VOGTMANN, M. VON HIPPEL, W. WALTERS, Y. WAN, M. WANG, J. WARREN, K. C. WEBER, C. H. D. WILLIAMSON, A. D. WILLIS, Z. Z. XU, J. R. ZANEVELD, Y.

ZHANG, Q. ZHU, R. KNIGHT & J. G. CAPORASO Reproducible, interactive, scalable and extensible microbiome data science using QIIME 2. *Nature Biotechnology*, **2019**, 37(8), 852-857. doi: 10.1038/s41587-019-0209-9

BOULARD, L., G. DIERKES, M. P. SCHLUSENER, A. WICK, J. KOSCHORRECK & T. A. TERNES Spatial distribution and temporal trends of pharmaceuticals sorbed to suspended particulate matter of German rivers. *Water Research*, **2020**, 171, 9. doi: 10.1016/j.watres.2019.115366

CALLAHAN, B. J., P. J. MCMURDIE, M. J. ROSEN, A. W. HAN, A. J. JOHNSON & S. P. HOLMES DADA2: High-resolution sample inference from Illumina amplicon data. *Nature Methods*, **2016**, 13(7), 581-583. doi: 10.1038/nmeth.3869

CHALUPNIK, S., M. WYSOCKA, E. JANSON, I. CHMIELEWSKA & M. WIESNER Long term changes in the concentration of coal mines and Upper Silesian rivers of radium in discharge waters. *Journal of Environmental Radioactivity*, **2017**, 171, 117-123. doi: 10.1016/j.jenvrad.2017.02.007

CHEUNG, M. K., C. H. AU, K. H. CHU, H. S. KWAN & C. K. WONG Composition and genetic diversity of picoeukaryotes in subtropical coastal waters as revealed by 454 pyrosequencing. *The ISME Journal*, **2010**, 4(8), 1053-1059. doi: 10.1038/ismej.2010.26

CISZEWSKI, D. & J. TURNER Storage of sediment-associated heavy metals along the channelized Odra River, Poland. *Earth Surface Processes and Landforms*, **2009**, 34(4), 558-572. doi: 10.1002/esp.1756

DIETRICH, C., A. WICK & T. A. TERNES Open-source feature detection for non-target LC-MS analytics. *Rapid Communications in Mass Spectrometry*, **2022**, 36(2), 9. doi: 10.1002/rcm.9206

DIN Deutsche Einheitsverfahren zur Wasser-, Abwasser- und Schlammuntersuchung; Testverfahren mit Wasserorganismen (Gruppe L); Bestimmung der nicht akut giftigen Wirkung von Abwasser gegenüber Daphnien über Verdünnungsstufen (L 30), DIN 38412-30:1989-03. Berlin: **1989**.

DIN Deutsche Einheitsverfahren zur Wasser-, Abwasser- und Schlammuntersuchung; Testverfahren mit Wasserorganismen (Gruppe L); Bestimmung der nicht giftigen Wirkung von Abwasser gegenüber Grünalgen (Scenedesmus-Chlorophyll-Fluoreszenztest) über Verdünnungsstufen (L 33), DIN 38412-33:1991-03. Berlin: **1991**.

DIN Wasserbeschaffenheit - Bestimmung der Hemmwirkung von Wasserproben auf die Lichtemission von Vibrio fischeri (Leuchtbakterientest) - Teil 2: Verfahren mit flüssig getrockneten Bakterien (ISO 11348-2:2007); Deutsche Fassung EN ISO 11348-2:2008, DIN EN ISO 11348-2:2009-05. Berlin: **2008**.

DUCZMAL-CZERNIKIEWICZ, A., A. BAIBATSHA, A. BEKBOTAYEVA, G. OMAROVA & A. BAISALOVA Ore Minerals and Metal Distribution in Tailings of Sediment-Hosted Stratiform Copper Deposits from Poland and Kazakhstan. *Minerals*, **2021**, 11(7), 20. doi: 10.3390/min11070752

DULIAS, R. A Brief History of Mining in the Upper Silesian Coal Basin. In R. DULIAS ed. *The Impact of Mining on the Landscape.* Cham: Springer, **2016**, p. 31-49. doi: 10.1007/978-3-319-29541-1_2

ECKFORD-SOPER, L. K. & N. DAUGBJERG Examination of six commonly used laboratory fixatives in HAB monitoring programs for their use in quantitative PCR based on Taqman probe technology. *Harmful Algae*, **2015**, 42, 52-59. doi: https://doi.org/10.1016/j.hal.2014.12.007

EDVARDSEN, B., W. EIKREM, J. THRONDSEN, A. G. SÁEZ, I. PROBERT & L. K. MEDLIN Ribosomal DNA phylogenies and a morphological revision provide the basis for a revised taxonomy of the Prymnesiales (Haptophyta). *European Journal of Phycology*, **2011**, 46(3), 202-228. doi: 10.1080/09670262.2011.594095

ERICSSON, B. & B. HALLMANS Treatment of saline wastewater for zero discharge at the Debiensko coal mines in Poland. *Desalination*, **1996**, 105(1-2), 115-123. doi: 10.1016/0011-9164(96)00065-3

ERRERA, R. M., D. L. ROELKE, R. L. KIESLING, B. W. BROOKS, J. P. GROVER, L. SCHWIERZKE, F. URENA-BOECK, J. W. BAKER & J. L. PINCKNEY Effect of imbalanced nutrients and immigration on Prymnesium parvum community dominance and toxicity: Results from in-lake microcosm experiments. *Aquatic Microbial Ecology*, **2008**, 52(1), 33-44. doi: 10.3354/ame01199

EU Richtlinie 2000/60/EG zur Schaffung eines Ordnungsrahmens für Maßnahmen der Gemeinschaft im Bereich der Wasserpolitik. **2000** https://eur-lex.europa.eu/eli/dir/2000/60?locale=de

FAMERA, M., T. M. GRYGAR, D. CISZEWSKI, A. CZAJKA, M. A. ALVAREZ-VAZQUEZ, K. HRON, K. FACEVICOVA, V. HYLOVA, S. TUMOVA, I. SVETLIK, K. ZIMOVA, K. DVORAKOVA, B. SZYPULA, M. HOSEK & J. HENYCH Anthropogenic records in a fluvial depositional system: The Odra River along The Czech-Polish border. *Anthropocene*, **2021**, 34, 11. doi: 10.1016/j.ancene.2021.100286

FEIST, S. M. & R. F. LANCE Genetic detection of freshwater harmful algal blooms: A review focused on the use of environmental DNA (eDNA) in Microcystis aeruginosa and Prymnesium parvum. *Harmful Algae*, **2021**, 110, 102124. doi: 10.1016/j.hal.2021.102124

FGG WESER Die wichtigen Fragen der Gewässerbewirtschaftung in der Flussgebietseinheit Weser. Hildesheim: Geschäftsstelle der FGG Weser, 44 Seiten, **2020**. https://www.fgg-weser.de/component/rsfiles/download-file/files?path=EG-WRRL%252Fwichtige_fragen_gewaesserbewirtschaftung_weser_20200.pdf&Itemid=111

FISTAROL, G. O., C. LEGRAND & E. GRANELI Allelopathic effect of *Prymnesium parvum* on a natural plankton community. *Marine Ecology Progress Series*, **2003**, 255, 115-125. doi: 10.3354/meps255115

FREE, G., W. VAN DE BUND, B. GAWLIK, L. VAN WIJK, M. WOOD, E. GUAGNINI, K. KOUTELOS, A. ANNUNZIATO, B. GRIZZETTI, O. VIGIAK, M. GNECCHI, S. POIKANE, T. CHRISTIANSEN, C. WHALLEY, F. ANTOGNAZZA, B. ZERGER, R. HOEVE & H. STIELSTRA An EU analysis of the ecological disaster in the Oder River of 2022. Luxembourg: Publications Office of the European Union, **2023**. 10.2760/067386

FREI, C. R. R package 'trend 1.5.1' (Functions for trend estimation and testing). 2013.

GALLUZZI, L., E. BERTOZZINI, A. PENNA, F. PERINI, A. PIGALARGA, E. GRANELI & M. MAGNANI Detection and quantification of Prymnesium parvum (Haptophyceae) by real-time PCR. *Letters in Applied Microbiology*, **2008**, 46(2), 261-266. doi: 10.1111/j.1472-765X.2007.02294.x

GAONKAR, C. C. & L. CAMPBELL Metabarcoding reveals high genetic diversity of harmful algae in the coastal waters of Texas, Gulf of Mexico. *Harmful Algae*, **2023**, 121, 102368. doi: 10.1016/j.hal.2022.102368

GIBSON, C. E. The Algicidal Effect of Copper on a Green and a Blue-Green Alga and some Ecological Implications. *Journal of Applied Ecology*, **1972**, 9(2), 513-518. doi: 10.2307/2402449

GOBLER, C. J., J. M. BURKHOLDER, T. W. DAVIS, M. J. HARKE, T. JOHENGEN, C. A. STOW & D. B. VAN DE WAAL The dual role of nitrogen supply in controlling the growth and toxicity of cyanobacterial blooms. *Harmful Algae*, **2016**, 54, 87-97. doi: 10.1016/j.hal.2016.01.010

GREEN, J. C., D. J. HIBBERD & R. N. PIENAAR The taxonomy of Prymnesium (Prymnesiophyceae) including a description of a new cosmopolitan species, P. Patellifera sp. nov., and further observations on P. parvum N. carter. *British Phycological Journal*, **1982**, 17(4), 363-382. doi: 10.1080/00071618200650381

GREENPEACE Ergebnisbericht - So schlecht geht es der Oder wirklich (Laboranalysen von Wasser-, Sediment- und Fischproben aus der Oder nach dem Fischsterben vom 26.07.-13.08.2022). Greenpeace, **2022**. https://www.greenpeace.de/publikationen/20220929_greenpeace_factsheet_fischsterben_oder_analyse.pdf

GUILLOU, L., D. BACHAR, S. AUDIC, D. BASS, C. BERNEY, L. BITTNER, C. BOUTTE, G. BURGAUD, C. DE VARGAS, J. DECELLE, J. DEL CAMPO, J. R. DOLAN, M. DUNTHORN, B. EDVARDSEN, M. HOLZMANN, W. H. KOOISTRA, E. LARA, N. LE BESCOT, R. LOGARES, F. MAHE, R. MASSANA, M. MONTRESOR, R. MORARD, F. NOT, J. PAWLOWSKI, I. PROBERT, A. L. SAUVADET, R. SIANO, T. STOECK, D. VAULOT, P. ZIMMERMANN & R. CHRISTEN The Protist Ribosomal Reference database (PR2): a catalog of unicellular eukaryote small sub-unit rRNA sequences with curated taxonomy. *Nucleic Acids Research*, **2013**, 41(Database issue), D597-604. doi: 10.1093/nar/gks1160

GZYL, G., E. JANSON & P. ŁABAJ. Mine Water Discharges in Upper Silesian Coal Basin (Poland). In *Assessment, Restoration And Reclamation Of Mining Influenced Soils.* Elsevier, **2017**, p. 463-486. doi: 10.1016/B978-0-12-809588-1.00017-7

HAGSTRÖM, J. A. *Fate of marine algal toxins in presence of bacteria and mussel or copepod faecal matter*. Department of Biology and Environmental Science, University of Kalmar, Sweden, **2006**.

HAGSTRÖM, J. A. & E. GRANÉLI Removal of Prymnesium parvum (Haptophyceae) cells under different nutrient conditions by clay. *Harmful Algae*, **2005**, 4(2), 249-260. doi: https://doi.org/10.1016/j.hal.2004.03.004

HAGSTRÖM, J. A., M. R. SENGCO & T. A. VILLAREAL Potential Methods for Managing *Prymnesium parvum* Blooms and Toxicity, With Emphasis on Clay and Barley Straw: A Review. *JAWRA Journal of the American Water Resources Association*, **2010**, 46(1), 187-198. doi: 10.1111/j.1752-1688.2009.00402.x

HAMBRIGHT, K. D., J. D. EASTON, R. M. ZAMOR, J. BEYER, A. C. EASTON & B. ALLISON Regulation of growth and toxicity of a mixotrophic microbe: implications for understanding range expansion in Prymnesium parvum. *Freshwater Science*, **2014**, 33(3), 745-754. doi: 10.1086/677198

HARAT, A., N. RAPANTOVA, A. GRMELA & Z. ADAMCZYK Impact of mining activities in the Upper Silesian coal basin on surface water and possibilities of its reduction. *Journal of Ecological Engineering*, **2015**, 16(3), 61-69. doi: 10.12911/22998993/2806

IFB Fische in der Oder – Erste Untersuchungen nach dem Fischsterben. Nicht alle Fische sind verendet! Institut für Binnenfischerei e. V. Potsdam-Sacrow (IfB), **2023**. https://daten2.verwaltungsportal.de/dateien/seitengenerator/39e60e9485fbb087a783632dbdd20658216970/fische_in_der_oder.pdf

IGB IGB Befischung nach der Oder-Katastrophe zeigt: von Erholung keine Spur 2022a, https://www.igb-berlin.de/news/befischung-nach-der-oder-katastrophe-zeigt-von-erholung-keine-spur, abgerufen am 05.04.2023

IGB Die Zukunft der Oder: Forschungsbasierte Handlungsempfehlungen nach der menschengemachten Umweltkatastrophe. Berlin: Leibniz-Institut für Gewässerökologie und Binnenfischerei, IGB Policy Brief **2022b**. 10.4126/FRL01-006431249

IGB IGB Nach der Oder-Katastrophe: Fischbestände massiv gesunken 2022c, https://www.igb-berlin.de/news/nach-der-oder-katastrophe-fischbestaende-massiv-gesunken, abgerufen am 05.04.2023

IKSO Havarieplan für die Oder. Wrocław: 28 Seiten, **2018**. http://www.mkoo.pl/index.php?mid=4&aid=763&lang=DE

IKSO Einzugsgebiet der Oder 2020, http://www.mkoo.pl/index.php?mid=2&lang=DE, abgerufen am 13.05.2020

IKSO Strategie zur Nährstoffreduzierung in den Gewässern der Internationalen Flussgebietsgemeinschaft Oder. Wrocław: 102 Seiten, **2022a**. http://www.mkoo.pl/show.php?fid=7068&lang=DE

IKSO Zweite Aktualisierung des Bewirtschaftungsplans für die Internationale Flussgebietseinheit Oder für den Bewirtschaftungszeitraum 2022-2027. Wrocław: 139 Seiten, **2022b**. http://www.mkoo.pl/show.php?fid=6996&lang=DE

INSTITUT DR. NOWAK Bericht zum Einzelauftrag AF1_WSV_20210426134955_1121 der Bundesanstalt für Gewässerkunde (BfG) für das WSA Oder-Havel zur Entnahme und Untersuchung von Sedimentproben aus dem Vorhaben „Sedimentmanagementkonzept Oder (2021)". Koblenz: Bundesanstalt für Gewässerkunde, **2021**.

IOŚ-PIB Wstępny raport zespołu ds. sytuacji na rzece Odrze. Instytut Ochrony Środowiska-Państwowy Instytut Badawczy, 260 Seiten, **2022**. https://ios.edu.pl/projekt/prezentacja-wnioskow-ze-wstepnego-raportu-zespolu-ds-sytuacji-na-rzece-odrze/

IOŚ-PIB Raport kończący prace Zespołu ds. sytuacji w Odrze. Instytut Ochrony Środowiska-Państwowy Instytut Badawczy, 191 Seiten, **2023**. https://ios.edu.pl/wp-content/uploads/2022/12/raport-konczacy-prace-zespolu-ds-sytuacji-w-odrze-2.pdf

JAMES, S. V., T. W. VALENTI, K. N. PROSSER, J. P. GROVER, D. L. ROELKE & B. W. BROOKS Sunlight amelioration of Prymnesium parvum acute toxicity to fish. *Journal of Plankton Research*, **2011**, 33(2), 265-272. doi: 10.1093/plankt/fbq082

JASKULA, J. & M. SOJKA Assessment of spatial distribution of sediment contamination with heavy metals in the two biggest rivers in Poland. *Catena*, **2022**, 211, 13. doi: 10.1016/j.catena.2021.105959

JEWELL, K. S., U. KUNKEL, B. EHLIG, F. THRON, M. SCHLUSENER, C. DIETRICH, A. WICK & T. A. TERNES Comparing mass, retention time and tandem mass spectra as criteria for the automated screening of small molecules in aqueous environmental samples analyzed by liquid chromatography/quadrupole time-of-flight tandem mass spectrometry. *Rapid Communications in Mass Spectrometry*, **2020**, 34(1), 9. doi: 10.1002/rcm.8541

JOHANSSON, N. & E. GRANÉLI Influence of different nutrient conditions on cell density, chemical composition and toxicity of Prymnesium parvum (Haptophyta) in semi-continuous cultures. *Journal of Experimental Marine Biology and Ecology*, **1999**, 239(2), 243-258. doi: https://doi.org/10.1016/S0022-0981(99)00048-9

JONES, M., J. WILLIAMS, K. GARTNER, R. PHILLIPS, J. HURST & J. FRATER Low copy target detection by Droplet Digital PCR through application of a novel open access bioinformatic pipeline, 'definetherain'. *Journal of Virological Methods*, **2014**, 202(100), 46-53. doi: 10.1016/j.jviromet.2014.02.020

KAHLENBORN, W., L. PORST, M. VOß, L. DORSCH, S. LACOMBE, B. HUBER, M. ZEBISCH, A. BOCK, J. KLEMM, A. CRESPI, K. RENNER, C. LUTZ, L. BECKER, P. ULRICH, M. DISTELKAM, J. BEHMER, A. WALTER, N. LEPS, S. WEHRING, E. NILSON & K. JOCHUMSEN Klimawirkungs- und Risikoanalyse 2021 für Deutschland. Teilbericht 1: Grundlagen **2021** https://www.umweltbundesamt.de/publikationen/KWRA-Teil-1-Grundlagen

KARCZEWSKA, A., J. KASZUBKIEWICZ, C. KABAŁA, P. JEZIERSKI, Z. SPIAK & K. SZOPKA. Tailings impoundments of polish copper mining industry - environmental effects, risk assessment and reclamation. In *Assessment, restoration and reclamation of mining influenced soils.* Elsevier, **2017**, p. 149-202. doi: 10.1016/B978-0-12-809588-1.00006-2

KCEPIŃSKI, J. Desalination and Utilization of saline mine waters in Poland. *Desalination*, **1980**, 32, 399-408. doi: 10.1016/S0011-9164(00)86040-3

KENEFICK, S. L., S. E. HRUDEY, H. G. PETERSON & E. E. PREPAS Toxin Release from Microcystis Aeruginosa after Chemical Treatment. *Water Science and Technology*, **1993**, 27(3-4), 433-440. doi: 10.2166/wst.1993.0387

KORNEVA, L. Recent invasion of planktonic diatom algae in the Volga River basin and their causes. *Biology of Inland Waters*, **2007**, 1, 28-36. doi:

KREBS, F. Der pT-Wert: Ein Gewässertoxikologischer Klassifizierungs-Maßstab. *GIT Fachzeitschrift für das Laboratorium*, **1988**, 32, 293-296. doi: nicht vorhanden

KREBS, F. Ökotoxikologische Bewertung von Baggergut aus Bundeswasserstraßen mit Hilfe der pT-Wert-Methode. *Hydrologie und Wasserbewirtschaftung*, **2000**, 44, 301-307. doi: https://www.hywa-online.de/oekotoxikologische-bewertung-von-baggergut-aus-bundeswasserstrassen-mit-hilfe-der-pt-wert-methode/

LARSEN, A. & B. EDVARDSEN Relative ploidy levels in Prymnesium parvum and P. patelliferum (Haptophyta) analyzed by flow cytometry. *Phycologia*, **1998**, 37(6), 412-424. doi: 10.2216/i0031-8884-37-6-412.1

LEAL, P. R., V. MOSCHINI-CARLOS, J. C. LÓPEZ-DOVAL, J. P. CINTRA, J. K. YAMAMOTO, M. D. BITENCOURT, R. F. SANTOS, G. C. ABREU & M. L. M. POMPÊO Impact of copper sulfate application at an urban Brazilian reservoir: A geostatistical and ecotoxicological approach. *Science of The Total Environment*, **2018**, 618, 621-634. doi: https://doi.org/10.1016/j.scitotenv.2017.07.095

LFU Automatisches Gewässergütemessnetz im Land Brandenburg. Messstationen zur Gewässergüteüberwachung und Gefahrenabwehr an Oder, Elbe und Havel 111, 30 Seiten, **2009**. https://lfu.brandenburg.de/lfu/de/ueber-uns/veroeffentlichungen/detail/~23-10-2009-automatisches-gewaesserguetemessnetz-fachbeitraege-heft-111

LUO, N., H. HUANG & H. JIANG Establishment of methods for rapid detection of Prymnesium parvum by recombinase polymerase amplification combined with a lateral flow dipstick. *Frontiers in Marine Science*, **2022**, 9. doi: https://www.frontiersin.org/articles/10.3389/fmars.2022.1032847

LYDZBA, D., A. RÓŻAŃSKI, M. SOBÓTKA & P. STEFANEK Optimization of technological measures increasing the safety of the Żelazny Most tailings pond dams with the combined use of monitoring results and advanced computational models. *Archives of Civil Engineering*, **2022**, 68(1), 503-518. doi: 10.24425/ace.2022.140182

MACHER, T. H., A. J. BEERMANN & F. LEESE TaxonTableTools: A comprehensive, platform-independent graphical user interface software to explore and visualise DNA metabarcoding data. *Molecular Ecology Resources*, **2021**, 21(5), 1705-1714. doi: 10.1111/1755-0998.13358

MALBROUCK, C. & P. KESTEMONT Effects of microcystins on fish. *Environmental Toxicology and Chemistry*, **2006**, 25(1), 72-86. doi: 10.1897/05-029r.1

MANNING, S. R. & J. W. LA CLAIRE Multiplex PCR methods for the species-specific detection and quantification of Prymnesium parvum (Haptophyta). *Journal of Applied Phycology*, **2010**, 22(5), 587-597. doi: 10.1007/s10811-009-9498-6

MARY, M. A., R. H. RASHEL & R. PATIÑO Growth inhibition of the harmful alga Prymnesium parvum by plant-derived products and identification of ellipticine as highly potent allelochemical. *Journal of Applied Phycology*, **2021**, 33(6), 3853-3860. doi: 10.1007/s10811-021-02545-6

MATYSIK, M. Hazards to the quality of surface water from discharge of saline mining waters in the upper Oder River Basin. *AIP Conference Proceedings*, AIP Publishing LLC, 120007, **2019**. doi: 10.1063/1.5138038

MEYER, A. Die Belastung der Oder - Ergebnisse des Internationalen Oderprojekts Hamburg: **2002**. ISBN 3-924330-54-9 https://docplayer.org/storage/17/81770/1675869715/_4e5N4TKru-_O8R4qJOEjQ/81770.pdf

MILLER, M. A., W. PFEIFFER & T. SCHWARTZ 2010. Creating the CIPRES Science Gateway for inference of large phylogenetic trees. *2010 Gateway Computing Environments Workshop (GCE)*, 1-8.

MISCHKE, U. & H. BEHRENDT *Handbuch zum Bewertungsverfahren von Fließgewässern mittels Phytoplankton zur Umsetzung der EU-WRRL in Deutschland*. Schweizerbart, **2015**. ISBN 9783510653287.

MITKO, K., M. TUREK, H. JAROSZEK, E. BERNACKA, M. SAMBOR, P. SKORA & P. DYDO Pilot studies on circular economy solution for the coal mining sector. *Water Resources and Industry*, **2021**, 26, 9. doi: 10.1016/j.wri.2021.100161

MORA, D., N. ABARCA, S. PROFT, J. H. GRAU, N. ENKE, J. CARMONA, O. SKIBBE, R. JAHN & J. ZIMMERMANN Morphology and metabarcoding: a test with stream diatoms from Mexico highlights the complementarity of identification methods. *Freshwater Science*, **2019**, 38(3), 448-464. doi: 10.1086/704827

MÜLLER, A., P. HEININGER, M. WESSELS, J. PELZER, K. GRUNWALD, S. PFITZNER & M. BERGER Contaminant levels and ecotoxicological effects in sediments of the river Odra. *Acta Hydrochimica Et Hydrobiologica*, **2003**, 30(5-6), 244-255. doi: 10.1002/aheh.200390006

MÜLLER, K., J. MÜLLER, C. NEINHUIS & D. QUANDT. PhyDE–Phylogenetic Data Editor, version 0.9971. Program distributed by the authors. 2010. http://www.phyde.de/.

NA, G.-H., W.-J. CHOI & Y.-Y. CHUN A study on red tide control with loess suspension. *Journal of Aquaculture*, **1996**, 9(3), 239-245. doi: https://koreascience.kr/article/JAKO199607523622911.pdf

NEWMAN, J. Control of algae with barley straw. Crowmarsh Gifford, Wallingford, Oxon: United Kingdom: Centre for Aquatic Plant Management, **2004**. https://nora.nerc.ac.uk/id/eprint/19957/1/BarleyStrawtocontrolalgae.pdf

NÜRENBERG, G., M. SCHULZ, U. KUNKEL & T. A. TERNES Development and validation of a generic nontarget method based on liquid chromatography - high resolution mass spectrometry analysis for the evaluation of different wastewater treatment options. *Journal of Chromatography A*, **2015**, 1426, 77-90. doi: 10.1016/j.chroma.2015.11.014

OGEWV Verordnung zum Schutz von Oberflächengewässern (Oberflächengewässerverordnung - OGewV) **2016** https://www.gesetze-im-internet.de/ogewv_2016/OGewV.pdf

PAZDERSKI, L., M. PAZDERSKA-SZABŁOWICZ & A. MERES Salinisation of Poland's Two Major Rivers by Mining Companies - A Greenpeace study. Warsaw: Greenpeace, **2023**. https://www.greenpeace.de/publikationen/20230302-greenpeace-report-oder-en.pdf

PORCO, D., S. HERMANT, C. A. PURNOMO, M. HORN, G. MARSON & G. COLLING Getting rid of 'rain' and 'stars': Mitigating inhibition effects on ddPCR data analysis, the case study of the invasive crayfish Pacifastacus leniusculus in the streams of Luxembourg. *PLoS One*, **2022**, 17(11), e0275363. doi: 10.1371/journal.pone.0275363

RAMBAUT, A. FigTree-version 1.4. 3, a graphical viewer of phylogenetic trees.: Computer program distributed by the author 2017. http://tree.bio.ed.ac.uk/software/figtree.

RASMUSSEN, S. A., S. MEIER, N. G. ANDERSEN, H. E. BLOSSOM, J. O. DUUS, K. F. NIELSEN, P. J. HANSEN & T. O. LARSEN Chemodiversity of Ladder-Frame Prymnesin Polyethers in Prymnesium parvum. *Journal of Natural Products*, **2016**, 79(9), 2250-2256. doi: 10.1021/acs.jnatprod.6b00345

RENSEL, J. E. J. & D. M. ANDERSON Effects of phosphatic clay dispersal at two divergent sites in Puget Sound, Washington. *Xth International Conference on Harmful Algae, October 2002*, K.A. STEIDINGER, J.H. LANDSBERG, C.R. TOMAS & G.A. VARGO eds. Florida Fish and Wildlife Conservation Commission 522-524, **2004**. doi:

RODGERS, J. H. J., B. M. JOHNSON & W. M. BISHOP Comparison of Three Algaecides for Controlling the Density of *Prymnesium parvum*. *JAWRA Journal of the American Water Resources Association*, **2010**, 46(1), 153-160. doi: 10.1111/j.1752-1688.2009.00399.x

ROELKE, D. L., A. BARKOH, B. W. BROOKS, J. P. GROVER, K. D. HAMBRIGHT, J. W. LACLAIRE, P. D. R. MOELLER & R. PATINO A chronicle of a killer alga in the west: ecology, assessment, and management of Prymnesium parvum blooms. *Hydrobiologia*, **2016**, 764(1), 29-50. doi: 10.1007/s10750-015-2273-6

ROELKE, D. L., R. M. ERRERA, R. KIESLING, B. W. BROOKS, J. P. GROVER, L. SCHWIERZKE, F. URENA-BOECK, J. BAKER & J. L. PINCKNEY Effects of nutrient enrichment on Prymnesium parvum population dynamics and toxicity: Results from field experiments, Lake Possum Kingdom, USA. *Aquatic Microbial Ecology*, **2007**, 46(2), 125-140. doi: 10.3354/ame046125

SAG CULTURE COLLECTION SAG 18.97 *Prymnesium parvum* 2023, https://sagdb.uni-goettingen.de/detailedList.php?str_number=18.97, abgerufen am 01.03.2023

SAGER, D. R., L. L. FRIES, L. SINGHURST, G. M. SOUTHARD & I. FISHERIES Guidelines for Golden Alga *Prymnesium parvum* Management Options for Ponds and Small Reservoirs (Public Waters) in Texas. Austin, Texas, USA: **2007**. https://tpwd.texas.gov/publications/pwdpubs/media/pwd_rp_t3200_1404.pdf

SAYERS, E. W., M. CAVANAUGH, K. CLARK, K. D. PRUITT, C. L. SCHOCH, S. T. SHERRY & I. KARSCH-MIZRACHI GenBank. *Nucleic Acids Research*, **2022**, 50(D1), D161-D164. doi: 10.1093/nar/gkab1135

SCHINDLER, D. W., S. R. CARPENTER, S. C. CHAPRA, R. E. HECKY & D. M. ORIHEL Reducing Phosphorus to Curb Lake Eutrophication is a Success. *Environmental Science & Technology*, **2016**, 50(17), 8923-8929. doi: 10.1021/acs.est.6b02204

SCHWIERZKE-WADE, L., D. L. ROELKE, B. W. BROOKS, J. P. GROVER & T. W. VALENTI *Prymnesium parvum* bloom termination: role of hydraulic dilution. *Journal of Plankton Research*, **2011**, 33(2), 309-317. doi: 10.1093/plankt/fbq108

SENGCO, M. & D. ANDERSON Removal of *Prymnesium parvum* Through Clay and Chemical Flocculation. Austin, Texas, USA: **2005**. https://tpwd.texas.gov/publications/pwdpubs/media/pwd_rp_t3200_1177.pdf

SENGCO, M. R., J. A. HAGSTRÖM, E. GRANÉLI & D. M. ANDERSON Removal of Prymnesium parvum (Haptophyceae) and its toxins using clay minerals. *Harmful Algae*, **2005**, 4(2), 261-274. doi: https://doi.org/10.1016/j.hal.2004.05.001

SHIROTA, A. Red tide problem and countermeasures. II. *Int. J. Aqua. Fish. Technol.*, **1989**, 1, 195-223. doi: https://cir.nii.ac.jp/crid/1571980076264681856

SHUMWAY, S. E., D. M. FRANK, L. M. EWART & J. EVAN WARD Effect of yellow loess on clearance rate in seven species of benthic, filter-feeding invertebrates. *Aquaculture Research*, **2003**, 34(15), 1391-1402. doi: https://doi.org/10.1111/j.1365-2109.2003.00958.x

SOLLINGER, L., L. HEERMANN & S. STAAS 2023. Leben am Limit: Konsequenzen von Niedrigwasserereignissen für die Fischfauna von Fließgewässern. *Internationales Wasserbau-Symposium (vIWASA)* Aachen, Januar 2023.

SOUTHARD, G. M. Use of Hydrogen Peroxide as an Algaecide for *Prymnesium parvum*. In A. BARKOH & L.T. FRIES eds. *Management of Prymnesium parvum at Texas State Fish Hatcheries.* Austin, TX, USA: Texas Parks and Wildlife Department, **2005**, p. 35-38. doi: https://tpwd.texas.gov/publications/pwdpubs/media/pwd_rp_t3200_1138_chapter7.pdf

SPAULDING, S. A., C. KILROY & M. B. EDLUND. Diatoms as non-native species. In E.F. STOERMER & J.P. SMOL eds. *The Diatoms: Applications for the Environmental and Earth Sciences.* Cambridge: Cambridge University Press, **2010**, p. 560-569. doi: 10.1017/CBO9780511763175.033

SPAULDING, S. A., M. G. POTAPOVA, I. W. BISHOP, S. S. LEE, T. S. GASPERAK, E. JOVANOSKA, P. C. FUREY & M. B. EDLUND Diatoms.org: supporting taxonomists, connecting communities. *Diatom Research*, **2021**, 36(4), 291-304. doi: 10.1080/0269249X.2021.2006790

STAMATAKIS, A. RAxML version 8: a tool for phylogenetic analysis and post-analysis of large phylogenies. *Bioinformatics*, **2014**, 30(9), 1312-1313. doi: 10.1093/bioinformatics/btu033

STAMATAKIS, A., P. HOOVER & J. ROUGEMONT A rapid bootstrap algorithm for the RAxML Web servers. *Systematic Biology*, **2008**, 57(5), 758-771. doi: 10.1080/10635150802429642

STEPIEN, D. K. & W. PUTTMANN Source identification of high glyme concentrations in the Oder River. *Water Research*, **2014**, 54, 307-317. doi: 10.1016/j.watres.2014.01.067

SVENSSEN, D. K., S. B. BINZER, N. MEDIC, P. J. HANSEN, T. O. LARSEN & E. VARGA Development of an Indirect Quantitation Method to Assess Ichthyotoxic B-Type Prymnesins from Prymnesium parvum. *Toxins*, **2019**, 11(5). doi: 10.3390/toxins11050251

SWOLKIEŃ, J. & K. FILEK Wpływ zmian technologicznych w kolektorze „Olza" na skład chemiczny wód rzeki Odry i jej dopływów. *Rocznik Ochrona Środowiska*, **2012**, 14, 945-959. doi: http://www.towarzystwo.ros.edu.pl/images/roczniki/archive/pp_2012_076.pdf

SZPOR, A. & K. ZIÓŁKOWSKA Transformation of the Polish coal sector. International Institute for Sustainable Development (IISD), GSI report 25 Seiten, **2018**. https://www.iisd.org/system/files/publications/transformation-polish-coal-sector.pdf

TANG, Y. Z. & C. J. GOBLER The green macroalga, Ulva lactuca, inhibits the growth of seven common harmful algal bloom species via allelopathy. *Harmful Algae*, **2011**, 10(5), 480-488. doi: https://doi.org/10.1016/j.hal.2011.03.003

TSALIDIS, G. A., K. P. TOURKODIMITRI, K. MITKO, G. GZYL, A. SKALNY, J. A. POSADA & D. XEVGENOS Assessing the environmental performance of a novel coal mine brine treatment technique: A case in Poland. *Journal of Cleaner Production*, **2022**, 358, 9. doi: 10.1016/j.jclepro.2022.131973

TUREK, M., P. DYDO & R. KLIMEK Salt production from coal-mine brine in ED-evaporation-crystallization system. *Desalination*, **2005**, 184(1-3), 439-446. doi: 10.1016/j.desal.2005.03.047

TUSZYNSKI, J. R. R package 'caTools 1.17' (Tools: moving window statistics, GIF, Base64, ROC AUC, etc.). 2014. https://cran.r-project.org/web/packages/caTools/caTools.pdf.

UK GOV. ENVIRONMENT AGENCY Quarter of a million fish rescued in Norfolk Broads 2015, https://www.gov.uk/government/news/quarter-of-a-million-fish-rescued-in-norfolk-broads, abgerufen am 21.03.2023

VAN DAM, H., A. MERTENS & J. SINKELDAM A coded checklist and ecological indicator values of freshwater diatoms from The Netherlands. *Netherland Journal of Aquatic Ecology*, **1994**, 28(1), 117-133. doi: 10.1007/BF02334251

VIDAKOVIĆ, D., J. KRIZMANIĆ, G. SUBAKOV-SIMIĆ & V. KARADŽIĆ Distribution of invasive species Actinocyclus normanii (Hemidiscaceae, Bacillariophyta) in Serbia. *Studia Botanica Hungarica*, **2016**, 47(2), 201-212. doi: 10.17110/StudBot.2016.47.2.201

WAGSTAFF, B. A., E. S. HEMS, M. REJZEK, J. PRATSCHER, E. BROOKS, S. KUHAUDOMLARP, E. C. O'NEILL, M. I. DONALDSON, S. LANE, J. CURRIE, A. M. HINDES, G. MALIN, J. C. MURRELL & R. A. FIELD Insights into toxic Prymnesium parvum blooms: the role of sugars and algal viruses. *Biochemical Society Transactions*, **2018**, 46(2), 413-421. doi: 10.1042/BST20170393

WAGSTAFF, B. A., J. PRATSCHER, P. P. L. RIVERA, E. S. HEMS, E. BROOKS, M. REJZEK, J. D. TODD, J. C. MURRELL & R. A. FIELD Assessing the Toxicity and Mitigating the Impact of Harmful Prymnesium Blooms in Eutrophic Waters of the Norfolk Broads. *Environmental Science & Technology*, **2021**, 55(24), 16538-16551. doi: 10.1021/acs.est.1c04742

WALSH, P. S., D. A. METZGER & R. HIGUCHI Chelex 100 as a medium for simple extraction of DNA for PCR-based typing from forensic material. *Biotechniques*, **1991**, 10(4), 506-513. doi: https://www.ncbi.nlm.nih.gov/pubmed/1867860

WIEDERHOLD, J. G. & A. SCHMIDT. Radioaktive Stoffe in Binnengewässern. In *Umweltradioaktivität in der Bundesrepublik Deutschland : Bericht der Leitstellen des Bundes und des Bundesamtes für Strahlenschutz ; Stand 2021, Daten und Bewertung.* Bundesministerium für Umwelt, Naturschutz, nukleare Sicherheit und Verbraucherschutz (BMUV), **2022**, p. 52-60. doi: http://nbn-resolving.de/urn:nbn:de:0221-2022010530428

WIESNER-SĘKALA, M. & B. KOŃCZAK Assessment of the Impact of Industrial and Municipal Discharges on the Surface Water Body Status (Poland). *Sustainability*, **2023**, 15(2), 997. doi: 10.3390/su15020997

WITECKI, K. & A. GROTOWSKI Technical, technological and environmental aspects of the management of technological waters in mines and concentrators owned by KGHM Polska Miedź SA. *IOP Conference Series: Materials Science and Engineering*, IOP Publishing, 012021, **2019**. doi: 10.1088/1757-899X/641/1/012021

WOLKERSDORFER, C., R. BOWELL, I. F. WALDER, S. NILSSEN, M. RAISANEN, P. HEIKKINEN, K. PULKKINEN, K. KORKKA-NIEMI, V. P. SALONEN, G. DESTOUNI, A. HASCHE, A. J. WITKOWSKI, A. BLACHERE, A. MOREL, D. LEFORT, S. MIDZIC, I. SILAJDZIC, R. H. COULTON, K. P. WILLIAMS, B. REES, K. B. HALLBERG & D. B. JOHNSON Contemporary Reviews of Mine Water Studies in Europe, Part 2. *Mine Water and the Environment*, **2005**, 24, 2-37. doi: 10.1007/s10230-005-0068-0

WYSOCKA, M., S. CHALUPNIK, I. CHMIELEWSKA, E. JANSON, W. RADZIEJOWSKI & K. SAMOLEJ Natural Radioactivity in Polish Coal Mines: An Attempt to Assess the Trend of Radium Release into the Environment. *Mine Water and the Environment*, **2019**, 38(3), 581-589. doi: 10.1007/s10230-019-00626-0

XU, C., S. YU, J. HU, K. EFFIONG, Z. GE, T. TANG & X. XIAO Programmed cell death process in freshwater Microcystis aeruginosa and marine Phaeocystis globosa induced by a plant derived allelochemical. *Science of The Total Environment*, **2022**, 838, 156055. doi: https://doi.org/10.1016/j.scitotenv.2022.156055

YARIMIZU, K., S. SILDEVER, Y. HAMAMOTO, S. TAZAWA, H. OIKAWA, H. YAMAGUCHI, L. BASTI, J. I. MARDONES, J. PAREDES-MELLA & S. NAGAI Development of an absolute quantification method for ribosomal RNA gene copy numbers per eukaryotic single cell by digital PCR. *Harmful Algae*, **2021**, 103, 102008. doi: 10.1016/j.hal.2021.102008

YUE, S. & C. Y. WANG The Mann-Kendall test modified by effective sample size to detect trend in serially correlated hydrological series. *Water Resources Management*, **2004**, 18(3), 201-218. doi: 10.1023/b:Warm.0000043140.61082.60

ZAMOR, R. M., N. R. FRANSSEN, C. PORTER, T. M. PATTON & K. D. HAMBRIGHT Rapid recovery of a fish assemblage following an ecosystem disruptive algal bloom. *Freshwater Science*, **2014**, 33(2), 390-401. doi: 10.1086/675508

ZAMOR, R. M., K. L. GLENN & K. D. HAMBRIGHT Incorporating molecular tools into routine HAB monitoring programs: Using qPCR to track invasive Prymnesium. *Harmful Algae*, **2012**, 15, 1-7. doi: https://doi.org/10.1016/j.hal.2011.10.028

ZGORSKA, A., J. BONDARUK, M. DUDZIAK & A. HAMERLA Impact of Industrial Discharge on Aquatic Ecosystems of the Klodnica River with Reference to Water Framework Directive Objectives. *Polish Journal of Environmental Studies*, **2020**, 29(4), 2945-2953. doi: 10.15244/pjoes/112931

ZHU, P., H.-L. HUANG, C.-X. ZHOU, J. XU, L.-L. QIAO, C.-Y. DANG, J.-H. PANG, W.-F. GAO & X.-J. YAN Sensitive and rapid detection of Prymnesium parvum (Haptophyceae) by loop-mediated isothermal amplification combined with a lateral flow dipstick. *Aquaculture*, **2019**, 505, 199-205. doi: https://doi.org/10.1016/j.aquaculture.2019.02.059

ZIELIŃSKI, S., S. KOSTECKI & P. STEFANEK Numerical analysis of the transport of brine in the Odra River downstream of a mine's discharge. *Studia Geotechnica et Mechanica*, **2021**, 43(4), 366-379. doi: 10.2478/sgem-2021-0036

Annex 1: Description of methods

A1.2.2 Trend analysis statistical procedure

Statistical processing of the long-term measurement data was carried out with the help of the Trendanalist program (see https://www.amo-nl.com/software/trendanalist and BAGGELAAR & VAN DER MEULEN 2012). This included identification of existing long-term trends by means of the non-parametric Mann-Kendall test at a significance level $p \leq 0.05$. This process also involved evaluating seasonal variations in the data series by means of seasonal component (s), and existing trends between the same points in time in the individual years analysed were examined.

The Mann-Kendall test has a tendency to underestimate the prevalent variance when there is an autocorrelation, i.e. a serial dependency within a data set, e.g. when an annual data series correlates with itself at an earlier point in time. The data sets were therefore examined to determine whether an autocorrelation (a) was present. If it was, it was corrected automatically using the approach described by YUE & WANG (2004).

A1.5.3 Element analysis

Sample preparation:

The water samples were filtered through 0.45 µm syringe filters (CA, cellulose acetate) into 50 ml centrifuge tubes (PP). Distilled, concentrated nitric acid was added to acidify the samples to an acidity of 1.3% HNO_3 (= 2 vol%). For the whole water samples, microwave digestion was performed on 25 ml of unfiltered water sample with 6 ml concentrated hydrochloric acid and 2 ml concentrated nitric acid (= aqua regia digestion). The digested samples were subsequently topped up with water to 50 ml and allowed to settle, and an aliquot of the supernatant was removed for further analysis. Once the suspended particulate matter samples had been freeze-dried, 1 g of each sample was digested in the microwave with 10 ml concentrated nitric acid. It was then transferred and topped up to 100 ml with ultrapure water. Depending on the expected concentration range, some of the solutions were also diluted with matrix solution (1.3% HNO_3 or 1:50 aqua regia) by a factor of 2, 10 or 50 prior to the ICP-QQQ-MS measurement.

ICP-QQQ-MS:

A triple quadrupole inductively coupled plasma mass spectrometer (ICP-QQQ-MS, Agilent 8900) was used for the measurements. The multi-element method used has been developed and validated at BfG over recent years (BELKOUTEB et al. 2023). This method makes it possible to measure the concentrations of 68 elements (Li, Be, B, C, Na, Mg, Al, Si, P, S, Cl, K, Ca, Sc, Ti, V, Cr, Mn, Fe, Co, Ni, Cu, Zn, Ga, Ge, As, Se, Br, Rb, Sr, Y, Nb, Mo, Ru, Pd, Ag, Cd, In, Sn, Sb, Te, Cs, Ba, La, Ce, Pr, Nd, Sm, Eu, Gd, Tb, Dy, Ho, Er, Tm, Yb, Lu, Hf, Ta, W, Ir, Pt, Hg, Tl, Pb, Bi, Th, U) in a single analysis run. It involves use of three different multi-element standard solutions, each with an adapted acid matrix and an element-specific calibration range extending over more than four orders of magnitude. Rhodium (Rh) and rhenium (Re) are used as the internal standard for correcting instrumental drift and matrix effects, since measurable concentrations of these elements are not normally found in environmental samples. However, after elevated Re signals were unexpectedly detected during the first measurement series of water samples from the Oder, Re was added as a calibrated analyte for the method in the second and third measurement series, and only Rh was used as the internal standard.

The quality of the measured concentration data was verified by means of measurements of several reference materials (SPS-SW1, SPS-SW2, TMDA 51.5, BAM U115) and measurements of standard solutions as a sample in all three measurement series. With the exception of a few outliers for certain elements, the results were consistently within the range of 90-110% of the certified values. In each measurement series, the limit of quantification was individually calculated as the mean value plus tenfold standard deviation of replicate measurements (n ≥10) of the acid matrix (1.3% HNO_3) used to dilute the samples and standards. In the first and third measurement series of the samples from the Oder being discussed here, there was an elevated background signal for Si, which was probably caused by contamination; this was also the case for Zn in the first measurement series. It was therefore not possible to determine concentrations for these elements in these measurement series. However, highly elevated values for these elements in the samples measured could be semiquantitatively excluded by means of the registered measurement signals (cps).

X-ray fluorescence analysis (XRF)

Once the suspended particulate matter samples from the BfG Hohenwutzen monitoring station for the months of March to July 2022 and for 1 to 15 August 2022 had been freeze-dried, energy-dispersive X-ray fluorescence analysis (Spectro XEPOS) was performed on powder preparations in order to measure the total element concentrations. The measured element concentrations (Al, P, Si, As, Br, Ca, Cl, Co, Cr, Cu, Fe, Ga, Ge, K, Mg, Mn, Ni, S, Se, Ti, V, Y, Zn, Zr, Ag, Ba, Bi, Cd, Hg, Mo, Na, Nb, Pb, Rb, Sb, Sn, Sr, Tl) can be used for comparison of the values determined by means of ICP-QQQ-MS following nitric acid digestion.

A1.5.4 Organic compound analysis

Non-target screening by means of LC-ESI-QqToF-MS (section 5.4.1)

Non-target screening by means of LC-ESI-QqToF-MS was used to analyse trace organic compounds. This is a generic method that can be used to detect a broad range of substance classes.

Sample preparation:

Water: Samples were only filtered (0.45 µm), and a mix of three internal standards was added.

Suspended particulate matter: The samples were measured according to BOULARD et al. (2020) with the non-target method.

Algal biomass: The sample preparation protocol for detecting algal toxins from the biomass by means of LC-NTS was as follows:

Step	Procedure
1	Filter a 500 ml sample via a glass fibre filter (Whatman GF6 glass fibre filter, 55 mm diameter, ref. no. 10 370 003). Also filter 500 ml MilliQ water as a blank value.
2	Put the filtrate into a 500 ml Schott bottle.
3	Using rinsed tweezers, transfer the filter into 50 ml PP centrifuge tubes (VWR 50 ml Centrifuge Tubes, Metal-Free, cat. no. 525-0462).
4	Add 20 ml LC/MS methanol.
5	Vortex for 10 seconds.
6	Ultrasonic bath for 30 min.
7	Centrifuge for 15 min at 4,248 g and 4 °C.
8	Put the extract into a 50 ml PP centrifuge tube.
9	Repeat the extraction (steps 4 to 7).
10	Combine extract from the second extraction with extract from the first extraction -> 40 ml/sample.
11	Completely evaporate the extract in a water bath at 35 °C in a stream of nitrogen.
12	Reconstitute with 1.2 ml LCMS methanol/MilliQ water 90:10.
13	Vortex for 10 seconds.
14	Transfer to 1.5 ml centrifuge vials.
15	Centrifuge for 5 min at 12,100 g and room temperature.
16	Transfer the supernatant to glass HPLC vials.

Analysis

Non-target measurements were performed using high-resolution mass spectrometry (ESI-QqToF-MS) coupled with liquid chromatography (C18 column, water/acetonitrile gradient). Full-scan measurements were made from 100 to 1,200 Da, and MS^2 measurements from 30 Da (NÜRENBERG et al. 2015). Peak detection software was used to process the data (DIETRICH et al. 2022), and screening of known substances was performed with the help of several substance libraries (JEWELL et al. 2020).

For the retrospective quantification, either external calibration series or individual standards with known concentration of the substances to be quantified were created in ultrapure water, and a mix of three internal standards was added. The analysis was carried out using the method described. The evaluation of the quantification by means of the calibration series was performed using the MultiQuant software, and the quantification by means of individual standards was conducted using R and the peak detection software.

Quantification of organic compounds in suspended particulate matter using GC-MS (section 5.4.2)

The suspended particulate matter samples were analysed for various groups of organic compounds.

Sample preparation for analysis of PAHs, mineral oil hydrocarbons (MOHs), chlorinated organic compounds and polybrominated diphenyl ethers:

The suspended particulate matter samples were first freeze-dried and ground in a ball mill. A quantity of 5 g of the milled suspended particulate matter was weighed out and extracted by means of pressurised liquid extraction (PLE) at an increased temperature (120 °C) with a mixture of isohexane and acetone. For desulphurisation, 2 g of copper powder were added to the extraction cells. Deuterated or ^{13}C-labelled internal standard substances were added to the extract for all analyte groups (apart from MOHs). The volume of the extract was reduced to 1 ml by means of vacuum parallel evaporation, and the obtained extract was divided up between the different measurement methods. While the PAHs were measured directly from the obtained extract by means of GC-MS/MS, the mineral oil hydrocarbons were purified with Florisil before being measured by GC-FID. For the chlorinated organic compounds and polybrominated diphenyl ethers, the extract was purified over a column with silica sulphuric acid and then quantified with GC-MS/MS.

Sample preparation for detecting organotin compounds:

Internal standard was first added to the homogenised, wet suspended particulate matter samples, which were then treated with methanolic potassium hydroxide solution. The samples were then buffered with glacial acetic acid and modified with the derivatisation reagent bromomagnesium tetraethylborate before extraction took place with isohexane on a horizontal shaker. A clean-up was performed on an aluminium oxide / silver nitrate column to purify the extract (DIN EN ISO 23161:2019-04). The extract obtained was concentrated and measured by means of GC-MS/MS.

Analysis by means of ion chromatography mass spectrometry (section 5.4.3)

A combination of ion chromatography and tandem mass spectrometry was available for analysing anions, oxohalides, haloacetic acids and other small organic compounds with a negative charge.

Sample preparation

Approximately 1 ml of the homogenised sample was filtered. A pipette was used to transfer 800 µl of the filtered sample to an HPLC vial, and 800 µl ACN and 10 µl of internal standard were added.

Analysis

The analyses were performed following US EPA method 300.A and B and US EPA 557. The IC separation took place on an A Supp 5 column (100 × 4 mm, Metrohm) under a Na_2CO_3 / $NaHCO_3$ gradient.

A1.5.5 Ecotoxicology

Luminescent bacteria test according to DIN EN ISO 11348-2 (DIN 2008)

In the investigations with the luminescent bacteria test, the acute impact on the *Aliivibrio fischeri* bacterium was recorded. In the test, the inhibition of the bioluminescence produced by the bacteria was measured before and after a 30-minute period of exposure, with this inhibition expressed as a percentage. According to the standard used, inhibition of 20% is considered a significant effect. In this case, further sample dilutions with a dilution factor of 2 are analysed.

The luminescent bacteria test was first carried out as a screening test on microplates (MPLs) and then performed in glass cuvettes in line with the standard.

Freshwater algal growth inhibition test according to DIN 38412-33 (DIN 1991)

In the freshwater algal growth inhibition test, the inhibition of the biomass production of the limnic alga *Desmodesmus subspicatus* was measured in comparison to a control, with this inhibition expressed as a percentage. The tests took place in rotating light exposure cabinets in the semi-micro standard, i.e. the test preparations were exposed in glass reagent tubes containing a test volume of 4 ml for 72 hours in the exposure chamber. According to the standard, growth inhibition of 20% is considered significant.

The freshwater algal growth inhibition tests were carried out on unfiltered and filtered samples (Whatman GF 6 glass fibre filter). The purpose of the filtration step was to ensure that the potential presence of other algae would not have any influence on the measurement results.

Daphnia acute immobilisation test according to DIN 38412-30 (DIN 1989)

The Daphnia acute immobilisation test was used to record the impact on the *Daphnia magna* microcrustacean. The inhibition of the creatures' ability to move, i.e. their immobility, expressed as a percentage, was measured after 24 and 48 hours. The smallest dilution level at which at least 9 out of 10 Daphnia retain their ability to swim is key to the classification of a sample.

A1.5.6 Phytoplankton

A1.5.6.2.1 Light microscopy analysis of environmental samples and clonal cultures

Isolation of single cells and subsequent cultivation:

Eleven days after the start of the enrichment cultures (see section 5.6.2.1), single cells were isolated from an enrichment culture with a salt content of 10 g/l, since this exhibited the highest abundance of *Prymnesium* cells. The cells were isolated using micro-capillaries that were produced manually in house from glass Pasteur pipettes under a light microscope (Leitz DM IRBE) with 100-fold magnification (MORA et al. 2019). A drop of the enrichment culture was first applied to a slide and diluted with an algal culture medium (Alga-Gro; Carolina Biology Supply Comp.) with the same salt concentration. Each isolated cell was transferred to a clean slide, and a drop of culture medium was added. From there, each cell was then isolated again. This two-stage isolation technique ensured a higher probability that a single cell would be successfully isolated, without also transferring contaminating cells of non-target organisms that were present in the

enrichment culture. Approximately 30 single cells were isolated in total. These were distributed between eight 0.5 ml microcentrifuge tubes and used for subsequent DNA extraction (see Annex A1.5.6.2.2). In order to establish clonal cultures, 12 single cells were put into a sterile 12-well cell culture plate (i.e. one cell in each well), which was filled to around 75% of its capacity with freshly prepared algal culture medium with the same salt concentration (10 g/l). The culture plate was incubated at room temperature under ambient light conditions. When the plate was examined under a light microscope after one week and after two weeks, no cells could be detected. Observations after five weeks revealed dense growth of *Prymnesium*-typical cells in 4 of the 12 cultures, while one other culture also contained a high abundance of a centric diatom. Examinations under a light microscope with magnification by a factor of 630 and 1,000 confirmed the identity of the cells as *Prymnesium*. The five cultures were then divided into aliquots of approximately 50 µl on another 12-well culture plate, with one complete plate being used per culture. After 10 days, 1 ml aliquots from one culture in each plate (well A1) were transferred to sterile Petri dishes and topped up with nutrient medium. After another 12 days, the contents of each Petri dish were transferred to 15 ml microcentrifuge tubes (approx. 7 ml) and used for subsequent DNA extraction (see Annex A1.5.6.2.2). The Petri dishes were again topped up with nutrient medium, sealed with Parafilm and further cultivated at room temperature. Aliquots of each of the four successfully established unialgal clonal cultures of *Prymnesium parvum* from the Oder were deposited in the Central Collection of Algal Cultures (CCAC) at the University of Duisburg-Essen.

A1.5.6.2.2 Molecular phylogenetic analysis for species and phylotype identification

DNA extraction from single cells:

The DNA was extracted from single cells using Chelex resin (Bio-Rad) in solutions of 10% and 20% (four samples in each case). Firstly, 150 µl of the Chelex solution was added to each microcentrifuge tube, and the tubes were incubated for 2 min at 98 °C. The samples were then placed in a cooled rack (-20 °C) and kept in a freezer for 15 min at -20 °C. Next, the samples were thawed, homogenised briefly and centrifuged for 1 min at 3,000 rpm. The supernatant was then transferred to a new 0.5 ml microcentrifuge tube. This supernatant, which contained the extracted DNA, was used for the PCR amplification and stored at -20 °C until its further use.

DNA extraction from clonal cultures:

To extract DNA from the *P. parvum* clonal cultures, 7 ml of each culture was taken, transferred to separate sterile 15 ml centrifuge tubes and then centrifuged for 5 min at 4,000 rpm. The supernatant was discarded without disturbing the pellet. The pellet and the remaining liquid were transferred to a sterile 1.5 ml microcentrifuge tube and centrifuged again at 11,000 rpm. The supernatant was then discarded. The DNA was subsequently extracted using the NucleoSpin® Plant II Mini Kit (Macherey-Nagel, Germany), following the manufacturer’s instructions and using 60 µl of Elution Buffer PE in two steps (30 µl in each case). The concentrations of the extracted DNA were then measured by spectrophotometer (NanoDrop™ OneC, Thermo Fisher Scientific; concentration between 1.6 and 3.3 ng/µl), and the extracted DNA was then stored at -20 °C until its further use.

PCR amplification:

For the DNA extracted from single cells, amplifications were performed for the V4 region of the 18S rRNA gene with primers TAReuk454FWD1 (5′-CCAGCASCYGCGGTAATTCC-3′; Stoeck et al. 2010) and TAReukREV3_mod (5′-ACTTTCGTTCTTGATYRATGA-3′; Piredda et al. 2017). Details of the PCR reactions and cycler conditions can be found in Table A1.5.6.2.2. The resultant PCR products were used for re-amplification with 2 µl of the PCR product. The PCR conditions were identical to the first PCR. The PCR products were separated by electrophoresis in a 2% agarose gel and visualised.

Using the DNA extracted from the clonal cultures, PCR reactions were performed with primers 1F (5′-AACCTGGTTGATCCTGCCAGT-3′) and 1528R (5′-TGATCCTTCTGCAGGTTCACCTAC-3′) for the almost complete 18S rRNA gene (Medlin et al. 1988) and with primers ITS1 (5′-TCCGTAGGTGAACCTGCGG-3′) and ITS4 (5′-TCCTCCGCTTATTGATATGC-3′) for the internal transcribed spacer regions (ITS1-5.8S-ITS2) (White et al. 1990). Details of the PCR reactions and cycler conditions can be found in Table A1.5.6.2.2. The PCR products were separated by electrophoresis in a 2% agarose gel and visualised. PCR products to be sequenced were then cleaned up using the Exo-CIP Rapid PCR Cleanup Kit (New England Biolabs) in accordance with the manufacturer's instructions. The bidirectional sequencing with the amplification primers was carried out by the sequencing service company GENEWIZ Germany GmbH (Leipzig, Germany). In addition, amplicons of the 18S rRNA gene were sequenced with internal primers targeted at the hypervariable 18S-V4 region (TAReuk454FWD1/ TAReukREV3_mod) in order to increase the sequence overlapping for a more reliable sequence assembly.

Table A1.5.6.2.2 *Details of the PCR reactions and cycler conditions.*

Marker	18S-V4 region	18S rDNA	ITS
PCR mix			
Forward primer (10 µM)	1 µl	1 µl	1 µl
Reverse primer (10 µM)	1 µl	1 µl	1 µl
Polymerase mix*	16 µl	12.5 µl	12.5 µl
Nuclease-free water		3.5 µl	3.5 µl
Template DNA	12 µl	3 µl	3 µl
Reaction volume	30 µl	21 µl	21 µl
PCR mix re-amplification			
Forward primer (10 µM)	1 µl		
Reverse primer (10 µM)	1 µl		
Polymerase mix*	12.5 µl		

Nuclease-free water		8.5 µl							
Template DNA		2 µl							
Reaction volume		25 µl							
PCR conditions									
	Temp.	Time	Cycles	Temp.	Time	Cycles	Temp.	Time	Cycles
Initial denaturation	94 °C	2 min	1	94 °C	6 min	1	95 °C	12 min	1
Denaturation	94 °C	45 sec		94 °C	1 min		95 °C	30 sec	
Hybridisation	50 °C	45 sec	35	55 °C	1 min	35	54 °C	30 sec	35
Elongation	72 °C	1 min		68 °C	2 min		72 °C	40 sec	
Final elongation	72 °C	10 min	1	68 °C	5 min	1	72 °C	5 min	1

*DreamTaq™ Hot Start Green PCR Master Mix (Thermo Scientific™)

Sequence assembly and phylogenetics:

The sequence data obtained by means of Sanger sequencing was reviewed manually and assembled with the Phyde® program (MÜLLER et al. 2010) to obtain consensus sequences for the respective marker region. The resulting consensus sequences were then compared with the NCBI nucleotide collection (ALTSCHUL et al. 1990) using the BLASTn search (SAYERS et al. 2022). Since all the consensus sequences obtained for the respective marker regions were identical, only one sequence per marker was used for the subsequent phylogenetic analyses. Three data sets were created for this purpose: 1) 18S-rDNA; consisting of the 18S-rDNA sequences in almost full length, 2) 18S-V4; consisting of the same sequences as the previous data set, plus one sequence from the single cell analysis, but limited to the hypervariable V4 region, and 3) ITS; consisting of sequences that cover the ITS1-5.8S-ITS2 region. The 18S-rDNA/18S-V4 data sets were supplemented by 32 sequences of various Haptophyta that were contained in the NCBI database based on EDVARDSEN et al. (2011), including three *Phaeocystis* strains as an outgroup. The ITS data set contained 31 *P. parvum* sequences, including the 26 sequences that were analysed in BINZER et al. (2019). Phylogenetic maximum likelihood (ML) analyses were carried out on the CIPRES platform (MILLER et al. 2010) with RAxML (STAMATAKIS et al. 2008; STAMATAKIS 2014). The general time reversible (GTR) model with gamma distribution (Γ) and a proportion of invariant sites (I) was selected for all three data sets, and a bootstrap analysis with 1,000 pseudo-replicates was carried out (based on EDVARDSEN et al. (2011) for the 18S data sets and BINZER et al. (2019) for ITS). The resulting phylogenies were visualised in the FigTree program, version 1.4.3 (RAMBAUT 2017), and processed in Inkscape 1.0.

A1.5.6.3.1 Rapid detection with the PCR method

DNA extraction:

For each water sample tested, 200 to 300 ml of water was filtered (Pall MicroFunnel GN-6, 0.45 µm), and the filters were stored at -20 °C. The DNA was then extracted from one half of the filter using a Qiagen Powerwater Kit and following the manufacturer's instructions (with slight modifications). Once Buffer PW1 had been added, the filters were secured horizontally on a vortex mixer, shaken for 1 min at 3,000 rpm and then incubated for 15 min at 65 °C and 500 rpm. Following the wash step with ethanol, the spin columns were air-dried for 5 min. The DNA was then dissolved in 100 µl of warm Buffer EB (55 °C) and stored at -20 °C until its further use.

Amplification primers:

The following specific primers for *Prymnesium parvum* were used for the end-point PCR reaction: PrymF/R-3 for the internal transcribed spacer 2 region (ITS2; GALLUZZI et al. 2008, ZAMOR et al. 2012), FUCO-F1/R1 for the fucoxanthin chlorophyll a/c-binding protein (MANNING & LA CLAIRE 2010) and GST-F1/R1 for glutathione S-transferase (MANNING & LA CLAIRE 2010). For the quantitative droplet digital PCR, only the PrymF/R-3 primer pair for ITS2 was used.

PCR reaction conditions:

For the end-point PCR, all DNA extracts were diluted to 10 ng/µl, and 2 µl of each was used in a 20 µl PCR reaction. The PCR was performed with the DreamTaq HotStart Mastermix Green (Thermo Scientific™) and a final primer concentration of 250 nM for PrymF/R-3 and 500 nM for FUCO-F1/R1 and GST-F1/R1. The amplification conditions were as follows: 5 min at 95 °C; 40 cycles with 15 sec at 95 °C, 30 sec at 60 °C, 30 sec at 72 °C; 5 min at 72 °C; hold at 16 °C.

For the ddPCR, the DNA extracts were diluted in various ways, based on the results of the conventional PCR. All the daily composite samples from Hohenwutzen (HW_TM) and the environmental sample from the Rhine that was used were diluted to 20 ng/µl. The two grab samples taken from Hohenwutzen and Frankfurt (Oder) on 24 August 2022 were diluted to 2 ng/µl, and the grab sample taken from Hohenwutzen on 16 August 2022 was diluted to 200 pg/µl. Next, 5 µl of each of these DNA dilutions was used in a 20 µl PCR mixture that also contained the QX200™ EvaGreen™ ddPCR SuperMix (Bio-Rad) and a final primer concentration of 250 nM. The amplification conditions for the droplet PCR were as follows: 5 min at 95 °C; 40 cycles with 30 sec at 95 °C, 1 min at 60 °C; 5 min at 4 °C; 5 min at 90 °C; hold at 10 °C; all steps with a ramp rate of 2 °C/min.

Analysis process:

The amplification products of the conventional PCR were separated on 2% agarose gel by means of electrophoresis (25 min at 120V). The agarose gel was stained with peqGREEN DNA dye (VWR, Germany) following the manufacturer's instructions, and 5 µl of the PCR product was used. The DNA bands were then visualised under UV light (UVP Gelstudio Plus, Analytik Jena).

The ddPCR products were analysed using the QX200 ddPCR System (Bio-Rad Laboratories, Inc., Germany), and the raw data (amplitude values) was then exported and processed further. The mean values and their standard deviations (SD) were first calculated for the positive and negative droplets using a k-means algorithm (JONES et al. 2014). Based on these values, an upper and lower threshold value for the positive droplets was set (mean value ± 5*SD, modified according to PORCO et al. 2022) to reduce

false-positive and false-negative results to the greatest possible extent. The number of copies and the 95% confidence interval was then calculated with the “Poisson Law” web-based application (Stilla Technologies, https://www.gene-pi.com/statistical-tools/poisson-law/).

A1.5.6.3.2 DNA metabarcoding

Aliquots of the DNA extracted from the environmental samples (see Annex A1.5.6.3.1 Rapid detection with the PCR method) were sent to sequencing service provider Novogene Co. Ltd. (UK) for DNA analysis by means of amplicon sequencing. The V4 region of the 18S rRNA gene (18S-V4) was amplified with primers 528F (5'-GCGGTAATTCCAGCTCCAA-3') and 706R (5'-AATCCRAGAATTTCACCTCT-3') (CHEUNG et al. 2010). The amplicons that were obtained were sequenced on an Illumina NovaSeq 6000 platform (250bp paired-end reads); the amplification, library preparation, sequencing and demultiplexing were carried out by Novogene. The bioinformatic analysis of the demultiplexed sequence files was then carried out in QIIME2 (BOLYEN et al. 2019) with the DADA2 denoising algorithm (CALLAHAN et al. 2016) in order to derive amplicon sequence variants (ASVs). The taxonomic classification of the ASVs was carried out using the QIIME2 Naïve Bayes classification algorithm and a pre-trained classifier of the curated database PR2 v.4.14.0 (GUILLOU et al. 2013). The resulting taxonomy table was then imported into TaxonTableTools for data exploration and visualisation (MACHER et al. 2021). The de.NBI Cloud, which is within the German Network for Bioinformatics Infrastructure (de.NBI) and funded by the German Federal Ministry of Education and Research (BMBF), was used for the bioinformatic analysis.

A1.5.6.4 Algal toxins

LC-HRMS measurements

See section A1.5.4

Extraction of the algal biomass

The algal biomass was extracted as described by SVENSSEN et al. (2019) and briefly described here. Filtration of 200 ml of surface water (Whatman GF 6, Ø 55 mm, Dassel, Germany) and transfer of the filter to a 50 ml polypropylene tube. Double extraction of the filter with methanol (LCMS grade, 20 ml in each case) in an ultrasonic bath for 30 min with subsequent centrifugation (15 min, 4,220 g, 4 °C). Transfer and combination of the supernatants to a new 50 ml polypropylene tube. Evaporation of the extract under nitrogen at 35 °C until dryness, re-uptake in 1 ml methanol / ultrapure water (90:10) and transfer to an HPLC glass vial using a membrane syringe filter (Spartan 13/0.45 RC, Whatman, Dassel, Germany). The extract was stored in the refrigerator at 8 °C for a maximum of seven days until LC-HRMS measurement.

Annex 2: Additional figures and remarks (in German only)

A2.2.3 Informationen zu anthropogenen Einflüssen

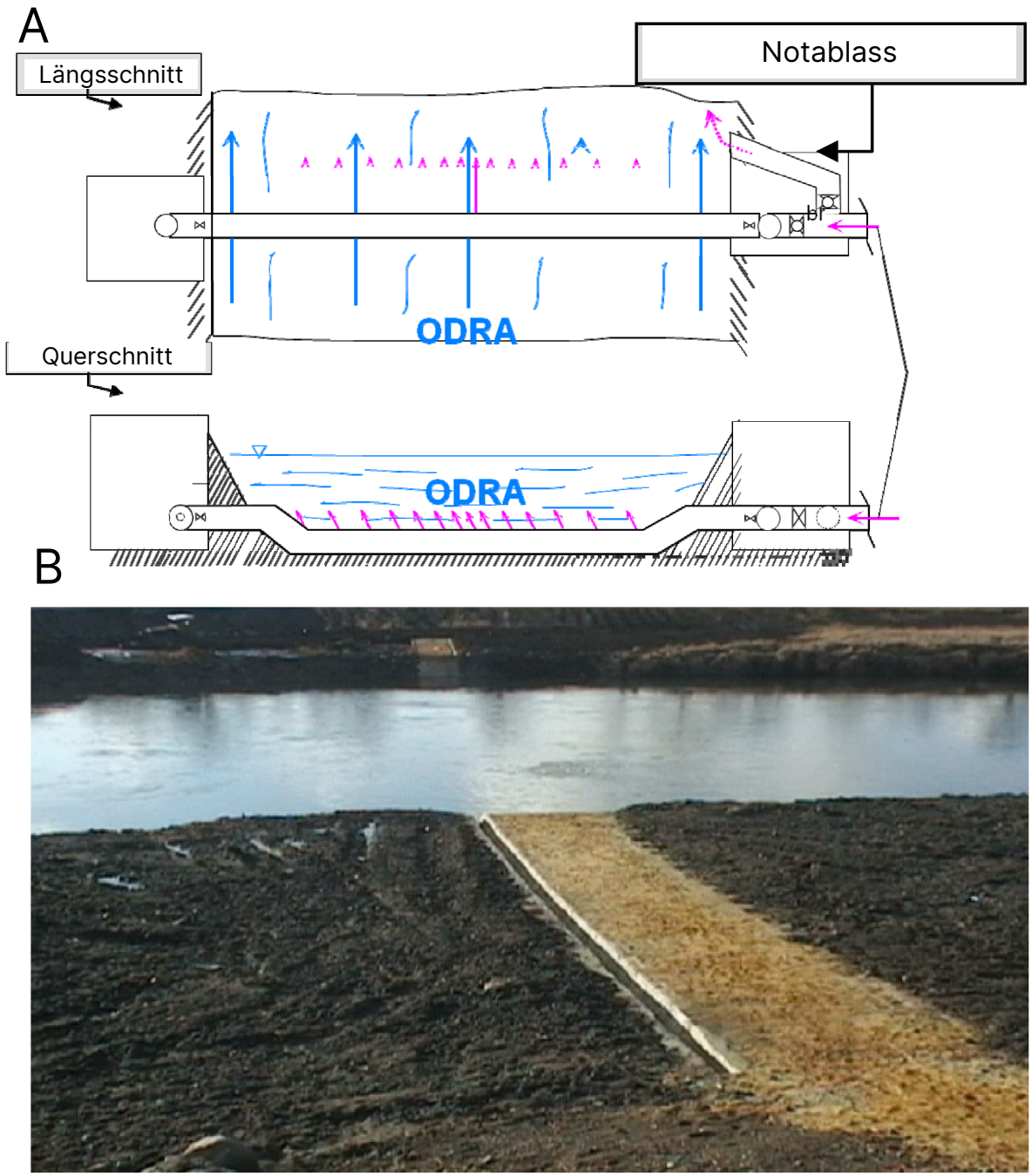

Abbildung A2.2.3.1 *(A) Schema des Einleitsystems für salzhaltige Abwässer der oberschlesischen Kohleminen in die Oder über den „Olza Kollektor“ (verändert nach SWOLKIEŃ & FILEK 2012) kurz hinter der tschechisch-polnischen Grenze vor Krzyżanowice, (B) Foto der Einleitstelle des „Olza Kollektor“ in die Oder (SWOLKIEŃ & FILEK 2012)*

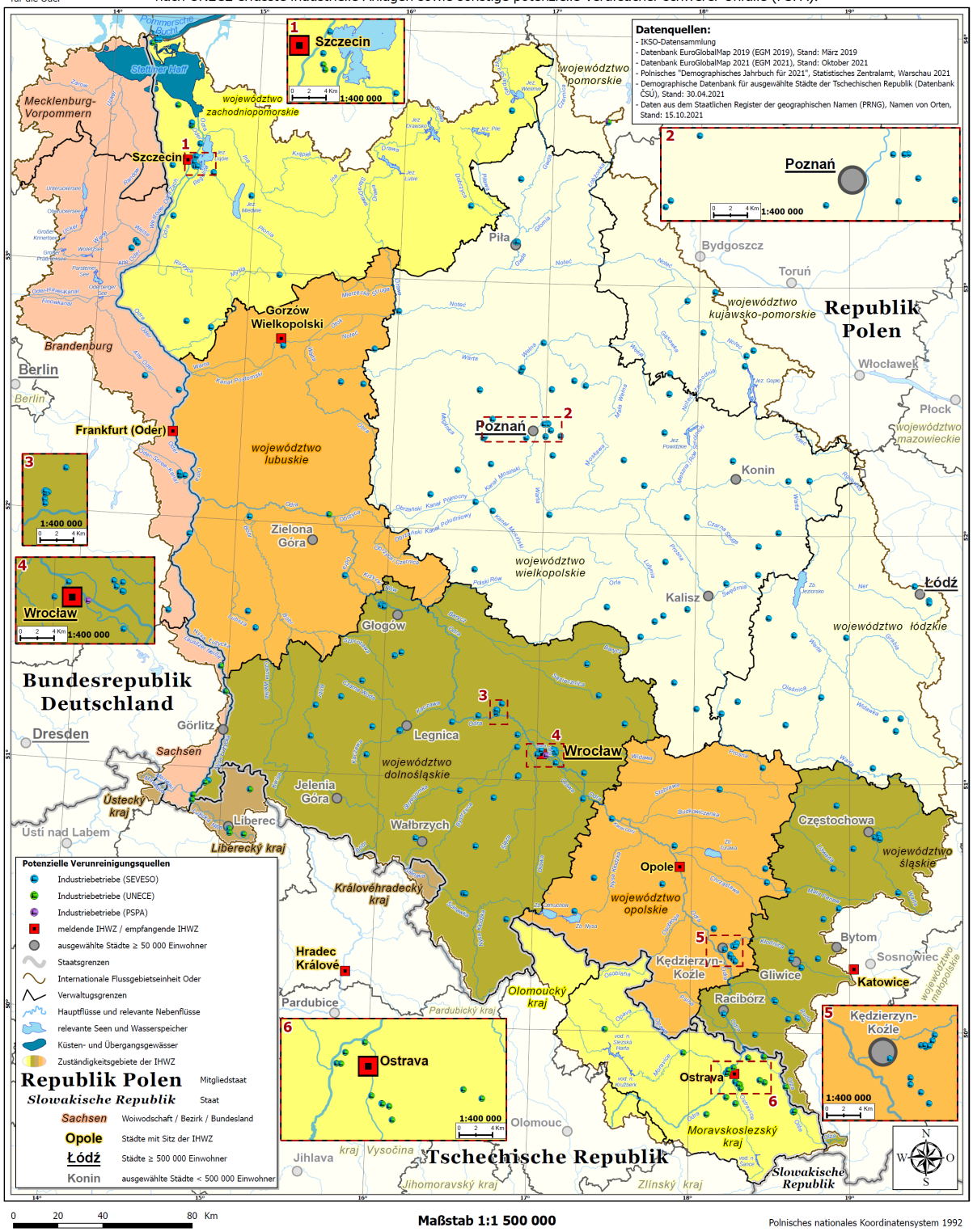

Abbildung A2.2.3.2 *Anlage 4 des „Havarieplan für die Oder“ (IKSO, 2018)*

A2.4.1 Radioaktivitätsmessungen

Die BfG-Messstation Hohenwutzen ist eine von 40 Stationen des Radioaktivitätsmessnetzes an den Bundeswasserstraßen, das die BfG gemeinsam mit der WSV (Wasserstraßen- und Schifffahrtsverwaltung des Bundes) im gesetzlichen Auftrag (StrlSchG §161) betreibt (WIEDERHOLD & SCHMIDT 2022). Als Online-Messung wird dabei in einer mit Flusswasser durchströmten Messschale kontinuierlich der Summenparameter Gesamt-Gamma-Aktivitätskonzentration bestimmt. Die Messwerte des Oderwassers waren im Zeitraum 01.-15.8.2022 (Abbildung A2.4.1.2) genauso wie in den Vormonaten unauffällig und zeigten die üblichen und durch natürliche Radionuklide (z. B. K-40 und U-Th-Zerfallsprodukte) erklärbaren Hintergrundwerte von ca. 5-7 Bq/l. Einzelne kurzzeitige Anstiege auf >10 Bq/l lassen sich durch den Vergleich mit veröffentlichten Daten des DWD teilweise auf kleinere Niederschlagsereignisse zurückführen, die zu einem Auswaschen natürlicher Radionuklide aus der Atmosphäre und damit einem kurzzeitigen Anstieg im Flusswasser führen. Die im IMIS (Integriertes Mess- und Informationssystem des Bundes zur Überwachung der Radioaktivität in der Umwelt) festgelegte Warnschwelle von 25 Bq/l, deren Überschreiten über einen längeren Zeitraum zu einer näheren Untersuchung bezüglich eines möglichen Eintrages künstlicher Radionuklide in das Flusswasser führen würde, wurde im untersuchten Zeitraum nicht erreicht. Es kann somit festgehalten werden, dass das in der Oder beobachtete Fischsterben mit größter Wahrscheinlichkeit nicht durch einen Eintrag radioaktiver Stoffe in den Fluss ausgelöst wurde.

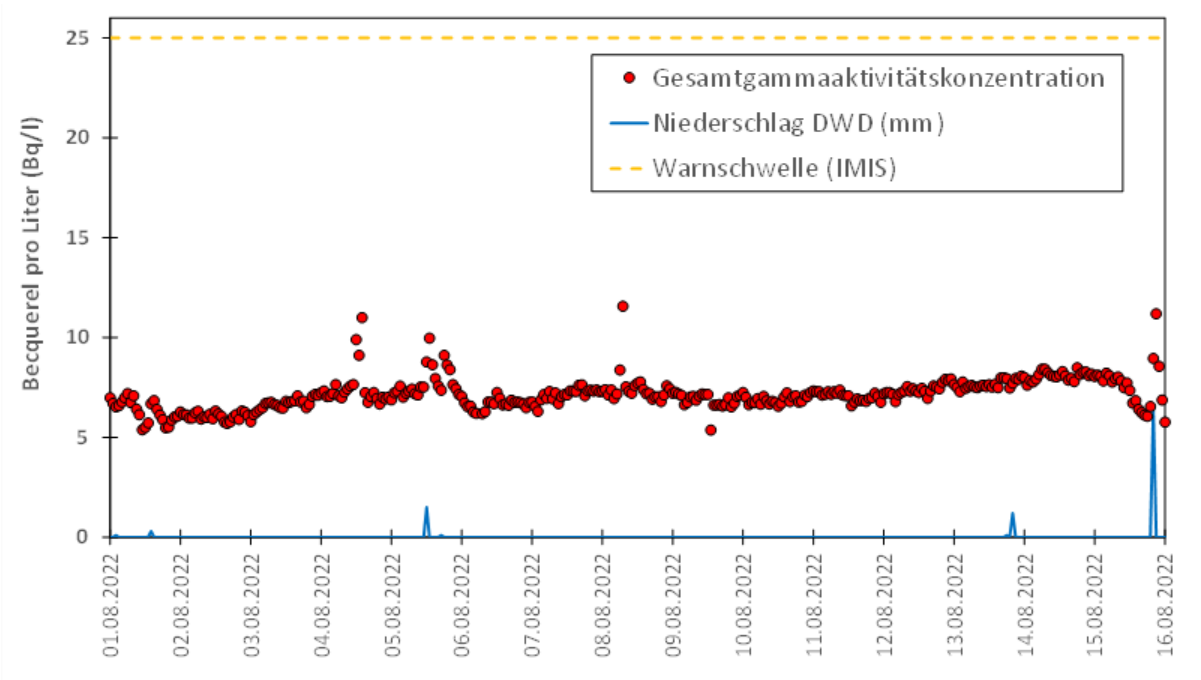

Abbildung A2.4.1.2 *Stundenmittelwerte der Gesamt-Gamma-Aktivitätskonzentration (Summenparameter Umweltradioaktivität) im Oderwasser an der BfG-Messstation Hohenwutzen im Zeitraum 01.-16.08.2022.*

A2.5.3 Elementzusammensetzung

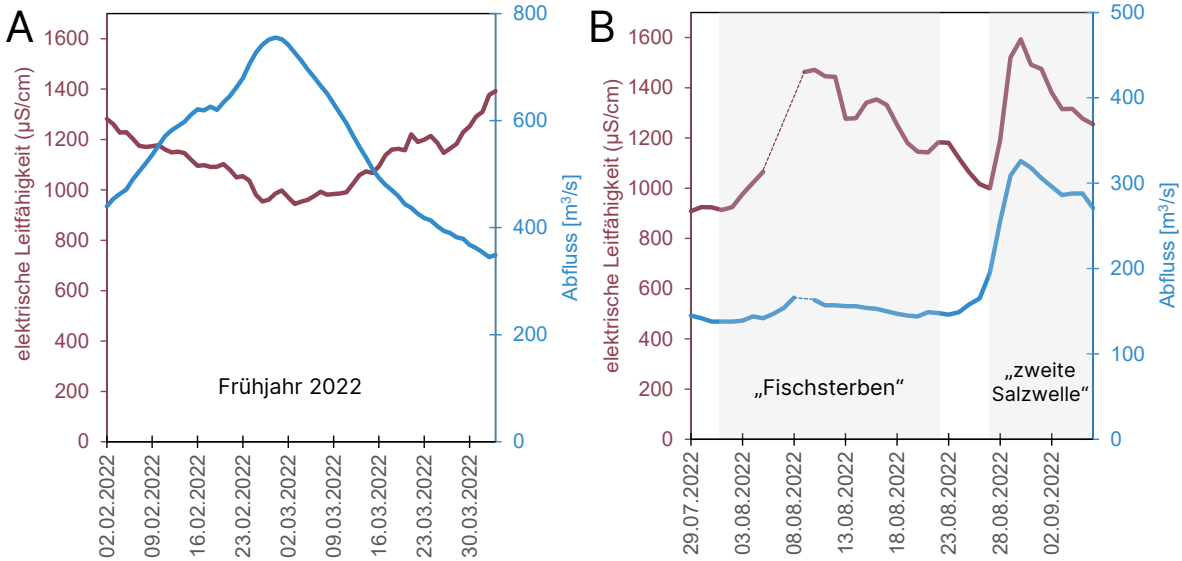

Abbildung A2.5.3.1.1 *Zeitlicher Verlauf von elektrischer Leitfähigkeit in Hohenwutzen (linke y-Achsen) und Abfluss am Pegel Hohensaaten-Finow (rechte y-Achsen) (A) im Frühjahr 2022 (02.02.-03.04.2022) und (B) im Zeitraum 29.07.-06.09.2022.*

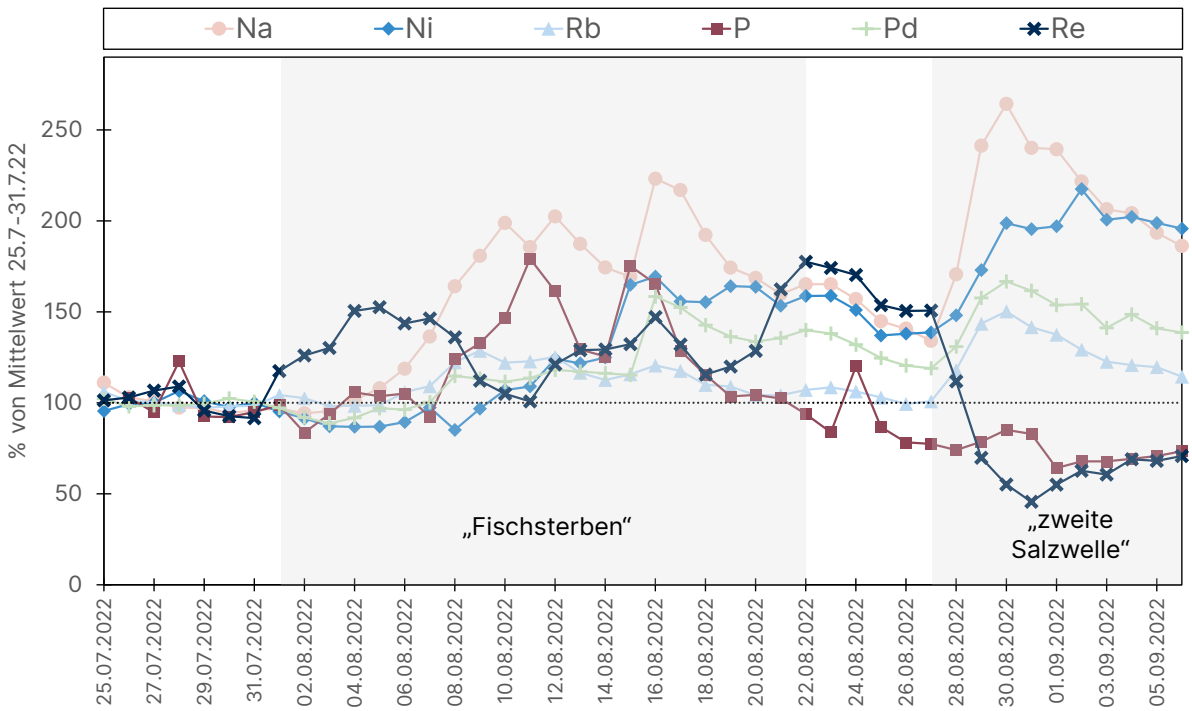

Abbildung A2.5.3.2.3 *Relativer Konzentrationsverlauf der sich in den beiden „Salzwellen“ unterschiedlich verhaltenden Elemente Na, Ni, Rb, P, Pd und Re in filtrierten Oderwasserproben aus Hohenwutzen vom 25.07.-06.09.2022. Die dargestellten Werte sind jeweils auf den Mittelwert der letzten Juliwoche (25.-31.07.2022) als 100% normalisiert.*

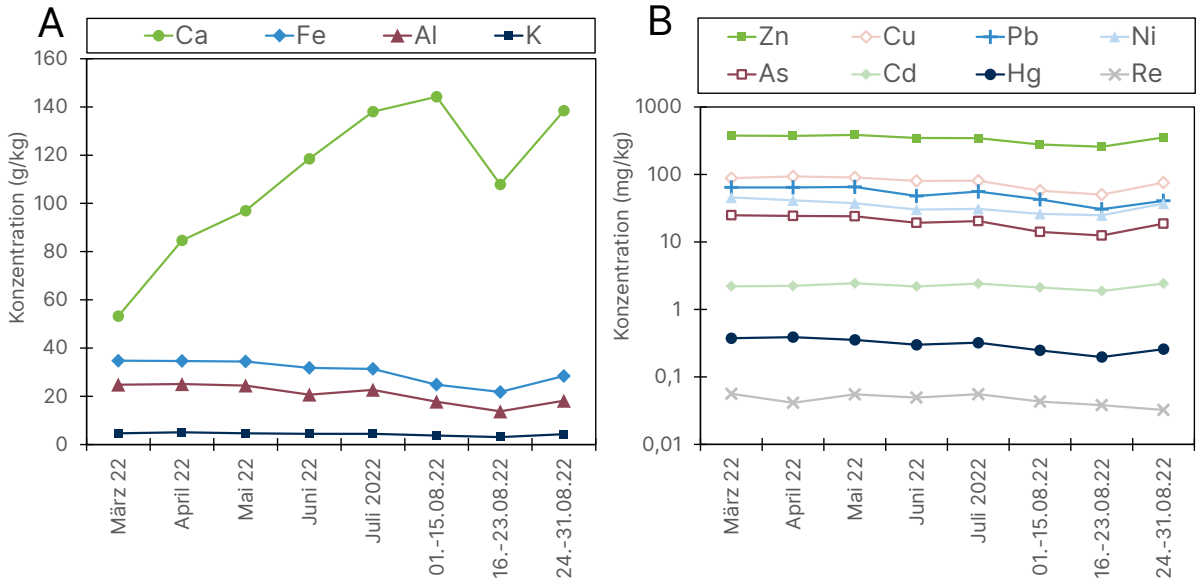

Abbildung A2.5.3.2.3 *Elementkonzentrationen in den Schwebstoffen der Oder in Hohenwutzen (Monatsmischproben März-Juli 2022 und Mischproben 01.-15.08., 16.-23.08. und 24.-31.08.22) für (A) die Hauptelemente Ca, Fe, Al, K und (B) die Spurenelemente Zn, Cu, Pb, Ni, As, Cd, Hg, Re (in logarithmischer Auftragung).*

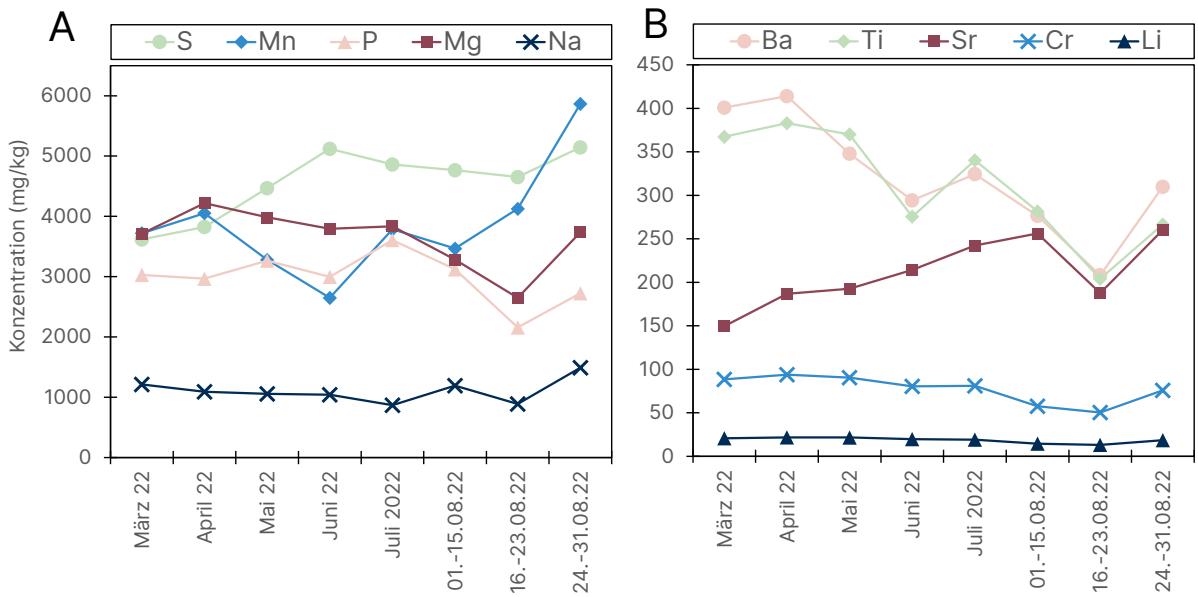

Abbildung A2.5.3.2.3 *Elementkonzentrationen in den Schwebstoffen der Oder in Hohenwutzen (Monatsmischproben März-Juli 2022 und Mischproben 01.-15.08., 16.-23.08. und 24.-31.08.22) für (A) S, Mn, P, Mg, Na und (B) Ba, Ti, Sr, Cr, Li.*

A2.5.6 Phytoplankton

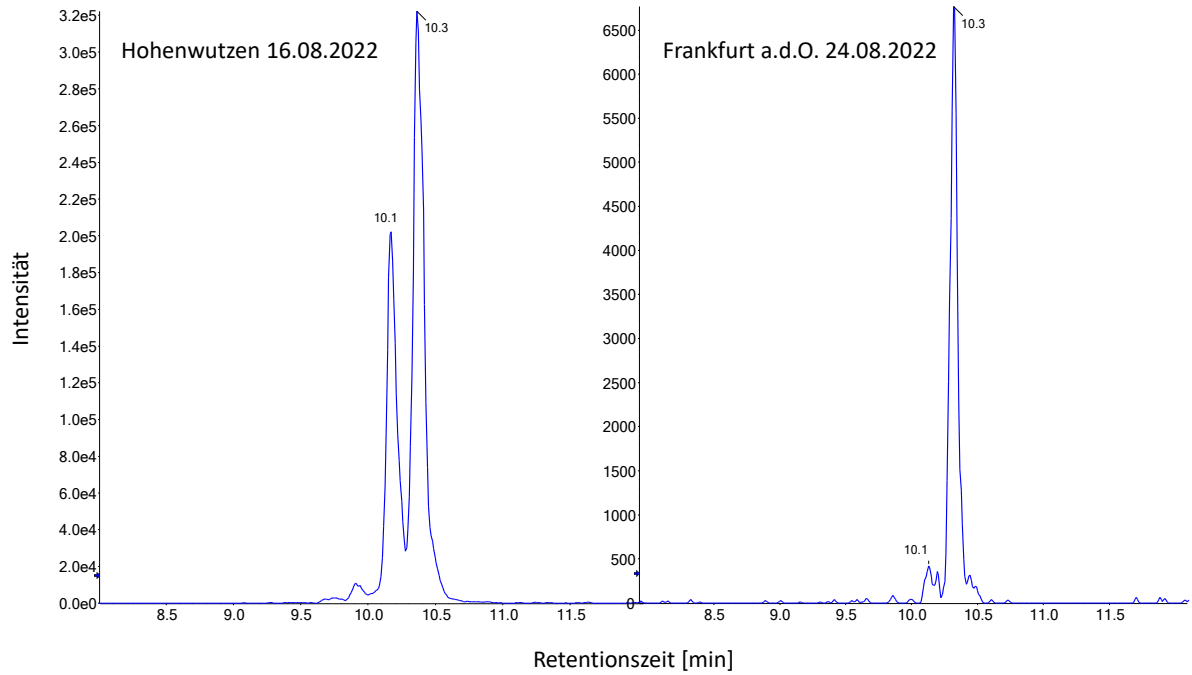

Abbildung A2.5.6.4.1 *Extrahiertes Ionenchromatogramm (828.8968 ± 0.01 Da) der extrahierten Algenbiomasse der Wasserprobe vom 16.8.2022 aus Hohenwutzen und 24.8.2022 aus Frankfurt (Oder).*

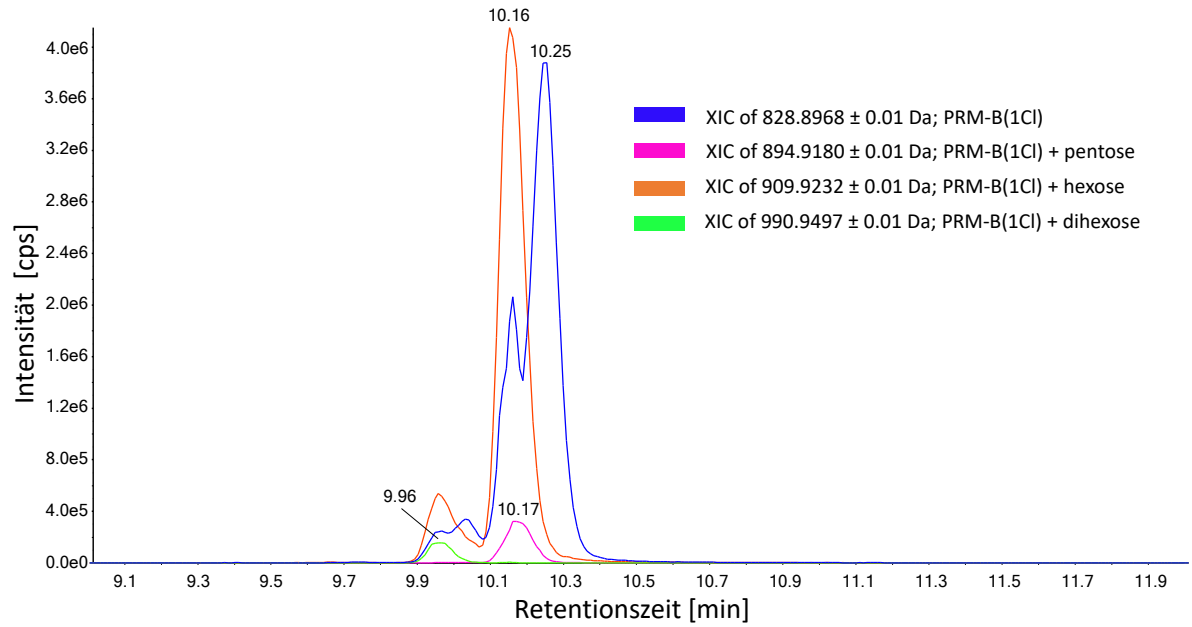

Abbildung A2.5.6.4.2 *Überlagerte extrahierte Ionenchromatogramme (XICs) von Prymnesin-B1, nachgewiesen in einer Klonkultur von Prymnesium parvum. Nach BINZER et al. (2019) wurden PRM-B(1Cl) bei 10,25 Min., PRM-B(1Cl) + pentose bei 10,17 Min., PRM-B(1Cl) + hexose bei 10,16 Min. und PRM-B(1Cl) + dihexose bei 9,96 Min. identifiziert.*

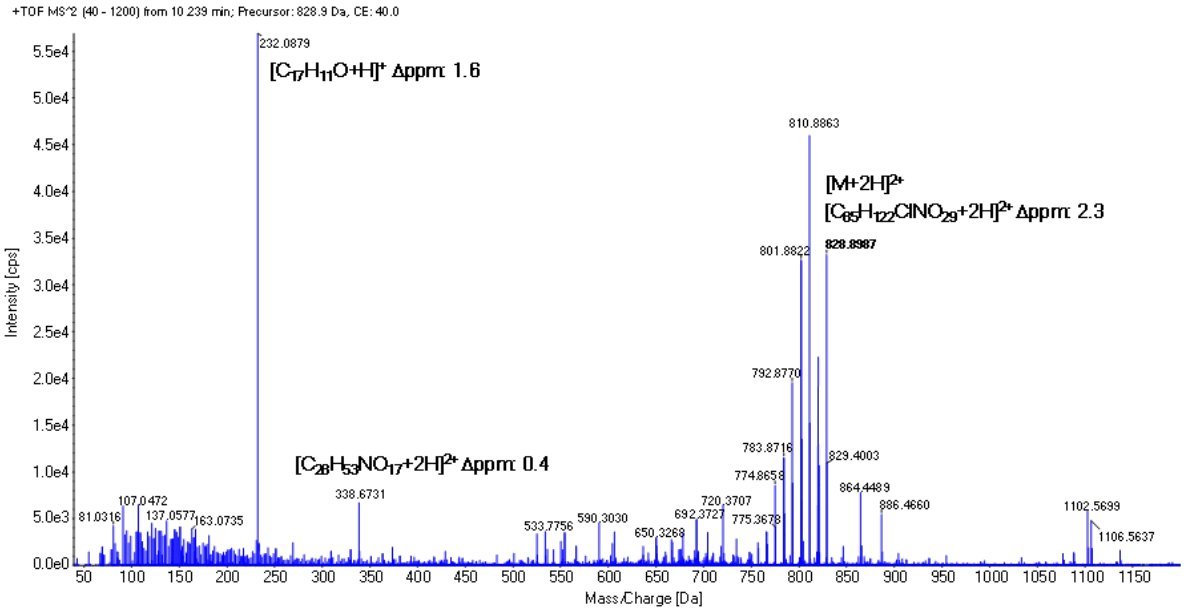

Abbildung A2.5.6.4.3 *Produktionenspektrum von 828.9 Da bei 10.25 min, identifiziert als PRM-B(1Cl).*

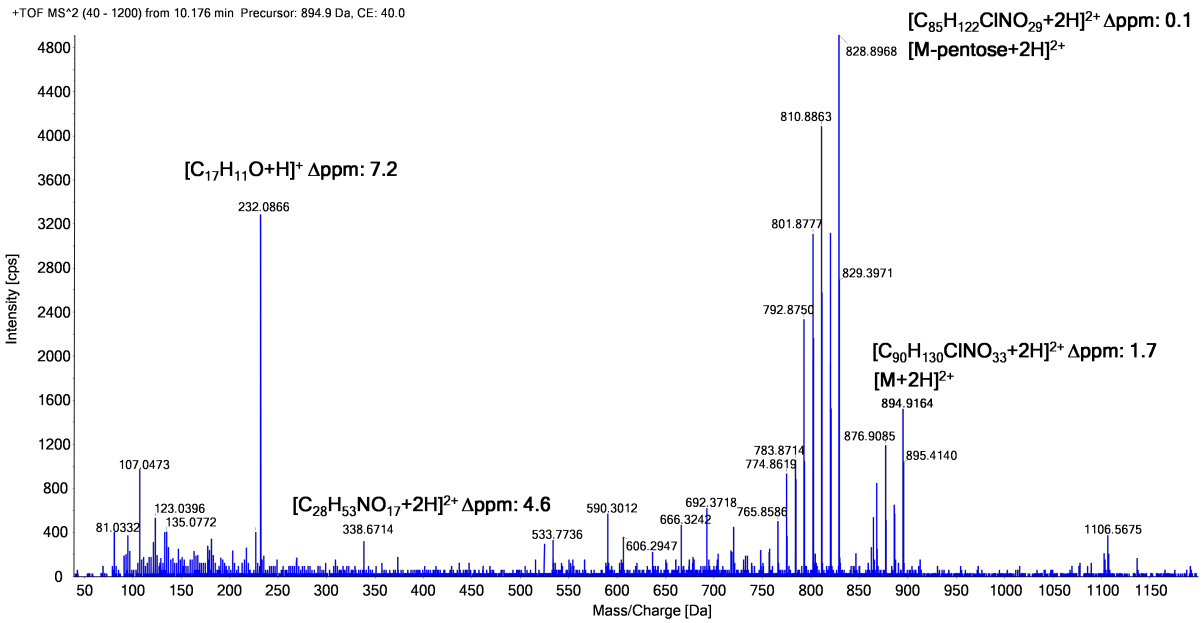

Abbildung A2.5.6.4.4 *Produktionenspektrum von 894.9 Da bei 10.17 min, identifiziert als PRM-B(1Cl) + pentose.*

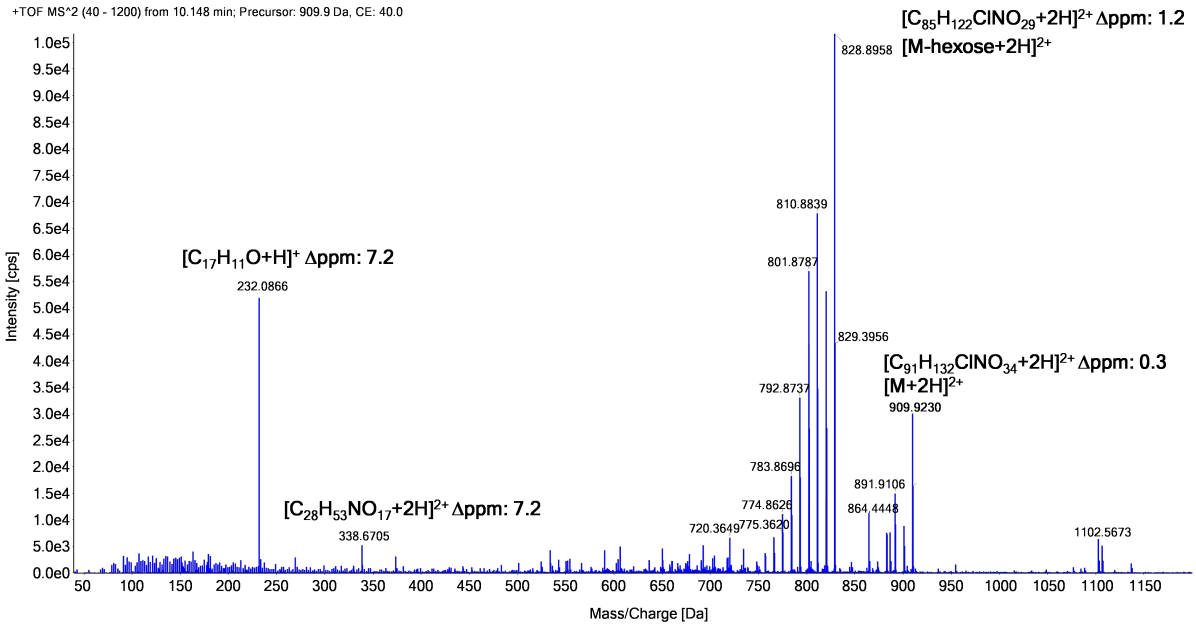

Abbildung A2.5.6.4.5 *Produktionenspektrum von 909.9 Da bei 10.16 min, identifiziert als PRM-B(1Cl) + hexose.*

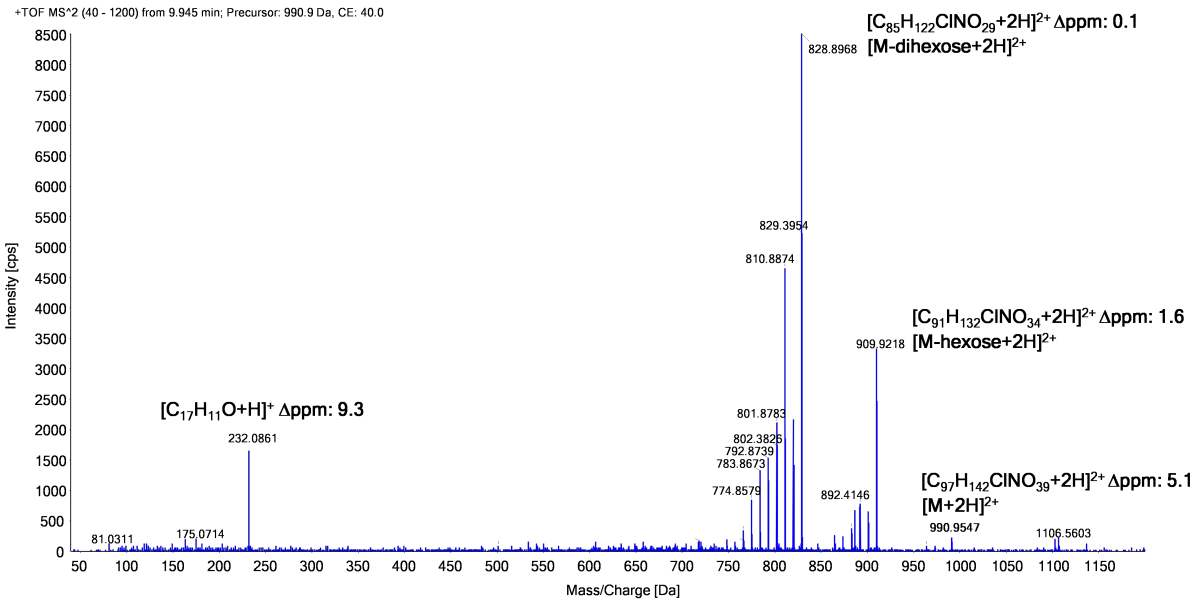

Abbildung A2.5.6.4.6 *Produktionenspektrum von 990.9 Da bei 9.96 min, identifiziert als PRM-B(1Cl) + dihexose*

Annex 3: Data tables (in German only)

Tabelle A3.4.2.1 *Übersicht über die an der BfG untersuchten Proben:*

Proben-bezeichnung	BfG-Nummer	Proben-ID	Datum	Gewässer	Fluss-km	Ort	Station
HW_TM_01/07	220747	W44 7 1	01.07.2022				
HW_TM_02/07	220748	W44 7 2	02.07.2022				
HW_TM_03/07	220749	W44 7 3	03.07.2022				
HW_TM_04/07	220750	W44 7 4	04.07.2022				
HW_TM_05/07	220751	W44 7 5	05.07.2022				
HW_TM_06/07	220752	W44 7 6	06.07.2022				
HW_TM_07/07	220753	W44 7 7	07.07.2022				
HW_TM_08/07	220754	W44 7 8	08.07.2022				
HW_TM_09/07	220755	W44 7 9	09.07.2022				
HW_TM_10/07	220756	W44 7 10	10.07.2022				
HW_TM_11/07	220757	W44 7 11	11.07.2022				
HW_TM_12/07	220758	W44 7 12	12.07.2022				
HW_TM_13/07	220759	W44 7 13	13.07.2022				
HW_TM_14/07	220760	W44 7 14	14.07.2022				
HW_TM_15/07	220761	W44 7 15	15.07.2022				
HW_TM_16/07	220762	W44 7 16	16.07.2022				
HW_TM_17/07	220763	W44 7 17	17.07.2022				
HW_TM_18/07	220764	W44 7 18	18.07.2022				
HW_TM_19/07	220765	W44 7 19	19.07.2022				
HW_TM_20/07	220766	W44 7 20	20.07.2022				
HW_TM_21/07	220767	W44 7 21	21.07.2022				
HW_TM_22/07	220768	W44 7 22	22.07.2022				
HW_TM_23/07	220769	W44 7 23	23.07.2022	Oder	661	Hohenwutzen	BfG
HW_TM_24/07	220770	W44 7 24	24.07.2022				
HW_TM_25/07	220771	W44 7 25	25.07.2022				
HW_TM_26/07	220772	W44 7 26	26.07.2022				
HW_TM_27/07	220773	W44 7 27	27.07.2022				
HW_TM_28/07	220774	W44 7 28	28.07.2022				
HW_TM_29/07	220775	W44 7 29	29.07.2022				
HW_TM_30/07	220776	W44 7 30	30.07.2022				
HW_TM_31/07	220777	W44 7 31	31.07.2022				
HW_TM_01/08	220731	W44 8 1	01.08.2022				
HW_TM_02/08	220732	W44 8 2	02.08.2022				
HW_TM_03/08	220733	W44 8 3	03.08.2022				
HW_TM_04/08	220734	W44 8 4	04.08.2022				
HW_TM_05/08	220735	W44 8 5	05.08.2022				
HW_TM_06/08	220736	W44 8 6	06.08.2022				
HW_TM_07/08	220737	W44 8 7	07.08.2022				
HW_TM_08/08	220738	W44 8 8	08.08.2022				
HW_TM_09/08	220739	W44 8 9	09.08.2022				
HW_TM_10/08	220740	W44 8 10	10.08.2022				
HW_TM_11/08	220741	W44 8 11	11.08.2022				
HW_TM_12/08	220742	W44 8 12	12.08.2022				
HW_TM_13/08	220743	W44 8 13	13.08.2022				
HW_TM_14/08	220744	W44 8 14	14.08.2022				
HW_TM_15/08	220745	W44 8 15	15.08.2022				

Proben-bezeichnung	BfG-Nummer	Proben-ID	Datum	Gewässer	Fluss-km	Ort	Station
HW_TM_16/08	220806	W44 8 16	16.08.2022				
HW_TM_17/08	220807	W44 8 17	17.08.2022				
HW_TM_18/08	220808	W44 8 18	18.08.2022				
HW_TM_19/08	220809	W44 8 19	19.08.2022				
HW_TM_20/08	220810	W44 8 20	20.08.2022				
HW_TM_21/08	220811	W44 8 21	21.08.2022				
HW_TM_22/08	220812	W44 8 22	22.08.2022				
HW_TM_23/08	220813	W44 8 23	23.08.2022				
HW_TM_24/08		W44 8 24	24.08.2022				
HW_TM_25/08		W44 8 25	25.08.2022				
HW_TM_26/08		W44 8 26	26.08.2022				
HW_TM_27/08		W44 8 27	27.08.2022				
HW_TM_28/08		W44 8 28	28.08.2022				
HW_TM_29/08		W44 8 29	29.08.2022				
HW_TM_30/08		W44 8 30	30.08.2022				
HW_TM_31/08		W44 8 31	31.08.2022				
HW_TM_01/09		W44 9 1	01.09.2022				
HW_TM_02/09		W44 9 2	02.09.2022				
HW_TM_03/09		W44 9 3	03.09.2022				
HW_TM_04/09		W44 9 4	04.09.2022				
HW_TM_05/09		W44 9 5	05.09.2022				
HW_TM_06/09		W44 9 6	06.09.2022				
HW_S_16/08			16.08.2022				
HW_S_24/08			24.08.2022				
HW_LfU_TM_10/08	220783	22-034010	10.08.2022				
HW_LfU_TM_11/08	220784	22-034011	11.08.2022				LfU
HW_LfU_TM_12/08	220786	22-034471	12.08.2022				
FFO_TM_05/08	220778	22-033954	05.08.2022				
FFO_TM_06/08	220779	22-033955	06.08.2022				
FFO_TM_07/08	220780	22-033956	07.08.2022				
FFO_TM_08/08	220781	22-033957	08.08.2022		584	Frankfurt (Oder)	LfU
FFO_TM_10/08	220785	22-034012	10.08.2022				
FFO_TM_12/08	220787	22-034464	12.08.2022				
FFO_S_24/08		22-035381	24.08.2022				
EHS_SOK_S_06/09	220885		06.09.2022	Spree-Oder-WStr	125,68	Eisenhüttenstadt	SOK
EHS_ZSS_S_06/09	220886		06.09.2022	Spree-Oder-WStr	127,14	Eisenhüttenstadt	ZSS
Schwebstoffproben:							
HW_Schw_03	220574		März 2022				
HW_Schw_04	220575		April 2022				
HW_Schw_05	220576		Mai 2022				
HW_Schw_06	220679		Juni 2022				
HW_Schw_07	220692		Juli 2022	Oder	661	Hohenwutzen	BfG
HW_Schw_08-1	220746		01.-15. 08.2022				
HW_Schw_08-2	220797		16.-23. 08.2022				
HW_Schw_08-3	220884		24.-31. 08.2022				

HW = Hohenwutzen, FFO = Frankfurt (Oder), SOK = Spree-Oder-Kanal, ZSS = Zwillingsschachtschleuse, TM = Tagesmischprobe, S = Stichprobe, Schw = Schwebstoff

A3.5.4.1 Schadstoffscreening mittels Non-Target Verfahren

Tabelle A3.5.4.1.1 *Über die Spektrendatenbank annotierte Substanzen, deren maximalen Intensitäten, Detektionsfrequenzen und maximalen Konzentrationen im Juli und August in Hohenwutzen sowie in Frankfurt (Oder); BG = Bestimmungsgrenze, maxI = maximale Intensität, Freq = Detektionsfrequenz, maxK = maximale Konzentration, n.v. = nicht vergeben, PSM = Pflanzenschutzmittel*

					Hohenwutzen						**Frankfurt (Oder)**		
Substanz	**CAS**	**Summenformel**	**Klasse**	**BG**	**maxI Juli**	**maxI Aug**	**Freq Juli**	**Freq Aug**	**maxK Juli**	**maxK Aug**	**maxI**	**Freq**	**maxK**
				ng/l	**counts**	**counts**	**%**	**%**	**ng/l**	**ng/l**	**counts**	**%**	**ng/l**
1,3-Diphenylguanidin	102-06-7	C13H13N3	n.v.	-	68	49	100	100	-	-	40	100	-
2,4,6-Trichlorophenoxyacetic acid	575-89-3	C8H5Cl3O3	PSM	600*	6	8	10	22	838	1027	59	100	6226
2,4-Dichlorophenoxyacetic acid	94-75-7	C8H6Cl2O3	PSM	150*	7	114	10	61	156	2422	380	100	8461
2,6-Dichlorophenoxyacetic acid	575-90-6	C8H6Cl2O3	PSM	800*	6	14	10	30	< BG	1735	120	100	17618
2,6-Dimethylquinoline	877-43-0	C11H11N	n.v.	-	88	79	100	87	-	-	13	50	-
2`-Deoxyadenosine	16373-93-6	C10H13N5O3	Natürlich	-	0	0	0	0	-	-	29	33	-
2-Hydroxybenzothiazole	934-34-9	C7H5NOS	Industrie	40**	5	56	6	70	< BG	552	0	0	< BG
2-Phenylbenzimidazole-5-sulfonic acid	27503-81-7	C13H10N2O3S	Personal Care	-	61	37	71	83	-	-	33	100	-
3-(Diethylcarbamoyl)benzoic acid	72236-23-8	C12H15NO3	n.v.	20**	14	34	97	100	22	55	24	100	41
4-Acetamidoantipyrine	83-15-8	C13H15N3O2	Pharma	10*	105	108	100	100	166	177	127	100	178
4-Formylaminoantipyrine	1672-58-8	C12H13N3O2	Pharma	20*	87	76	100	100	351	309	78	100	258
4-Toluenesulfonic acid	104-15-4	C7H8O3S	Industrie	100*	3	56	3	52	< BG	154	82	67	293

5(and 4-)-Methyl-1H-benzotriazole	4: 29878-31-7, 5: 136-85-6	C7H7N3	Industrie	10**	59	63	100	100	76	77	78	100	96
Adenosine	58-61-7	C10H13N5O4	Natürlich	30**	12	214	3	43	< BG	1857	66	50	536
AMPS	15214-89-8	C7H13NO4S	n.v.	-	13	8	77	65	-	-	4	33	-
Atenolol acid	56392-14-4	C14H21NO4	Pharma	5*	22	29	52	87	39	63	45	100	76
Atrazine-desisopropyl-2-hydroxy	7313-54-4	C5H9N5O	PSM	-	0	52	0	17	-	-	0	0	-
Azoxystrobin	131860-33-8	C22H17N3O5	PSM	-	5	0	6	0	-	-	0	0	-
Azoxystrobin R234886	1185255-09-7	C21H15N3O5	PSM	-	40	10	87	74	-	-	0	0	-
Bentazone	25057-89-0	C10H12N2O3S	PSM	-	127	163	100	100	-	-	240	100	0
Benzothiazole-2-sulfonic acid	941-57-1	C7H5NO3S2	n.v.	2*	125	114	100	100	315	274	102	100	236
Benzotriazole	95-14-7	C6H5N3	Industrie	5*	257	251	100	100	1765	1822	234	100	1315
Candesartan	139481-59-7	C24H20N6O3	Pharma	20*	37	50	61	83	57	77	47	100	65
Carbamazepine	298-46-4	C15H12N2O	Pharma	20*	119	99	100	100	283	242	109	100	270
Cyclamate	100-88-9	C6H13NO3S	Weitere	-	0	16	0	48	-	-	22	100	-
DEET	134-62-3	C12H17NO	Personal Care	5*	49	46	100	100	39	39	38	100	34
Denatonium	47324-98-1	C21H29N2O	Weitere	50*	37	30	90	91	< BG	< BG	38	100	< BG
Desamino-metamitron	36993-94-9	C10H9N3O	PSM	10*	33	15	97	91	99	40	7	17	16
Desethylterbuthylazine	30125-63-4	C7H12ClN5	PSM	-	19	9	90	52	-	-	10	83	-
Diphenylphosphinic acid	1707-03-5	C12H11O2P	Industrie	10**	21	16	100	100	41	< BG	23	100	43
Fexofenadin N-Oxid		C32H39NO5	Pharma	-	16	16	68	83	-	-	11	100	-

Fexofenadine	83799-24-0	C32H39NO4	Pharma	50*	51	43	97	100	51	< BG	38	100	< BG
Fluconazole	86386-73-4	C13H12F2N6O	Pharma	50*	28	46	13	22	76	100	31	50	83
Flutriafol	76674-21-0	C16H13F2N3O	PSM	-	43	12	100	87	-	-	0	0	-
Gabapentin	60142-96-3	C9H17NO2	Pharma	20*	48	50	100	100	151	159	84	100	210
Guanosine	118-00-3	C10H13N5O5	Natürlich	145**	0	9	0	4	< BG	< BG	19	33	1122
Imidacloprid	138261-41-3	C9H10ClN5O2	PSM	50*	14	0	10	0	144	< BG	0	0	< BG
Lamotrigine	84057-84-1	C9H7Cl2N5	Pharma	10*	113	135	100	100	275	361	104	100	242
Lidocaine	137-58-6	C14H22N2O	Pharma	50*	32	33	52	74	< BG	< BG	38	83	< BG
Losartan carboxylic acid	124750-92-1	C22H21ClN6O2	Pharma	40**	6	11	10	43	< BG	44	6	17	< BG
Metazachlor ESA	172960-62-2	C14H17N3O4S	PSM	-	40	31	68	70	-	-	40	100	-
Metolachlor	51218-45-2	C15H22ClNO2	PSM	20*	13	6	100	39	26	< BG	10	100	26
Metolachlor ESA	171118-09-5	C15H23NO5S	PSM	-	24	24	100	100	-	-	29	100	-
N-Desmethyltramadol	73806-55-0	C15H23NO2	Pharma	10*	51	47	100	100	54	55	52	100	54
N-Ethyl-4-menthane-3-carboxamide	39711-79-0	C13H25NO	Personal Care	-	23	24	100	100	-	-	38	100	-
Nicosulfuron	111991-09-4	C15H18N6O6S	PSM	-	16	9	29	9	-	-	0	0	-
Oxipurinol	2465-59-0	C5H4N4O2	Pharma	200*	40	44	90	96	1860	1888	40	100	1626
P-Cumolsulfonsaeure	16066-35-6	C9H12O3S	Industrie	-	19	27	100	100	-	-	23	100	-
Sitagliptin	486460-32-6	C16H15F6N5O	Pharma	20*	0	0	0	0	25	< BG	27	67	51
Sulfamethoxazole	723-46-6	C10H11N3O3S	Pharma	20*	17	12	100	100	74	61	14	100	62
Sulpiride	15676-16-1	C15H23N3O4S	Pharma	10*	112	92	84	91	91	101	116	100	102

Tebuconazole	107534-96-3	C16H22ClN3O	PSM	10*	27	55	100	96	24	54	7	83	< BG
Telmisartan	144701-48-4	C33H30N4O2	Pharma	50*	36	0	48	0	53	< BG	0	0	< BG
Terbuthylazine	5915-41-3	C9H16ClN5	PSM	5*	70	29	100	100	48	21	36	100	24
Terbutryn	886-50-0	C10H19N5S	PSM	2*	17	11	100	96	8	5	8	83	3
Terbutylazine-2-hydroxy	66753-07-9	C9H17N5O	PSM	100*	34	22	100	100	245	238	27	100	235
Tetrabutylammonium	10549-76-5	C16H36N	Industrie	20*	16	20	100	100	< BG	< BG	14	100	< BG
Tetraglyme	143-24-8	C10H22O5	Industrie	100*	80	379	100	100	441	2153	80	100	413
Tiapride	51012-32-9	C15H24N2O4S	Pharma	5**	77	84	61	35	51	54	83	67	66
Tramadol	27203-92-5	C16H25NO2	Pharma	5*	183	150	100	100	121	106	184	100	117
Triethyl phosphate	78-40-0	C6H15O4P	Industrie	100*	14045	77571	100	100	104099	557192	6037	100	44868
Triphenylphosphine oxide	791-28-6	C18H15OP	Industrie	-	44	26	65	65	-	-	36	100	-
Tris(1-chloro-2-propyl) phosphate	13674-84-5	C9H18Cl3O4P	Industrie	40**	65	52	100	100	< BG	97	27	100	< BG
Tris(2-butoxyethyl) phosphate	78-51-3	C18H39O7P	Industrie	-	34	20	23	9	-	-	22	50	-
Tris(2-chloroethyl) phosphate	115-96-8	C6H12Cl3O4P	Industrie	250**	23	18	100	100	< BG	< BG	0	0	< BG
Tyrosine	60-18-4	C9H11NO3	Natürlich	-	0	8	0	9	-	-	30	33	-
Uric acid	69-93-2	C5H4N4O3	Natürlich	-	26	53	39	74	-	-	205	83	-
Valsartan	137862-53-4	C24H29N5O3	Pharma	10*	5	14	19	100	10	26	20	100	35
Valsartanic acid	164265-78-5	C14H10N4O2	Pharma	50*	57	55	100	100	329	327	67	100	347
Venlafaxine	93413-69-5	C17H27NO2	Pharma	5*	50	41	100	100	30	27	41	100	24
Xanthosine	146-80-5	C10H12N4O6	Natürlich	200**	0	34	0	17	< BG	1505	47	50	1186

Bestimmung BG und Quantifizierung über Kalibrationsreihen (*) und Ein-Punkt-Kalibrierungen (**)

Tabelle A3.5.4.1.2 *Über die Spektrendatenbank annotierte Substanzen in den Schwebstoff-Proben*

m/z	tR	Name	CAS	Summenformel
120.0542	5.97	Benzotriazole	95-14-7	C6H5N3
139.0371	5.49	4-Hydroxybenzoic acid	99-96-7	C7H6O3
152.0146	7.9	2-Hydroxybenzothiazole	934-34-9	C7H5NOS
153.0535	6.53	Methyl 4-(or 3)-hydroxybenzoate	99-76-3	C8H8O3
180.0796	5.82	Acridine	260-94-6	C13H9N
155.1051	7.97	Godecke	7236-78-4	C9H14O2
161.1051	5.26	Tryptamine	61-54-1	C10H12N2
198.1255	6.3	Dibenzylamine	103-49-1	C14H15N
198.1829	12.47	N-Octyl-2-pyrrolidone	2687-94-7	C12H23NO
212.1169	5.91	1,3-Diphenylguanidin	102-06-7	C13H13N3
225.1943	10.77	1,3-Dicyclohexylurea	2387-23-7	C13H24N2O
196.0739	8.37	Acridone	578-95-0	C13H9NO
199.0580	5.86	Syringic acid	530-57-4	C9H10O5
242.2830	9.41	Tetrabutylammonium	10549-76-5	C16H36N
242.2828	12.17	N,N-Dimethyltetradecylamine	112-75-4	C16H35N
243.0866	7.17	Lumichrome	1086-80-2	C12H10N4O2
233.1097	9.27	N-Cyclohexyl-1,3-benzothiazol-2-amine	28291-75-0	C13H16N2S
226.1563	6.52	Dibenzyldimethyl ammonium	14800-26-1	C16H20N
270.3136	11.88	Dimethyldioctylammonium	20256-55-7	C18H40N
282.2781	17.58	Oleamide	301-02-0	C18H35NO
242.1415	9.62	Terbutryn	886-50-0	C10H19N5S
284.3292	13.82	Hexadecyl-trimethylammonium	6899-10-01	C19H42N
250.1794	6.23	N-Desmethyltramadol	73806-55-0	C15H23NO2
264.1946	6.2	Tramadol	27203-92-5	C16H25NO2
264.1939	5.81	O-desmethyl-venlafaxine	93413-62-8	C16H25NO2
293.1025	8.91	Climbazole	38083-17-9	C15H17ClN2O2
268.1892	6.15	Metoprolol	51384-51-1	C15H25NO3
278.2093	6.98	Venlafaxine	93413-69-5	C17H27NO2
313.1420	14.78	Benzyl-butylphthalate	85-68-7	C19H20O4
273.0749	8.94	Naringenin	67604-48-2	C15H12O5

279.0910	10.48	Triphenylphosphine oxide	791-28-6	C18H15OP
326.2301	7.01	Bisoprolol	66722-44-9	C18H31NO4
327.0053	11.63	Tris(1-chloro-2-propyl) phosphate	13674-84-5	C9H18Cl3O4P
327.0759	13.79	Triphenyl phosphate	115-86-6	C18H15O4P
277.1118	7.64	Methyltriphenylphosphonium	15912-74-0	C19H18P
291.1281	8.05	Ethyltriphenylphosphonium	39895-79-9	C20H20P
298.0961	5.01	5`-Deoxy-5`-(methylthio)adenosin	2457-80-9	C11H15N5O3S
300.0771	9.8	Fenbendazole	43210-67-9	C15H13N3O2S
308.1493	12.37	Tebuconazole	107534-96-3	C16H22ClN3O
311.1529	7.81	N-desmethyl-citalopram	62498-67-3	C19H19FN2O
315.2301	13.36	Progesterone	57-83-0	C21H30O2
369.1239	15.83	Tris(4-methylphenyl) phosphate	78-32-0	C21H21O4P
325.1696	7.96	Citalopram	59729-33-8	C20H21FN2O
325.2262	8.21	Denatonium	47324-98-1	C21H29N2O
329.1519	5.16	Tiapride	51012-32-9	C15H24N2O4S
342.0743	13.02	Propiconazole	60207-90-1	C15H17Cl2N3O2
342.1467	4.98	Sulpiride	15676-16-1	C15H23N3O4S
326.3771	14.32	Didecyl-dimethylammonium	20256-56-8	C22H48N
370.1785	5.69	Amisulpride	71675-85-9	C17H27N3O4S
392.2197	7.77	Trospium	47608-32-2	C25H30NO3
408.1242	6.58	Sitagliptin	486460-32-6	C16H15F6N5O
502.2912	8.76	Fexofenadine	83799-24-0	C32H39NO4
515.2444	8.94	Telmisartan	144701-48-4	C33H30N4O2
577.1326	14.24	Ethylene Terephthalate Cyclic Trimer	7441-32-9	C30H24O12
151.0394	6.51	Methyl 4-hydroxybenzoate	99-76-3	C8H8O3
163.0399	6.42	4-Acetylbenzoic acid	586-89-0	C9H8O3
209.0845	9.46	Octyl hydrogen sulfate	110-11-2	C8H18O4S
213.9634	5.84	Benzothiazole-2-sulfonic acid	941-57-1	C7H5NO3S2
271.0598	8.95	Naringenin	67604-48-2	C15H12O5
498.2812	8.9	Microcystin LR	101043-37-2	C49H74N10O12
523.2713	8.7	Microcystin YR	101064-48-6	C52H72N10O13

A3.5.4.1 Schadstoffscreening mittels Non-Target Verfahren (Fortsetzung)

Steckbriefe zur Identifizierung unbekannter Substanzen

Vorgehen bei der Identifizierung am Beispiel der „Unbekannten 2“

Über die Korrelationsanalyse wurde eine unbekannte Verbindung mit m/z 274.8724 (neg. ESI) bei einer Retentionszeit von 8.5 min ermittelt.

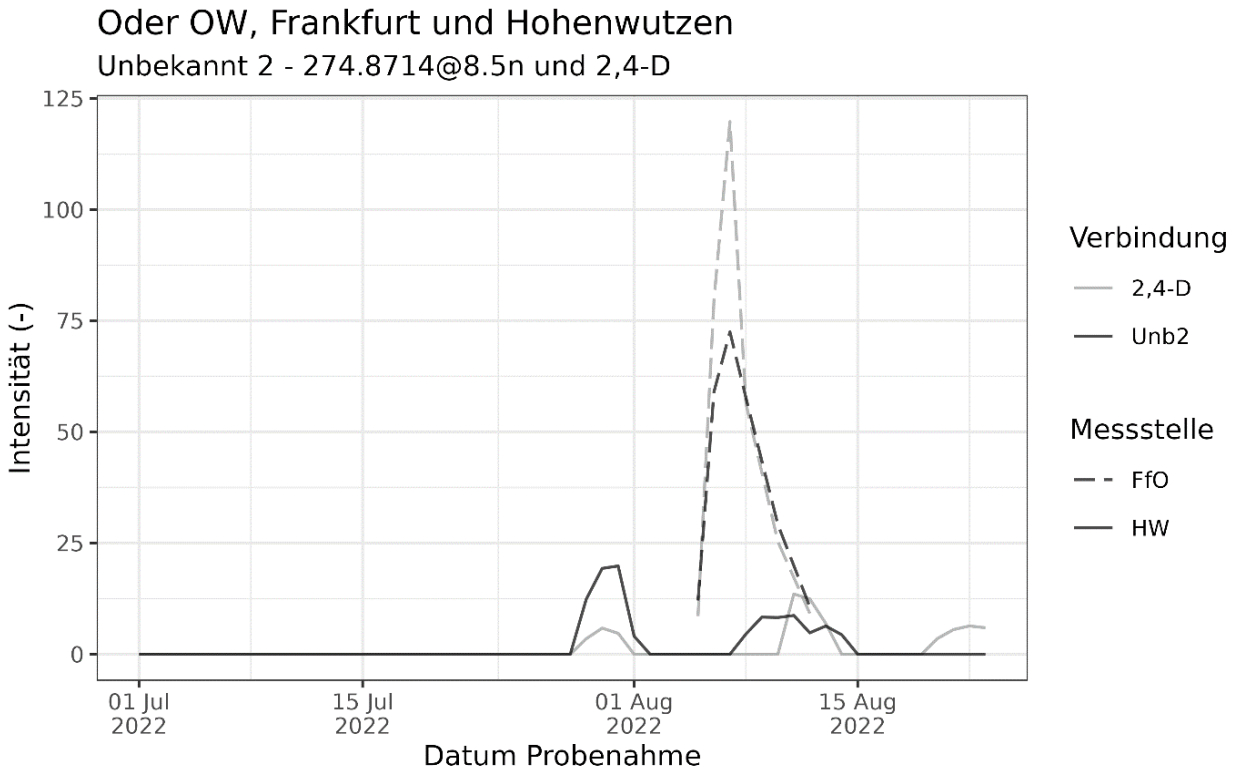

Für diese Verbindung ergaben sich 10 Addukte, Isotopologe sowie Bruchstücke der Ionisierung. Das Isotopenmuster im MS^1-Spektrum des Features m/z 274.8724 konnte nicht eindeutig dem Muster von Cl_3 oder Cl_3S zugeordnet werden. Für das Isotopenmuster im MS^1-Spektrum des Quellfragments m/z 194.9152 kommen das Isotopenmuster Cl_2 und Cl_3 in Frage (s. Steckbrief). Der Massenunterschied von 79.9572 Da zwischen dem Molekularpeak und dem Quellfragment deutet zudem auf das Vorhandensein einer Sulfonsäuregruppe hin. Anhand der Intensität des ^{13}C Peaks (m/z 275.1269) wurde eine Anzahl von 4 - 12 C-Atomen abgeschätzt. Mittels Genform wurden für diese Verbindung potenzielle Summenformeln gebildet. Diese wurden anhand der Isotopenmuster sowie der abgeschätzten Anzahl von C-Atomen und dem Vorhandensein von HSO_3 gefiltert. Auf Basis dieser Vorbedingungen wurde die Summenformel $C_6H_3O_4SCl_3$ berechnet. Aufgrund des MS^2-Spektrums und der Recherche in PubChem über die in-silico Fragmentierung MetFrag wurde zwei Kandidaten ermittelt (s. Steckbrief). Für beide Kandidaten wurde jeweils das Quellfragment als Trichlorphenolat erklärt. Dieses wurde auch für das Feature „Unbekannt 1“ identifiziert. Für eine weitergehende Verifizierung dieser vorläufigen Identifizierung müssten im weiteren Verlauf Referenzstandards erworben, mittels der verwendeten NTS-Methode eingemessen und mit den gemessenen Daten verglichen werden.

Überblick der erstellten Steckbriefe

ID (mz_RT[p/n])	Steckbrief	Kandidat
320.9100_10.8n	Unb1	-
274.8714_8.5n	Unb2	2,3,5,6-tetrachloro-4-nitro-phenol oder 4-bromo-2,3-dichloro-6-(difluoromethyl)pyridine
240.9091_6.7n & **240.9098_8.3n**	Unb3 & Unb4	3,5-Dichlor-4-hydroxybenzolsulfonsäure oder Isomer
289.1612_6.3p	Unb7	-
564.2840_9.5p	Unb13	-
301.2120 _ 13.6p	Unb14	-
209.0276 _ 6.2n	Unb15	2,3-Diethenylbenzene-1-sulfonic acid oder Propargyl p-toluenesulfonate
169.0083_4.7n	Unb16	O,O-Diethylthiophosphat
345.1866_9.3p	Unb17	Hexamethoxymethylmelamin

Steckbrief Feature: Unbekannt 1 (320.9100@10.8_neg)

Das Feature wurde über die Korrelation mit der Substanz 2,4-D für die Identifizierung priorisiert.

Zeitverlauf

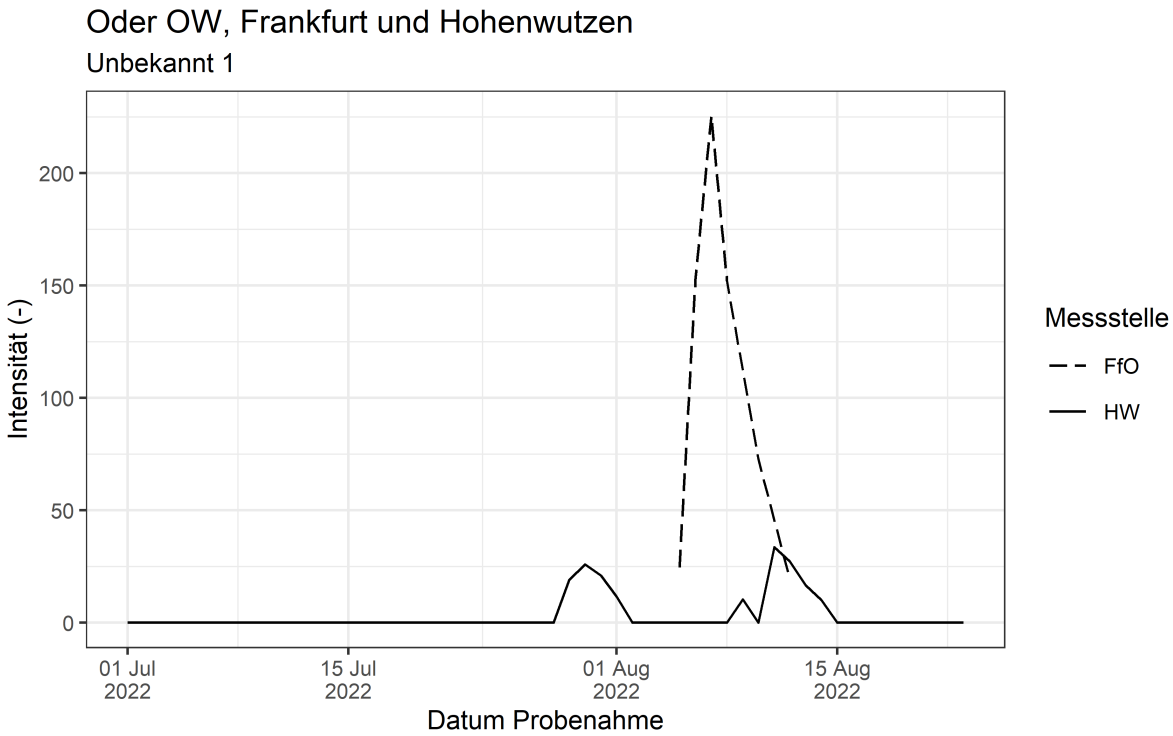

Addukte und Isotopologe

Über 70 detektierte Features gehören zu dieser Substanz. Der postulierte Molekularpeak hat ein m/z von 320.9085 (ESIneg) und eluiert bei 10.8 min. Das intensivste Feature ist das Quellenfragment m/z 194.913 bei 10.8 min.

Spektren

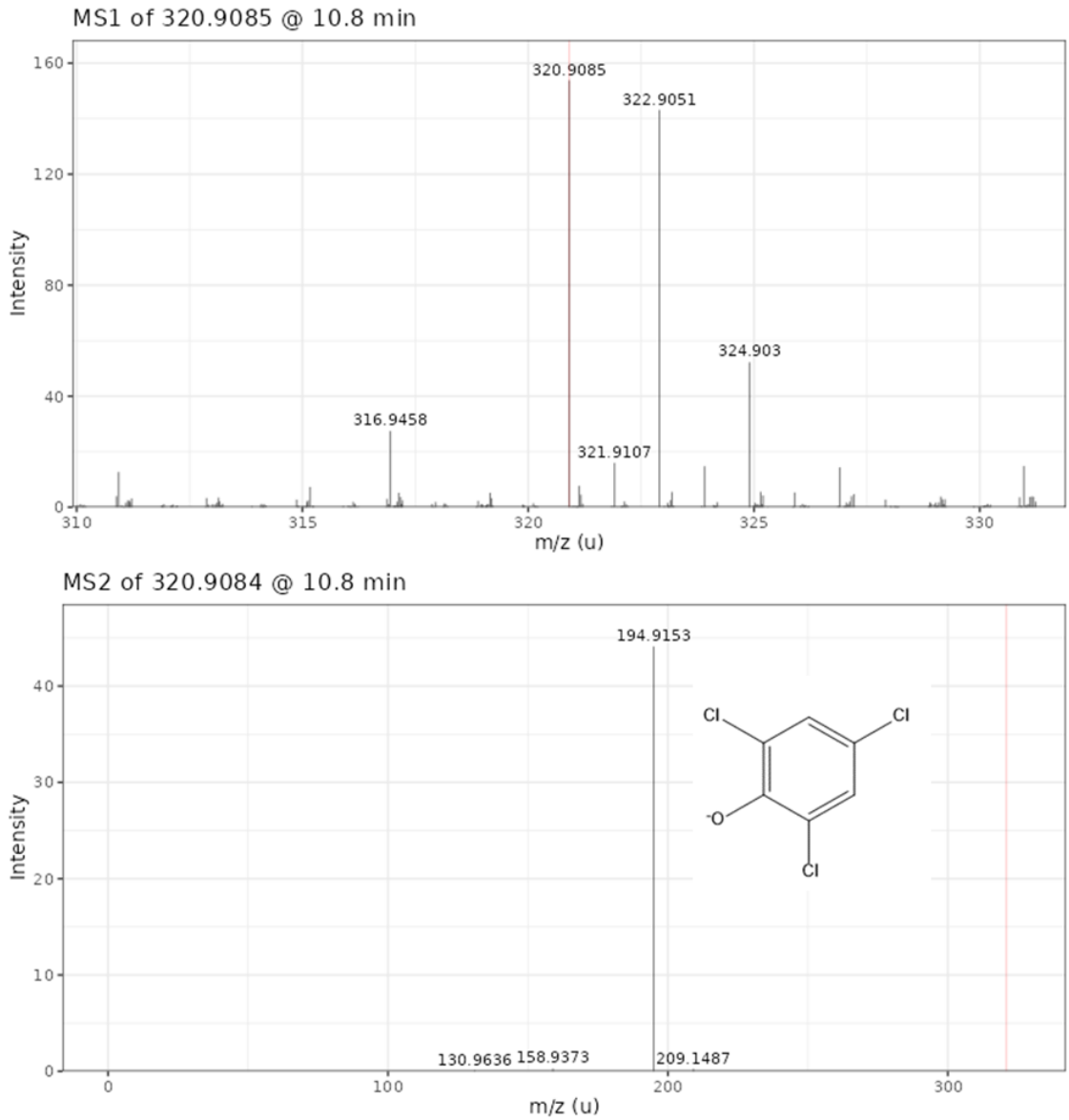

Summenformel

Es konnte keine eindeutige Summenformel über GenForm generiert werden. Jedoch konnte anhand des charakteristischen Cl_3 Isotopenmusters das Fragment m/z 194.9158 als Benzolring mit 3 Chloratomen und einem Sauerstoff identifiziert werden. An diesem hängt vermutlich eine Struktur mit der Summenformel C5H2O4 und einer Masse von 125.9925 Da.

Abgleich möglicher Summenformeln mit Datenbanken:

For-Ident: Keine Kandidaten

PubChem: Keine Kandidaten

CompTox: Keine Kandidaten

Steckbrief Feature: Unbekannt 2 (274.8714@8.5_neg)

Das Feature wurde über die Korrelation mit der Substanz 2,4-D für die Identifizierung priorisiert.

Zeitverlauf

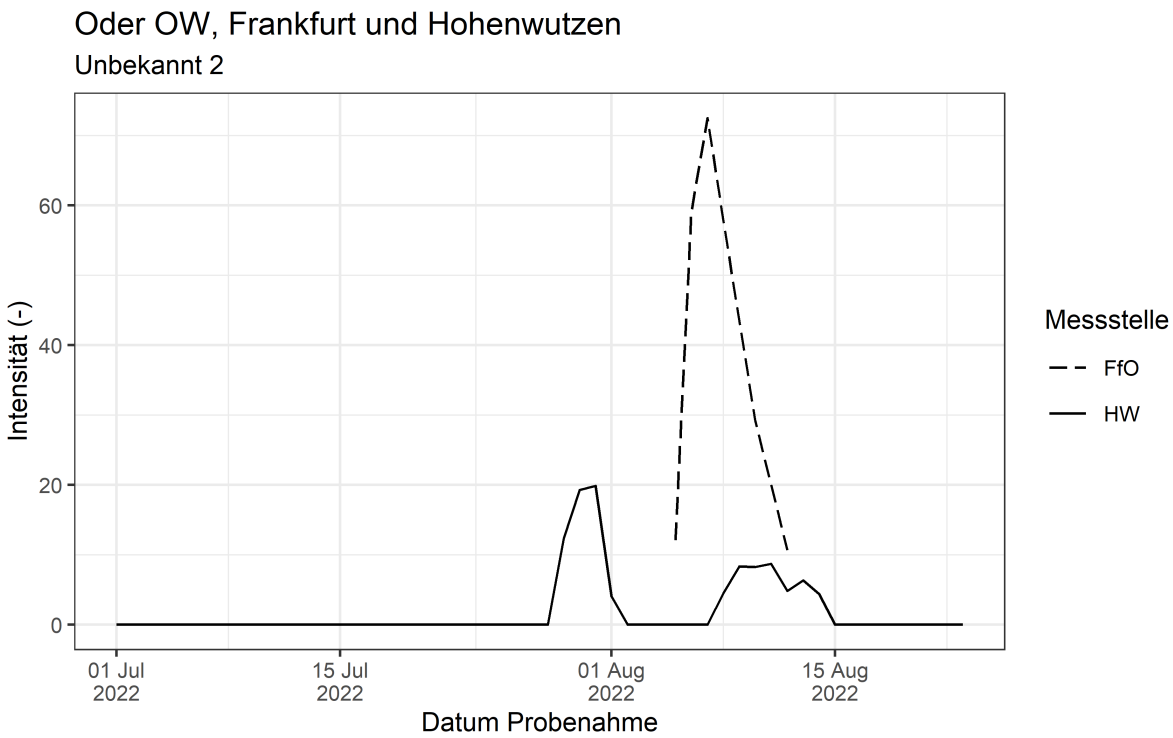

Addukte und Isotopologe

10 detektierte Features gehören zu dieser Substanz. Der postulierte Molekularpeak ist m/z 274.8724 (ESIneg) und eluiert bei 8.6 min. Das intensivste Feature ist das Quellenfragment m/z 194.9152 bei 8.5 min.

Das Isotopenmuster im MS^1-Spektrum des Features m/z 274.8724 konnte nicht eindeutig dem Muster von Cl_3 oder Cl_3S zugeordnet werden. Auch für das Isotopenmuster im MS^1-Spektrum des Quellfragments m/z 194.9152 kommen das Isotopenmuster Cl_2 und Cl_3 in Frage. Der Massenunterschied von 79.9572 Da zwischen dem Molekularpeak und dem Quellfragment deutet zudem auf das Vorhandensein einer Sulfonsäuregruppe hin. Anhand der Intensität des ^{13}C Peaks (m/z 275.1269) wurde eine Anzahl von 4 - 12 C-Atomen abgeschätzt.

Spektren

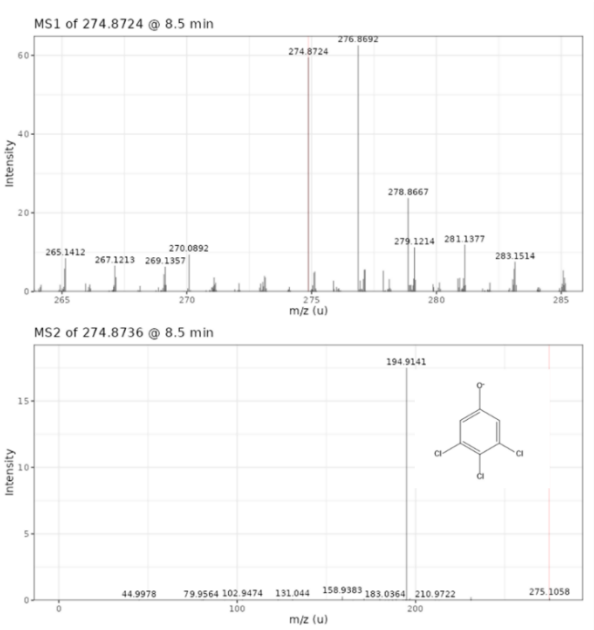

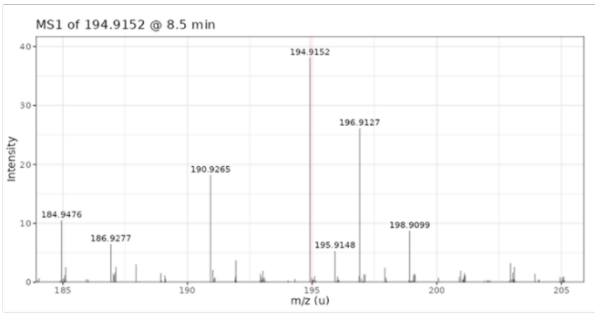

Summenformel

Mittels Genform wurde für diese Verbindung potenzielle Summenformeln gebildet. Diese wurden anhand der Isotopenmuster sowie der abgeschätzten Anzahl von C-Atomen und dem Vorhandensein von HSO_3 gefiltert. Auf Basis dieser Vorbedingungen wurde die Summenformel $C_6H_3O_4SCl_3$ berechnet.

Aufgrund des MS^2-Spektrums und der Recherche in PubChem über die in-silico Fragmentierung des Online-tools MetFrag wurden zwei Kandidaten ermittelt (siehe Tabelle). Für beide Kandidaten wurde jeweils das Quellfragment als Trichlorphenolat erklärt. Dieses wurde auch für das Feature „Unbekannt 1“ identifiziert.

	Kandidat 1	Kandidat 2
Name	2,3,6-Trichlor-4-hydroxy-benzensulfonsäure	(2,4,6-Trichlorphenyl)-hydrogensulfat
Anzahl der Isomere nach PubChem	1	3
Struktur	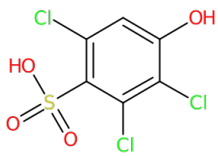	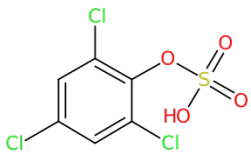

Steckbrief Feature: Unbekannt 3 (240.9091_6.7n) und 4 (240.9098_8.3n)

Die Features wurden über die Korrelation mit der Substanz 2,4-D für die Identifizierung priorisiert.

Zeitverlauf

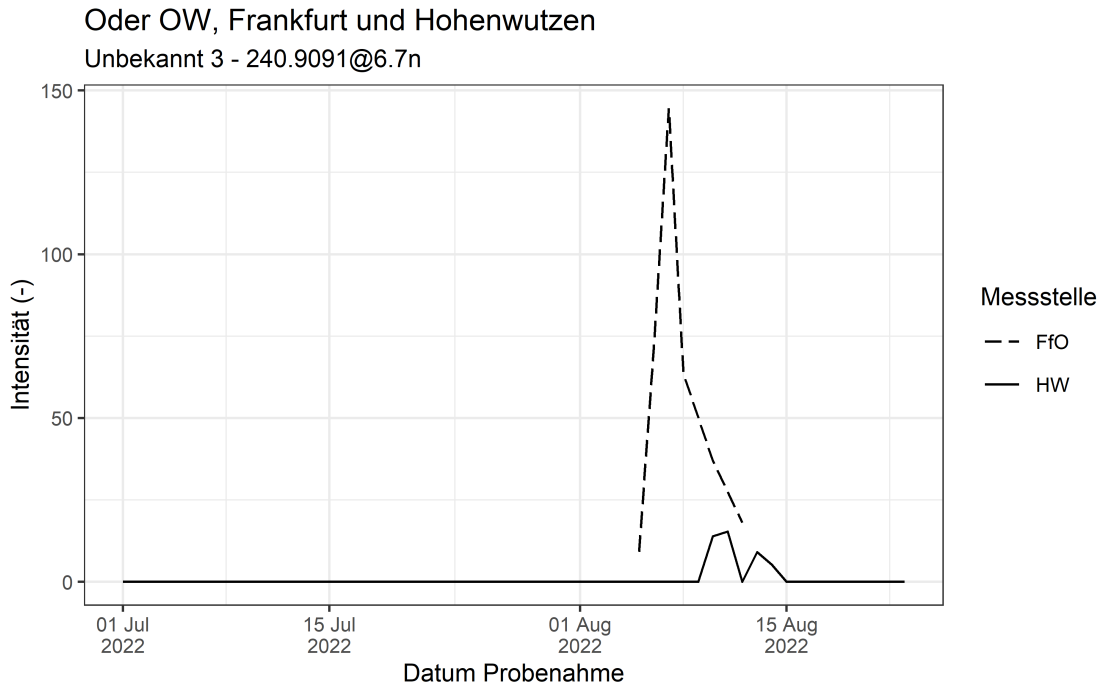

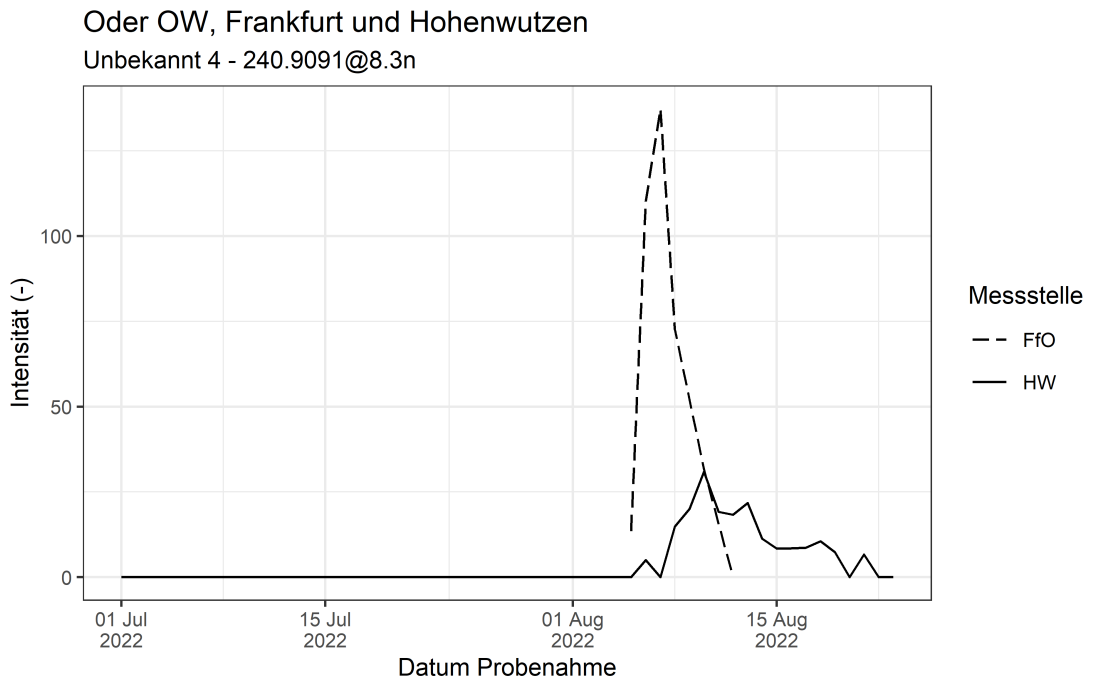

Addukte und Isotopologe

Das Isotopenmuster zeigt eindeutig ein Cl_2 Pattern.

Spektren

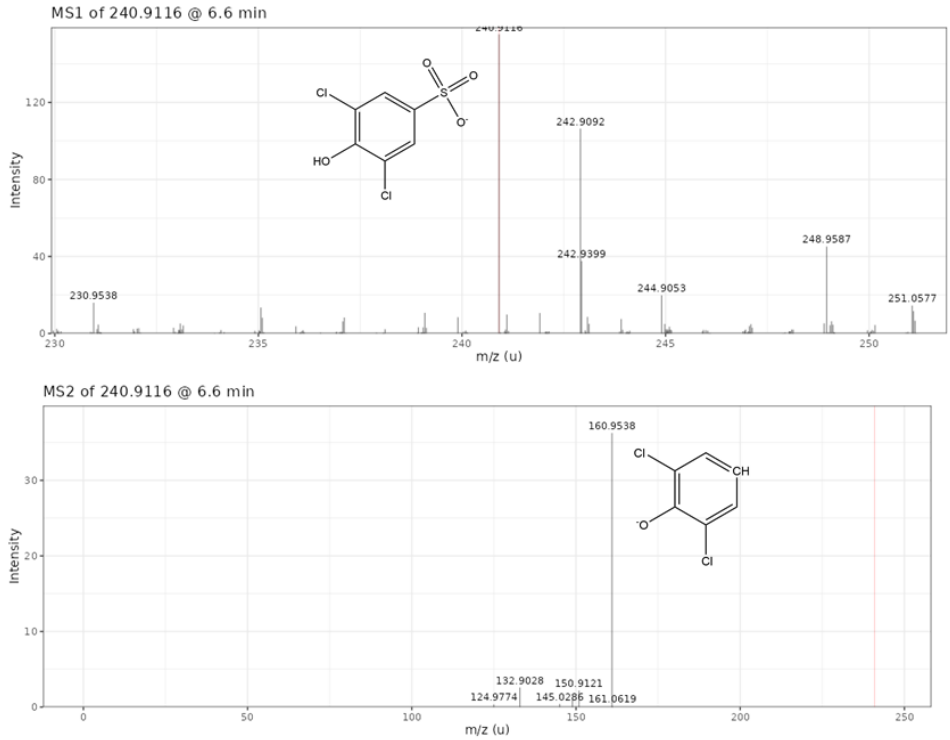

Das MS^2 Spektrum zeigt ein Verlust von 79.9 Da (SO_3) und vermutlich Dichlorphenolat als Fragmentmasse (160.95). Beide Isomere (Unb3 und Unb 4) zeigten identische MS^2 Spektren.

Abgleich mit Online-Datenbanken

Eine Suche nach der Masse 240.9091 in NORMAN Susdat ergab 3,5-Dichlor-4-hydroxybenzolsulfonsäure als einen möglichen Treffer. Mit dieser Ausgangssubstanz kann das Fragment 160.95 erklärt werden. Die zwei Isomere deuten auf zwei Stellungsisomere, z. B. 3,5-Dichlor-4-hydroxybenzolsulfonsäure und 3,5-Dichlor-2-hydroxybenzolsulfonsäure, passend zu den Positionen von Cl in 2,4-D und 2,6-D, die in den Proben bereits eindeutig detektiert wurden.

Kandidaten:

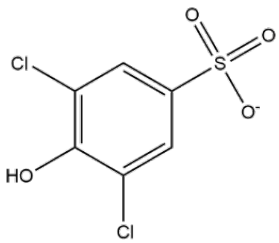

3,5-Dichlor-4-hydroxybenzolsulfonsäure

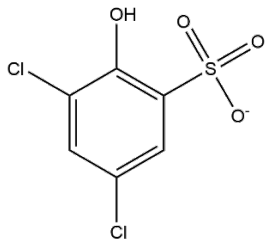

3,5-Dichlor-2-hydroxybenzolsulfonsäure

Steckbrief Feature: Unbekannt 7 (289.1612@6.3p)

Priorisierung: Korrelation mit Tetraglyme

Zeitverlauf

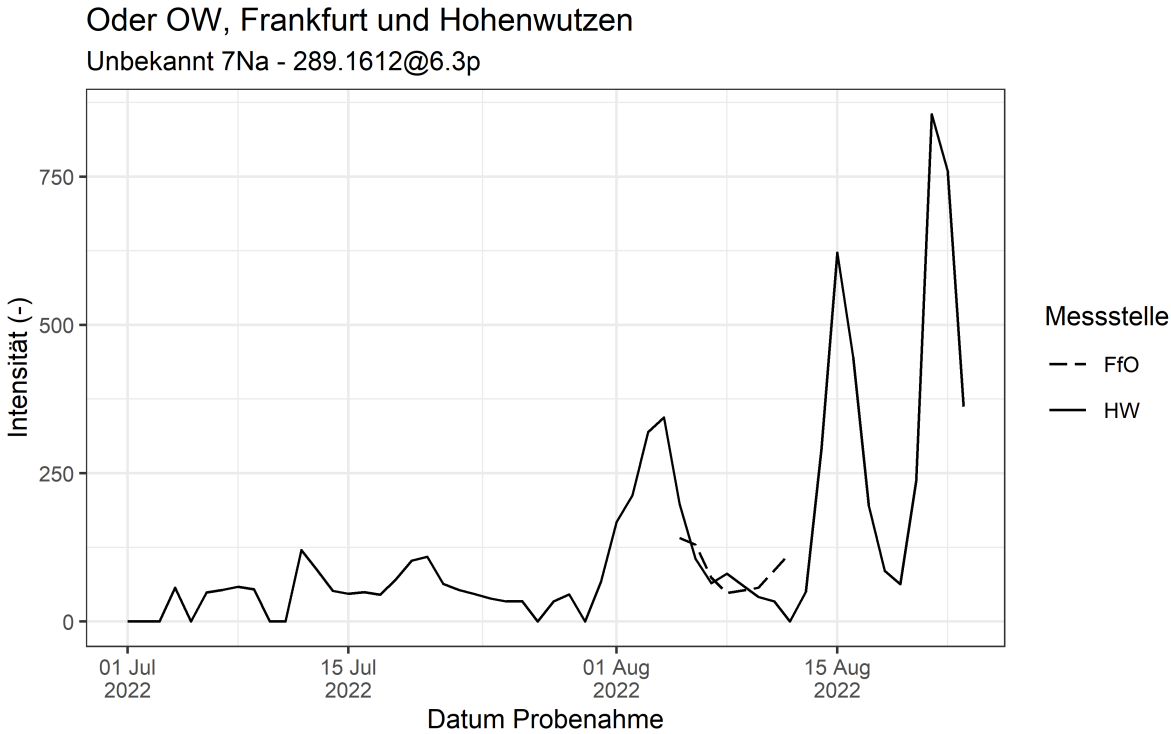

Die Substanz wird bei einer niedrigeren Intensität in Frankfurt (Oder) detektiert als in Hohenwutzen. Es gab jedoch nur Proben in Frankfurt (Oder) über sieben Tage und die Höchstintensität in Frankfurt (Oder) könnte deshalb möglicherweise vor oder nach diesem Zeitraum liegen.

Addukte und Isotopologe

Na-Addukt 289.1618 zeigt die höchste Intensität, diese wurde für die Erstellung des Zeitverlaufs benutzt. Molekülpeak wurde bei 267.1793@6.4 postuliert.

Spektren

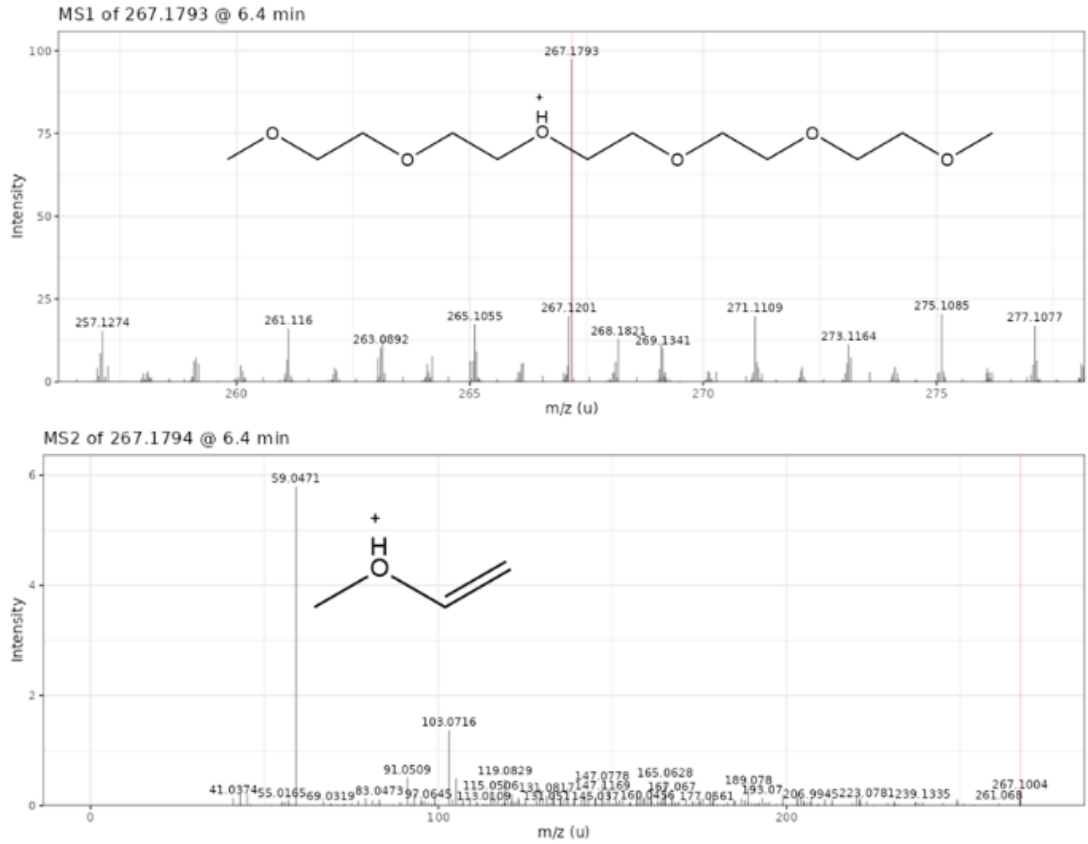

Das MS^2 Spektrum zeigt eine eindeutige Ähnlichkeit zu Tetraglyme. Die Berechnete Summenformel von $C_{12}H_{26}O_6$ und MS^2 Fragment 59 deutet auf eine Detektion von Pentaethylenglycoldimethylether hin.

Steckbrief Feature: Unbekannt 13 (644.2409@9.5p)

Das Feature wurde über die Korrelation mit der Substanz Adenosin für die Identifizierung priorisiert.

Zeitverlauf

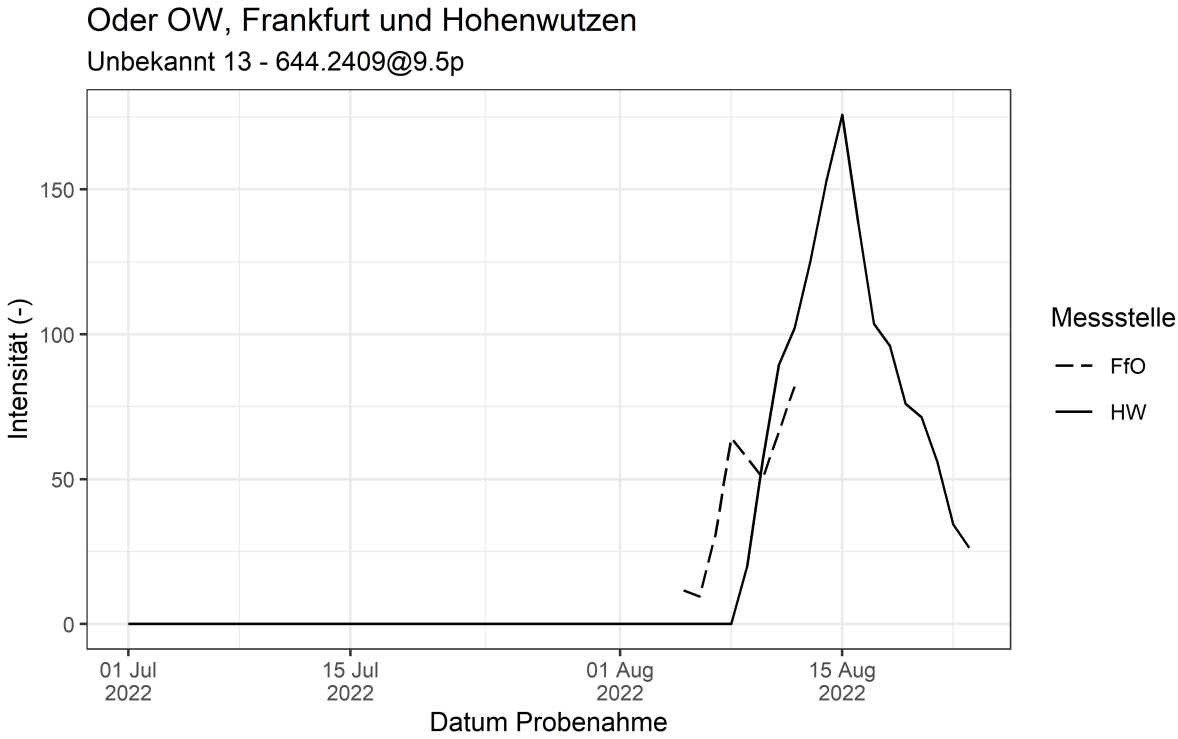

Addukte und Isotopologe

Der [M+H]+ Peak wurde bei 644.2409 vermutet, da es ein Feature bei 666.2197 ([M+Na]+) gab. Das Isotopenmuster deutet auf Cl2 hin.

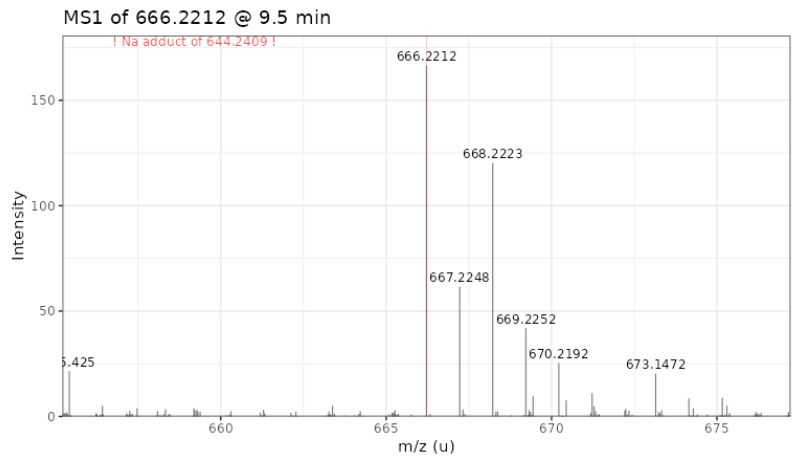

Isotopenmuster vom M+Na peak.

Spektren

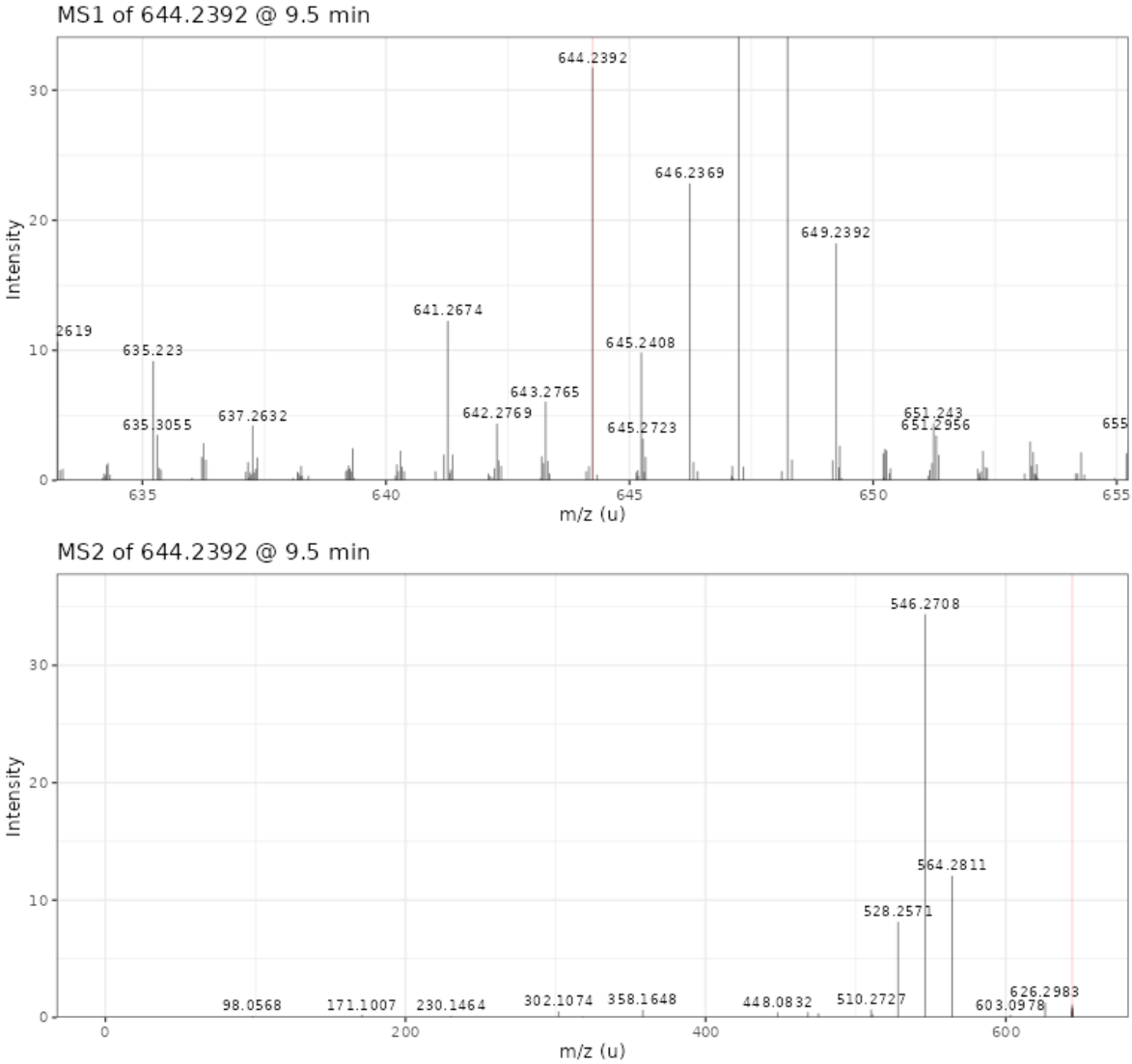

Summenformel

Berechnung der Summenformel mittels Genform ergab 399 Treffer mit Cl2, zu viele für eine eindeutige Zuordnung.

Abgleich möglicher Summenformel mit Datenbanken:

mzCloud: Keine Kandidaten

NORMAN MassBank: Keine Kandidaten

CompTox: Keine Kandidaten

Steckbrief Feature: Unbekannt 14 (301.2120@13.533_pos)

Das Feature wurde über einen t-Test für die Identifizierung priorisiert.

Zeitverlauf

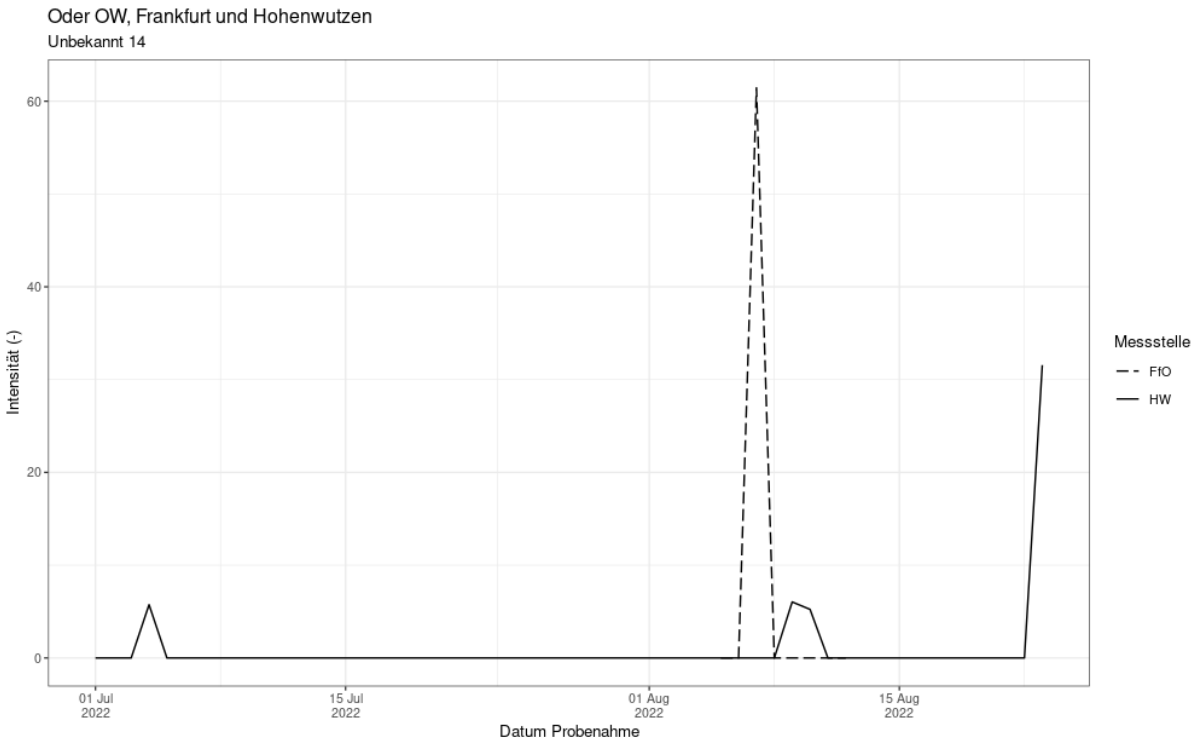

Addukte und Isotopologe

3 detektierte Features gehören zu dieser Substanz. Der postulierte Molekularpeak ist m/z 301.2150 (ESIpos) und eluiert bei 13.6 min. Dieser stellt auch das intensivste Feature der Substanz dar. Anhand der Intensität des ^{13}C Peaks (m/z 302.2177) wurde eine Anzahl von 17-25 C-Atomen abgeschätzt.

Spektren

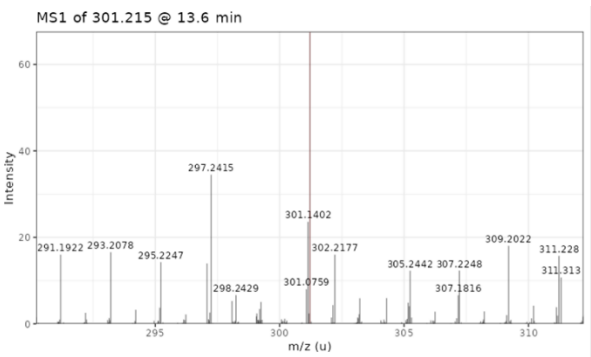

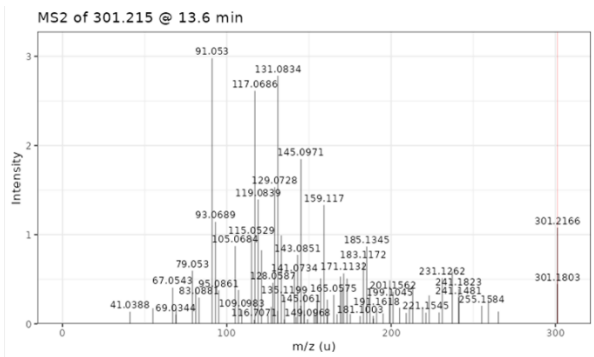

Summenformel

Mittels Genform wurden für diese Verbindung 9 potenzielle Summenformeln gebildet. Diese wurden anhand der abgeschätzten Anzahl von C-Atomen auf 2 potenzielle Summenformeln ($C_{20}H_{28}O_2$ und $C_{18}H_{27}F_3$) eingegrenzt.

Aufgrund des MS^2-Spektrums und der Recherche in NORMAN SusDat über die in-silico Fragmentierung des Online-tools MetFrag konnten für die Summenformel $C_{20}H_{28}O_2$ 10 Kandidaten und für $C_{18}H_{27}F_3$ 0 Kanditaten ermittelt werden. Die 3 an den besten bewerteten Vorschlägen sind in der folgenden Tabelle aufgeführt.

	Kandidat 1	Kandidat 2	Kandidat 3
Name	Dehydroabietic acid	Retinoic acid	Ethynodiol
Final Score	1.0	0.91	0.77
Anzahl der erklärten Fragmente (in-silico)	18/19	16/19	14/19
Struktur	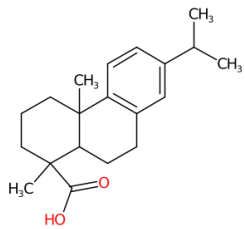	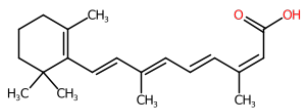	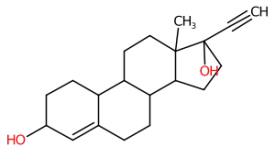
Funde in online Spektren-datenbanken (MassBank, mzCliud)	nein	Ja, keine Überinstimmung mit exp. MS2-Spektrum Ausschluss	nein

Steckbrief Feature: Unbekannt 15 (209.0276@6.248_neg)

Das Feature wurde über einen t-Test für die Identifizierung priorisiert.

Zeitverlauf

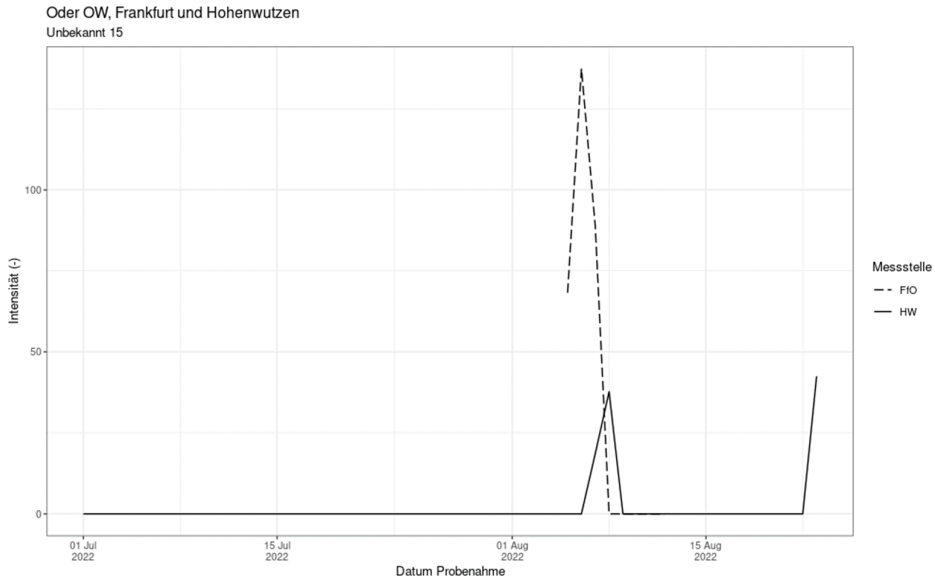

Addukte und Isotopologe

3 detektierte Features gehören zu dieser Substanz. Der postulierte Molekularpeak ist m/z 209.0261 (ESIneg) und eluiert bei 6.2 min. Dieser stellt auch das intensivste Feature der Substanz dar. Anhand der Intensität des ^{13}C Peaks (m/z 210.0289) wurde eine Anzahl von 8-12 C-Atomen abgeschätzt.

Spektren

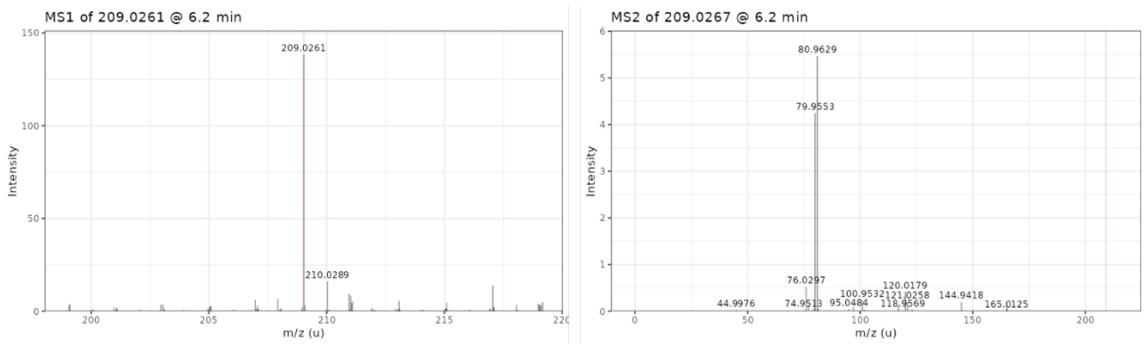

Summenformel

Mittels Genform wurden für diese Verbindung 27 potenzielle Summenformeln gebildet. Diese wurden anhand der abgeschätzten Anzahl von C-Atomen auf 8 potenzielle Summenformeln eingegrenzt. Aus dem MS2-Spektrum ging zudem hervor, dass die Verbindungen voraussichtlich eine Sulfonsäuregruppe enthält (SO_3, Fragmente 79.9553, 80.9629) was ausschließlich bei der Summenformel $C_{10}H_{10}O_3S$ gegeben war.

Aufgrund des MS^2-Spektrums und der Recherche in der Stoffdatenbank CompTox über die in-silico Fragmentierung des Online-tools MetFrag konnten für die Summenformel $C_{10}H_{10}O_3S$ zwei Kandidaten ermittelt werden. In beiden Fällen kann die Abspaltung der zwei Hauptfragmente (79.9553, 80.9629) durch die in-silico Fragmentierung simuliert werden. In der folgenden Tabelle sind die zwei Substanzen gegenübergestellt.

	Kandidat 1	Kandidat 2
Name	2,3-Diethenylbenzene-1-sulfonic acid	Propargyl p-toluenesulfonate
Final Score	1.0	0.39
Anzahl der erklärten Fragmente (in-silico)	4/10	3/10
Struktur	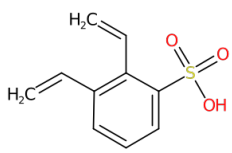	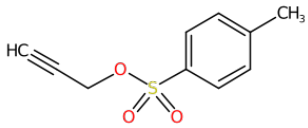

Steckbrief Feature: Unbekannt 16 (169.0083@4.747_neg)

Das Feature wurde über einen t-Test für die Identifizierung priorisiert.

Zeitverlauf

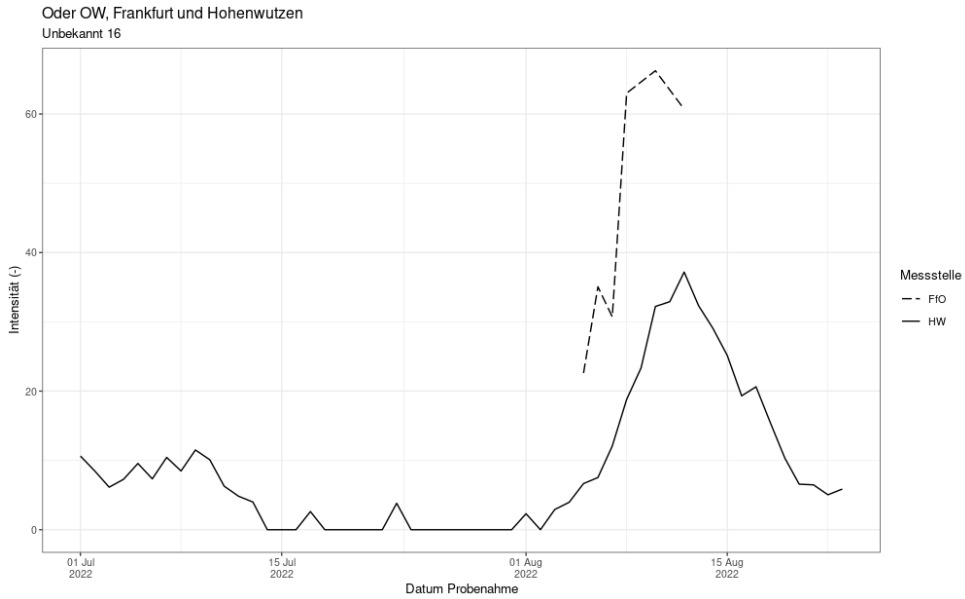

Addukte und Isotopologe

6 detektierte Features gehören zu dieser Substanz. Der postulierte Molekularpeak ist m/z 169.0074 (ESIneg) und eluiert bei 4.7 min. Dieser stellt auch das intensivste Feature der Substanz dar. Anhand der Intensität des ^{13}C Peaks (m/z 170.0102) wurde eine Anzahl von 4-7 C-Atomen abgeschätzt.

Spektren

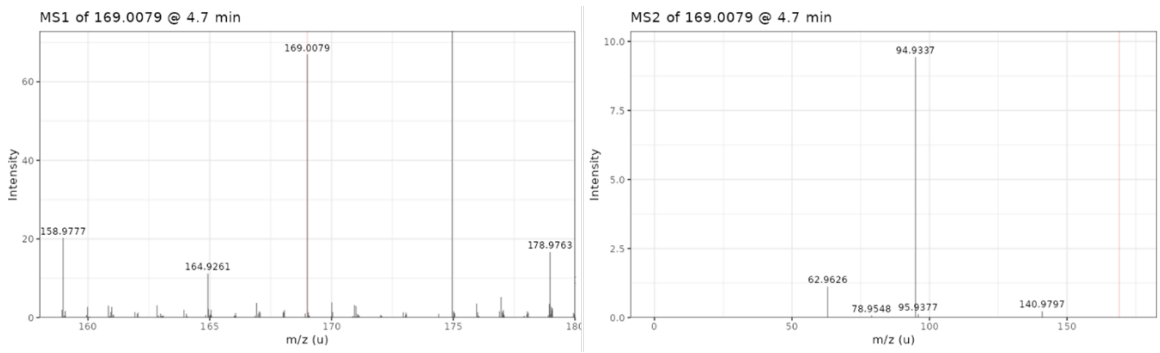

Summenformel

Mittels Genform wurden für diese Verbindung 39 potenzielle Summenformeln gebildet. Diese wurden anhand der abgeschätzten Anzahl von C-Atomen auf 14 potenzielle Summenformeln eingegrenzt.

Aufgrund der Übereinstimmung des experimentellen MS^2-Spektrums mit einem Referenzspektrum der Datenbank mzCloud wurde das Feature vorläufig als O,O-Diethylthiophosphat ($C_4H_{11}O_3PS$) identifiziert. In der folgenden Abbildung sind die zwei MS^2-Spektren gegenübergestellt. Eine abschließende Verifizierung der Identifizierung mit einem Referenzstandard wird empfohlen.

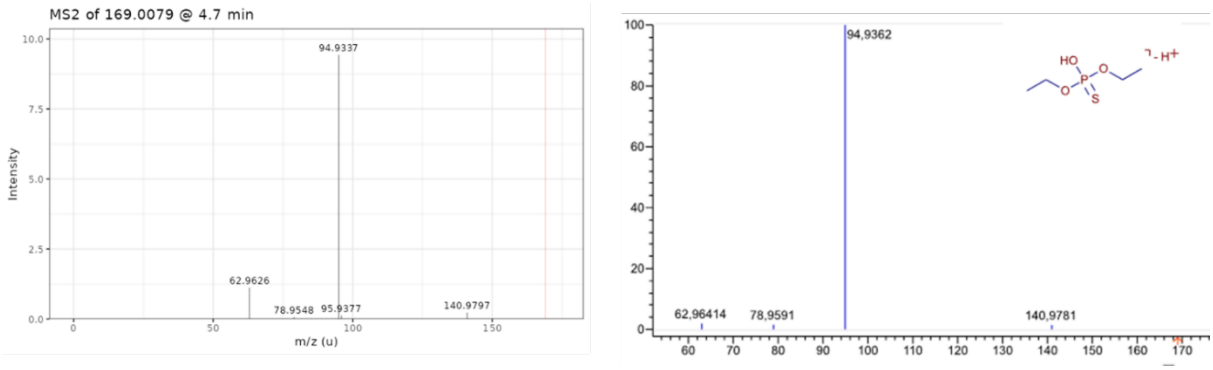

Gegenüberstellung des experimentellen MS^2-Spektrums von Feature 169.0083@4.747_neg (links) und dem Referenzspektrum von O,O-Diethylthiophosphat (rechts)

Steckbrief Feature: Unbekannt 17 (345.1866@9.347_pos)

Das Feature wurde über einen t-Test und die Korrelation mit Na^+ für die Identifizierung priorisiert.

Zeitverlauf

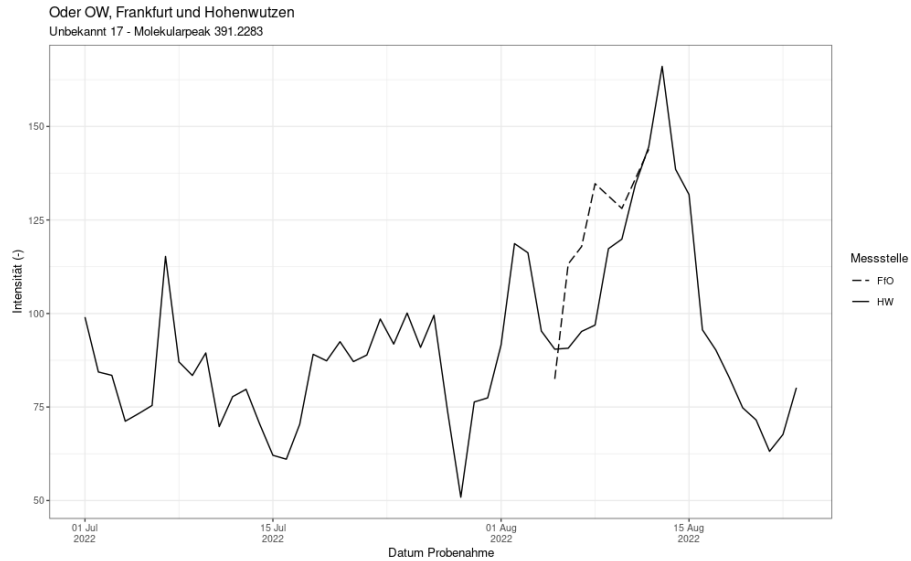

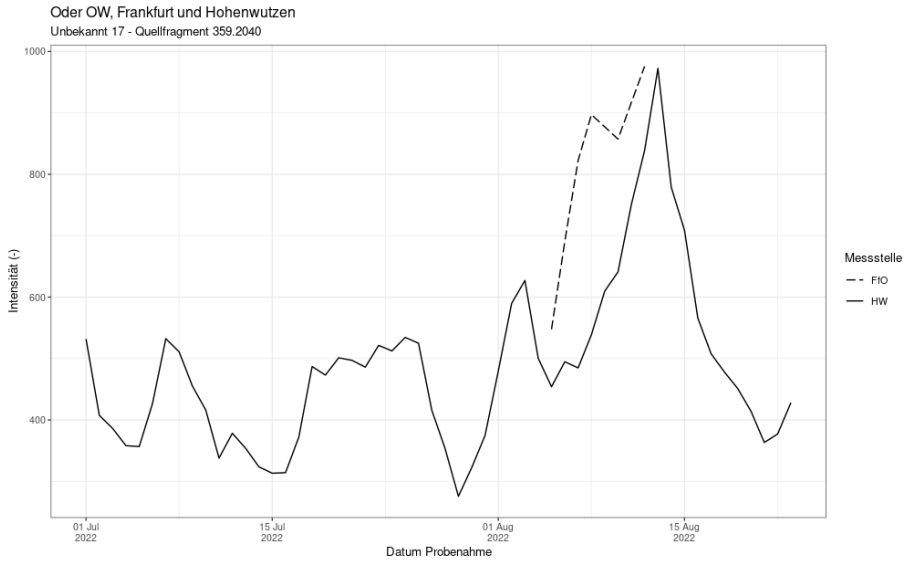

Addukte und Isotopologe

19 detektierte Features gehören zu dieser Substanz. Eines von diesen Features ist das priorisierte Feature m/z 345.1866. Der postulierte Molekularpeak ist m/z 391.2286 (ESIpos) und eluiert bei 9.4 min. Das Quellfragment m/z 359.2040 stellt das intensivste Feature der Substanz dar. Anhand der Intensität des ^{13}C Peaks (m/z 391.2286) wurde eine Anzahl von 15-22 C-Atomen abgeschätzt.

Spektren

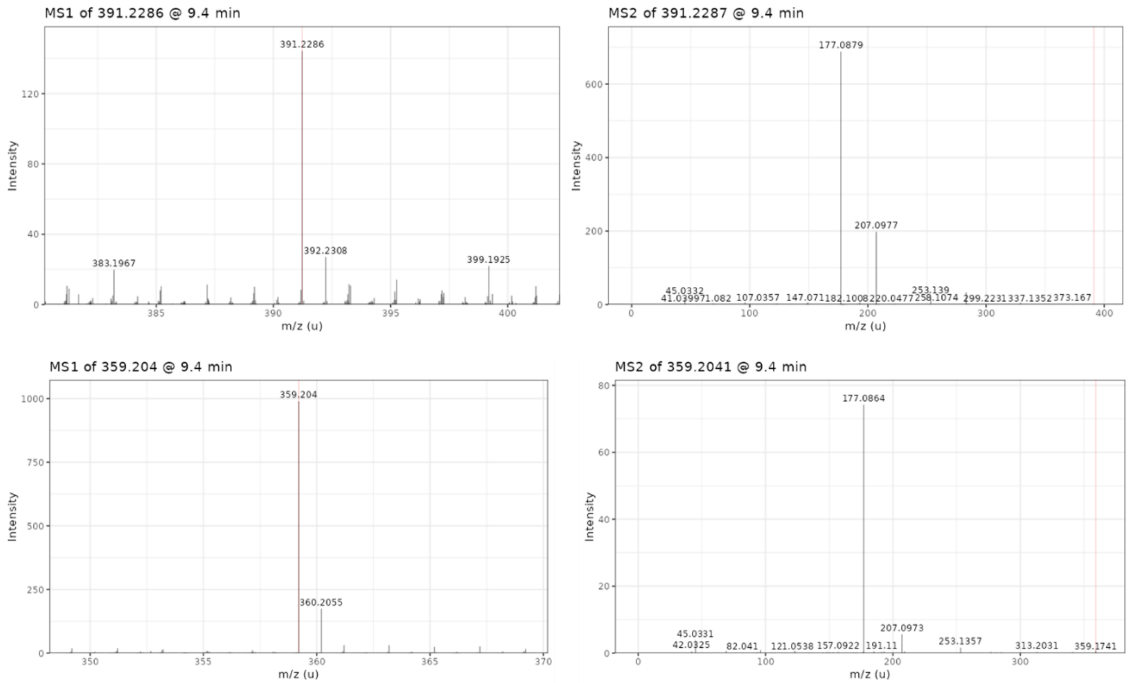

Summenformel

Mittels Genform wurden für diese Verbindung 44 potenzielle Summenformeln gebildet. Diese wurden anhand der abgeschätzten Anzahl von C-Atomen auf 22 potenzielle Summenformeln eingegrenzt.

Aufgrund der Übereinstimmung des experimentellen MS^2-Spektrums mit einem Referenzspektrum der Datenbank mzCloud wurde das Feature vorläufig als Hexamethoxymethylmelamin ($C_{15}H_{30}N_6O_6$) identifiziert. In der folgenden Abbildung sind die zwei MS^2-Spektren gegenübergestellt. Eine abschließende Verifizierung der Identifizierung mit einem Referenzstandard wird empfohlen.

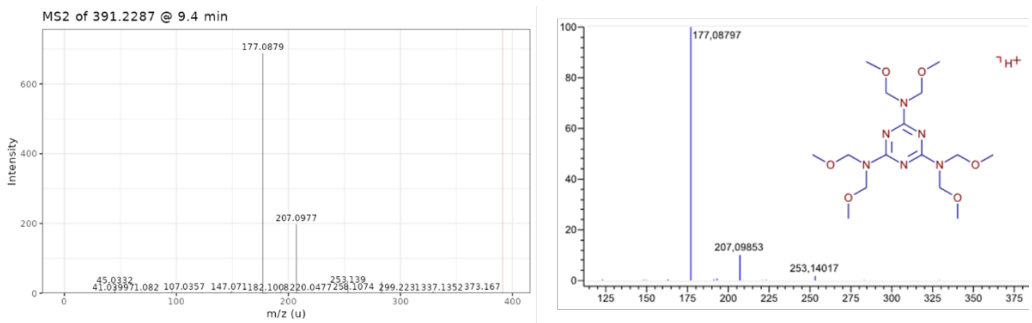

Gegenüberstellung des experimentellen MS^2-Spektrums von Feature 391.2287@9.4_pos (links) und dem Referenzspektrum von Hexamethoxymethylmelamin (rechts)

A3.5.4.2 Target Screening mittels GC-MS/MS

Tabelle A3.5.4.2.1 *Konzentrationen organischer Schadstoffe in Oderschwebstoffen*

			Sammelzeitraum								
Parameter	**Einheit**	**BG**	**01.-31. 03.22**	**01.-30. 04.22**	**01.-31. 05.22**	**01.-30. 06.22**	**01.-31. 07.22**	**01.-15. 08.22**	**16.- 23. 08.22**	**24.-31. 08.22**	**März-August 22 Mittelwert**
Polyzyklische aromatische Kohlenwasserstoffe											
Naphtalin	mg/kg TS	0,006	0,59	0,70	0,60	0,50	0,51	0,40	0,27	0,46	0,55
Acenaphthylin	mg/kg TS	0,002	0,09	0,10	0,10	0,08	0,07	0,06	0,04	0,05	0,08
Acenaphthen	mg/kg TS	0,002	0,13	0,15	0,14	0,13	0,13	0,10	0,07	0,10	0,13
Fluoren	mg/kg TS	0,002	0,17	0,21	0,19	0,17	0,17	0,12	0,09	0,12	0,17
Dibenzothiophen	mg/kg TS	0,002	0,04	0,05	0,04	0,03	0,03	0,03	0,02	0,03	0,03
Phenanthren	mg/kg TS	0,002	0,53	0,61	0,51	0,45	0,45	0,36	0,28	0,29	0,48
Anthracen	mg/kg TS	0,002	0,15	0,17	0,15	0,14	0,13	0,11	0,08	0,11	0,14
Fluoranthen	mg/kg TS	0,002	0,73	0,80	0,81	0,68	0,59	0,60	0,42	0,33	0,68
Pyren	mg/kg TS	0,002	0,66	0,65	0,67	0,57	0,51	0,45	0,31	0,32	0,57
Benzo(b)fluoren	mg/kg TS	0,002	0,20	0,25	0,21	0,17	0,17	0,14	0,11	0,13	0,19
Benzo(a)fluoren	mg/kg TS	0,002	0,11	0,13	0,12	0,09	0,09	0,08	0,07	0,09	0,10
Benzo(a)anthracen	mg/kg TS	0,002	0,38	0,44	0,45	0,38	0,31	0,30	0,20	0,16	0,37
Cyclopenta(c,d)pyren	mg/kg TS	0,002	0,07	0,09	0,09	0,07	0,06	0,05	0,04	0,03	0,07
Triphenylen	mg/kg TS	0,002	0,17	0,19	0,16	0,14	0,14	0,11	0,08	0,06	0,15
Chrysen	mg/kg TS	0,002	0,46	0,51	0,54	0,45	0,41	0,34	0,22	0,15	0,44
Benzo(b)fluoranthen	mg/kg TS	0,002	0,55	0,65	0,69	0,56	0,48	0,45	0,22	0,25	0,54
Benzo(k)fluoranthen	mg/kg TS	0,002	0,17	0,19	0,19	0,16	0,14	0,13	0,09	0,13	0,16
Benzo(a)fluoranthen	mg/kg TS	0,012	0,14	0,17	0,15	0,14	0,12	0,10	0,09	0,07	0,13
Benzo(e)pyren	mg/kg TS	0,002	0,28	0,31	0,27	0,21	0,23	0,16	0,14	0,19	0,24
Benzo(a)pyren	mg/kg TS	0,002	0,40	0,45	0,52	0,42	0,34	0,33	0,17	0,23	0,40
Perylen	mg/kg TS	0,002	0,17	0,16	0,16	0,13	0,13	0,11	0,09	0,10	0,14
Indeno(1,2,3-c,d)pyren	mg/kg TS	0,002	0,39	0,43	0,47	0,40	0,35	0,33	0,19	0,14	0,38
Dibenzo(a,h)anthracen	mg/kg TS	0,002	0,05	0,06	0,05	0,04	0,04	0,04	0,03	0,03	0,05
Benzo(b)chrysen	mg/kg TS	0,002	0,08	0,09	0,09	0,07	0,07	0,07	0,05	0,06	0,08
Benzo(g,h,i)perylen	mg/kg TS	0,002	0,34	0,38	0,40	0,33	0,28	0,27	0,16	0,19	0,32
Summe PAK 16 (EPA)	mg/kg TS	0,002	5,8	6,5	6,5	5,4	4,9	4,4	2,8	3,1	5,5
Mineralölkohlen-wasserstoffe	mg/kg TS	10	168	172	214	199	213	186	146	139	188
Organozinnverbindungen (als Organozinnkation)											
Monobutylzinn	µg/kg OZK TS	5,0	24	14	12	9,3	9,8	9,3	7,7	29,0	13,9
Dibutylzinn	µg/kg OZK TS	1,5	5,6	3,5	3,2	2,2	2,8	2,4	2,8	3,0	3,3
Tributylzinn	µg/kg OZK TS	0,7	1,4	0,83	0,78	0,77	0,59	< 0,7	2,0	0,3	0,9
Tetrabutylzinn	µg/kg OZK TS	0,8	< 0,8	< 0,8	< 0,8	< 0,8	< 0,8	< 0,8	< 0,8	< 0,8	< 0,8
Monooctylzinn	µg/kg OZK TS	0,7	3,7	2,9	3,0	2,2	2,4	2,0	1,8	7,9	2,9
Dioctylzinn	µg/kg OZK TS	1,5	7,3	7,4	7,3	4,9	5,2	4,6	4,5	3,9	6,1
Triphenylzinn	µg/kg OZK TS	0,7	< 0,7	< 0,7	< 0,7	< 0,7	< 0,7	< 0,7	< 0,7	< 0,7	< 0,7
Tricyclohexlyzinn	µg/kg OZK TS	0,8	< 0,8	< 0,8	< 0,8	< 0,8	< 0,8	< 0,8	< 0,8	< 0,8	< 0,8

BG = Bestimmungsgrenze

Tabelle A3.5.4.2.2 *Konzentrationen organischer Schadstoffe in Oderschwebstoffen*

			Sammelzeitraum								
Parameter	**Einheit**	**BG**	**01.-31. 03.22**	**01.-30. 04.22**	**01.-31. 05.22**	**01.-30. 06.22**	**01.-31. 07.22**	**01.-15. 08.22**	**16.- 23. 08.22**	**24.-31. 08.22**	**März-August 22 Mittelwert**
Chlororganische Verbindungen											
1,3,5-Trichlorbenzol	µg/kg TS	0,02	2,6	3,0	2,5	1,9	2,4	1,8	1,4	2,0	2,4
1,2,4-Trichlorbenzol	µg/kg TS	0,02	6,1	6,9	6,5	5,5	5,5	5,0	3,4	5,4	5,8
1,2,3-Trichlorbenzol	µg/kg TS	0,02	1,2	1,0	0,96	0,81	0,78	0,80	0,60	0,71	0,91
1,2,3,5-Tetrachlorbenzol + 1,2,4,5-Tetrachlorbenzol	µg/kg TS	0,02	0,78	0,77	0,88	0,66	0,52	0,66	0,51	0,65	0,70
1,2,3,4-Tetrachlorbenzol	µg/kg TS	0,02	0,65	0,87	0,60	0,48	0,57	0,46	0,30	0,49	0,60
Pentachlorobenzen	µg/kg TS	0,02	1,0	1,1	0,88	0,79	0,84	0,68	0,48	0,71	0,88
Hexachlorbenzol	µg/kg TS	0,02	3,7	4,0	3,4	2,8	2,7	2,3	1,7	2,5	3,1
α–Hexachlorcyclohexan	µg/kg TS	0,02	0,50	0,32	0,31	0,20	0,25	0,21	0,12	0,19	0,29
β-Hexachlorcyclohexan	µg/kg TS	0,02	1,3	1,2	0,81	0,73	0,62	0,56	0,42	0,55	0,86
γ-Hexachlorcyclohexan	µg/kg TS	0,02	0,11	0,12	0,08	0,06	0,08	0,12	0,08	0,18	0,10
δ-Hexachlorcyclohexan	µg/kg TS	0,10	0,17	< 0,1	< 0,1	< 0,1	< 0,1	< 0,1	< 0,040	< 0,040	< 0,1
ε-Hexachlorcyclohexan	µg/kg TS	0,02	< 0,02	< 0,02	< 0,02	< 0,02	< 0,02	< 0,02	< 0,02	< 0,02	< 0,02
PCB 28	µg/kg TS	0,02	0,35	0,38	0,31	0,27	0,28	0,21	0,19	0,22	0,30
PCB 52	µg/kg TS	0,02	0,33	0,28	0,25	0,23	0,24	0,20	0,20	0,19	0,25
PCB 101	µg/kg TS	0,02	1,1	0,64	0,55	0,53	0,45	0,37	0,38	0,37	0,60
PCB 118	µg/kg TS	0,10	0,48	0,46	0,40	0,34	0,32	0,26	0,23	0,23	0,37
PCB 138	µg/kg TS	0,02	2,7	1,8	1,6	1,4	0,94	0,84	0,9	0,91	1,54
PCB 153	µg/kg TS	0,10	3,9	2,6	2,4	2,3	1,5	1,2	1,4	1,2	2,3
PCB 180	µg/kg TS	0,10	2,7	1,6	1,9	1,4	1,1	0,89	1,0	1,0	1,59
Summe PCB 7	µg/kg TS	0,38	12	7,7	7,4	6,4	4,8	4,0	4,2	4,1	7,0
o,p-DDE	µg/kg TS	0,02	0,19	0,26	0,24	0,16	0,19	0,13	0,11	0,12	0,19
o,p-DDD	µg/kg TS	0,02	1,6	1,8	1,5	1,3	1,3	1,0	0,8	1,0	1,4
o,p-DDT	µg/kg TS	0,20	0,24	0,24	0,31	0,21	0,33	< 0,2	0,09	0,15	0,25
p,p-DDE	µg/kg TS	0,02	5,0	6,1	7,2	4,4	5,3	3,6	2,4	3,7	5,2
p,p-DDD	µg/kg TS	0,10	4,7	4,6	4,3	3,5	3,7	2,8	2,3	3,0	3,9
p,p-DDT	µg/kg TS	0,10	1,2	1,3	1,3	0,6	1,0	0,75	0,5	1,2	1,04
Summe DDX 6	µg/kg TS	0,46	13	14	15	10	12	8,3	6	9	12,0
Octachlorstyrol	µg/kg TS	0,10	0,32	0,33	0,32	0,22	0,17	0,16	0,15	0,17	0,25
Hexachlorbutadien	µg/kg TS	0,02	1,6	0,58	0,38	0,40	0,37	0,36	0,18	0,29	0,60
Polybromierte Diphenylether											
BDE 28	µg/kg TS	0,01	< 0,01	< 0,01	< 0,01	< 0,01	< 0,01	< 0,01	< 0,01	< 0,01	< 0,01
BDE 47	µg/kg TS	0,01	0,12	0,20	0,11	0,09	0,11	0,09	0,11	0,09	0,12
BDE 99	µg/kg TS	0,01	0,13	0,29	0,12	0,10	0,11	0,08	0,13	0,08	0,14
BDE 100	µg/kg TS	0,01	0,04	0,08	0,04	0,04	0,04	0,04	0,04	0,02	0,05
BDE 153	µg/kg TS	0,01	0,03	0,05	0,03	0,03	0,03	0,02	0,02	0,02	0,03
BDE 154	µg/kg TS	0,01	0,03	0,04	0,03	0,03	0,03	0,03	0,02	0,02	0,03
BDE 183	µg/kg TS	0,10	0,12	0,19	0,14	0,14	0,18	0,17	0,20	0,08	0,16
BDE 209	µg/kg TS	0,10	27	35	33	28	37	37	45	28	33
TOC	%	0,1	6,4	6,4	6,4	6,6	6,6	5,8	5,5	6,8	6,4

BG = Bestimmungsgrenze

A3.5.4.3 Analytik Oxohalogenide, Halogenessigsäuren und Sulfonsäuren

Substanzliste

Standard-Anionen	**Oxohalogenide**	**HalAc und Sulfonsäuren**
Fluorid, Chlorid, Bromid, Iodid, Nitrit, Nitrat, Phosphat, Sulfat, Formiat, Acetat	Chlorit, Chlorat, Perchlorat, Bromat, Iodid, Iodat, Selenit, Selenat, Chromat	Methansulfonsäure, Sulfaminsäure, Heptansulfonsäure, p-Toluolsulfonsäure, p-Phenolsulfonsäure, Perfluorbutansulfonsäure, 2-Brompropionsäure, Mono-/ Di-/ Trichloressigsäure, Bromchloressigsäure, Mono-/ Dibromessigsäure, Trifluroessigsäure, Iodessigsäure

A3.5.5 Ökotoxikologie

Tabelle A3.5.5.1 *Ökotoxikologische Ergebnisse der Proben von den Messstationen des LfU Brandenburg, der BfG-Messstation Hohenwutzen und aus der Spree-Oder-Wasserstraße.*

Probenbezeichnung	Entnahmestelle	Gewässer-Km	Entnahme-datum	Datum Probeneing.	physiko-chemische Parameter Testgut					
					pH	O_2 n. Gew. [mg/l]	LF [mS/cm]	Sali-nität	Sali-nität TG vor LB-Test	NH_4^+-N [mg/l]
FFO_TM_05/08	Frankfurt (Oder), Messstation LFU	585,229	05.08.2022	17.08.2022						
FFO_TM_06/08		585,229	06.08.2022	17.08.2022						
FFO_TM_07/08		585,229	07.08.2022	17.08.2022						
FFO_TM_08/08		585,229	08.08.2022	17.08.2022						
FFO_TM_10/08		585,229	10.08.2022	17.08.2022	7,7	8,0	2,1	1,0	20,3	<1
FFO_TM_10/08 (Nachunters.)		585,229	10.08.2022	17.08.2022	8,2	9,1	2,2	1,1		
FFO_TM_12/08		585,229	12.08.2022	17.08.2022	7,6	8,1	2,1	1,1	20,3	<1
FFO_TM_12/08 (Nachunters.)		585,229	12.08.2022	17.08.2022	8,2	9,2	2,2	1,1		
FFO_BP_12/08		585,229	12.08.2022	17.08.2022						
FFO_BP_15/08		585,229	15.08.2022	17.08.2022	7,7	7,8	0,0	0,0	20,9	<1
FFO_S_24/08 (unfiltriert)		585,229	24.08.2022	25.08.2022	8,4	8,3	1,5	0,7	20,4	0,1
FFO_S_24/08 (filtriert)		585,229	24.08.2022	25.08.2022	8,4	8,3	1,5	0,7	20,3	0,0
HW_LfU_TM_10/08	Hohenwutzen, Messstation LfU	661,585	10.08.2022	17.08.2022	8,1	8,9	1,5	0,7	20,4	0,0
HW_LfU_TM_11/08		661,585	11.08.2022	17.08.2022	8,0	8,8	1,5	0,7	20,7	0,0
HW_LfU_TM_12/08		661,585	12.08.2022	17.08.2022	7,9	8,6	1,5	0,7	20,0	0,1
HW_TM_01/08	Hohenwutzen, BfG-Messstation	661,585	01.08.2022	17.08.2022	8,5	9,0	1,1	0,5	21,6	0,2
HW_TM_02/08		661,585	02.08.2022	17.08.2022	8,5	9,0	1,0	0,5	20,0	<1
HW_TM_03/08		661,585	03.08.2022	17.08.2022	8,4	9,3	1,0	0,4	20,1	<1
HW_TM_04/08		661,585	04.08.2022	17.08.2022	8,3	8,8	1,1	0,5	20,5	<1
HW_TM_05/08		661,585	05.08.2022	17.08.2022	8,2	9,5	1,1	0,5	20,4	<1
HW_TM_06/08		661,585	06.08.2022	17.08.2022	8,3	8,5	1,1	0,5	20,3	<1
HW_TM_07/08		661,585	07.08.2022	17.08.2022	8,2	8,3	1,3	0,6	21,2	<1
HW_TM_08/08		661,585	08.08.2022	17.08.2022	8,1	9,3	1,5	0,7	19,9	<1
HW_TM_09/08		661,585	09.08.2022	17.08.2022	7,9	7,5	1,5	0,7	20,0	<1
HW_TM_10/08		661,585	10.08.2022	17.08.2022	7,9	8,2	1,5	0,7	20,3	<1
HW_TM_11/08		661,585	11.08.2022	17.08.2022	7,7	9,6	1,5	0,7	20,1	<1
HW_TM_12/08		661,585	12.08.2022	17.08.2022	7,7	9,9	1,6	0,7	21,6	<1
HW_TM_13/08		661,585	13.08.2022	17.08.2022	7,7	10,1	1,5	0,7	20,2	<1
HW_TM_14/08		661,585	14.08.2022	17.08.2022	7,7	9,9	1,4	0,7	21,6	<1
HW_TM_15/08		661,585	15.08.2022	17.08.2022	7,5	8,2	1,4	0,7	20,1	1,8
EHS_SOK_S_06/09 (unfiltriert)	Eisenhüttenstadt, Brücke Straße der Republik	125,68	06.09.2022	06.09.2022	8,9	8,0	1,2	0,5	19,8	0,5
EHS_SOK_S_06/09 (filtriert)		125,68	06.09.2022	06.09.2022	8,8	7,9	1,2	0,5	19,7	0,7

Tabelle A3.5.5.1 (Fortsetzung) *Ökotoxikologische Ergebnisse der Proben von den Messstationen des LfU Brandenburg, der BfG-Messstation Hohenwutzen und aus der Spree-Oder-Wasserstraße.*

Probenbezeichnung	Entnahmestelle	Leuchtb.-Test DIN EN ISO 11348-2						Grünalgentest DIN 38412-33									
		MTP			Norm			unfiltriert					filtriert				
		G1 [%]	LID	pT	G1 [%]	LID	pT	G1 [%]	G2 [%]	G4 [%]	G_A	pT	G1 [%]	G2 [%]	G4 [%]	G_A	pT
FFO_TM_05/08	Frankfurt (Oder), Messstation LFU	-11	**2,2**	1,1		-	-				-	-				-	-
FFO_TM_06/08		-12	**2,2**	1,1		-	-				-	-				-	-
FFO_TM_07/08		-13	**2,2**	1,1		-	-				-	-				-	-
FFO_TM_08/08		-11	**2,2**	1,1		-	-				-	-				-	-
FFO_TM_10/08		-9	**2,2**	1,1	-5	**1**	0	0	-9	-13	**1**	0	-38	-34	-26	**1**	0
FFO_TM_10/08 (Nachunters.)		-9	**2,2**	1,1		-	-				-	-				-	-
FFO_TM_12/08		-8	**2,2**	1,1	-10	**1**	0	35	19	2	**1**	0	-39	-35	-27	**1**	0
FFO_TM_12/08 (Nachunters.)		-9	**2,2**	1,1		-	-				-	-				-	-
FFO_BP_12/08		0	**2,2**	1,1		-	-				-	-				-	-
FFO_BP_15/08		-2	**2,2**	1,1	-6	**1**	0	-7			**1**	0	4	-1		**1**	0
FFO_S_24/08 (unfiltriert)		-2	**2,2**	1,1	3	**1**	0	14	4	-15	**1**	0				-	-
FFO_S_24/08 (filtriert)		-3	**2,2**	1,1	0	**1**	0	-41	-39	-29	**1**	0				-	-
HW_LfU_TM_10/08	Hohenwutzen, Messstation LfU	-8	**2,2**	1,1	-4	**1**	0	-61	-52	-31	**1**	0				-	-
HW_LfU_TM_11/08		-5	**2,2**	1,1	0	**1**	0	-50	-50	-33	**1**	0				-	-
HW_LfU_TM_12/08		-3	**2,2**	1,1	3	**1**	0	-18	-34	-26	**1**	0				-	-
HW_TM_01/08	Hohenwutzen, BfG-Messstation	-9	**2,2**	1,1	-6	**1**	0	-42			**1**	0	-37	-35		**1**	0
HW_TM_02/08		-11	**2,2**	1,1	1	**1**	0	-49			**1**	0	-34	-28		**1**	0
HW_TM_03/08		-8	**2,2**	1,1	3	**1**	0	-56			**1**	0	-32	-30		**1**	0
HW_TM_04/08		-10	**2,2**	1,1	3	**1**	0	-55			**1**	0	-44	-39		**1**	0
HW_TM_05/08		-9	**2,2**	1,1	-2	**1**	0	-50	-44	-30	**1**	0	-34	-29	-20	**1**	0
HW_TM_06/08		-7	**2,2**	1,1	-2	**1**	0	-46	-42	-28	**1**	0	-31	-23	-19	**1**	0
HW_TM_07/08		-8	**2,2**	1,1	-4	**1**	0	-44	-44	-34	**1**	0	-30	-23	-19	**1**	0
HW_TM_08/08		-6	**2,2**	1,1	-2	**1**	0	-42	-41	-26	**1**	0	-31	-31	-27	**1**	0
HW_TM_09/08		-6	**2,2**	1,1	6	**1**	0	-23	-32	-24	**1**	0	-38	-33	-25	**1**	0
HW_TM_10/08		-10	**2,2**	1,1	2	**1**	0	-19	-28	-4	**1**	0	-31	-29	-20	**1**	0
HW_TM_11/08		-10	**2,2**	1,1	9	**1**	0	-249	-255	-231	**1**	0	-34	-28	-25	**1**	0
HW_TM_12/08		-11	**2,2**	1,1	9	**1**	0	-242	-259	-224	**1**	0	-31	-26	-23	**1**	0
HW_TM_13/08		-11	**2,2**	1,1	3	**1**	0	-56	-70	-70	**1**	0	-29	-27	-21	**1**	0
HW_TM_14/08		-11	**2,2**	1,1	4	**1**	0	-196	-235	-240	**1**	0	-31	-27	-24	**1**	0
HW_TM_15/08		-17	**2,2**	1,1	7	**1**	0	-277	-274	-295	**1**	0	-45	-40	-35	**1**	0
EHS_SOK_S_06/09 (unfiltriert)	Eisenhüttenstadt, Brücke Straße der Republik	-4	**2,2**	1,1	13	**1**	0	23	3	-4	**1**	0				-	-
EHS_SOK_S_06/09 (filtriert)		0	**2,2**	1,1	3	**1**	0	-16	-6	1	**1**	0				-	-

Tabelle A3.5.5.1 (Fortsetzung) *Ökotoxikologische Ergebnisse der Proben von den Messstationen des LfU Brandenburg, der BfG-Messstation Hohenwutzen und aus der Spree-Oder-Wasserstraße.*

Probenbezeichnung	Entnahmestelle	Daphnientest DIN 38412-30																max. G-Wert	pT_{max}
		24h								48h									
		G1 [%]	G2 [%]	G4 [%]	G8 [%]	G16 [%]	G32 [%]	G_D	pT	G1 [%]	G2 [%]	G4 [%]	G8 [%]	G16 [%]	G32 [%]	G_D	pT		
FFO_TM_05/08	Frankfurt (Oder), Messstation LFU							-	-							-	-	2,2	0
FFO_TM_06/08								-	-							-	-	2,2	0
FFO_TM_07/08								-	-							-	-	2,2	0
FFO_TM_08/08								-	-							-	-	2,2	0
FFO_TM_10/08		70	70	70	70	0	0	**16**	4	90	80	90	80	0	0	**16**	4	**16**	4
FFO_TM_10/08 (Nachunters.)		0	0	0	0	0	10	**1**	0	0	0	0	0	0	10	**1**	0	**1**	0
FFO_TM_12/08		50	80	60	70	10	0	**16**	4	70	90	70	70	20	0	**32**	5	**32**	5
FFO_TM_12/08 (Nachunters.)		0	0	0	0	0	0	**1**	0	0	0	0	0	0	0	**1**	0	**1**	0
FFO_BP_12/08								-	-							-	-	2,2	**0**
FFO_BP_15/08		0						**1**	0	0						**1**	0	**1**	0
FFO_S_24/08 (unfiltriert)		0	0	0	0	0	0	**1**	0	0	0	0	10	0	0	**1**	0	**1**	0
FFO_S_24/08 (filtriert)		0	10	0	0	0	0	**1**	0	0	10	0	10	0	0	**1**	0	**1**	0
HW_LfU_TM_10/08	Hohenwutzen, Messstation LfU	0	0					**1**	0	0	0					**1**	0	**1**	0
HW_LfU_TM_11/08		0	0					**1**	0	0	0					**1**	0	**1**	0
HW_LfU_TM_12/08		0	0					**1**	0	0	0					**1**	0	**1**	0
HW_TM_01/08	Hohenwutzen, BfG-Messstation	0	0	0				**1**	0	0	0	0				**1**	0	**1**	0
HW_TM_02/08		0	0	0				**1**	0	0	0	0				**1**	0	**1**	0
HW_TM_03/08		0	0	0				**1**	0	0	0	0				**1**	0	**1**	0
HW_TM_04/08		0	0	0				**1**	0	0	0	0				**1**	0	**1**	0
HW_TM_05/08		0	0	0				**1**	0	0	0	0				**1**	0	**1**	0
HW_TM_06/08		0	0	0				**1**	0	0	0	0				**1**	0	**1**	0
HW_TM_07/08		0	0	0	0	0	0	**1**	0	0	10	0	0	0	0	**1**	0	**1**	0
HW_TM_08/08		0	0	0	0	0	0	**1**	0	10	0	0	0	0	0	**1**	0	**1**	0
HW_TM_09/08		0	0	0	0	0	0	**1**	0	0	0	0	0	0	0	**1**	0	**1**	0
HW_TM_10/08		0	0	0	0	0	0	**1**	0	0	0	0	0	0	0	**1**	0	**1**	0
HW_TM_11/08		0	0	0	0	0	0	**1**	0	0	0	0	0	0	0	**1**	0	**1**	0
HW_TM_12/08		0	0	0	0	0	0	**1**	0	0	0	0	0	0	0	**1**	0	**1**	0
HW_TM_13/08		0	0	0	0	0	0	**1**	0	0	0	0	0	0	0	**1**	0	**1**	0
HW_TM_14/08		0	0	0	0	0	0	**1**	0	10	0	0	0	0	10	**1**	0	**1**	0
HW_TM_15/08		0	0	0	0	0	0	**1**	0	0	0	0	0	0	0	**1**	0	**1**	0
EHS_SOK_S_06/09 (unfiltriert)	Eisenhüttenstadt, Brücke Straße der Republik	80	30	10	0	0	0	**4**	2	90	90	20	0	0	0	**8**	3	**8**	3
EHS_SOK_S_06/09 (filtriert)		50	30	10	0	0	0	**4**	2	50	30	10	0	0	0	**4**	2	**4**	2

Fördereffekte sind mit negativen Vorzeichen gekennzeichnet!

A3.5.6.1 Lichtmikroskopische Analyse von Umweltproben und zeitliche Trends von Chlorophyll und Algenabundanzen

Tabelle A3.5.6.1 *Abundanz von Prymnesium parvum und Anteil an der Gesamtbiomasse des Phytoplanktons. Werte mit > 20 Millionen Zellen P. parvum pro Liter sind in Fettdruck dargestellt. Enthalten sind die Ergebnisse aus Proben des LfU und der BfG (kursiv). Bestimmung und Zählung: AquaEcology GmbH, Oldenburg.*

Ort	Datum	Abundanz (Mio. Zellen/l)	Biovolumen (mm^3/l)	Biomasse (µg C/l)
Staffelder Westoder	18.08.	**75**	14	2583
(NP Unteres Odertal)	22.08.	**47**	8,8	1622
	26.08.	**28**	5,3	978
	30.08.	0,69	0,13	24
	03.09.	1,1	0,20	36
Lunower Dammhaus	18.08.	**65**	12	2244
(Stromoder)	22.08.	16	3,0	557
	26.08.	2,2	0,41	76
	30.08.	0,29	0,054	9,8
	03.09.	0,17	0,031	5,7
Wriezener Alte Oder	19.08.	0	0	0
	22.08.	0	0	0
	26.08.	0,80	0,15	28
	30.08.	0,54	0,10	19
	03.09.	**93**	18	3211
Oder bei Hohenwutzen	*16.08.*	***141***	*31*	*5622*
(BfG Messstation)	*24.08.*	*10*	*2,3*	*410*
Oder bei Lebus	19.08.	**97**	18	3363
(nördl. Frankfurt)	23.08.	8,1	1,5	280
	24.08.	*4,5*	*0,98*	*178*
	27.08.	0,50	0,094	17
	31.08.	0,54	0,10	19
	04.09.	0,21	0,039	7,2
Oder-Spree-Kanal	27.08.	**75**	14	2596
(Eisenhüttenstadt)	31.08.	**56**	10	1920
	04.09.	**54**	10	1877
Oder-Spree-Kanal	19.08.	0	0	0
(o. Schleuse Kersdorf)	23.08.	0	0	0
	27.08.	0,03	0,006	1,1
	31.08.	0	0	0
	04.09.	0	0	0
Spree	19.08.	0	0	0
(o. Wehr Große Tränke)	23.08.	0	0	0

Federal Institute of Hydrology (BfG)

Federal Institute of Hydrology (BfG)
Am Mainzer Tor 1
56068 Koblenz
Germany

Phone: +49 261 1306-0
Fax: +49 261 1306-5302
Email: posteingang@bafg.de

www.bafg.de/EN